STUDIES ON THE CYTOSKELETAL PROTEIN α-ACTININ.

ALISTAIR McGREGOR

Thesis submitted to the
University of Leicester in part fulfilment for the requirements
for the Degree of Doctor of Philosophy.

June 1992.

ProQuest LLC
789 East Eisenhower Parkway
P.O. Box 1346
Ann Arbor, MI 48106-1346

ACKNOWLEDGEMENTS

This work was carried out at Leicester University under the supervision of Dr. David Critchley. I am indebted to him for the guidance and encouragement that he gave me during my time in his laboratory. I am also grateful to the members of his laboratory, past and present, that have provided advice and discussion. Special thanks must go to Bipin Patel for technical advice, Gillian Waites for ear bending, and to Betsy Colley for the cakes. I am also grateful for the advice and discussion of Drs. Arthur Rowe and Ken Jones. Thankyou to Ian Riddell for all the photographs here and elsewhere. I acknowledge SERC for funding this research.

I would like to thank Dr. Paul Bolger for carrying out the electron microscopy and Dr. Arthur Rowe for carrying out the sedimentation equilibrium centrifugation.

Finally I would like to thank my parents and family for their ever constant support and encouragement. Also to my friends, especially Kathryn, Stumpy, Sarah, and Simon, who bore the brunt of the hard times.

CONTENTS

INVESTIGATION OF POSSIBLE STRUCTURAL HOMOLOGIES BETWEEN THE ACTIN BINDING DOMAIN OF α-ACTININ AND FILAMIN

ABSTRACT

The interaction between the cytoskeletal proteins α-actinin and vinculin is considered to be fundamental to the link between actin microfilaments and the cytoplasmic face of integral membrane proteins that support cell adhesion. Evidence is provided here for an interaction between α-actinin and vinculin. Electron microscopy of negatively stained samples was used to directly visualise α-actinin/vinculin complexes. The micrographs showed that an α-actinin dimer could bind two vinculin molecules, one at each end of the α-actinin rod. Low speed equilibrium centrifugation demonstrated that the two proteins interacted with a K_d of approximately $1.6x10^{-5}$M. An interaction between α-actinin and vinculin was also demonstrated using a ^{125}I-vinculin overlay technique. Appropriate concentrations of unlabelled vinculin or α-actinin inhibited the binding of ^{125}I-vinculin to α-actinin electroblotted onto nitrocellulose. The vinculin binding site of α-actinin has been localised to a 37 amino acid sequence (residues 713 to 749). Thermolysin generated fragments of α-actinin and glutathione-S-transferase linked α-actinin fusion proteins were used to define the binding site. Their ability to bind vinculin was assayed using ^{125}I-vinculin overlays, by their ability to compete in ^{125}I-vinculin overlays, and in a solid phase binding assay.

Determination of the three dimensional structure of α-actinin may prove useful in elucidating a number of α-actinin/protein interactions. As yet, intact α-actinin has not been crystallised. The actin binding domain of α-actinin (residues 1 to 268) was expressed in *E. coli*. A purification protocol that produces milligram quantities for crystallisation studies was devised. No crystals have as yet been

produced. The repeats of α-actinin (residues 240 to 749) were expressed. However, a satisfactory purification protocol could not be devised.

The possible homology between the actin binding domains of α-actinin and filamin was investigated. An immunological approach, in conjunction with peptide mapping, was used to identify the actin binding domain of filamin for N-terminal sequencing.

ABBREVIATIONS

AMP	adenosine monophosphate
bp	base pair
BSA	bovine serum albumin
cAMP	cyclic adenosine monophosphate
CEF	chicken embryo fibroblasts
CM	carboxymethyl
D	daltons
DEAE	diethyl amino ethyl
DNA	deoxyribonucleic acid
DTT	dithiothreitol
E coli	Escherichia coli
E	extinction coefficient
E64	(trans-Epoxysuccinyl-L-leucylamido-(4-guanidino)-butane)
EDTA	ethylene diamine tetraacetic acid
EGTA	ethylene glycol-bis(β-aminoethyl ether)N,N,N',N'-tetraacetic acid
FPLC	Fast protein liquid chromatography^{Tm} (Pharmacia)
GST	Glutathione-S-Transferase
HEPES	N-2-hydroxy ethyl piperazine-N'-2-ethane sulphonic acid
K_d	dissociation constant
kV	kilovolts
M	molar
mA	milli-amps
μF	microfarads
MES	2-(N-morpholino) ethane sulphonic acid
MPD	2-methyl-2,4-pentanediol
MT-PBS	phosphate buffered saline
NMR	nuclear magnetic resonance
PAGE	polyacrylamide gel electrophoresis
PCR	polymerase chain reaction
PDGF	platelet-derived growth factor
PEG	polyethylene glycol
PMA	phorbol 12-myristate 13-acetate
PMSF	phenyl methyl sulphonyl fluoride

psi	pounds per square inch
PVDF	Polyvinylidene Difluoride membrane
rpm	revolutions per minute
RSV	Rous sarcoma virus
SDS	sodium dodecyl sulphate
TBS	Tris buffered saline
TBS-T	Tris buffered saline-Tween 20
TEMED	N,N,N',N'-tetramethylethylenediamine
TPA	12-O-tetradecanoylphorbol-13-acetate
Tris	Tris(hydroxymethyl)aminomethane

CHAPTER ONE
INTRODUCTION

1.1 THE IMPORTANCE OF CELL ADHESION.

The adhesion of cells to other cells or to the extracellular matrix is thought to be fundamental to a wide variety of cellular processes including cell proliferation (Folkman and Moscona, 1978), cell migration in morphogenesis (McClay and Ettensohn, 1987), regulation of gene expression and differentiation (Edelman, 1986), and wound healing (Grinnell et al, 1987; Clark, 1989). Furthermore, cell-matrix junctions are disrupted to varying degrees in malignant tumours. There has therefore been major efforts made in characterising the molecules involved in the cell-matrix junction. One of the requirements for furthering our understanding of transformation on cell adhesion is a complete understanding of the cell-matrix adhesion site. However, our knowledge of cell-matrix junction components and how they interact is rather limited. Much of the information that has been obtained has come from studies on the focal contacts of cultured fibroblasts. Focal contacts, first described by Abercrombie et al (1971), are prominent cell-matrix junctions with dimensions of 2-10μm by 0.25-0.5μm. The membrane-substrate separation at focal contacts is 10-15nm (Izzard and Lochner, 1976). Focal contacts are a specific type of adherens junction. Adherens junctions are cell-cell and cell-matrix structures characterised by their association with actin microfilament bundles and the presence of vinculin (Geiger et al, 1985).

1.2 THE MODEL OF THE FOCAL CONTACT.

The focal contact is thought to consist of three domains, the extracellular, transmembrane, and cytoskeletal domains (Figure 1.1). The model of the focal contact proposed by Burridge et al (1988) is a

FIGURE 1.1

THE FOCAL CONTACT MODEL

The figure depicts the interactions within the focal contacts formed when fibroblasts adhere and spread on extracellular matrix proteins (from Burridge et al, 1988). Where possible the approximate regions involved in the protein-protein interactions are shown. However, the region of interaction between α-actinin and vinculin is not known. The 190kDa fragment of talin interacts with β_1 integrin and vinculin, but the binding site has not been defined further (Horwitz et al, 1986). Although not depicted, talin and vinculin may each form oligomers (Milam, 1985; Molony et al, 1987).

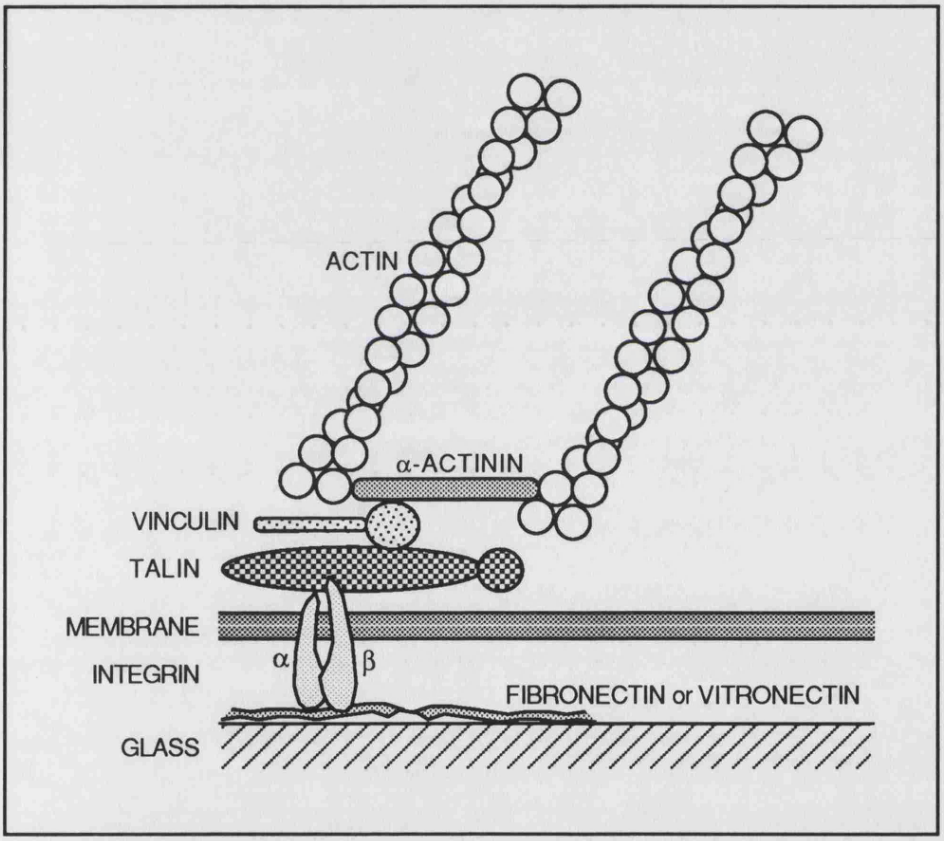

simple chain of interacting proteins. The extracellular matrix proteins are recognised by members of the integrin family that span the cell membrane, the cytoplasmic domain of integrin binds to talin, talin binds to vinculin, vinculin binds to α-actinin, and ultimately α-actinin binds to actin. As will be discussed later, further research strongly suggests that this is a grossly over simplified model. However, it does provide a good introduction to the major components of the focal contact.

1.21 THE EXTRACELLULAR MATRIX.

Fibroblasts adhere poorly to, and fail to spread when directly plated onto glass (unless serum is present) or glass coated with proteins such as bovine serum albumin. Two main extracellular matrix proteins have been implicated in the formation of focal contacts, namely fibronectin and vitronectin. Fibronectin is a multifunctional disulphide linked dimeric glycoprotein. In addition to promoting cell attachment it binds to a number of other proteins, including collagen, proteoglycans, and fibrin(ogen) (Ruoslahti, 1988). Sequence analysis of the approximately 2500 residues shows that fibronectin is composed of three types of repeating segments termed type I, II, and III (Figure 1.2a) (Skorstengaard et al, 1986). There are twelve type I repeats, each about 45 residues long. Homologous repeats have been observed in plasminogen activator and Factor XIII. There are two type II repeats (60 amino acids) that have homologies in Factor XII, prothrombin, plasminogen, and seminal plasma protein. The bulk of fibronectin is composed of type III repeats. These repeats of approximately 90 residues are also found in a number of proteins, including tenascin, collagen (types VI, XII, XIV), β_4 integrin, and titin (reviewed in Engel, 1991). A number of alternatively spliced variants

FIGURE 1.2a

THE STRUCTURE OF FIBRONECTIN

The stucture of the fibronectin monomer is depicted, showing the three types of repeat and the identified functional binding domains (from Skorstengaard et al, 1986). The type III repeats are numbered. The alternatively spliced domains, EIIIA, EIIIB, and V or IIICS, are shown. The disulphide bonds responsible for fibronectin dimerisation are close to the C-terminus.

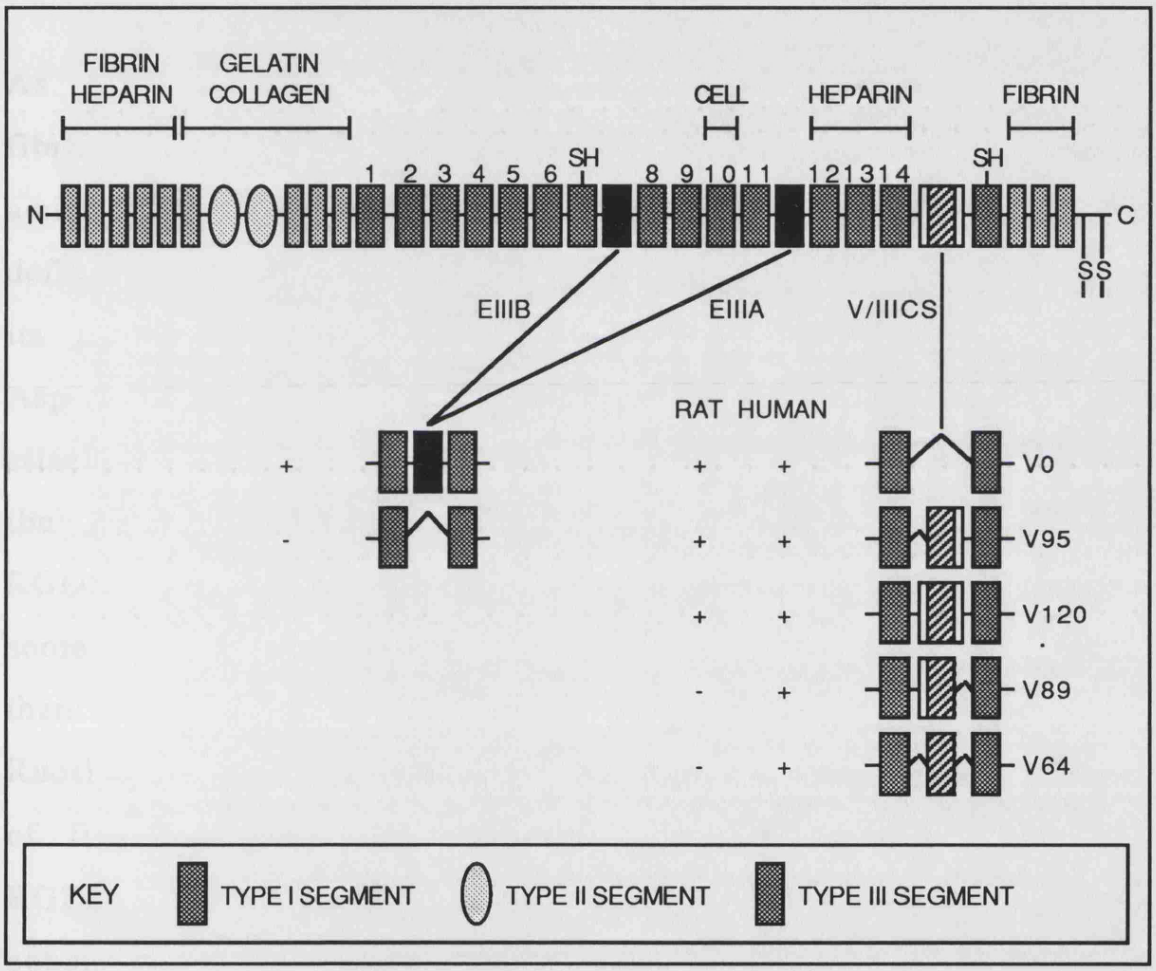

of fibronectin exist. Three regions of alternative splicing have been identified. Two variants involve the inclusion or exclusion of a type III repeat (IIIA or IIIB) (Kornblihtt et al, 1984). The third splice variant involves the inclusion/exclusion in full or in part (Figure 1.2a) of a 120 residue sequence, termed the IIICS or V segment (Tamkun et al, 1984; Paul et al, 1986).

As depicted in Figure 1.2a, a number of functional domains in fibronectin have been identified using limited proteolysis. The 108 amino acid 'cell binding domain' (termed III-10, where the first figure defines the type of fibronectin repeat and the second figure denotes its position within similar repeats) contains the sequence Arg-Gly-Asp-Ser (RGDS) that has been shown to be important in cell attachment (Pierschbacher and Ruoslahti, 1984a). When immobilised, the RGDS tetrapeptide (and an 11.5kDa fragment containing the RGDS sequence) will enable cell attachment although the activity is some 10 to 100 fold lower than intact fibronectin or fragments larger than 75kDa that encompass the RGDS sequence (Pierschbacher and Ruoslahti, 1984a; Akiyama et al, 1985). Interestingly a second region of fibronectin has been identified that acts cooperatively with the RGDS sequence (Obara et al, 1987). The III-9 repeat markedly enhances the cell attachment activity if the III-8 repeat is also present. Replacement of the III-9 repeat by other repeats resulted in a much lower activity (Kimizuka et al, 1991). Two further distinct integrin binding sites (designated CS1 and CS5) have been recognised in separate independently-spliced segments of the IIICS region of fibronectin (Humphries et al, 1986). Both the CS1 and CS5 regions bind to the same (or closely associated) site on $\alpha_4\beta_1$ integrin (Mould et al, 1990; Mould et al, 1991).

Vitronectin is also a multifunctional glycoprotein (Figure 1.2b) (Barnes and Silnutzer, 1983). Vitronectin does not exhibit any homology with fibronectin (Jenne and Stanley, 1987; Sato et al, 1990). However, vitronectin does contain the sequence Arg-Gly-Asp-Val (RGDV) which is a similar integrin binding motif to that found in fibronectin. The RGDV tetrapeptide promotes a degree of cell attachment similar to that produced by the RGDS tetrapeptide (Pierschbacher and Ruoslahti, 1984b). Vitronectin also contains a heparin binding site although it is not homologous to that in fibronectin (Suzuki et al, 1984). The C-terminal two thirds of vitronectin is mostly composed of repeats homologous to those found in the heme binding plasma protein called hemopexin. In hemopexin eight repeats (1 to 8) are divided into two domains by a flexible hinge. In vitronectin the repeat analagous to repeat 4 (possibly 5) of hemopexin is absent and that analagous to repeat 7 has been converted to the heparin binding domain (Jenne and Stanley, 1987).

Vitronectin is a serum protein that binds tenaciously to glass (Barnes and Silnutzer, 1983). The majority of adhesion promoting activity of serum can be accounted for by vitronectin. Fibroblasts also adhere to and spread when plated onto fibronectin coated glass. However, in the presence of serum, fibronectin is removed from focal contacts whereas in the absence of serum it is retained. Since vitronectin is not removed from focal contacts, it has been suggested that vitronectin is the preferred substrate for fibroblasts and that this is used in preference to fibronectin (Grinnell, 1986). Both the cell binding domain and heparin binding domain of fibronectin appear to be important in cell attachment. Whilst some fibroblast cell lines

FIGURE 1.2b

THE STRUCTURE OF VITRONECTIN

The cell (RGD), collagen, and heparin binding domains are depicted (from Preissner, 1991). The series of hemopexin-like repeats are also shown.

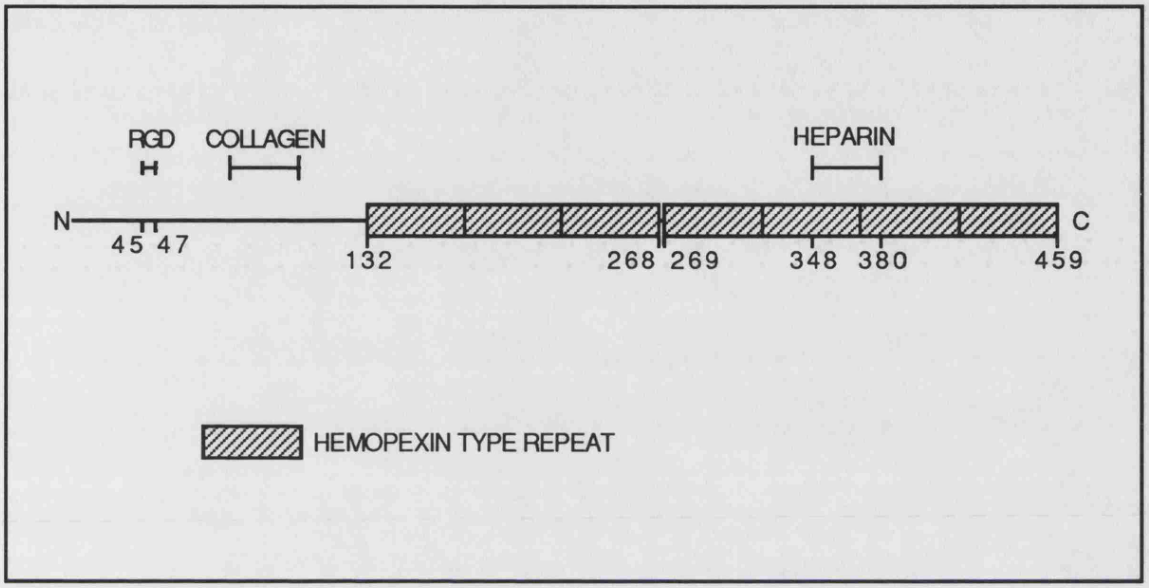

adhere well to the RGD peptide, others adhere poorly and do not form focal contacts (Singer et al, 1987). Cells that bind poorly to the RGD containing domain could be induced to form focal contacts if the heparin-binding domain was adsorbed with the RGD containing domain, or if it is added as a solution (Woods et al, 1986). The requirement of the heparin binding domain suggests that some cells require surface heparin sulphate proteoglycans to form focal contacts, though the heparin binding domain alone is insufficient to induce focal contact formation (Laterra et al, 1983)

1.22 INTEGRINS.

The integrins are a family of transmembrane proteins that mediate cell-matrix and cell-cell adhesion (Figure 1.3). In focal contacts they are linked to actin microfilaments via talin, vinculin, and α-actinin. They are αβ heterodimers that were initially identified using antibodies that perturbed cell adhesion (Horwitz et al, 1985), and by affinity chromatography using an immobilised RGD containing fragment of fibronectin (Pytela et al, 1985; Cheresh, 1987). Since their initial discovery, various techniques have been used to identify many distinct α and β subunits. At least 14 α and 8 β subunits, and over 20 combinations of these subunits have been identified (Table 1.1) (Hynes, 1992). Furthermore, a number of integrin subunits are alternatively spliced. For example, the isoform of β_1 integrin, termed $\beta_1$3'v, has a cytoplasmic domain that is 9 residues shorter than that of β_1 integrin. Unlike β_1 integrin, $\beta_1$3'v integrin does not contain a tyrosine residue that fits the consensus phosphorylation sequence (Altruda et al, 1990). The cytoplasmic domains of the β_3, β_4, α_3, and α_6 subunits and the extracellular domain of the α_{IIb} subunit are also alternatively spliced (reviewed in Hynes, 1992). The integrin

FIGURE 1.3

A MODEL OF THE STRUCTURE OF INTEGRIN

The figure gives an impression of the overall shape of integrin as observed by electron microscopy. The ligand binding region, cystine rich repeats, and divalent cation binding sites (M^{++}) are indicated (from Hynes, 1992).

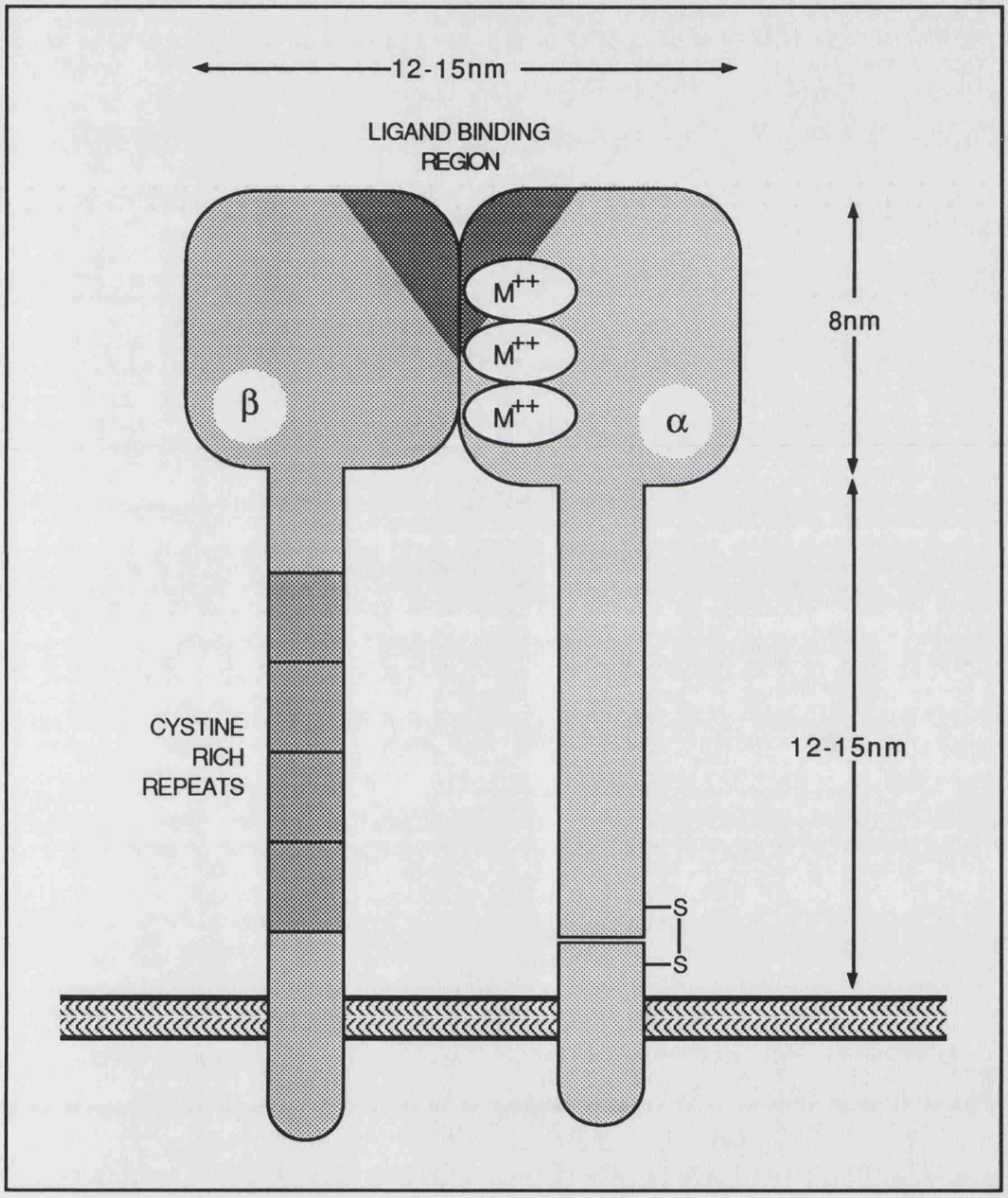

TABLE 1.1

THE MEMBERS OF THE INTEGRIN SUPERFAMILY

The table shows the integrin heterodimers identified, their ligands if known, and the sequence of the binding site of the ligand where identified (from Hynes, 1992).

Integrin		Ligands/Counter-receptors	Binding Site	α Subunit Type[5]
β_1	α_1	C, LM		I
	α_2	C, LM	DGEA[2]	I
	α_3	FN, LM, C	RGD(?)	C
	α_4	FN (V25), VCAM-1	EILDV[3]	C[6]
	α_5	FN (RGD)	RGD	C
	α_6	LM		C
	α_7	LM		C
	α_8	?		?
	α_V	VN, FN (?)	RGD	C
β_2	α_L	ICAM-1, ICAM-2		I
	α_M	C3b[1], FB, Factor X, ICAM-1		I
	α_X	FB, C3b[1]	GPRP	I
β_3	α_{IIb}	FB, FN, vWF, VN, TSP	RGD, KQAGDV[4]	C
	α_V	VN, FB, vWF, TSP, FN, C	RGD	C
β_4	α_6	LM (?)		C
β_5	α_V	VN	RGD	C
β_6	α_V	FN	RGD	C
β_7	α_4	FN (V25), VCAM-1	EILDV[3]	C[6]
	α_{IEL}	?		?
β_8	α_V	?		C

The ligands/counter-receptors are as follows: C - collagens; LM - laminin; FN - fibronectin; FN (V25) - alternatively spliced V segment of FN; VCAM and ICAM - integral membrane proteins of the immunoglobulin superfamily; FB - Fibrinogen; vWF - von Willebrand factor; TSP - Thrombospondin. [1] component of complement (inactivated). [2] determined for type I collagen. [3] from the alternatively spliced V segment of fibronectin. [4] RGD recognised in all ligands, whereas KQAGDV only recognised in fibrinogen. [5] this column denotes whether the α subunit is cleaved (C) or if it contains an I-domain (I) (see below). [6] The cleavage of α_4 occurs in a region distinct from that of the other subunits.

superfamily is divided into sub-families based on which β subunit the heterodimer contains. Most α subunits only associate with a single type of β subunit. However, a number of α subunits, most notably α_v, can associate with multiple β subunits (Table 1.1). The β_1 sub-family have a widespread distribution and are generally involved in binding extracellular matrix proteins. Interestingly, although the $\alpha_4\beta_1$ integrin binds to the IIICS region of fibronectin, it is also involved in cell-cell interactions (Mould et al, 1990). The β_2 sub-family appear to be confined to lymphoid and myeloid cells and are concerned with cell-cell adhesion. The β_3 sub-family binds certain extracellular matrix proteins and some serum borne proteins such as fibrinogen. The β_3 sub-family appears to be confined to platelets, endothelial cells and certain carcinomas (Hemler, 1990).

The α subunits range in size from 140kDa to 200kDa (under non-reducing conditions). They can be subdivided into two groups. One group is post-translationally cleaved to give two disulphide linked polypeptides. The cleavage site is typically near the C-terminus, but lies in the extracellular domain. The cleaved α subunits also contain four putative divalent cation sites whereas other α subunits have three. The α_4 subunit is cleaved, but the cleavage site is towards the middle of the subunit. The degree of cleavage ranges from 0-100%. The α_4 subunit only has three putative cation sites (Takada et al, 1989). The other type of α subunit contains an I-domain. The I-domain is a 180-200 amino acid sequence found in the α_2, α_L, α_M, and α_X integrin subunits. Due to its presence in cartilage matrix protein, von Willebrands factor, and $\alpha_2\beta_1$ integrin, each of which binds collagen, it has been suggested that the I-domain is responsible

for collagen binding. However, the ability of the β_2 integrins to bind collagen has not been demonstrated (Hemler, 1990).

Each α subunit has a C-terminal cytoplasmic tail of 15-53 residues. Although the α subunits share an overall homology of 20 to 30% there is very little homology between the cytoplasmic domains of the different α subunits. However, the α subunit cytoplasmic domains appear to be well conserved between species. For example, the cytoplasmic domain of the human α_3 subunit is 86% identical to that of the chicken (Hemler, 1990).

The molecular weights of the β subunits are generally between 90 and 100kDa, though the β_4 subunit is 210kDa. There is 44 to 47% similarity between the β_1, β_2, and β_3 subunits. The β_1, β_2, and β_3 subunits each contain 56 conserved cysteine residues, mainly in a four fold repeating motif in the extracellular domain. The conservation of the C-terminal cytoplasmic tail of the β_1 subunit is very high. Sequence comparison of the 41 C-terminal amino acids from the chicken, *Xenopus*, and human (residues 758 to 798) β_1 subunits showed them to be 98% identical (Marcantonio and Hynes, 1988). The high conservation of this domain suggests that it has an important role in the function of β_1 integrins, possibly with regard to cytoskeletal interactions (Marcantonio and Hynes, 1988).

The integrin heterodimer is essential for binding to its intracellular and extracellular ligands. Buck et al (1986) demonstrated that the α and β_1 subunits of avian integrin were individually unable to bind fibronectin, laminin, or talin. The sequences required for dimerisation are contained within the extracellular domains of the α

and β subunits. Truncated integrins that lack both their C-terminal and transmembrane domains form soluble heterodimers that are able to bind their extracellular ligands (Dana et al, 1991). An interesting feature of the integrins is their ligand specificity (Table 1.1). Whereas $\alpha_6\beta_1$ will only bind laminin, the $\alpha_1\beta_1$ receptor will bind collagen and laminin, whist the $\alpha_{IIB}\beta_3$ will bind fibrinogen, fibronectin, von Willebrands factor, and vitronectin. Initially variations in ligand specificity were attributed to the different α subunits. However, it is now apparent (Table 1.1) that both subunits can affect ligand specifity (Hynes, 1992). The tripeptide RGD is only recognised by some of the integrins. A number of the integrins bind RGD containing proteins but at a site distinct from the RGD sequence. Two regions involved in the binding of extracellular ligands have been identified by chemical cross linking studies. The binding of an RGD peptide has been localised to within 63 residues (residues 109 to 171) of the β_3 subunit. A synthetic fibrinogen peptide has been shown to bind within the second putative calcium binding motif of the α_{IIb} subunit.

A number of integrins have been shown to have an inactive and active states. The $\alpha_{IIB}\beta_3$ integrin of resting platelets does not bind to its appropriate ligands unless the platelets are activated (Elmore et al, 1990). Interestingly, the $\alpha_4\beta_1$, $\alpha_5\beta_1$, and $\alpha_6\beta_1$ integrins which are constitutively active on most cells are inactive on leucocytes until the leucocytes have been activated by antigens or phorbol esters (Shimizu et al, 1990).

1.23 TALIN.

Talin is a high molecular weight protein that localises to cell-matrix adherens junctions, but is absent from cell-cell adherens junctions

(Geiger et al, 1985). However, talin has also been implicated in the cell-cell interactions of lymphocytes (Kupfer et al, 1986).

The binding of talin (and a 190kDa proteolytic fragment of talin) to integrin was demonstrated using an equilibrium gel filtration assay. The avian integrin complex of a talin/integrin mixture eluted from a gel filtration column at a position equivalent to integrin. However, the avian integrin complex eluted earlier from the gel filtration column if the column had been pre-equilibrated with talin (or the 190kDa fragment of talin) (Horwitz et al, 1986). This indicated that a complex formed but dissociated rapidly during the time course of the experiment. The shift in elution position of integrin increased with increasing talin concentration, being half maximal at 150μg/ml. Hence the K_d was estimated to be approximately $7x10^{-7}M$ (Horwitz et al, 1986). The talin binding site of integrin was distinct from the fibronectin binding site of integrin as the RGDS peptide did not perturb the talin/integrin interaction (Horwitz et al, 1986). Native heterodimeric integrin was required for talin binding (Buck et al, 1986) which may explain why attempts to demonstrate an interaction using Western Blotting were unsuccessful. Sucrose density gradient centrifugation also failed to show a talin/integrin interaction, presumably due to rapid dissociation of the complex (Horwitz et al, 1986).

Talin has a deduced molecular weight of 270kDa (Rees et al, 1990). Previously the molecular weight had been estimated as 225-235kDa as judged on SDS-PAGE. This discrepancy may be due to the unusual amino acid composition of talin which has 14% alanine residues and low levels of aromatic residues (Rees et al, 1990). Secondary

structure predictions suggest a high degree of α-helix, but no coiled-coil structure. Talin is monomeric at concentrations below 0.72 mg/ml but can dimerise at higher concentrations. It has been suggested that such oligomer formation may be relevant in focal contact formation (Molony et al, 1987). Protease digestion of talin by calpain and V8 protease indicated the presence of two domains (Figure 1.4) (O'Halloran et al, 1985). The C-terminal 190kDa fragment (220kDa from sequence analysis) is rich in alanine (18%) and has a highly polar (>30%) C-terminal domain of 60 residues (Rees et al, 1990). The N-terminal 47kDa fragment (50kDa from sequence analysis) is also markedly polar (28%) (Rees et al, 1990). Electron microscopy of talin at physiological salt concentrations showed it to be an elongated, flexible, rod shaped molecule of 60nm, whereas in low ionic strength buffers it was globular (Molony et al, 1987). Interestingly, the 190kDa fragment of talin maintains an elongated conformation in solutions of both high and low ionic strength. It has been suggested that the 47kDa fragment is necessary for this conformational change (O'Halloran and Burridge, 1986). A further interesting result of calpain cleavage is the effect on localisation of talin, especially considering that talin appears to be a physiological substrate for calpain II which is present in focal contacts (O'Halloran and Burridge, 1986; Beckerle et al, 1987). When microinjected into cultured epithelial cells, the 190kDa fragment of talin localised to both cell-matrix and cell-cell adherens junctions (Nuckolls et al, 1990). A proportion of the 47kDa talin fragment localised to focal contacts when microinjected into fibroblasts but most was diffusely dispersed through the cytoplasm. Whether the 47kDa fragment localised to cell-cell junctions in

FIGURE 1.4

THE DOMAIN STRUCTURE OF TALIN

The domain structure of talin is shown. The region of talin that is homologous to the N-terminal domains of Band 4.1 (Conboy et al, 1986), ezrin (Turunen et al, 1989), moesin (Lankes and Furthmayr, 1991), radixin (Funayama et al, 1991), and a protein-tyrosine phosphatase termed PTPH1 (Yang and Tonks, 1991) is indicated. The N- and C-terminal highly polar regions are depicted (from Rees et al, 1990).

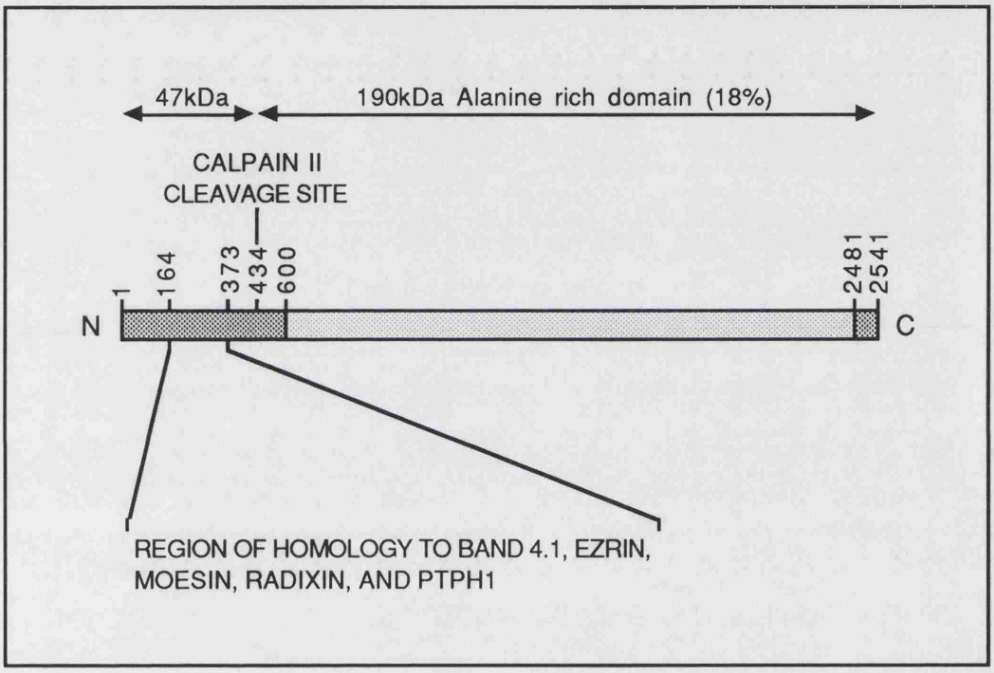

epithelial cells was unclear due to the cytoplasmic staining (Nuckolls et al, 1990).

A 200 to 220 amino acid segment within the 47kDa talin fragment is homologous to the N-terminal domain of Band 4.1 (Conboy et al, 1986), ezrin (Turunen et al, 1989), moesin (Lankes and Furthmayr, 1991), radixin (Funayama et al, 1991), and a protein-tyrosine phosphatase termed PTPH1 (Yang and Tonks, 1991). As yet the significance of this similarity is unclear. The N-terminal domain of Band 4.1 binds to the integral membrane protein glycophorin (Leto et al, 1986), whereas the C-terminal domain is reported to bind to spectrin (Correas et al, 1986). The role of the homologous domain has not yet been determined in ezrin or radixin. However, ezrin has a submembranous distribution (Pakkanen et al, 1987) whilst radixin localises to cell-cell adherens junctions (Tsukita et al, 1989). Although talin binds integrin and vinculin via the 190kDa fragment (Burridge and Mangeat, 1984; Horwitz et al, 1986), the 47kDa fragment may also have a binding site for an as yet unidentified adherens junction component (Nuckolls et al, 1990).

1.24 VINCULIN.

Vinculin is a monomeric protein that localises to adherens junctions (cell-matrix and cell-cell). The molecular weight deduced from the DNA sequence is 117kDa (Price et al, 1989). On the basis of V8 protease data and sequence analysis of vinculin, the molecule can be divided into two domains (Figure 1.5). The 90kDa N-terminal domain contains three 112 residue repeats which have no known homologies with repeat sequences observed in other cytoskeletal proteins. The 27/32kDa C-terminal domain is separated from the N-terminal

FIGURE 1.5

THE DOMAIN STRUCTURE OF VINCULIN

The domains within vinculin are shown, as described by Price et al (1989). The location of the metavinculin insert is shown (Gimona et al, 1988b). The domain that contains the paxillin binding site is indicated (Turner et al, 1990).

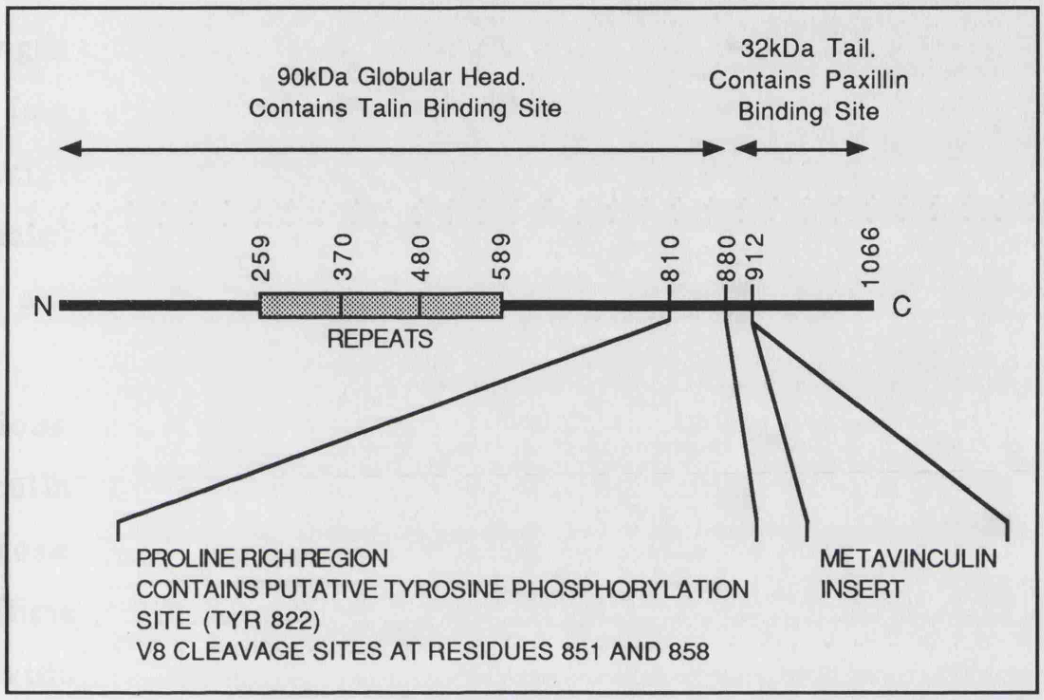

domain by a proline rich region that contains two V8 protease cleavage sites (Price et al, 1989). The N- and C-terminal domains correspond respectively to the globular head of 8nm diameter and the elongated tail of 20nm length observed in electron microscopy (Milam, 1985). Interestingly, vinculin self associates at high ionic strength via head to head and tail to tail interactions into complexes of four to six individual vinculin molecules. The tail to tail association appears to be more stable than those between the head domains (Milam, 1985). The physiological significance of vinculin self association is unclear.

Various assays have been employed to demonstrate the binding of vinculin to talin. Initially the interaction was demonstrated using sucrose density gradient centrifugation. The sedimentation coefficients for vinculin and talin were 7.6 and 9.4 when centrifuged individually. However, a proportion of a vinculin/talin mixture migrated with a sedimentation coefficient of 10.5 (Burridge and Mangeat, 1984). A dissociation constant for the talin/vinculin interaction of approximately 10^{-8}M was determined using quantitative immunoprecipitation of talin/^{125}I-vinculin complexes with anti-talin antibodies. The talin binding site in vinculin was tentatively identified as a 41 residue sequence (residues 167 to 207) in the 90kDa head domain (Jones et al, 1989). Interestingly, the cDNA clone cVin5 lacks the corresponding 123 nucleotides (Bendori et al, 1989), and these 123 nucleotides are contained within a single exon (Gilmore et al, 1992). It has been suggested that alternative splicing of the single vinculin copy gene (Price et al, 1989; Weller et al, 1990) may generate talin binding and non-talin binding vinculin isoforms that localise to cell-matrix and cell-cell adherens junctions

respectively. However, a sensitive reverse transcriptase/polymerase chain reaction has not demonstrated the presence of a vinculin isoform lacking exon 5 (Gilmore et al, 1992). Sequence comparison of chicken (Price et al, 1989), human (Weller et al, 1990), and nematode vinculin (Barstead and Waterston, 1989) shows that the 41 amino acid region of nematode vinculin is quite divergent (39% identity) whereas the N- (residues 1 to 258) and C-terminal (residues 820 to 1066) domains are 54 and 61% identical respectively. Despite this divergence, each contains a block of eight conserved residues (residues 178 to 185). Two point mutations within this sequence that each alter the charge characteristics of the residue abolished the talin binding capacity of vinculin *in vitro* (Gilmore et al, 1992). Interestingly, when vinculin polypeptides (residues 1 to 398) incorporating the mutations were expressed in Cos cells they still localised to focal contacts suggesting that this domain may contain a binding site for another focal contact protein (Gilmore et al, 1992). The possible relevance of the block of eight conserved residues assumes that the nematode contains talin, though this has not yet been demonstrated. Vinculin residues 167 to 207 are not in themselves sufficient to support talin binding. The smallest talin binding fragment that has been generated contains residues 1 to 258. Further deletions of residues abolished talin binding activity (Gilmore et al, 1992).

A 150kDa isoform of vinculin, termed metavinculin, is present in smooth and cardiac muscle tissue (Belkin et al, 1988). Metavinculin contains a 68 amino acid insert between residues 912 to 913 of chicken vinculin (Gimona et al, 1988) that arises due to alternative

splicing of the vinculin gene (Koteliansky et al, 1992). The function of the metavinculin insert is not known.

Vinculin shows similarities to the 102kDa cadherin associated protein, termed CAP102 or α-catenin (Herrenknecht et al, 1991; Nagafuchi et al, 1991). CAP102 localises to cell-cell adherens junctions. It binds to the cytoplasmic domain of the transmembrane protein E-cadherin. The CAP102 binding site lies within the last 72 residues of the 151 amino acid C-terminal domain of E-cadherin (Ozawa et al, 1990). The N-terminal domain of CAP102 shares 26% identity with the N-terminal domain of vinculin. This region of vinculin contains the talin binding site (Gilmore et al, 1992). Interestingly, a five residue sequence of CAP102 (residues 194 to 198) is identical to a region within the block of eight conserved eight residues in vinculin (residues 178 to 185, see above). Although intact talin does not localise to cell-cell adherens junctions (Geiger et al, 1985) it would be interesting to see whether CAP102 could bind to talin. The central regions of CAP102 and vinculin are 32% identical. The significance of this domain is unclear. The C-terminal 150 residues of vinculin and CAP102 share 34% identity. This region is involved in vinculin self association (Bendori et al, 1989). It has been suggested that CAP102 may self associate in a similar manner or be able to form vinculin/CAP102 complexes (Herrenknecht et al, 1991).

Recently vinculin has been shown to be essential for the development of the nematode *Caenorhabditis elegans* , where it is present in dense bodies. Nematode embryos lacking vinculin grew more slowly than wild type embryos, and died soon after hatching. They did not demonstrate muscle twitching during embryogenesis, as had the wild

type embryos. The muscle structure was disorganised suggesting that vinculin has an essential role in muscle development (Barstead and Waterston, 1991).

1.25 α-ACTININ.

α-Actinin is a 2x100kDa antiparallel homodimer found in a variety of cytoskeletal structures. It is an F-actin cross-linking and bundling protein. Three main isoforms exist, referred to as the skeletal muscle, smooth muscle, and non-muscle isoforms. As yet the only functional difference appears to be that the binding of skeletal and smooth muscle α-actinins to F-actin is calcium insensitive whilst that of the non-muscle isoform is calcium sensitive (Burridge and Feramisco, 1981; Bennett et al, 1984; Duhaiman and Bamburg, 1984; Landon et al, 1985). However, it appears that individual cell types can express more than one of the isoforms. Endo and Masaki (1984) have shown that myotubes express both the skeletal and smooth (and/or non) muscle isoforms of α-actinin. The skeletal muscle isoform was restricted to the Z-lines whilst the smooth/non-muscle isoform was confined to membrane associated structures. More recently a smooth muscle α-actinin cDNA clone was isolated from a fibroblast cDNA library (Baron et al, 1987a) and a non-muscle α-actinin cDNA was isolated from a skeletal muscle cDNA library (Arimura et al, 1988), further supporting the suggestion that cells can express more than one α-actinin isoform.

Sequence analysis of chick smooth muscle, chick skeletal, and *Dictyostelium discoideum* α-actinins (Baron et al, 1987a; Noegel et al, 1987; Arimura et al, 1988) suggested that the α-actinin sequence could be divided into three domains (Figure 1.6). The N-terminal

FIGURE 1.6

THE DOMAIN STRUCTURE OF CHICKEN α-ACTININ

The domains within α-actinin are depicted. The two EF-hand calcium binding motifs are shown as black boxes. The binding sites for F-actin (Mimura and Asano, 1986), β integrin (Otey et al, 1990), and zyxin (Crawford et al, 1992) are indicated.

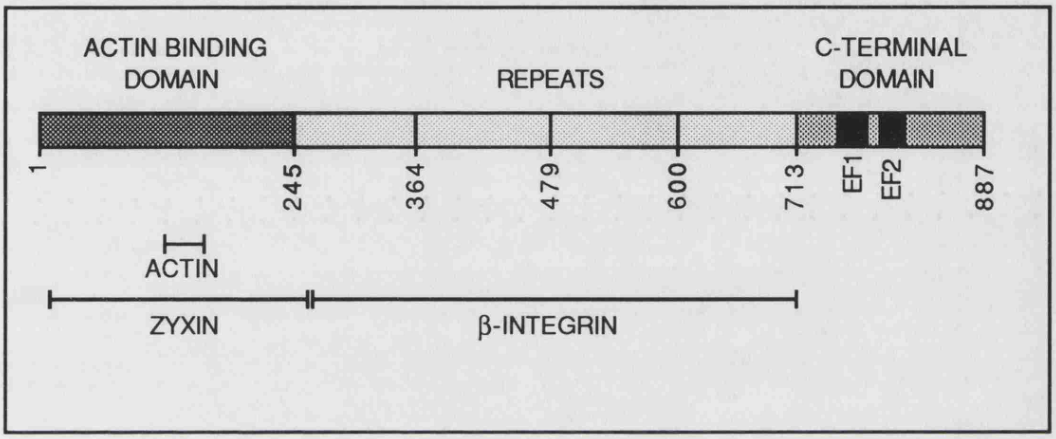

domain (residues 1 to 245) contains the actin binding site (Mimura and Asano, 1986). The actin binding domain is homologous to that of β-spectrin, dystrophin, and the *Dictyostelium discoideum* 120kDa gelation factor (termed ABP-120) (Koenig et al, 1988; Byers et al, 1989; Noegel et al, 1989). A 27 residue surface accessible sequence of ABP-120 has been shown to be capable of binding F-actin (Bresnick et al, 1990; Bresnick et al, 1991). It is thought that this region (66% identity to residues 107 to 133 of chick smooth muscle α-actinin) is also involved in the binding of α-actinin to F-actin, though this remains to be demonstrated. The central region of α-actinin contains four repeats of about 122 amino acids. The repeats are homologous to the approximately 106 and 110 residue repeats found in spectrin and dystrophin respectively (Speicher and Marchesi, 1984; Koenig et al, 1988). Consistent with circular dichroism data (Imamura et al, 1988), secondary structure predictions for the repeats suggest that it is composed of four α-helices (Davison et al, 1989). The repeats are thought to be responsible for the dimerisation of α-actinin as a thermolysin generated 53kDa fragment of α-actinin that contains most of the repeats (residues 266 to approximately 750) is dimeric (Mimura and Asano, 1987). The C-terminal domain contains two EF-hand calcium binding motifs. The EF-hands are predicted to be non-functional in chicken skeletal and smooth muscle isoforms whereas the first EF-hand of chicken fibroblast α-actinin is predicted to be functional (Arimura et al, 1988).

Separate single-copy genes for chicken smooth and skeletal muscle α-actinins have been demonstrated by genomic Southern analysis (Baron et al, 1987a; Arimura et al, 1988). The smooth and non-muscle α-actinin isoforms arise due to alternative splicing of the

"smooth muscle" gene (Waites et al, 1992). Interestingly, the smooth and non-muscle isoforms only differ slightly. The latter half of the first EF-hand is different such that the first EF-hand of the non-muscle isoform is predicted to be functional whilst that of the smooth muscle isoform is predicted to be non-functional. (Baron et al, 1987a; Baron et al, 1987b; Arimura et al, 1988). However, the difficulties in predicting whether or not an EF-hand is functional based on sequence comparisons are well recognised (Da Silva and Reinach, 1991). The non-muscle α-actinin isoform also has five more residues between the two EF-hands than the smooth muscle isoform. Since *Dictyostelium discoideum* α-actinin lacks the five amino acid sequence the significance of this region remains to be established (Noegel et al, 1987). Furthermore, the latter half of the first skeletal muscle EF-hand also appears to be alternatively spliced. However, both resulting EF-hands are predicted to be non-functional (Dr. Tim Parr, personal communication).

It is generally assumed that α-actinin interacts with vinculin. The evidence for this interaction is based on the following observations. Immunofluoresence microscopy and immunogold electron microscopy have shown that α-actinin and vinculin co-localise to adherens junctions (Geiger, 1979; Chen and Singer, 1982). A number of laboratories have demonstrated an interaction using an overlay technique. Overlays showed that radiolabelled vinculin bound to α-actinin that had been resolved on a sodium dodecyl sulphate-polyacrylamide gel (SDS-PAGE) and electroblotted onto nitrocellulose (Otto, 1983; Wilkins et al, 1983; Belkin and Koteliansky, 1987). Wachsstock et al (1987) also demonstrated an interaction between α-actinin and vinculin using equilibrium gel filtration

chromatography and fluoresence energy transfer. An approximate K_d for the interaction was calculated from Scatchard analysis of the fluorescence energy transfer data (discussed further in section 3.1).

1.26 THE IMPORTANCE OF THE INTEGRIN/CYTOSKELETAL LINK IN FOCAL CONTACT FORMATION.

The linkage between integrin and the cytoskeleton appears to be important to integrin function. A polyclonal anti-talin antibody labelled the focal contacts of well spread fibroblasts. However, the same antibody had dramatic effects on fibroblasts that were spreading, as the talin was precipitated and the cells rounded up completely. Hence talin is required in focal contact formation and integrin mediated matrix adhesion (Nuckolls and Burridge, 1990). Integrins with deletions in the cytoplasmic domain of β_1 subunit failed to localise to focal contacts (Solowska et al, 1989; Hayashi et al, 1990). Furthermore, integrins with C-terminal deletions of the β_1 subunit appeared to be unable to bind to the extracellular matrix (Hayashi et al, 1990).

1.3 A RE-EVALUATION OF THE FOCAL CONTACT MODEL.

It has become increasingly apparent that the model of the focal contact is far too simplistic. A number of the interactions within the model are of low affinity and it has been suggested that these interactions may be physiologically irrelevant (Burridge et al, 1988). However, low affinity interactions does not necessarily mean that they are physiologically unimportant. For example, The K_d of the α-actinin/F-actin interaction is only of the order of 10^{-6}M (Sato et al,

1987). Many other interactions have been described that could conceivably be involved in the actin microfilament/membrane connection. Novel focal contact proteins are still being identified. The kinetics of protein incorporation into focal contacts is unclear but suggests that some of the proteins may have a stabilising function rather than a structural role. A clearer evaluation of the spatial positions of focal contact proteins is only just becoming apparent. These various interactions and the timing of incorporation will be described below.

1.31 PROTEIN INTERACTIONS NOT DESCRIBED BY THE FOCAL CONTACT MODEL.

INTEGRIN/α-ACTININ INTERACTION.

Otey et al (1990) have shown that α-actinin will bind to a synthetic peptide of the entire cytoplasmic domain (residues 752 to 798) of β_1 integrin when the β_1 integrin peptide is linked to a Sepharose column or is adsorbed onto microtitre wells ("solid phase binding assay"). Scatchard analysis of the solid phase binding assay data revealed a K_d of 1.6×10^{-8}M for the α-actinin/β_1 integrin peptide interaction. Binding of α-actinin to avian smooth muscle integrin (a β_1 integrin) and to the β_3 integrin, $\alpha_{IIb}\beta_3$, has also been demonstrated using the solid phase binding assay. However, the interaction of α-actinin with the native avian and $\alpha_{IIb}\beta_3$ integrins was weaker than that with the β_1 peptide (2.5 and 2.1×10^{-6}M respectively). α-Actinin could also bind to $\alpha_{IIb}\beta_3$ that had been incorporated into liposomes. There were anomalies with the solid phase binding assay. The synthetic peptide of β_1 integrin also appeared to exhibit specific binding to tropomyosin. It was suggested that the peptide may be binding to certain proteins containing coiled coil structure, and this remains to

be resolved. Another protein, designated fibulin, has also been isolated by affinity chromatography with a similar synthetic β_1 integrin peptide (residues 762 to798) (Argraves et al, 1989). It is unlikely that this interaction is physiologically relevant as fibulin was subsequently shown to be an extracellular protein (Argraves et al, 1990). It would be interesting to know if fibulin contains coiled coil structure, but the secondary structure of fibulin has not as yet been determined. An interaction between fibulin and the native fibronectin receptor ($\alpha_5\beta_1$) was also demonstrated using a solid phase binding assay similar to that of Otey et al (1990). However, in contrast to Otey et al (1990), the fibronectin receptor did not bind to α-actinin when examined by Argraves et al (1989). The affinity column prepared using the β_1 integrin peptide failed to bind to talin (Otey et al, 1990). Talin had previously been shown to bind integrin in an equilibrium gel filtration assay (Horwitz et al, 1986). This apparent discrepancy may be due to the requirement of the talin/integrin interaction on the integrin being a heterodimer (Buck et al, 1986). Why the α-actinin/integrin interaction was not detected by equilibrium gel filtration (Horwitz et al, 1986) is unclear. Conceivably the α-actinin/integrin complex has a similar Stokes radius to integrin alone.

The thermolysin generated 53kDa fragment (residues 266 to approximately 750) of α-actinin inhibits the binding of ^{125}I-α-actinin to the synthetic β_1 integrin peptide adsorbed to microtitre wells (Otey et al, 1990). The 27kDa α-actinin fragment (residues 24 to approximately 269) had no effect on the α-actinin/β_1 peptide interaction. This suggests that the integrin binding site is within the spectrin-like repeats. When microinjected into REF-52 (rat embryo

fibroblast) cells, the 53kDa fragment localised to focal contacts. This is consistent with the repeats containing the integrin binding site (Pavalko and Burridge, 1991). However, a construct encoding residues 222 to 887 of smooth muscle α-actinin did not localise to focal contacts or stress fibres when expressed in COS cells (Hemmings et al, 1992). The explanation for this discrepancy has not been determined. The cytoplasmic domain of the α_v subunit of the vitronectin receptor has been shown to bind to a 100kDa protein from placental tissue (Armstrong and Molony, 1991). Whether this protein is α-actinin or an as yet unidentified protein remains to be established.

TALIN/LIPID AND TALIN/ACTIN INTERACTIONS.

It has recently been suggested that platelet talin binds to lipid bilayers (Heise et al, 1991). Integration of talin into lipid vesicles required cycles of freeze/thawing and sonicating. Whether the protein retained its native conformation was not investigated. The same group (Kaufmann et al, 1991) have also shown that platelet talin (95-98% pure) bound to actin and promoted filament nucleation. Actin (both F and G) binding and filament nucleation have also been demonstrated with chicken gizzard talin (Muguruma et al, 1990). Curiously Muguruma et al (1990) demonstrated that talin could be co-sedimented by F-actin whereas Burridge and Mangeat (1984-unpublished results) failed to show a similar interaction. It appears that the slightly different talin purification protocols used (Molony et al, 1987; Muguruma et al, 1990) may explain this difference. Indeed, the talin purified according to Muguruma et al (1990) migrated slightly slower on SDS-PAGE than that purified according to Molony et al (1987) suggesting that the

method of purification could be relevant. Alternatively the buffer used in the sedimentation assay could be responsible for the differences observed by Muguruma et al (1990) and Burridge and Mangeat (1984). The 190kDa proteolytic fragment of talin was also shown to co-sediment with F-actin (Muguruma et al, 1990).

As noted previously, the 47kDa fragment of talin localised to focal contacts despite the 190kDa fragment having binding sites for both vinculin and integrin (Nuckolls et al, 1990). Whether the 47kDa fragment of talin has a second binding site for integrin or binds to another constituent of the focal contact remains to be shown.

VINCULIN/LIPID INTERACTION.

On the basis of experiments with lipid monolayers and vesicles, various groups have suggested that vinculin interacts directly with the lipid bilayer (Ito et al, 1983; Niggli et al, 1986; Meyer, 1989). Ito et al (1983) demonstrated an interaction between vinculin and anionic phospholipid vesicles using gel filtration chromatography. When a vinculin and phospholipid mixture was applied to the gel filtration column, a large fraction of the vinculin co-eluted in the void volume along with the phospholipid rather than being retarded. Niggli et al (1986) demonstrated a vinculin/phospholipid interaction using a photoactivatable phosphatidylcholine analogue that can chemically modify membrane embedded proteins. Vinculin was labelled by the phosphatidylcholine analogue when incubated with photoactivated liposomes. No labelling occurred when the sample was not photolysed. For labelling to occur a proportion of the phospholipid had to be acidic. Meyer (1989) used a lipid monolayer maintained at constant pressure in a Langmuir trough. He showed

that vinculin in the aqueous phase could penetrate the lipid monolayer and form protein patches at the air/liquid interface. The predicted pI of the vinculin C-terminal 'tail' (residues 857 to 1066) is 9.7 and it has been proposed that it could interact with acidic phospholipids of the membrane (Coutu and Craig, 1988). Two stretches of hydrophobic amino acids have been identified in the amino terminal domain of the deduced sequence of vinculin that, if exposed, were potentially long enough to partially insert into the membrane (Coutu and Craig, 1988).

Kellie and Wigglesworth (1987) demonstrated that the vinculin isolated from chick embryo fibroblasts (CEF) was myristylated but not palmitoylated. The level of myristylation was low with approximately four percent of vinculin being labelled. This could provide a mechanism for a direct interaction between vinculin and the cell membrane, although not all myristylated proteins are associated with the membrane (Aitken et al, 1982; Pellman et al, 1985). However, vinculin lacks an N-terminal glycine which is an apparent requirement for myristylation (reviewed in Sefton and Buss, 1987). However, using a technique similar to Kellie and Wigglesworth, Burn and Burger (1987) have shown that vinculin was palmitoylated. The reason for this contradiction is unclear. Transformation by Rous Sarcoma Virus (RSV) caused a reduction of the lipid to protein ratio of approximately 3.3 fold (Burn and Burger, 1987). Whether transformation affected the incorporation of palmitate or promoted the cleavage of palmitate from vinculin was not examined.

VINCULIN/ACTIN INTERACTION.

There was (and remains) controversy concerning whether or not vinculin can interact directly with F-actin. Initial reports using vinculin purified by the method of Burridge and Feramisco (1980), and in some cases further purified by gel filtration, suggested that vinculin would bind F-actin (Isenberg et al, 1982; Wilkins and Lin, 1982). However, a contaminant was isolated from vinculin preparations whose activity could account for most, if not all, of the actin binding properties previously attributed to vinculin. The contaminant was a protein of 23 to 33 kDa, called HA1, that could be removed from vinculin by chromatography on carboxymethyl cellulose or hydroxylapatite. Vinculin treated in this manner did not bind actin (Evans et al, 1984; Schroer and Wegner, 1985; Wilkins and Lin, 1986). Higher molecular weight proteins of 150 and 200kDa, immunologically related to HA1 have been identified in smooth muscle and fibroblasts, and HA1 may represent a degradation product of the larger proteins. The 150kDa band, called tensin, was subsequently purified and shown to bind vinculin in an overlay assay (see below) (Wilkins et al, 1986; Risinger et al, 1987; Wilkins et al, 1987). Using hydroxylapatite chromatography, Ruhnau et al (1989) have isolated another contaminant of vinculin preparations. They suggest that this protein of approximately 30kDa, designated insertin, binds to vinculin and the barbed end of actin microfilaments where it can permit the addition of actin monomers.

More recently Ruhnau and Wegner (1988) demonstrated binding of fluorescently labelled F-actin to vinculin that had been electroblotted onto nitrocellulose. They also demonstrated the apparent co-sedimentation of vinculin with F-actin, but the results are of

questionable significance as their vinculin purification procedure would probably not have removed the HA1 protein. Westmeyer et al (1990) showed that vinculin adsorbed to nitrocellulose would bind fluorescently labelled F-actin and that a monoclonal antibody to a site within vinculin (residues 587 to 851) would inhibit that binding. Whether the final vinculin purification step was a gel filtration or hydroxylapatite column was unclear so that HA1 may still have been a contaminant. Curiously, this monoclonal antibody did not disrupt the cytoskeleton when microinjected into chicken fibroblasts whereas two other monoclonal antibodies (to sites within residues 131 to 220 and 349 to 357) were able to do so (Westmeyer et al, 1990; Gilmore et al, 1992).

VINCULIN/PAXILLIN INTERACTION.

The carboxy terminal domain of vinculin has been shown to bind to a 68kDa protein called paxillin. Paxillin did not bind to talin, filamin, α-actinin, or actin (Turner et al, 1990). Like talin, paxillin localises to focal contacts but not cell-cell contacts. Paxillin contains high levels of phosphoserine and phosphothreonine and was shown to be heavily phosphorylated on tyrosine after transformation by RSV (Glenney Jr and Zokas, 1989). Since it also has a low abundance in the cell, it has been suggested that paxillin may play a regulatory role rather than a structural one. During the embryonic development of chicken tissue, paxillin was shown to be one of three major phosphotyrosine containing proteins (Turner, 1991). Initially (8 day old embryos) some 20% of the paxillin was phosphorylated on tyrosine. Although the levels of paxillin remained constant the degree of phosphorylation dropped steadily and was undetectable in the adult.

These results are consistent with the proposed regulatory role of paxillin. However, a structural role has not been discounted.

α-ACTININ/LIPID INTERACTION.

α-Actinin has been reported to interact with a number of cellular components. Some of the reported interactions have implications at sites distinct from adherens junctions. Examples of these were interactions with skeletal muscle nebulin (Nave et al, 1990) and clathrin (Merisko et al, 1988).

Meyer et al (1982) have demonstrated that α-actinin can insert into a lipid monolayer. In addition, a number of trypsin and chymotrypsin cleavage sites within α-actinin were protected by incubation of the α-actinin in liposomes. Diacylglycerol and palmitic acid were specific requirements of this interaction. Further to this, Burn et al (1985) have shown that platelet α-actinin formed large diacylglycerol/palmitic acid/F-actin complexes that could be sedimented by low speed centrifugation. This was interesting as activated platelets rapidly produce diacylglycerol.

α-ACTININ/ZYXIN INTERACTION.

Recently zyxin, a phosphoprotein that localises to adherens junctions (Beckerle, 1986; Crawford and Beckerle, 1991) has been shown to bind to the N-terminal domain of α-actinin (Crawford et al, 1992). The interaction was shown to be of relatively low affinity (K_d approximately 1μM) using a solid phase binding assay. As well as localising to adherens junctions, immunofluoresence has also demonstrated that zyxin extends along the stress fibres near their

site of attachment to the focal contact (Crawford and Beckerle, 1991). However, the function of zyxin is as yet unclear.

OTHER PROTEINS OF THE FOCAL CONTACT.

Various other proteins (other than those with a presumed regulatory role such as calpain and type 3 protein kinase C) have been identified in the focal contact. Filamin is a high molecular weight (2x250kDa) dimeric actin cross linking protein of the peripheral cytoplasm (Wang et al, 1975; Langanger et al, 1984). Indirect immunofluoresence shows an almost continuous staining of the actin microfilament bundles and marked, though punctate, staining of the cortical network. The cortical network is the anisotropic array of F-actin fibres found in the cortical region of the cell (Langanger et al, 1984). Interestingly an isoform of filamin (Mab 6E) has been identified that is enriched at the end of microfilament bundles and in focal contacts (Pavalko et al, 1989). What determines the localisation of the Mab 6E isoform of filamin is unknown. Fimbrin also localises to the focal contact (Bretscher and Weber, 1980). Fimbrin is a 68kDa monomeric protein that bundles F-actin microfilaments (Bretscher, 1981; Matsudaira et al, 1983). Sequence analysis has shown that the 58kDa C-terminal domain of fimbrin contains two regions (denoted AB and A'B') that are homologous (18 and 21% sequence similarity respectively) to the actin binding domain of α-actinin (De Arruda et al, 1990). Interestingly, further sequence analysis of AB and A'B' indicates that B arose from gene duplication of A and that A'B' subsequently arose from gene duplication of AB (De Arruda et al, 1990). The 10kDa N-terminal head domain contains two EF-hands. However, F-actin bundling does not appear to be affected by physiological levels of calcium (Bretscher, 1981), although this may

be modulated by phosphorylation (De Arruda et al, 1990). An F-actin cross linking protein termed MARCKS (myristolated alanine-rich C kinase substrate) has also been identified in the focal contacts of macrophages (Stumpo et al, 1989; Rosen et al, 1990; Seykora et al, 1991). Interestingly the molecular weight of MARCKS determined from the cDNA sequence was 30 to 32kDa, whereas that determined by SDS-PAGE was 80 to 87kDa. Phosphorylation of MARCKS by protein kinase C inhibits the F-actin cross linking (Hartwig et al, 1992). Cross linking of F-actin by MARCKS is also regulated by calcium/calmodulin complexes. Calcium/calmodulin complexes will bind to non-phosphorylated MARCKS and inhibit F-actin cross linking (Hartwig et al, 1992). However, the role of MARCKS in focal contacts remains to be elucidated.

Other proteins that have been identified in focal contacts include a protein called FC1 (Oesch and Birchmeier, 1982), 200kDa protein (Maher and Singer, 1983), 25kDa IAP (Inhibitor of actin polymerisation) (Miron et al, 1991), and 80/75 kDa protein (54kDa protein in other cell types) (Senecal et al, 1987). However, little further research has been undertaken on these proteins.

1.32 TIMING OF INCORPORATION OF PROTEINS INTO THE FOCAL CONTACT.

Studies of the formation of the focal contact suggested that vinculin was initially absent (DePasquale and Izzard, 1987; Izzard, 1988). A focal contact precursor was observed to develop rapidly (approximately 1 second) below an advancing actin microfilament bundle. Vinculin immunostaining on newly formed contacts (up to about 30 seconds) was virtually absent. Contacts of 30 to 60 seconds

stained weakly, whilst after 90 seconds strong staining typical for vinculin was observed. Since actin was present in the nascent contact it seemed unlikely that vinculin was necessary for the initial linkage. Talin had accumulated to significant levels in the new focal contact before vinculin was detectable (DePasquale and Izzard, 1991). The timing of α-actinin or integrin incorporation was not investigated. Mueller et al (1989) have shown that the focal contacts of fibroblasts spreading on fibronectin coated beads contained integrin, talin, α-actinin, and actin. However, two points distinguish the results of DePasquale and Izzard (1987) to those of Mueller et al (1989). The data of Mueller et al (1989) indicates that vinculin did not localise to focal contacts during the 30 minute period examined. In contrast, the data of DePasquale and Izzard (1987) shows that vinculin is rapidly incorporated into the focal contact, although it is not present in the nascent focal contact. The results of Mueller et al (1989) show that integrin aggregation precedes the attachment of actin, whereas the data of DePasquale and Izzard (1987) suggests the converse. Whether this discrepancy reflects the initial attachment state of the fibroblast is unclear. The fibroblasts examined by DePasquale and Izzard (1987) were motile whilst those examined by Mueller et al (1989) were initially not attached to the substrate.

A similar situation was found in the dense plaques of chicken smooth muscle using immunofluoresence and immunoelectron microscopy. Dense plaques are thought to be analagous to focal contacts, but their formation is slower and therefore easier to follow. During embryonic growth, talin was shown to be incorporated into dense plaques at a similar time to the association of the dense plaques with

the microfilament bundles. Vinculin was not incorporated until 1-3 days post-hatching (Volberg et al, 1986).

The formation of focal contacts and stress fibres can be induced in stationary F9 embryonal carcinoma cells by adding retinoic acid to the culture. The formation of stress fibres was preceded by the formation of vinculin containing plaques (Lehtonen et al, 1983). It has been suggested that vinculin may be a stabilizing component of focal contacts rather than being part of the primary link. The presence of vinculin in focal contacts associated with stress fibres but its absence from more dynamic focal contacts is consistent with this hypothesis.

1.33 SPATIAL CONSIDERATIONS.

The spatial positions of proteins within the focal contact have been technically difficult to ascertain. The major problem has been the density of protein within the focal contact making microscope images difficult to interpret. Consistent with the focal contact model, α-actinin was shown to be further from the membrane than vinculin, with actin still further removed (Geiger et al, 1980; Chen and Singer, 1982). However, in dense plaques vinculin appears to be closer to the membrane than talin (Volberg et al, 1986). Recently, apparently intact fibroblast focal contacts have been examined that have had much 'extraneous' material removed by 'wet cleaving' (Feltkamp et al, 1991). The remaining electron dense plaque consists of bands parallel to the focal contact with occasional cross ribs between the bands. Immunogold electron microscopy has shown that the bands and the cross ribs contain both talin and vinculin. The vinculin and

talin (or at least an accessible epitope on talin) are equi-distant from the membrane (Feltkamp et al, 1991).

1.34 SUMMARY.

Despite evidence for other chains of interaction between the actin microfilaments and the membrane, these are potentially additional rather than alternative linkages. Variations on the structure may reflect the maturity or structural requirements of the focal contact. In *Dictyostelium discoideum* at least, it has become apparent that the actin microfilament system has a large degree of redundancy (Redundancy is the phenomena where a chain of events has parallel pathways). Mutants have been isolated that individually and almost entirely lack a motor molecule (myosin-II) (DeLozanne and Spudich, 1987; Knecht and Loomis, 1987), a major actin-filament severing protein (severin) (Andre et al, 1989), and an actin cross-linking protein (α-actinin) (Walraff et al, 1986; Schleicher et al, 1988). By many criteria the α-actinin and severin mutants were unaffected. The myosin mutant was more severely affected, but was still motile. Whether the actin cytoskeleton of higher eucaryotic cells share similar levels of redundancy to that seen in *Dictyostelium* has not been shown. However, a degree of redundancy as effective as that demonstrated by *Dictyostelium* seems unlikely. For example, deficiencies of, or deletions within, the cytoskeletal protein dystrophin resulted in either Becker or Duchenne muscular dystrophy (Monaco, 1989). The embryos of a nematode mutant that lacks vinculin demonstrated very little movement during embryogenesis and died soon after hatching (Barstead and Waterston, 1991). Two forms of hereditary haemolytic anaemia

(pyropoikilocytosis and elliptocytosis) are due to abnormalities of spectrin oligomerisation (Marchesi, 1985).

1.4 REGULATION OF THE INTERACTIONS WITHIN CELL-MATRIX ADHERENS JUNCTIONS.

Very little is known about the regulation of focal contact formation and disassembly. Various mechanisms have been proposed that may be involved in the regulation of the focal contact.

1.41 PHOSPHORYLATION.

THE EFFECT OF TYROSINE KINASES.

Transformation of fibroblasts by RSV has been shown to disrupt focal contacts and cause the breakdown of microfilament bundles (David-Pfeuty and Singer, 1980; Brands et al, 1990). Research into the mechanisms and effects of transformation are fundamentally important for two reasons. Modulation of cell adhesion is thought to be involved in metastasis. In addition, since many oncogenes have normal cellular homologues, the modifications that result from viral transformation may be similar to those in the normal cell regulation of focal contacts and microfilament bundles (Maher and Pasquale, 1988).

The transforming agent of RSV is a 60kDa tyrosine kinase termed $pp60^{v\text{-}src}$ (Sefton et al, 1980). Using immunofluoresence microscopy, its presence has been demonstrated in residual focal contacts following transformation (Rohrschneider, 1980). Indeed, the association of $pp60^{v\text{-}src}$ with the cytoskeleton close to the cell membrane is required for RSV transformation (Hamaguchi and

Hanafusa, 1987). A number of the effects of $pp60^{v\text{-}src}$ have variously been attributed to phosphorylation of vinculin (Sefton et al, 1981), talin (Pasquale et al, 1986), integrin (Hirst et al, 1986), and more recently to paxillin (Glenney Jr and Zokas, 1989). Phosphorylation of α-actinin has not been observed (Sefton et al, 1981).

Vinculin from RSV transformed cells was shown to contain eight fold more phosphotyrosine than vinculin from untransformed cells (Sefton et al, 1981). However, tyrosine phosphorylation of vinculin alone is not enough to perturb cell morphology. The temperature sensitive mutant of RSV, *ts LA32*, localises to the focal contacts of CEF grown at either the restrictive or permissive temperatures. The cell morphology of *ts LA32* transformed CEF is normal unless the cells are grown at the permissive temperature. However, the mutant tyrosine kinase encoded by *ts LA32* is active and produces similar levels of vinculin phosphorylation at both restrictive and permissive growth temperatures. The level of vinculin phosphorylation was similar to that due to transformation of CEF by wild type RSV (Kellie et al, 1986). Interestingly CEF transformed with an RSV strain that expresses a non-myristilated $pp60^{v\text{-}src}$ do not acquire the transformed morphology. The non-myristylated $pp60^{v\text{-}src}$ does not localise to focal contacts but generates similar levels of tyrosine phosphorylation on vinculin as the wild type $pp60^{v\text{-}src}$ (Kamps et al, 1986). More recently Igarashi et al (1990) have shown that vinculin isolated from foetal rat neuronal growth cones can be phosphorylated on tyrosine by an endogenous tyrosine kinase. Adult synaptosomes exhibited much lower levels of phosphotyrosine. Whether the higher levels of $pp60^{c\text{-}src}$ in embryonic neurons is responsible for the tyrosine phosphorylation was not demonstrated.

The proportion of vinculin and talin that is phosphorylated on tyrosine in response to RSV transformation is approximately 1 and 3% respectively (Pasquale et al, 1986). It has been suggested only the vinculin and talin confined to the focal contact is phosphorylated significantly resulting in low overall levels of phosphorylation. Alternatively there may be a rapid turnover of phosphotyrosine (Pasquale et al, 1986). However the phosphorylation could simply reflect promiscuous activity of the $pp60^{v\text{-}src}$ tyrosine kinase (Burridge et al, 1988). A more likely candidate for mediating the effects of RSV transformation on focal contact stability is paxillin. Following RSV transformation, 20 to 30% of paxillin, which is in low abundance compared to vinculin and talin, is phosphorylated on tyrosine (Turner et al, 1990). Furthermore, paxillin is a major phosphotyrosine containing protein during embryogenesis. The tyrosine kinase responsible has not been identified (Turner, 1991).

The effects on integrin due to cellular transformation by RSV are complex. On fibroblasts and rat kidney cells the level of $\alpha_3\beta_1$ remains unchanged, that of $\alpha_5\beta_1$ is markedly reduced, whilst $\alpha_A\beta_1$ and $\alpha_B\beta_1$ are lost (Plantefaber and Hynes, 1989). The effect on ligand binding due to tyrosine phosphorylation of integrin appears to differ depending on the type of integrin affected. The β_1 subunit from CEF and rat kidney cells was phosphorylated on tyrosine in response to RSV transformation (Hirst et al, 1986). Using a gel equilibrium technique it was demonstrated that phosphorylated integrin no longer bound to fibronectin or talin. Integrin from transformed cells had an alternative pattern of glycosylation. The altered glycosylation was not responsible for inhibiting the binding of integrin to fibronectin or talin. Integrin from transformed CEF that had been

phosphorylated and dephosphorylated bound fibronectin and talin (Tapley et al, 1989). Interestingly, the $\alpha_{IIB}\beta_3$ integrin of platelets is phosphorylated by the cellular homologue of $pp60^{v\text{-}src}$, probably on a conserved tyrosine residue. The role of phosphorylation of β_3 integrins is unclear. The $\alpha_{IIB}\beta_3$ integrin is expressed but it does not bind to the extracellular matrix unless the platelets have been activated. However, no direct correlation between platelet activation, $pp60^{c\text{-}src}$, phosphorylation of integrin, and matrix binding have been demonstrated (Elmore et al, 1990).

TUMOUR PROMOTERS.

Tumour promoters can produce dramatic and rapid effects on the actin cytoskeleton. The action of phorbol esters is thought to act by stimulating the calcium-activated phospholipid dependent kinase termed protein kinase C (Nishizuka, 1984). Type 3 protein kinase C has been shown to be concentrated in the focal contacts of REF-52 cells (Jaken et al, 1989).

Vinculin has been shown to be a substrate for protein kinase C *in vitro*. Tryptic peptide analysis of vinculin phosphorylated by protein kinase C *in vitro* revealed two labelled peptides containing phosphoserine and phosphothreonine respectively (Werth et al, 1983). Similar phosphorylation of vinculin was achieved *in vivo* using phorbol 12-myristate 13-acetate (PMA). However, though PMA produced dramatic morphological changes in Swiss 3T3 cells, chick embryo fibroblasts were unaffected despite having similar levels of vinculin phosphorylation (Werth and Pastan, 1984). Both α-actinin and vinculin are depleted from the focal contacts of BSC-1 (an epithelial cell line) cells in response to the phorbol ester 12-O-tetra-

decanoylphorbol-13-acetate (TPA). α-Actinin also dissociated from the stress fibres as they fragmented (Meigs and Wang, 1986). However, what mediates the dissociation is unclear. The vinculin of BSC-1 cells was not phosphorylated in response to TPA treatment (Turner et al, 1989).

Talin is phosphorylated following treatment of BSC-1 cells with TPA. In contrast to phosphorylation by protein kinase C *in vitro* where threonine residues were labelled (Litchfield and Ball, 1986), the talin was labelled on serine residues in BSC-1 cells treated with TPA. Phosphorylation increased approximately four fold from 0.06 mol of phosphate/mol of talin. The phosphate was distributed between a number of separate talin residues (Turner et al, 1989). Interestingly, the focal contacts and degree of talin phosphorylation was unaffected when REF-52 cells were treated with TPA. The focal contacts and microfilaments of REF-52 cells were disrupted by agents that act via cAMP-dependent protein kinase, though with no concomitant increase in phosphorylation of talin. BSC-1 cells were unaffected by this treatment (Turner et al, 1989). These results suggest that more than one control mechanism exists and that these could be cell-type specific. Although talin phosphorylation by tumour promoters can be correlated to morphological changes, the physiological relevance is unclear. Less than 0.2% of talin was phosphorylated in BSC-1 cells in response to TPA treatment. It has been suggested that this may be due to talin within a specific compartment being modified or due to the action of phosphatases acting on talin that has dissociated from the focal contact (Turner et al, 1989). However, purified talin was phosphorylated to a similar degree by purified protein kinase C *in vitro* as by the the action of

TPA *in vivo*, suggesting that compartmentalisation of talin or the action of phosphatases is not responsible for the low degree of phosphorylation observed *in vivo* (Litchfield and Ball, 1986). Conceivably another focal contact protein is responsible for the effects of tumour promoters, with the talin/vinculin labelling being physiologically irrelevant. Paxillin was phosphorylated to a greater degree than talin by RSV transformation. Whether paxillin is phosphorylated to a significantly higher level than talin when epithelial cells are treated by tumour promoters has not been examined.

More recently it has been shown that phorbol esters and protein kinase C can promote focal contact formation in fibroblasts. Woods and Couchman (1992) demonstrated that the formation of focal contacts in rat embryo fibroblasts was inhibited by protein kinase C inhibitors. Phorbol 12-myristyl 13-acetate (PMA) promoted focal contact formation. Presumably an effect of TPA on REF-52 cells was not observed by Turner et al (1989) as the focal contacts were already formed prior to TPA treatment. Hence it appears that the effect of phorbol esters may be tissue specific. It has been suggested that the focal contacts of epithelial cells are disrupted by phorbol esters whereas focal contact formation is promoted in fibroblasts (Turner et al, 1989; Woods and Couchman, 1992).

Generally tissues express β_1 integrins that constitutively bind their ligands. However, there are examples of β_1 integrins being regulated. T-lymphocytes express a number of β_1 integrins. The binding of resting T-cells to substrates (such as fibronectin and laminin) was negligable. T-cells activated with TPA (or using a monoclonal

antibody to the CD3 receptor) showed dramatically increased ligand binding without increased integrin expression, implying that the activity of the integrin itself has been regulated. The mechanism of regulation was not examined (Shimizu et al, 1990). Similarly macrophages require activation by PMA or interferon-gamma for the laminin ($\alpha_6\beta_1$) receptor to be active. The α_6 subunit was phosphorylated following activation. Interestingly, the activated receptor would only bind to the cytoskeleton if it was bound to laminin (Shaw et al, 1990). Activation of lymphocytes also regulates the binding between integrin and talin. Burn et al (1988) demonstrated that the antibody-induced capping of β_1 integrin alone was insufficient for focal contact formation. However, talin (but not α-actinin or vinculin) co-localised with integrin if the lymphocytes were treated with phorbol ester prior to the antibody capping. The effect of phorbol ester alone was not examined.

HORMONES AND GROWTH FACTORS.

Agents that increase intracellular cAMP levels can generate diverse changes in morphology depending on cell type. In response to elevated cAMP levels, Chinese hamster ovary cells and many virally transformed cells will adhere to the matrix more strongly and develop focal contacts and stress fibres (Pastan and Willingham, 1978; Leader et al, 1983). However, Balb/c-3T3 cells treated with cholera toxin lose their stress fibres and vinculin dissociates from the focal contacts (Herman and Pledger, 1985). It is thought that these effects are mediated by the cAMP dependent protein kinase. Microinjection of the catalytic subunit of the cAMP dependent protein kinase initially caused the disruption of stress fibres followed by loss of the focal contacts (Burridge et al, 1988; Lamb et al, 1988).

How the focal contact and stress fibres are actually affected though is unclear. Neither vinculin (Werth et al, 1983) or talin (Litchfield and Ball, 1986) were significantly phosphorylated by cAMP dependent protein kinase *in vitro*. Platelet-derived growth factor (PDGF) induces a similar response to phorbol esters in Balb/c-3T3 cells. The effect appears to be mediated via phospholipase C activation and elevated calcium levels, with the subsequent activation of protein kinase C, as calcium chelators inhibit the effect. In contrast to phorbol esters, the disruption of focal contacts by platelet-derived growth factor disruption is reversible but requires the synthesis of new protein (Herman et al, 1986).

1.42 SPECIFIC PROTEOLYSIS.

A number of focal contact proteins have been reported to be degraded by calpain (calcium activated neutral protease). The presence of calpain II at focal contacts of epithelial (BSC-1) and fibroblast (MDBK) cells has been demonstrated using immunofluoresence microscopy. Calpain II was absent from cell to cell contacts (Beckerle et al, 1987). BSC-1 cells contained three to five fold less calpain I than calpain II. Calpain I appears to have a diffuse distribution and did not localise to adherens junctions (Beckerle et al, 1987).

A possible role of calpain proteolysis during platelet activation is easier to envisage than in other cell types. Calcium levels are elevated during the dramatic and irrevesible activation of platelets (Detwiler et al, 1978). Talin forms greater than 3% of the the platelet protein and is a likely substrate for calpain. Both platelet talin (P235) and smooth muscle talin are cleaved *in vitro* by calpain II, yielding

fragments of approximately 200kDa and 47kDa (O'Halloran et al, 1985; Beckerle et al, 1987). Since talin derived from activated platelets displays an identical peptide map to that obtained by calpain proteolysis *in vitro* , it is believed that the cleavage *in vitro* reflects the situation *in vivo* (Fox et al, 1985). Platelet actin-binding protein (filamin) is also degraded by calpain II upon platelet activation yielding fragments of 190, 100, and 90kDa. The latter fragment was derived from the 100kDa fragment (Fox et al, 1985). The cleaved filamin no longer cross links actin filaments (Ezzell et al, 1988) and its inhibition of the actomyosin ATPase is abolished (Onji et al, 1987). The 100kDa filamin fragment retained its capacity to bind to the membrane glycoprotein Ib (GPIb) whereas the 190kDa fragment retained the capacity to bind F-actin (Ezzell et al, 1988; Gorlin et al, 1990). Phosphorylation of platelet actin-binding protein may regulate the proteolysis of actin-binding protein by calpain. Zhuang et al (1984) showed that purified actin-binding protein contained four mol phosphate per mol protein and that removal of this with *Escherichia coli (E. coli)* phosphatase prevented the interaction between actin-binding protein and F-actin. Phosphorylation of actin-binding protein by cAMP-dependent protein kinase protected it from digestion with calpain *in vitro* and *in situ* (Zhang et al, 1988; Chen and Stracher, 1989). These results are consistent with the extensive actin cytoskeleton of resting platelets being destabilised to allow rapid formation of a stellate morphology upon activation. A small fragment (approximately 1kDa) of platelet α-actinin is cleaved by calpain (Gache et al, 1984). Whether the fragment was derived from the N- or C-terminus was not shown. However, the physiological relevance of this proteolysis is unclear as

higher calpain concentrations and longer incubation periods than those used in talin cleavage were required.

The focal contact is a dynamic structure and is subject to disassembly and assembly. Whether calpain is involved in focal contact integrity has not been demonstrated. Smooth muscle talin was degraded by calpain *in vitro* (Beckerle et al, 1987). Interestingly, a significant proportion of the talin extracted from embryonic smooth muscle is in the form of the 190kDa proteolytic fragment. This suggests that the 190kDa fragment may be physiologically important. Negligible amounts of talin have been similarly cleaved in tissue extracted from adult muscle (O'Halloran and Burridge, 1986). α-Actinin was unaffected unless higher calpain concentrations were used (Beckerle et al, 1987). Contradictory results have been obtained as to whether calpain digests vinculin (Evans et al, 1984; Beckerle et al, 1987). Presumably if disassembly involves proteolysis of focal contact components there must be new synthesis to replace the degraded proteins. The cytoplasmic pool of some focal contact proteins could provide an important reserve.

The role of calpain in skeletal muscle is unclear. The actin microfibrils do not undergo gross reorganisation suggesting that calpain is purely involved in protein turnover (Shoeman and Traub, 1990). Calpain (I or II) treatment of myofibrils results in the release of intact α-actinin from the Z-disc (Goll et al, 1991). However, the degradation of α-actinin by an endogenous calcium activated protease has also been reported following prolonged incubation (12 to 48 hours) (Kulesza-Lipka and Jakubiec-Puka, 1985). Whether the non-skeletal isoform of α-actinin that associates with skeletal muscle

membrane structures is cleaved by calpain has not been shown. In *mdx* mouse muscle cells (an animal model for Duchenne Muscular Dystrophy) there is an elevated level of calcium which correlates to the necrosis of the muscle fibers. It had been suggested that degradation of dystrophin by calpain may be involved in membrane instability (Shoeman and Traub, 1990). However, dystrophin deficiency may be due to the low levels of dystrophin mRNA often observed in Duchenne Muscular Dystrophy patients (Chelly et al, 1990) rather than degradation of dystrophin. It is unclear how this would affect the calcium levels, though it has been shown that *mdx* mouse muscle cells have decreased osmotic stability (Menke and Jockusch, 1991).

1.5 AIMS OF THE PROJECT.

The focal contact is an important and complex structure. Many proteins have been implicated in its formation and regulation. Proposals have been suggested for the proteins involved in the chain of attachment between F-actin and the membrane. However, novel focal contact proteins are still being identified, along with alternative suggestions for the F-actin/membrane linkage. The interaction between α-actinin and vinculin is not well documented, despite previously being regarded as an integral part of the linkage. One of the aims of the study was to re-evaluate this interaction *in vitro*. Providing the α-actinin/vinculin interaction could be substantiated, attempts would be made to determine the location of the vinculin binding site in α-actinin.

As yet, very little is known about the tertiary and quaternary structure of α-actinin. Similarly little is known about the tertiary structure of proteins that α-actinin interacts with, or the sites involved in these interactions. Three dimensional structural information would be invaluable in addressing these questions. Another aim of the project was to crystallise α-actinin, the actin binding domain of α-actinin, and the repeats of α-actinin.

Over recent years it has become apparent that many cytoskeletal proteins contain homologous domains. The possibility that the actin binding domains of α-actinin and filamin were homologous had been suggested (Mimura and Asano, 1986). One of the project aims was to identify the actin binding domain of filamin and determine whether it was homologous to the actin binding domain of α-actinin. If the two domains were similar, sequence comparison could highlight regions that were structurally or functionally important.

CHAPTER TWO
MATERIALS AND METHODS

2.1 INTRODUCTION.

This chapter describes the materials and general methods used throughout the experimental work presented in this thesis. In addition, methods relevant to specific chapters are described in those chapters.

2.2 MATERIALS.

2.21 SOLUTIONS.

Aqueous solutions were made with glass distilled water from a Fisons Fi-stream water still. The distilled water was further purified by a Millipore Milli-Q water purification system. Solutions used with the FPLC system were filtered before use through 0.2μm filters (Whatman) and degassed by the application of a water pump generated vacumn.

2.22 REAGENTS.

Unless otherwise stated reagents were of analytical grade. Most reagents were obtained from Fisons or BDH. Proteolytic enzymes and protease inhibitors were supplied by Sigma.

Bacto tryptone, yeast extract, and Bacto agar were supplied by Oxoid.

Restriction enzymes were obtained from Pharmacia. 'React Buffers' were supplied by BRL (Bethesda Research Laboratories). Taq polymerase was supplied by Cambio whilst the Taq polymerase buffer was supplied by Amersham. T4 DNA ligase and its buffer were obtained from Biolabs.

2.3 INSTRUMENTATION.

2.31 pH MEASUREMENT.

pH measurements were made on a Corning 140 pH meter with a BDH Gelplas electrode. Before use the pH meter was calibrated against solutions prepared from buffer tablets (Fisons).

2.32 WEIGHT MEASUREMENT.

Weights of 0.1mg to 5g were weighed on a Ohaus Galaxy 160 analytical balance. Larger amounts were weighed on a Ohaus Galaxy 1600D balance.

2.33 CENTRIFUGATION.

Various centrifuges were used, depending on sample size, temperature, and centrifugal force.

2.34 SPECTROPHOTOMETRY.

The optical density of bacterial cultures were determined using a LKB Biochron Ultrospec 4050. Protein concentrations were determined on a Pye Unicam scanning spectrophometer.

2.35 FAST PERFORMANCE LIQUID CHROMATOGRAPHY (FPLC).

Fast Performance Liquid Chromatography was carried out with a Pharmacia system. Buffers were filtered and degassed as previously mentioned.

2.4 GENERAL METHODS.

2.41 BUFFERS.

Phosphate buffers were prepared by titrating solutions of the required concentration of the dihydrogen phosphate salt with the monohydrogen salt until the desired pH was reached.

2.42 DIALYSIS TUBING.

Visking tubing (Scientific industries international Ltd) was successively boiled for 5 minutes in 2% Na_2CO_3, 2mM EDTA, and distilled water. It was rinsed with distilled water between washes. The dialysis tubing was stored in 0.2% sodium azide at 4°C. Immediately prior to use it was rinsed with distilled water

2.43 SODIUM DODECYL SULPHATE POLYACRYLAMIDE GEL ELECTROPHORESIS (SDS-PAGE).

SDS-PAGE was carried according to the method of Laemmli (1970). Electrophoresis was performed on either a LKB 2050 'Midget' electrophoresis unit (8cm by 10cm) (termed minigels) or a BioRad 'Protean' vertical electrophoresis system (16cm by 18cm). To samples of up to 50µg was added one fifth the sample volume of 320mM tris/HCl, pH6.8, 5% SDS, 5% β-mercaptoethanol, 25% glycerol, 0.5% bromophenol blue. The samples were boiled for 3 minutes before being loaded into individual wells in the stacking gel. 16 by 18cm and 8 by 10cm gels were run at 80mA and 50mA constant current per gel respectively. Gels were run until the bromophenol blue reached the base of the gel.

Gels were stained in 10% glacial acetic acid, 10% methanol, Coomassie blue for 15-30 minutes. Background staining was removed by washing the gel in 10% glacial acetic acid, 10% methanol.

Alternatively the more sensitive silver staining method was used on 16 by 18cm gels. Following thorough destaining of the gel it was washed with water (5 minutes) and then incubated in a 10% glutaraldehyde solution at room temperature for 30 minutes. The gel was then rinsed twice with distilled water before being allowed to soak in water overnight. The gel was then incubated in 5μg/ml dithiothreitol for 30 minutes and 0.1% silver nitrate (freshly prepared) for 30 minutes. It was again rinsed with water before the developer (3% sodium carbonate, 0.019% formaldehyde) was added. Development was stopped by placing the gel in 10% acetic acid for an hour. The gel was then rinsed with water.

2.44 ELECTROBLOTTING OF PROTEIN SAMPLES FROM POLYACRYLAMIDE GELS ONTO NITROCELLULOSE MEMBRANE.

Proteins were electroblotted onto nitrocellulose (Schleicher and Schuel) using a BioRad Mini Trans Blot (8cm by 10cm) or a BioRad Trans Blot system (16cm by 18cm). The blot buffer was 400mM glycine, 25mM tris, 10% methanol. The Mini Trans Blot was run at 200mA constant current for 30 to 60 minutes. The Trans Blot was run at 80V constant voltage for approximately 2 hours.

2.45 PROTEIN ESTIMATION.

The concentrations of α-actinin, filamin, actin, and vinculin were determined spectrophotometrically on a Pye Unicam scanning spectrophotometer. The absorption coefficients used were

$E_{1\%,280nm}$=10.0 for α-actinin, $E_{1\%,280nm}$=7.0 for filamin, $E_{1\%,280nm}$=11.0 for actin, and $E_{1\%,280nm}$=4.64 for vinculin (Langer et al, 1980; Wang, 1977; Shizuta et al, 1976; Hartwig and Stossel, 1981; Evans et al, 1984). The concentration of fusion proteins was determined using the method of Bradford (1976). Bradford reagent was filtered through Whatman Number 1 paper.

2.46 WESTERN BLOTTING.

Protein samples (or proteolytic fragments of) were run on SDS-polyacrylamide gels then electroblotted onto nitrocellulose as described. Protein transfer was checked by staining the nitrocellulose with Ponceau S (0.5% w/v 3-hydroxy-4-[2-sulpho-4-(4-sulphophenylazo)-phenylazo]-2,7-napthalenedisulphonic acid in 5% w/v trichloroacetic acid). Ponceau S was immediately removed by washing with tris-buffered saline (TBS) (20mM Tris, pH7.5, 0.9% NaCl). The nitrocellulose strips were then incubated for at least 30 minutes in a 3% bovine serum albumin/Tris-buffered saline (BSA/TBS) solution to block remaining nitrocellulose binding of protein. The nitrocellulose strip was then incubated in the primary antibody (or pre-immune serum) for at least 30 minutes. The strips were then washed (3x5 minutes) in Tris-buffered saline/tween (TBS-T) (20mM Tris, pH7.5, 0.9% NaCl, 1% tween 20). The alkaline phosphatase linked secondary antibody (Sigma) was then applied for at least 30 minutes. Both primary and secondary antibodies were diluted in BSA/TBS and stored at 4°C with 0.01% sodium azide. The strips were washed as before, then incubated in 'developer' solution (100mM Tris, pH9.5, 100mM NaCl, 5mM $MgCl_2$). NBT in 70% N,N-dimethylformamide, and BCIP in 100% N,N-dimethylformamide were added to the developer to 0.33 and 0.17mg/ml respectively

immediately prior to use. The colour reaction was stopped by rinsing the nitrocellulose strips with water. The nitrocellulose strips were then air dried.

2.47 THERMOLYSIN DIGESTION.

The protein to be digested was dialysed into 0.1M ammonium bicarbonate, 5mM $CaCl_2$, pH7.6. The thermolysin (type X protease from Bacillus thermoproteolyticus rokko) was 'preactivated' 30 minutes before use, by diluting the 20mg/ml stock solution 20 fold with 1mM $CaCl_2$. Digestions were carried out at 37°C, and stopped by adding EDTA or EGTA to a final concentration of 10mM.

2.48 PROTEIN CO-SEDIMENTATION WITH F-ACTIN BY AIRFUGE ASSAY.

Actin was freshly polymerised in 2mM Tris, pH8.0, 2mM $MgCl_2$, 1mM sodium azide, by the addition of NaCl to 100mM. Samples were incubated plus/minus F-actin at room temperature for 30-60minutes. The sedimentation buffer and protein concentrations used were stated in the figure legends. Sedimentation was carried out in a Beckman airfuge at 100,000g for 15 min at 4°C. The supernatant was removed with a drawn out pasteur pipette. The pellet was resuspended in the same volume as the supernatant. Equal volumes of the resuspended pellets and supernatants were analysed on SDS-polyacrylamide gels.

2.5 PREPARATION OF α-ACTININ, VINCULIN, AND ACTIN.

2.51 α-ACTININ PURIFICATION.

α-Actinin was purified from chicken gizzard according to the method of Feramisco and Burridge, (1980) with modifications. Approximately 50g of frozen chicken gizzard were cut into small pieces whilst thawing, then homogenised in approximately 700ml of 2mM EGTA, pH7.4, at 4°C. The homogenate was centrifuged and the pellet resuspended in about 700ml of buffer A (2mM Tris, pH9.0, 1mM EGTA, 0.5mM PMSF), at 37°C. The pH was maintained whilst stirring for 30 minutes. The solution was centrifuged and the supernatant retained. The pH was then lowered to 7.0-7.2 with acetic acid and $MgCl_2$ was added to a final concentration of 10mM. The solution was stirred for a further 15 minutes at room temperature before being centrifuged. The subsequent steps were carried out at 4°C. 20g of solid ammonium sulphate were added to each 100ml of supernatant. After centrifugation, the pellet was resuspended in buffer T (10mM Tris/acetate, pH7.6, 10mM NaCl, 0.1mM EDTA, 0.1% β-mercaptoethanol) and dialysed against the same buffer. Buffer T was used in all subsequent steps.

Particulate matter was removed from the sample by centrifugation before application to the DEAE-Sepharose Fast-Flow column (2.6x9cm, equilibrated with buffer T). The column was washed with approximately 100ml of buffer T. The gradient applied to the column was buffer T to buffer T plus 400mM NaCl (250ml). A flow rate of 2ml/min was used and 4ml fractions were collected. The fractions containing α-actinin were pooled and concentrated (by addition of an

purification and concentration was carried out on a MonoQ 5/5 column. A 30ml gradient of buffer T to buffer T plus 200mM NaCl, and a flow rate of 0.5ml/min were used. Vinculin fractions were dialysed into buffer B and stored in that buffer at 4°C for several weeks before noticeable proteolysis.

2.53 ACTIN PREPARATION.

Approximately 4g of rabbit muscle acetone powder (supplied by R. Ankrett, University of Leicester) were incubated on ice for 1 hour in 80ml of 0.5mM ATP, 0.5mM DTT, 0.2mM $CaCl_2$, 10mM Tris, pH8.5. This was filtered through a fine nylon net. The cloudy filtrate was centrifuged (40,000rpm, Sorvall 50.38 rotor) for 1 hour. The cloudy supernatant was filtered, and the solution adjusted to 50mM KCl, 1mM $MgCl_2$, 10mM sodium phosphate, pH 7.0. The mixture was allowed to stand for 1 hour at room temperature. KCl was added to a final concentration of 0.85M, and this solution was allowed to stand overnight. Following centrifugation at 40,000rpm for 2.5 hours, the actin pellet was resuspended in 100μM DTT, 100μM ATP, 2mM Tris, pH8.0. This was dialysed overnight against the same buffer with one change. A marble was placed inside the dialysis tubing to aid resuspension of the pellet. The dialysis buffer was then changed to 2mM Tris (pH8.0) for 4 hours. The dialysate was centrifuged to yield a clear supernatant. The concentration of the sample was determined spectrophotometrically. The G-actin was stored with 1mM sodium azide, 2mM $MgCl_2$, and polymerised by the addition of NaCl to 100mM.

2.6 MOLECULAR BIOLOGY TECHNIQUES.

2.61 BACTERIAL CULTURE MEDIA.

Liquid and solid media were prepared as follows:-

2xTY comprised 16g Bacto tryptone, 10g yeast extract, and 5g NaCl per litre of water. Media was sterilised by autoclaving at 15psi for 15 minutes.

Plasmid transformation plates comprised 10g Bacto tryptone, 5g yeast extract, and 10g NaCl, 1g glucose, 15g Bacto agar per litre of water. Media was sterilised by autoclaving. Ampicillin plates were made as plasmid transformation plates but with the addition of the stated amount of ampicillin immediately prior to pouring of the plates.

SOC media comprised 20g Bacto tryptone, 5g yeast extract, 0.5g NaCl, and 10ml of 250mM KCl in 1 litre of water. The pH was adjusted to 7.0. After autoclaving 20ml of 1M glucose (filter sterilised with a 0.2μm acrodisc) was added, and just prior to use a 1/200th the volume of 2M $MgCl_2$.

Minimal media comprised 6g disodium hydrogen phosphate, 3g potassium dihydrogen phosphate, 0.5g NaCl, 1g NH_4Cl, 15g Bacto agar in approximately 900ml of water. After autoclaving and cooling to 50-60°C, 1ml of 1M $MgSO_4$ (filtered sterilized), 10ml of 10mM $CaCl_2$ (filtered sterilized), 10ml 20% glucose (filtered sterilized), and 1ml of thiamine (10mg/ml) were added and the volume made to 1 litre with sterile water. The plates were then poured.

2.62 PLASMIDS AND BACTERIAL STRAINS.

α-Actinin fragments for high level protein expression were cloned into pMW172 (Way et al, 1990). These constructs were transformed into *E. coli* strain BL21(DE3) for expression (Studier and Moffat, 1986).

The vectors pGEX-1, pGEX-2T and pGEX-3X (Smith and Johnson, 1988) were used in the production of Glutathione-S-Transferase linked fusion proteins. pGEX constructs were transformed into *E. coli* strain JM101.

2.63 GENERAL DNA HANDLING PROCEDURES.

PHENOL, PHENOL/CHLOROFORM, AND CHLOROFORM EXTRACTION.

Protein was removed from DNA by vortexing the solution with an equal volume of phenol (equilibrated in 10mM Tris/HCl, pH8.0, 1mM EDTA) until an emulsion formed. The two phases were then separated by a 30 second spin in a Micro Centaur. The upper aqueous phase was retained whilst the lower phase was discarded. This procedure was then repeated successively with a phenol/chloroform (1:1) mix and chloroform. The DNA was then recovered by ethanol precipitation, as described below.

ETHANOL PRECIPITATION.

DNA was precipitated at low temperatures in the presence of monovalent cations using either ethanol or isopropanol. To the DNA solution was added a one tenth volume of 3M NaAc, pH4.8, and 2-2.5 volumes of ethanol at -20°C (or 1 volume of isopropanol). The solution was then spun in a Micro Centaur for 15 minutes. The pellet

was rinsed with 70% ethanol to remove any remaining salt and dried under a 60 Watt lamp. The pellet was resuspended in water.

ISOLATION OF PLASMID DNA.

Plasmid DNA was isolated using the alkaline lysis method of Birnboim and Dolby (1979). A 3ml overnight bacterial culture was divided into two microfuge tubes and the cells pelleted by centrifugation. Following aspiration of the supernatants, each pellet was resuspended with 100µl of GET buffer (50mM glucose, 10mM EDTA, 50mM Tris/HCl, pH8.0) and incubated on ice for 10 minutes. 200µl of freshly prepared 0.2M NaOH, 1% SDS at room temperature was then added to each tube and gently mixed. This was placed on ice for 5 minutes. To precipitate chromosomal DNA 150µl of 3M potassium acetate, pH5.2, was added and gently mixed. The glutinous pellet was removed by two centrifugations in a Micro Centaur. The supernatant was then phenol and phenol/chloroform extracted and ethanol precipitated as described above. The nucleic acid pellet was resuspended in 10-50µl of water and RNase A (10mg/ml in water and boiled for 10 minutes) added to 100µg/ml. Digestion was carried out at 37°C for 30 minutes.

Plasmid DNA was also obtained from 10ml bacterial cultures. The procedure used was as just described but using 1ml of GET buffer (plus 1-5mg of lysozyme), 2ml of NaOH/SDS, and 1.5ml of potassium acetate.

RESTRICTION ENZYME DIGESTS.

Unless otherwise stated, digests were carried out in the appropriate React Buffer (BRL) at 37°C for 1 hour. Digestion of the ends of

polymerase chain reaction (PCR) products to generate 'sticky ends' was carried out for two hours.

AGAROSE GEL ELECTROPHORESIS.

1.0-1.5% (w/v) horizontal agarose (Seakem H.G.T.) gels were prepared and run in TAE (40mM Tris/acetate, pH7.8, 1mM EDTA, 30mM sodium acetate) containing ethidium bromide (0.5µg/ml). The percentage agarose depended on the anticipated size of the DNA sample. To each sample was added one sixth the volume of sample buffer (30% glycerol, 0.25% bromophenol blue, 0.25% xylene cyanol FF). Appropriate size standards were also run. Gels were run at 60-120V constant for 30-90 minutes or overnight at 10-15V. Analytical gels were viewed on a UV transilluminator. Preparative gels were viewed under a long UV lamp so that the required bands could be excised and the DNA extracted using the 'Geneclean kit' as described below.

Small DNA fragments were purified on 0.8% (w/v) low melting point agarose (BRL) gels, as described below. Gels were prepared and run as above except that a different agarose was used and a lower voltage of 50-60V was used.

PURIFICATION OF DNA FROM AGAROSE GELS.

DNA fragments of over 0.4kb were generally purified from H.G.T. agarose using 'Geneclean' (Stratech Scientific) as per the manufacturers instructions. DNA was euted with 2 x 5-10µl of water.

Since low molecular weight DNA could not be recovered from 'glassbeads', it was purified from LMP agarose. 350µl of water was

added to the band excised from the gel. This was incubated at 65°C (5 minutes) and vortexed 3 times. The DNA was then phenol extracted twice and ethanol precipitated. The pellet was resuspended in 20µl of water.

2.64 LIGATION.

Ligations were set up as follows:-

10-20µg vector DNA,

An approximate 5 fold excess of insert,

1µl of 10x T4 DNA ligase buffer (includes 100mM ATP),

0.5µl T4 DNA ligase,

water to 10µl.

The mixture was incubated at 37°C for 1 hour or at room temperature overnight.

2.65 TRANSFORMATION.

Transformations were carried out using either the '$CaCl_2$ method' or electroporation, as described below:-

$CaCl_2$ METHOD.

The appropriate cells (*E. coli* strains JM101 or BL21(DE3)) were grown to an optical density at 600nm of 0.5. Following gentle centrifugation (MSE Chilspin, 2500rpm, 5 minutes) the cells were resuspended in one third the initial volume of ice cold $CaCl_2$ (50-100mM) and incubated on ice for 5 minutes. The cells were again centrifuged and the pellet was resuspended in one tenth the initial volume of ice cold $CaCl_2$ (50-100mM). The competent cells were kept at 0-4°C and used within 24 hours.

100µl of competent cells were transformed with 5µl of ligation mix. These were incubated together on ice for 30 minutes before 'heat shocking' the cells at 37°C for 5 minutes. The cells were placed on ice for a further 5-30 minutes. 400µl of 2xTY was added to the mix and transferred to a 30ml Sterilin tube. This was incubated with shaking at 37°C for 45 minutes before being plated out on ampicillin plates. The plates were incubated overnight at 37°C. Colonies were then assayed for the correct plasmid/insert (Maniatis et al, 1982).

ELECTROPORATION.

Bacterial cells were also transformed by the application of intense electrical fields (Dower et al, 1988). A 5ml culture (2xTY) of the appropriate cells was grown overnight from a colony picked from a fresh plate. 2mls of this was used to innoculate 100mls of pre-incubated 2xTY, and this was grown until the culture reached an optical density of 0.5. The cells were pelleted by centrifugation (MSE Chilspin, 4000rpm, 10 minutes), then resuspended in approximately 20mls of ice cold water. The pelleting and resuspension was performed 4 times to ensure that all the salt was removed. Finally the cells were resuspended in 160µl of 10% glycerol.

For the electroporation, 40µl of cells and 1µl of the ligation mix were added to the electroporation cuvette. The cell was pulsed by a waveform of 1.5kV peak voltage and total capacitance of 25µF. The electrical pulse was generated by a BioRad Gene Pulser. The cells were then immediately rinsed into a 30ml Sterilin tube with 1ml of SOC media and incubated at 37°C with shaking for 1 hour. The suspension was plated onto ampicillin plates and incubated overnight at 37°C. Colonies were then assayed for the correct plasmid/insert.

CHAPTER THREE
ANALYSIS OF THE INTERACTION BETWEEN α-ACTININ AND VINCULIN AND IDENTIFICATION OF THE VINCULIN BINDING DOMAIN IN α-ACTININ

3.1 INTRODUCTION.

An interaction between α-actinin and vinculin is widely assumed to be of key importance in the link between integrins and the actin cytoskeleton. However, the α-actinin/vinculin interaction has been characterised in far less detail than the talin/vinculin or α-actinin/actin interactions. An evaluation of the evidence for an interaction between α-actinin and vinculin is presented below.

3.11 EVIDENCE FOR AN α-ACTININ/VINCULIN INTERACTION.

The main evidence for an interaction between these two proteins is based on an overlay technique. Both Otto (1983) and Wilkins et al (1983) showed that ^{125}I-vinculin bound to purified smooth muscle α-actinin immobilised on a nitrocellulose blot. However, Otto (1983) failed to demonstrate that the binding of ^{125}I-vinculin (2nM) could be diminished by the presence of unlabelled vinculin (260nM). Wilkins et al (1983) did not examine the effect of unlabelled vinculin on the binding of ^{125}I-vinculin. It was suggested that these results were consistent with the existence of a low affinity* interaction between the two proteins. Using the same method, it has also been shown that ^{125}I-labelled α-actinin from smooth muscle binds to purified vinculin and metavinculin (Belkin and Koteliansky, 1987). The effect of unlabelled protein on the binding of iodinated ligand was not investigated.

---

* With respect to cytoskeletal proteins a K_a of $10^6 M^{-1}$ is regarded as low affinity whilst a K_a of $10^9 M^{-1}$ is regarded as being of high affinity (Burridge et al, 1988; Jones et al, 1989; Otey et al, 1990).

The possible interaction between α-actinin and vinculin has also been investigated using fluorescence energy transfer (Wachsstock et al, 1987). Vinculin was labelled with a donor fluorophore and α-actinin was labelled with an acceptor fluorophore. Mixing the two proteins resulted in a 28% quenching of fluorescence at 470nm. Since the degree of quenching is inversely proportional to the sixth power of the distance separating the fluorophores, the quenching was evidence that the two molecules were in close proximity. An eight fold excess of unlabelled α-actinin diminished the degree of quenching to 8%. Furthermore, Scatchard analysis of the degree of quenching of the labelled vinculin (donor fluorophore) by increasing concentrations of labelled α-actinin (acceptor fluorophore) indicated a K_d of 10^{-6}M. The same group also demonstrated that vinculin eluted earlier from a gel filtration column when the column was pre-equilibrated with a α-actinin solution instead of buffer alone. The shift in the elution profile of vinculin was small, but was considered consistent with there being an interaction between α-actinin and vinculin. These are the only studies where an α-actinin/vinculin interaction has been examined directly.

An interaction between α-actinin and vinculin is also supported by a variety of circumstantial evidence. Immunofluoresence has shown that α-actinin and vinculin co-localise at cell-cell and cell-substrate contacts. Vinculin staining was sharper and closer to the membrane than the α-actinin staining (Geiger, 1979). Immuno-electron microscopy studies have also shown that vinculin labelling was closer to the membrane than α-actinin labelling. This is consistent with their proposed positions in the actin-integrin linkage (Geiger, 1979; David-Pfeuty and Singer, 1980; Chen and Singer, 1982).

Stickel and Wang (1988) have shown that α-actinin and vinculin dissociated simultaneously from the focal contacts of cells treated with the synthetic peptide Gly-Arg-Gly-Asp-Ser. Focal contacts were also disrupted in cells treated with phorbol ester (Meigs and Wang, 1986). The sequence of events in the disappearance of the focal contacts differed slightly in that vinculin remained with the residual focal contact longer than the α-actinin and stress fibres. Following disruption of focal contacts by RSV induced transformation (Brands et al, 1990) or treatment with platelet-derived growth factor (Herman and Pledger, 1985), talin dissociated from the focal contact after vinculin or was unaffected. Taken together, these observations are consistent with a contiguous linkage between α-actinin, vinculin, and talin, with talin being more intimately associated with the membrane. Otey et al (1990) have shown that an affinity column of the cytoplasmic domain of β_1 integrin retained both α-actinin and vinculin from a chicken embryo fibroblast cell extract. However, when purified α-actinin and vinculin were used, only the α-actinin bound to the column. Though not examined further, this suggested that vinculin may be binding to integrin via an intermediary protein, which could be α-actinin.

3.12 APPROACHES USED TO ANALYSE THE α-ACTININ/VINCULIN INTERACTION.

Considering the limited evidence for a α-actinin/vinculin interaction, it was thought necesary to investigate the interaction further. The interaction was investigated using four different methods. Electron microscopy was used to try and directly visualise the α-actinin/vinculin complex. Although α-actinin and vinculin have

both been examined individually by electron microscopy, no attempts have been made to visualise possible α-actinin/vinculin complexes. The possible interaction between α-actinin and vinculin was also investigated by low speed equilibrium centrifugation. This method was also used to estimate a dissociation constant. The overlay technique originally used to demonstrate binding between α-actinin and vinculin was repeated. The theoretical aspects of the overlay assay were examined in an attempt to explain previous discrepancies that suggested the interaction between α-actinin and ^{125}I-vinculin was non-specific. The possibility that α-actinin/vinculin complexes could be isolated by co-sedimentation with F-actin was also investigated.

3.2 METHODS.

3.21 ELECTRON MICROSCOPY.

Vinculin, α-actinin, and α-actinin/vinculin mixtures at concentrations stated in the results were incubated at 4°C in 20mM Tris/acetate, pH7.6, 150mM NaCl, 0.1% β-mercaptoethanol, 0.1mM EDTA. Samples were mounted on copper grids that were covered by a celloidin film and carbon coated. The grid was subjected to a glow discharge immediately prior to sample application by applying a 1.5kV, 40mA supply across air at low pressure. The sample was fixed with glutaraldehyde vapour, rinsed with distilled water, and stained with a saturated uranyl acetate solution for approximately 30 seconds. Electron microscopy was carried out using a JEOL 100CX.

3.22 LOW SPEED EQUILIBRIUM CENTRIFUGATION.

Samples were centrifuged at 10,600rpm at 4°C, overnight in an MSE Centriscan 75 with absorption optics. The absorption profile across the samples was recorded. Samples were then centrifuged at 50,000rpm (1 hour) to sediment the protein. An absorption profile was again taken across the cell to provide a reference line. Using a graphics tablet the absorption profiles were entered into an Apple II microcomputer. The weight averaged molecular weight was then calculated using the program 'Sed Equil/Abs/Dig' (Dr. A Rowe, Leicester University). This programme utilises the equation:-

$$M_w = \frac{2RT}{(1-\bar{v}\rho)\omega^2} * \ln\frac{c_r}{c_a} * \frac{1}{r^2-a^2}$$

where M_w was the weight averaged molecular weight, R was the gas constant, T was the absolute temperature, $\bar{v}$ was the partial specific volume, ρ was the solvent density, and c was the solute concentration at distances from the axis of rotation of r and a.

3.23 PROTEIN IODINATION.

Vinculin was dialysed into 50mM sodium phosphate buffer, pH8.0, 1mM EDTA, 0.5mM DTT and iodinated using 500μCi of Bolton Hunter reagent (N-succinimidyl 3-(4-hydroxy, 5-[^{125}I]iodophenyl) propionate, supplied by Amersham). The reagent was supplied in benzene which was evaporated by a gentle flow of nitrogen across its surface. 1mg of protein (1mg/ml) was added and incubated on ice for 15-60 minutes. The solution was then transferred to dialysis tubing, and dialysed against at least 6x4 litres of 0.9% NaCl, 20mM Tris, pH7.7, 1mM EDTA, 0.1% β-mercaptoethanol, over 4 days. The

Binding was quantified by scanning autoradiographs using a LKB Bromma 2202 Ultroscan laser densitometer linked to an Apple II microcomputer. The program Gelscan (written by P. Heilmann, LKB) was used. The densitometer has been shown to give a linear response to autoradiograph band density, providing that the autoradiograph was not overexposed. The program's integration facility could not be used as the curves were often not symetrical. Plots were printed and the peak areas were calculated with the aid of the Apple graphics tablet and appropriate program. Generally three tracks of each sample were analysed. The area of each track was calculated three times and the mean value of the nine readings was used.

3.3 RESULTS.

3.31 THE PURIFICATION OF α-ACTININ AND VINCULIN.

α-ACTININ PURIFICATION.

α-Actinin was purified from chicken gizzards using the method of Feramisco and Burridge (1980) with the following modifications. The tissue was homogenised once in homogenisation buffer (2mM EGTA, pH7.4). The soluble cytosolic proteins were discarded following centrifugation of the homogenate. Cytoskeletal proteins were then extracted from the pellet by incubation in buffer A (2mM Tris, pH9.0, 1mM EGTA, 0.5mM PMSF) at 37°C. The supernatant after centrifugation was enriched in α-actinin, actin, desmin, filamin, myosin, talin, and vinculin. Some contaminants, including a large proportion of the actin, were then removed by precipitation with $MgCl_2$. The precipitate produced by the 34% ammonium sulphate cut was further enriched in α-actinin, filamin, and vinculin. The protein

remaining in solution was enriched in talin. The ammonium sulphate precipitate was resuspended in buffer T (10mM Tris/acetate, pH7.6, 10mM NaCl, 0.1mM EDTA, 0.1% β-mercaptoethanol) rather than buffer B (20mM Tris/acetate, pH7.6, 20mM NaCl, 0.1mM EDTA, 0.1% β-mercaptoethanol). The buffer was more important in the vinculin preparation (see below). The first chromatographic step was essentially similar to that of Feramisco and Burridge (1980), except that the DEAE-Sepharose Fast-Flow column matrix could permit a faster flow rate without any loss of resolution. The predominant α-actinin peak eluted between buffer T plus 190mM to 280mM NaCl (Figure 3.1). α-Actinin did elute outside of this region but these fractions were rejected mainly due to the presence of filamin. Most of the actin contamination in the α-actinin fractions was pelleted by high speed centrifugation (40,000rpm, 4°C, 1 hour). The supernatant was applied to a Superdex 200 Prep Grade column which provided a degree of purification similar to that obtained with the Sepharose Cl-6B column used by Feramisco and Burridge (1980), but it could be run at higher flow rates (Figure 3.2). Both the Superdex 200 Prep Grade and Sepharose 6B-CL columns removed contaminants with molecular weights of about 46, 47, 50, and 55kDa, along with many faint bands between 50 and 300kDa. Further purification was still required. A Q-Sepharose Hi-Load column was used as the final purification step (Figure 3.3). The α-actinin eluted between buffer B plus 285mM and 300mM NaCl. Occasionally a protein of 70-80kDa co-purified with the α-actinin. Western Blotting demonstrated that this fragment was a degradation product of α-actinin. A degradation product 1-2kDa smaller than α-actinin eluted at a slightly higher salt concentration and was removed by the Q-Sepharose Hi-Load column. The resolution was such that any residual filamin or actin was

FIGURE 3.1

PURIFICATION OF α-ACTININ AND VINCULIN: ELUTION PROFILE FROM THE DEAE-SEPHAROSE FAST-FLOW COLUMN.

The inserts show Coomassie stained SDS-PAGE minigels (12%) of (A) the applied sample; (B) and (C) the peak vinculin and α-actinin fractions at the positions indicated. 15µl aliquots of each was applied to the minigel. The column bed size was 2.6x9cm. A flow rate of 2ml/min was used. Buffer T with a salt gradient as indicated was used as the eluent. 4ml fractions were collected.

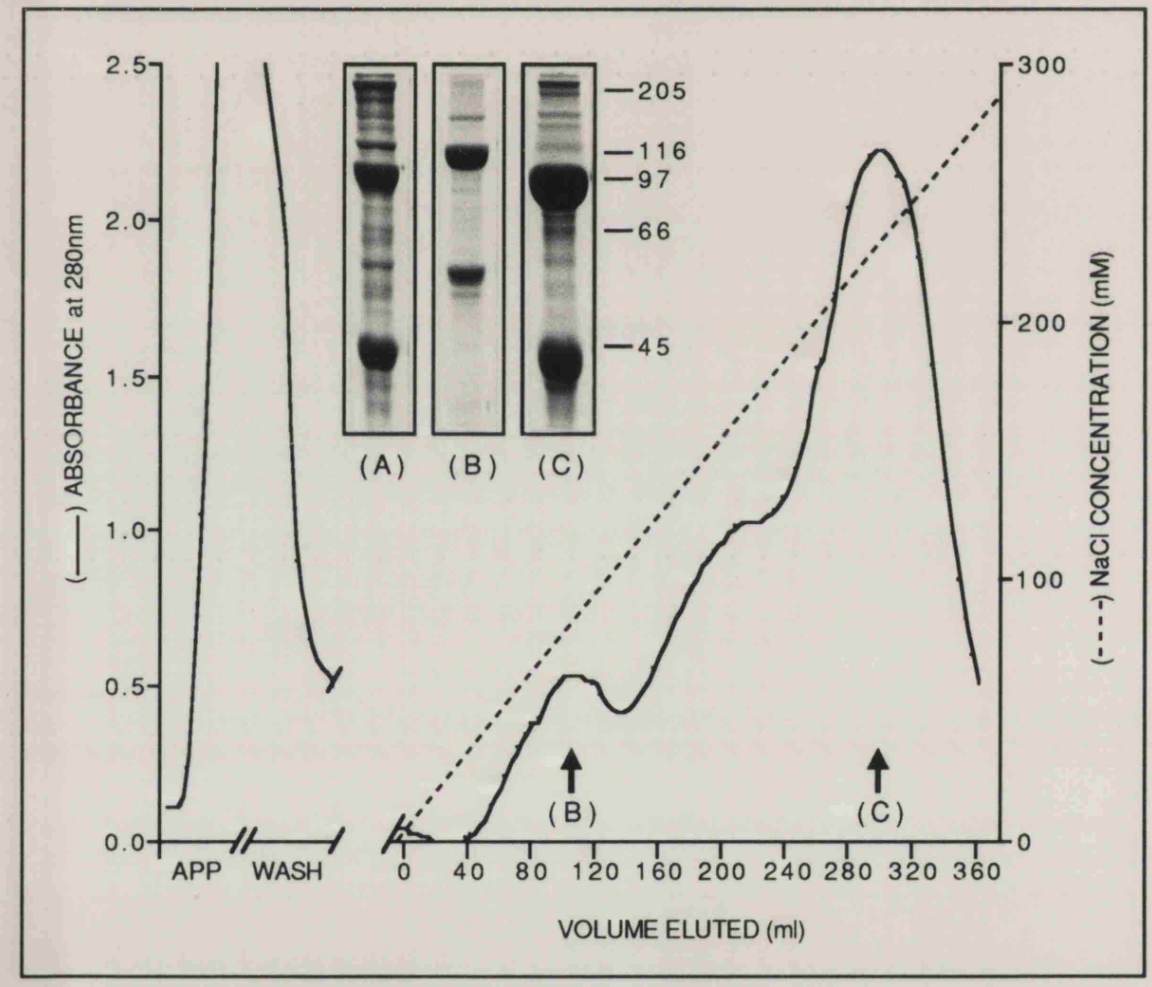

FIGURE 3.2

PURIFICATION OF α-ACTININ: ELUTION PROFILE FROM THE SEPHADEX 200 PREP-GRADE COLUMN.

The insert shows Coomassie stained SDS-PAGE minigels (10%) of (A) the applied sample and (B),(C), and (D) peak fractions as indicated. 10μl of the indicated fractions were applied for SDS-PAGE analysis. α-Actinin eluted in the peak labelled (B). The column bed size was 2.6x60cm. A flow rate of 2ml/min was used. The eluent was buffer B plus 100mM NaCl. Fractions of 3ml were collected.

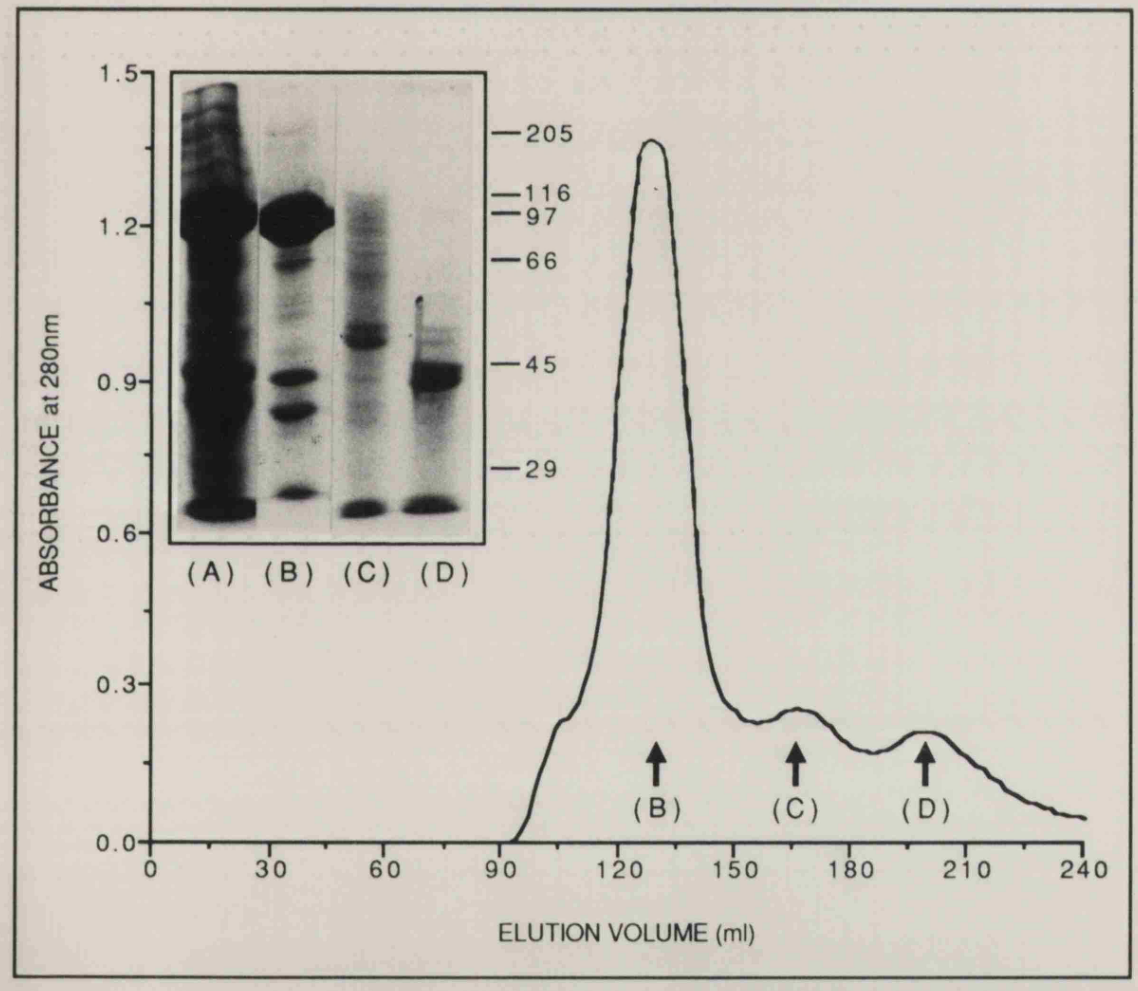

FIGURE 3.3
PURIFICATION OF α-ACTININ: ELUTION PROFILE FROM THE Q-SEPHAROSE COLUMN.

The inserts show Coomassie stained SDS-PAGE minigels (10%) of (A) the applied sample and (B) the peak fraction indicated. 15µl aliquots of the indicated samples were applied to the minigel. The column bed size was 2.6x10cm. A flow rate of 2ml/min was used. Buffer B with a salt gradient as indicated was used as the eluent. 3ml fractions were collected.

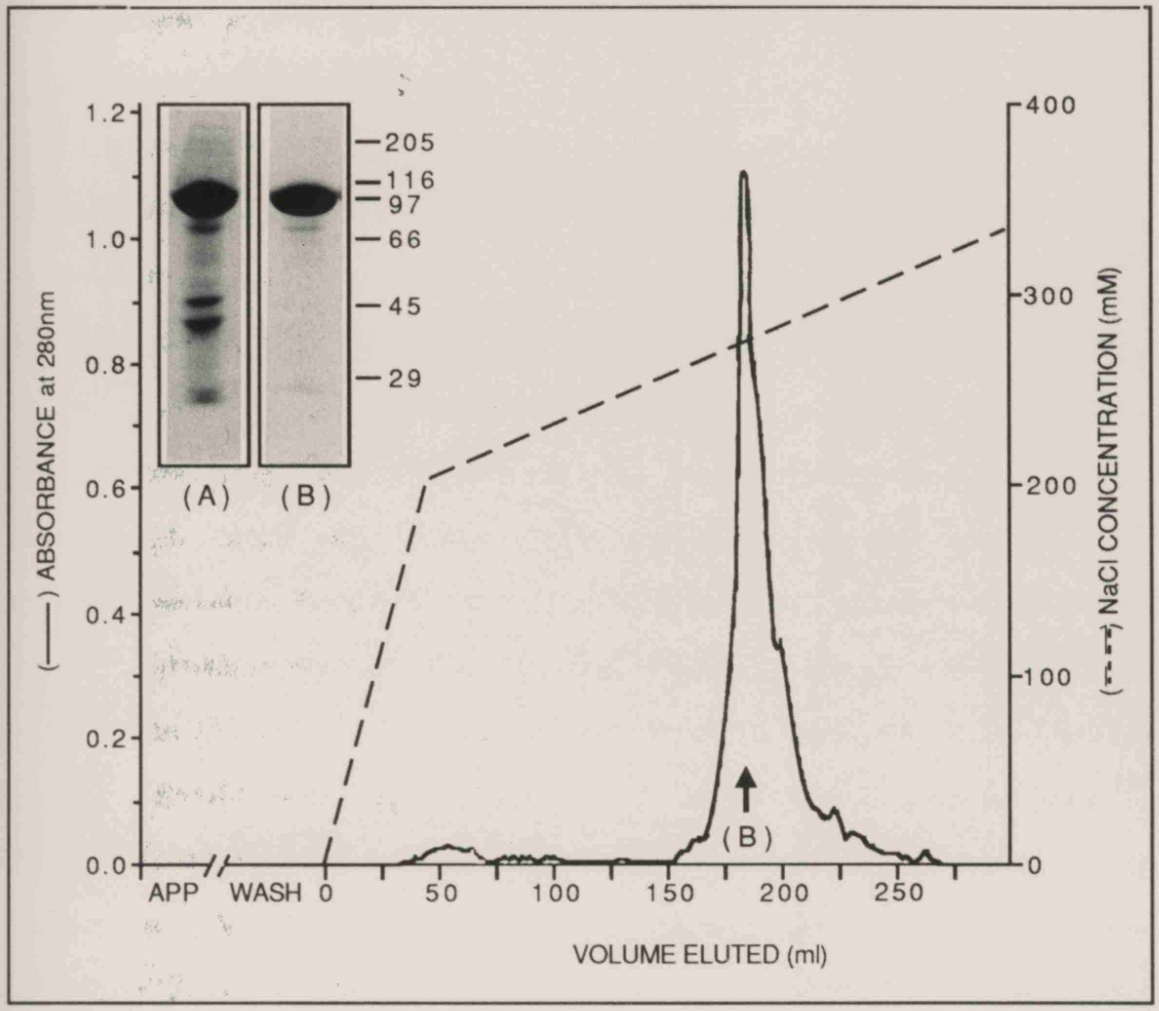

removed, negating the requirement for the phosphocellulose or hydroxylapatite column used by Feramisco and Burridge (1980). The hydroxylapatite column provided a good purification step if it initially bound the sample. However, since the binding of α-actinin to hydroxylapatite was inconsistent, the Q-Sepharose column was used in preference. Yields of 25-35mg of protein were obtained from 50g of chicken gizzard. α-Actinin was stored at 4°C in buffer B with 0.02% sodium azide, and was stable for several weeks.

VINCULIN PURIFICATION.

The initial steps were carried out as for α-actinin. Buffer T rather than buffer B was used in the first chromatographic step. If buffer B was used some vinculin failed to bind to the DEAE-Sepharose Fast-Flow column. Vinculin eluted between buffer T plus 50mM to 110mM NaCl (Figure 3.1). The vinculin at this stage was approximately 60% pure, though there was some slight contamination by proteins with molecular weights between 20 and 300kDa. More distinct bands were seen at approximately 20, 45, 60, and 70kDa. Though not specifically identified on SDS-PAGE gels, the contaminants such as HA1 (Wilkins and Lin, 1986) were presumably still present. Chromatography on CM-Sepharose Fast-Flow was reported to remove these contaminants (Schroer and Wegner, 1985). Vinculin eluted between buffer C plus 220mM to 260mM NaCl (Figure 3.4). Distinct bands of approximately 10, 20, 40, and 50kDa eluted prior to vinculin, along with many other minor bands. If necesary the vinculin was further purified on a MonoQ 5/5 column. The vinculin eluted at buffer T plus 70mM to 85mM NaCl. 2-4mg of vinculin were obtained from 50g of chicken gizzard. Vinculin was stable for several weeks in buffer B with 0.02%

FIGURE 3.4

PURIFICATION OF VINCULIN: ELUTION PROFILE FROM THE CM-SEPHAROSE FAST-FLOW COLUMN.

The insert shows a Coomassie stained SDS-PAGE minigel (10%) of (A) the applied sample and (B),(C), and (D) peak fractions as indicated. 20µl aliquots of the indicated fractions were applied to the minigel. Vinculin eluted in the peak labelled (D). The column bed size was 1.6x10cm. A flow rate of 2ml/min was used. Buffer C with a salt gradient as indicated was used as the eluent. 2ml fractions were collected.

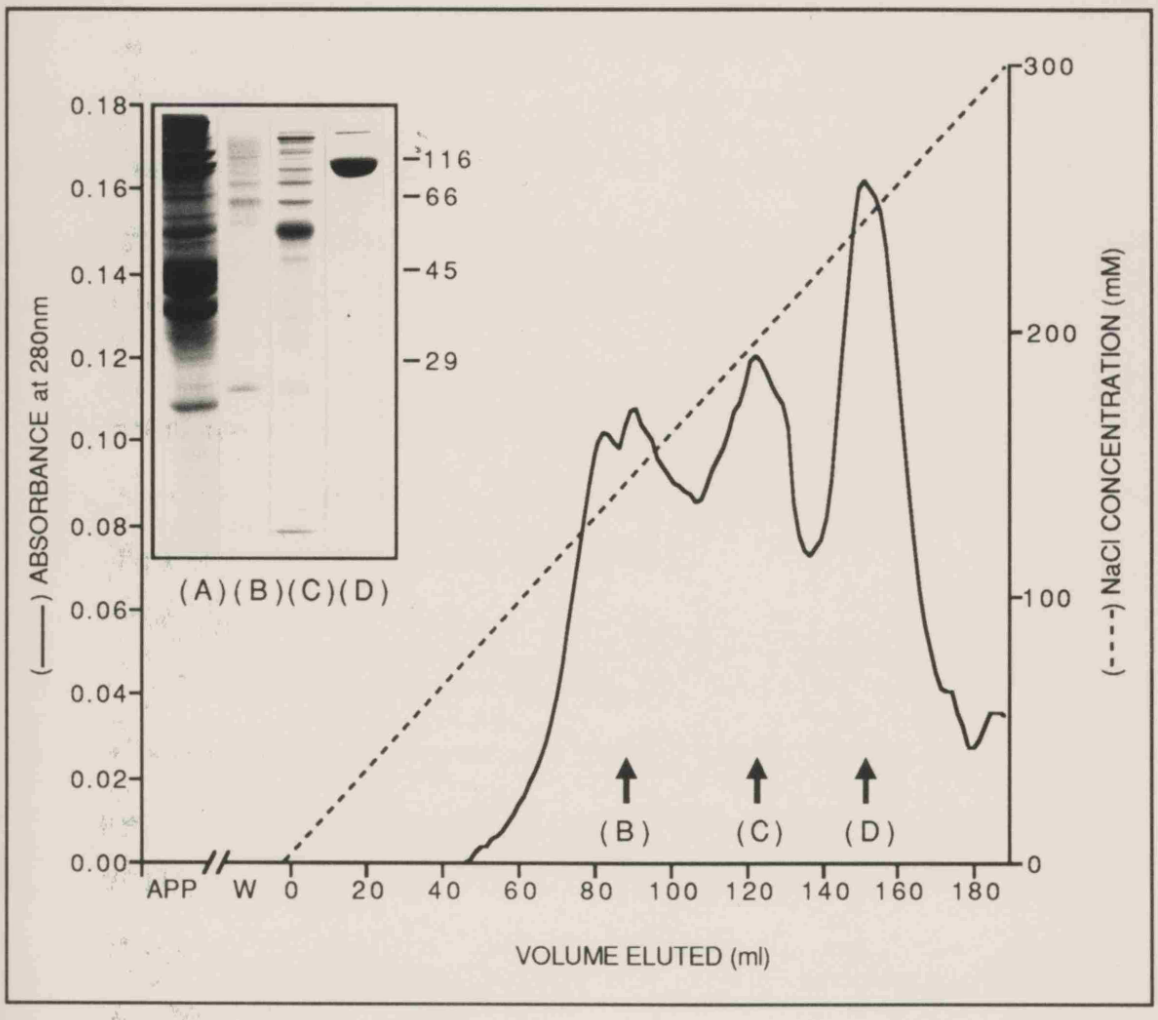

sodium azide at 4°C. Some degradation was detected during storage producing a fragment of about 100kDa.

3.32 ANALYSIS OF THE INTERACTION BETWEEN α-ACTININ AND VINCULIN USING ELECTRON MICROSCOPY.

Electron microscopy was used to investigate the interaction between α-actinin and vinculin. There are no reports in the literature of electron microscopy being used to examine the interaction of these two proteins, although electron microscopy has been used to examine binding of α-actinin to clathrin (Merisko et al, 1988). Samples of vinculin, α-actinin, and an α-actinin/vinculin mixture were prepared for electron microscopy. The proteins were negatively stained with uranyl acetate as described in section 3.21.

The electron micrographs of α-actinin alone (0.25μM) (Figure 3.5A) showed rods of 33nm (SD=3.3nm, n=23). Occasionally the rods had slightly bulbous ends (arrowed in figure).

Electron micrographs (Figure 3.5B) of vinculin alone (0.43μM) generally showed the molecule to be spherical. These were assumed to be vinculin monomers. Gel filtration and sedimentation of vinculin by Beck (1989) and Geiger (1981) have previously produced values compatible with it being a globular monomeric molecule of 116kDa (Geiger, 1981; Beck, 1989). There were occasions where the sphere had a "tail" protruding from it. The sphere had a diameter of 11.2nm (SD=1.7nm, n=21). As in a previous report (Isenberg et al, 1982), some of the spheres appeared to have a depression filled with stain (arrowed in figure).

FIGURE 3.5

ELECTRON MICROGRAPHS OF α-ACTININ AND VINCULIN.

The electron micrographs show negatively stained samples of (A) α-actinin alone and (B) vinculin alone. The slightly bulbous ends of α-actinin can be seen (arrow) in (A). Examples of vinculin molecules containing what may be a stained filled depression are arrowed in (B). The bar is 50nm.

A

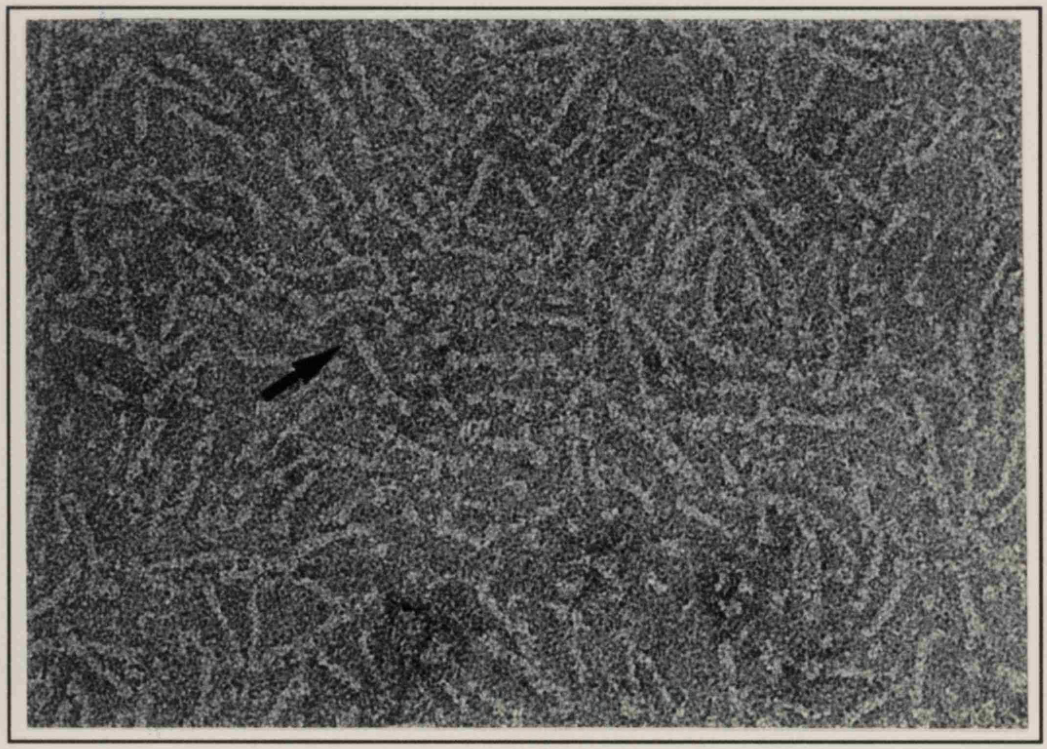

B

These results were consistent with previous reports. The globular head of vinculin has been reported as being 8-12nm in diameter (Isenberg et al, 1982; Milam, 1985; Gimona et al, 1987). The dimensions of α-actinin are generally reported to be between 30-40nm in length and 2-4nm in width (Podlbnaya et al, 1975; Suzuki et al, 1976; Bretscher et al, 1979; Bennett et al, 1984; Imamura et al, 1988), though the reported length of *Dictyostelium* α-actinin is 56nm (Walraff et al, 1986). The discrepancy may simply reflect experimental error.

Electron micrographs of a mixture of α-actinin (0.25μM) and vinculin (0.43μM) predominantly showed vinculin molecules. Two other structures were visible (Figure 3.6). These may be described as a disc attached to the end of a rod, "the lollipop" (arrowed in figure); and a rod with a disc at each end, "the dumbell" (arrowhead in figure). The discs differed distinctly from the slightly bulbous ends occasionally seen on α-actinin alone. The discs had diameters similar to those of vinculin molecules. The lengths of these structures was 41.3nm (SD=4.4nm, n=11) and 44.1nm (SD=4.8nm, n=16) respectively. The "lollipop" is consistent with an α-actinin dimer with a vinculin molecule bound at one end. The "dumbell" is consistent with an α-actinin dimer having a vinculin molecule bound at each end.

FIGURE 3.6
ELECTRON MICROGRAPHS OF A α-ACTININ/VINCULIN MIXTURE.
(A) The electron micrograph shows a negatively stained sample of a α-actinin/vinculin mixture. A "lollipop" and "dumbell" complex is indicated (arrow and arrowhead respectively. (B) shows selected examples of (i) "lollipop" and (ii) "dumbell" complexes. The bar is 50nm.

A

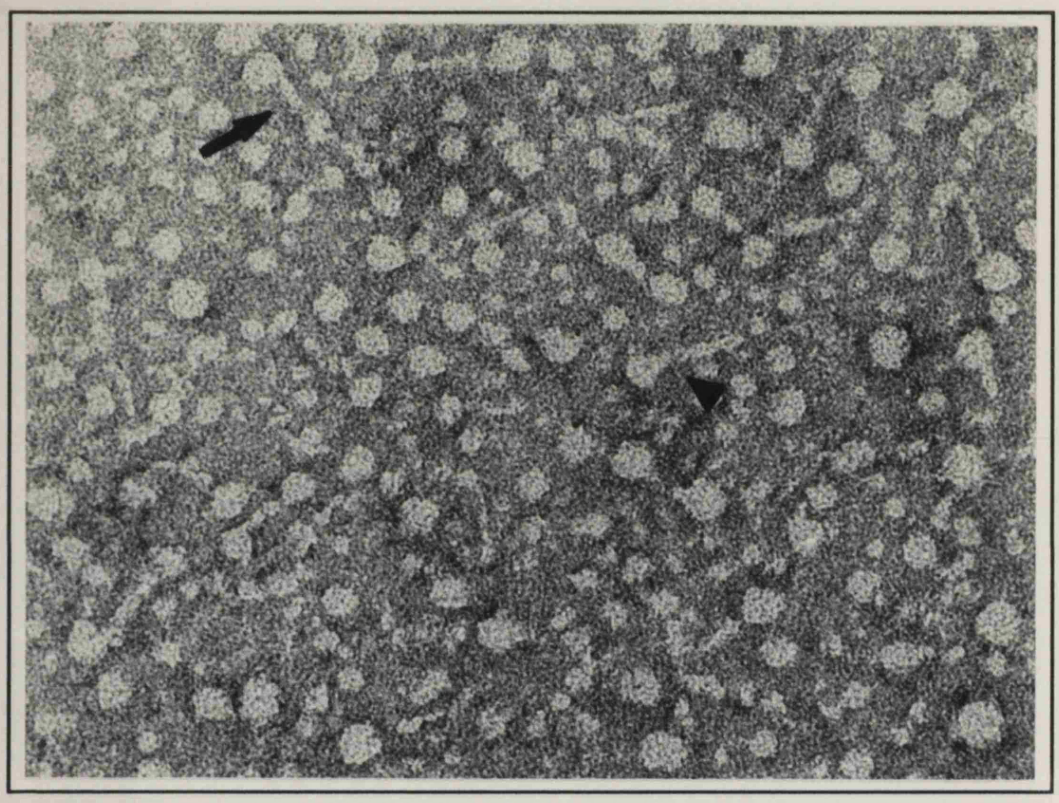

Bi

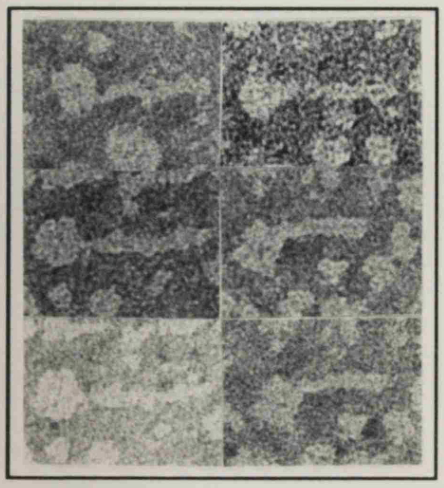

Bii

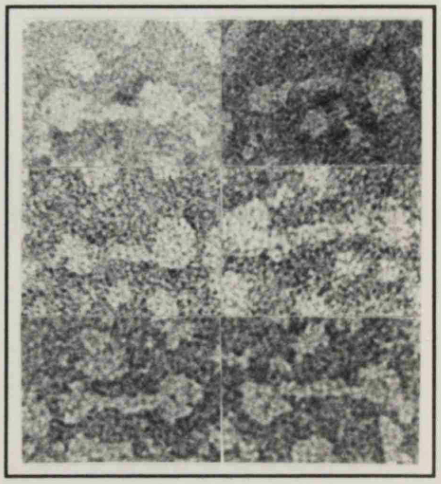

3.33 INVESTIGATION OF THE INTERACTION BETWEEN α-ACTININ AND VINCULIN USING LOW SPEED EQUILIBRIUM CENTRIFUGATION.

Low speed equilibrium (LSE) centrifugation was used to investigate the interaction of α-actinin with vinculin. LSE centrifugation yielded a weight averaged molecular weight, which could be expressed as:-

$$M_{r,w} = \Sigma n_i M^2_{r,i} / \Sigma n_i M_{r,i} = \Sigma c_i M_{r,i} / \Sigma c_i$$

where n and c respectively were the number and mass concentrations of the particle i which had a molecular weight M. Therefore, in a mixture of two proteins that interacted, there would be an increase in the weight averaged molecular weight above that expected if the two proteins did not interact. Initially a theoretical curve was derived relating K_d to the expected weight averaged molecular weight at the specified concentrations of the two proteins. This was based on the assumption that:-

$$K_d = [A2] \times [V] / [A2V]$$

where A2 was α-actinin dimer, V was vinculin monomer, and A2V was an α-actinin dimer/vinculin monomer complex. The electron microscopy data, and the fact that α-actinin is a dimer suggest that this is a simplistic view. A better model was devised where:-

$$A2 + V \leftrightarrow A2V \text{ with a } K_{d(\text{step } 1)}$$

$$A2V + V \leftrightarrow A2V2 \text{ with a } K_{d(\text{step } 2)}$$

where A2V2 represents an α-actinin dimer complexed with two vinculin molecules. It was assumed that $K_{d(step\ 1)}$ equals $K_{d(step\ 2)}$. This assumption will be discussed later. With the aid of the programming package "Stella", the final concentrations of A2, V, A2V, and A2V2, could be determined given the initial concentrations of A2, V, and the K_d (Figure 3.7). Hence a better relationship between K_d and weight averaged molecular weight was determined. The difference between the two models was negligible for interactions of low affinity but increased as the affinity increased.

α-Actinin, vinculin, and an α-actinin/vinculin mixture were used in LSE centrifugation. An approximate ratio of α-actinin dimer to vinculin monomer of 1:2 was used as this theoretically permitted a larger increase of the apparent weight averaged molecular weight. The resultant weight averaged molecular weights determined by LSE centrifugation are expressed in table 3.1. Hence a theoretical curve of weight averaged molecular weight against K_d was drawn (Figure 3.8) as described above. The K_d of the interaction was then deduced since the weight averaged molecular weight of the α-actinin/vinculin mixture was known (see table 3.1).

There was some disceprancy between the molecular weights determined for both α-actinin and vinculin using LSE and those published (Baron et al, 1987a; Price et al, 1989). It was therefore important to determine the molecular weights of the α-actinin and vinculin for each K_d determination. The value for the molecular weight of α-actinin (202kDa) was in good agreement with the deduced value for the α-actinin dimer (206kDa) (Baron et al, 1987a). However, the value of 185kDa was slightly below this expected value.

FIGURE 3.7
THE STELLA MODEL USED TO CALCULATE THE FINAL CONCENTRATIONS OF A_2, V, A_2V, AND A_2V_2, GIVEN SPECIFIED INITIAL CONCENTRATIONS OF A_2 AND V AND THE K_d OF THE INTERACTION

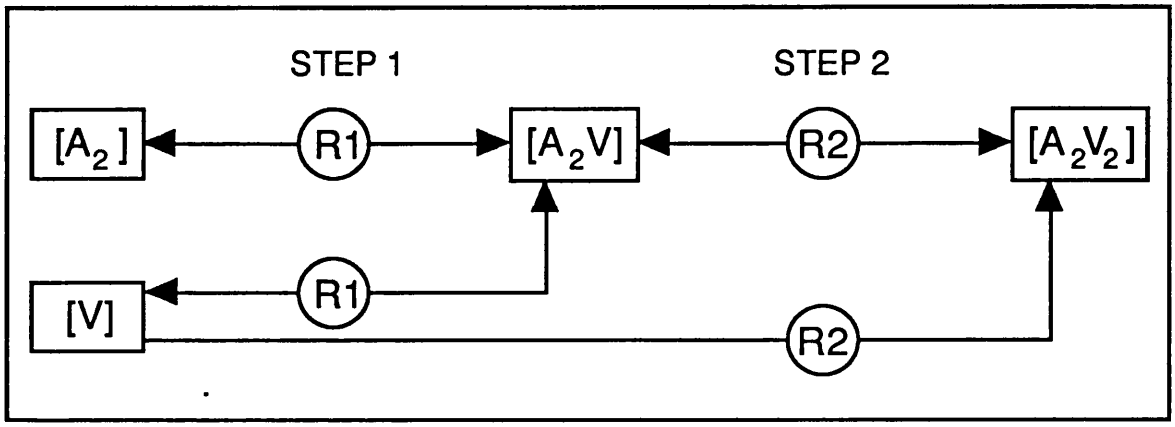

Stella was a computer software package that solved differential equations by numerical methods. It repeatedly calculated the fluxes R1 and R2. The fluxes were defined as:-

$$R1 = k_f[A_2][V] - k_r[A_2V]$$
$$R2 = k_f[A_2V][V] - k_r[A_2V_2]$$

k_f and k_r were the forward and reverse rate constants. These were chosen to define the equilibrium constant of each step. As shown steps 1 and 2 had the same equilibrium constant. The concentrations A_2, V, A_2V, and A_2V_2 were repeatedly calculated as follows:-

$$[A_2] = [A_2] + dt(-R1)$$
$$[A_2V] = [A_2V] + dt(R1-R2)$$
$$[A_2V_2] = [A_2V_2] + dt(R2)$$
$$[V] = [V] + dt(-R1-R2)$$

When both fluxes equalled zero the system was in equilibrium. The final values of A_2, V, A_2V, and A_2V_2 were then taken.

DIAGRAMATIC REPRESENTATION OF THE STELLA MODEL.

See Figure 3.7 for details of the equations utilised.

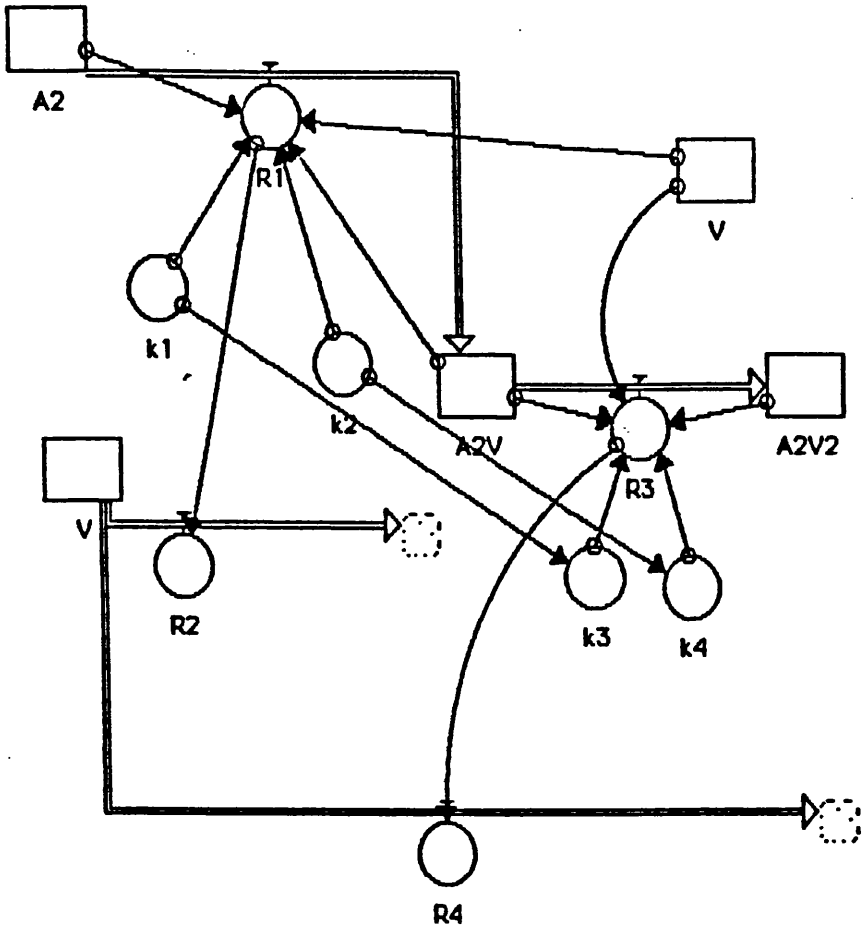

FIGURE 3.8

THE RELATIONSHIP BETWEEN DISSOCIATION CONSTANT AND EXPECTED WEIGHT AVERAGED MOLECULAR WEIGHT OF A MIXTURE OF α-ACTININ AND VINCULIN.

The curve was constructed with the aid of the Stella model (see figure 3.7). The total concentrations of α-actinin and vinculin were 0.715μM and 0.767μM respectively. The molecular weights of α-actinin and vinculin were derived from low speed equilibrium centrifugation. Molecular weights of 202kDa for α-actinin and 131kDa for vinculin were used in this example.

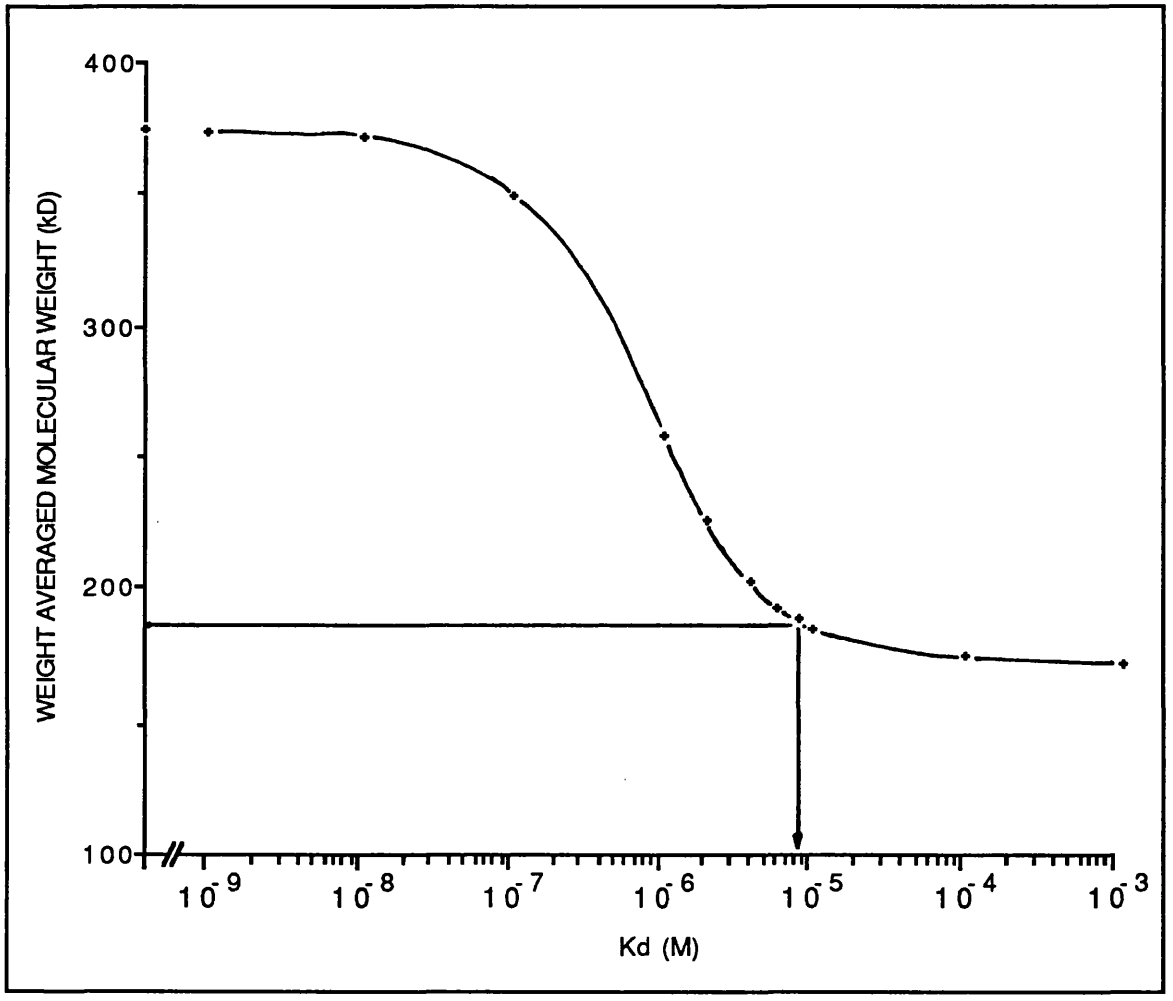

TABLE 3.1
Results of Low Speed Equilibrium Centrifugation of α-actinin, vinculin, and a α-actinin/vinculin mixture.

	Weight Averaged Molecular Weight (kDa)			Deduced K_d (M)
	α-Actinin	Vinculin	Mixture	
A	202	131	187 (173)†	8.8×10^{-6}
B	185	136	191 (159)†	2.0×10^{-5}

( )† indicated the weight averaged molecular weight expected if there was no interaction.
Buffers used were (A) buffer B without β-mercaptoethanol, and (B) buffer B plus 150mM NaCl without β-mercaptoethanol.

One possible explanation for this difference could have been partial degradation of the α-actinin. The values obtained by LSE for the molecular weight of vinculin (131 and 136kDa) were similar. However, these values were notably greater than the deduced value for the molecular weight of vinculin (117kDa) (Price et al, 1989). It was conceivable that this increase was due to a degree of self association of vinculin molecules (Milam, 1985). There was evidence for such an interaction indicated by a slight upward curvature in the plot of ln(concentration) against r^2 (where r was the distance from the axis of rotation). Indeed, if the weight averaged molecular weight was derived from the initial slope then molecular weights of 120kDa and 121kDa were obtained. If the weight averaged molecular weight was due to self association of 117kDa monomers then this would suggests that the affinity of self association was low. An association constant for the self association of vinculin has not been reported.

The average value for the K_d of the interaction between α-actinin and vinculin was $1.4x10^{-5}M$. This was approximately 6 fold greater than the value of $2.2x10^{-6}M$ obtained by Wachsstock et al (1987). Though the interpolated values for the K_d were high they were derived from a region of the curve (Figure 3.8) that was distinct from the region indicating negligible interaction. Considering the protein concentrations used, a K_d greater than $3x10^{-4}M$ was indicative of negligible interaction. The values obtained for the K_d differed by approximately 2.3 fold. Whether this was due to experimental error or a reflection of the different salt conditions used was not examined. Wachstock et al (1987) noted that increasing the concentration of NaCl reduced the amount of interaction slightly.

3.34 INVESTIGATION OF AN INTERACTION BETWEEN α-ACTININ AND VINCULIN USING AN ^{125}I-VINCULIN OVERLAY TECHNIQUE.

As expected, the binding of ^{125}I-vinculin to talin was readily demonstrated using this technique. Binding of ^{125}I-vinculin to talin was markedly reduced by a 17 fold excess of unlabelled vinculin showing that the interaction was specific. ^{125}I-Vinculin also bound to α-actinin, but the unlabelled vinculin did not markedly reduce the binding of ^{125}I-vinculin. A possible interpretation of this was that the interaction between α-actinin and vinculin was non-specific. The reported dissociation constant of α-actinin and vinculin is low, which may explain the inability of a 17 fold excess of unlabelled vinculin to reduce the binding of ^{125}I-vinculin to α-actinin. The binding of labelled ligand was examined on a theoretical basis. It is known (Freifelder, 1976) that:-

$$\frac{[\text{Ligand bound}]}{[\text{Binding sites}]} = \frac{[\text{Free ligand}]}{K_d + [\text{Free ligand}]}$$

Considering ligand, part of which was labelled, this expression can be written as:-

$$\frac{[H]f + [C]f}{K_d + [H]f + [C]f} = \frac{[H]b + [C]b}{[B]}$$

where H is labelled ligand, C is unlabelled ligand, f is free, b is bound, and B was the number of binding sites. It was assumed that labelled ligand had the same properties as unlabelled ligand. This expression

FIGURE 3.9

GRAPH DEMONSTRATING THE RELATIONSHIP (AT VARIOUS K_d's) BETWEEN THE NUMBER OF BINDING SITES OCCUPIED AND THE EXCESS OF UNLABELLED LIGAND OVER LABELLED LIGAND.

The vertical axis is the amount of occupied binding sites. The horizontal axis is the excess of unlabelled ligand over labelled ligand. The total concentrations of labelled ligand and binding sites were $1x10^{-8}M$ and $2x10^{-8}M$ respectively.

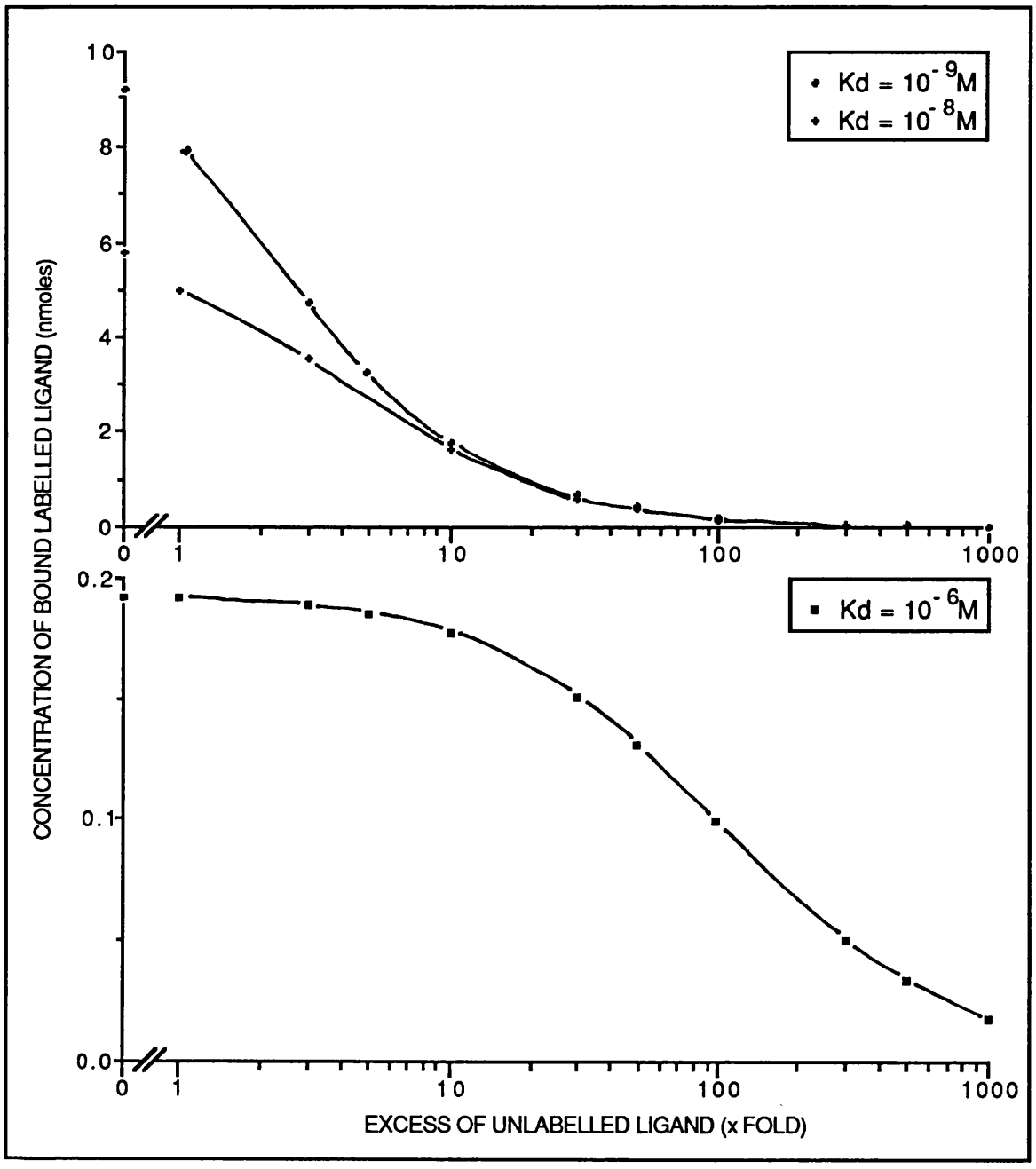

was expanded and solved for the concentration of labelled ligand bound:-

$$[H]b = \frac{\{(x+1)[H]t+K_d+[B]\}-\sqrt{\{sqr\{-(x+1)[H]t-K_d-[B]\}-4(x+1)[H]t[B]\}}}{2(x+1)}$$

where t was the total concentration, and x was the excess of unlabelled ligand. Graphs of percentage labelled ligand bound versus excess of unlabelled ligand were drawn for various K_d's (Figure 3.9). It was shown that considering the excess of unlabelled ligand alone was not enough. The excess had to be related to other factors, especially the K_d. When considering a labelled ligand concentration of $1x10^{-8}$M, $2x10^{-8}$ nmoles of binding site in an incubation volume of 5ml (similar to the amounts of α-actinin electroblotted) and a K_d of $1x10^{-9}$M, the amount of labelled ligand bound is 9.2nmoles. If there is a ten fold excess of unlabelled ligand this value drops to 1.8nmoles. This represents a greater than 80% reduction in the binding of labelled ligand. However, when considering a similar interaction but with a K_d of $1x10^{-6}$M, the amount of labelled ligand bound in the absence and presence of unlabelled ligand (ten fold excess) was 0.19nmoles and 0.18nmoles respectively. This represents a mere reduction of 5%. The overlay assay was not sensitive enough to detect such changes. A 49% reduction in binding of the labelled ligand would be obtained when a 100 fold excess of unlabelled ligand incubated with the labelled ligand. The low level of unlabelled vinculin required to reduce the binding of ^{125}I-vinculin to talin (reported K_d of $1x10^{-8}$M) (Burridge and Mangeat, 1984) is consistent with these calculations. They could also explain why a low level of unlabelled vinculin did not significantly reduce the binding of

^{125}I-vinculin to α-actinin, the reported K_d of which is approximately $1x10^{-6}$M (Wachsstock et al, 1987).

In subsequent overlays the concentrations of ^{125}I-vinculin and unlabelled vinculin were of the order of $1x10^{-8}$M and $1x10^{-6}$M respectively. Figure 3.10 shows that binding of ^{125}I-vinculin to α-actinin is significantly diminished by unlabelled vinculin when these conditions were used. The talin used was partially degraded. A significant proteolytic talin fragment of approximately 110kDa bound ^{125}I-vinculin specifically. The various marker proteins (rabbit skeletal muscle myosin, rabbit muscle phosphorylase B, *E. coli* β-galactosidase, BSA, hen egg albumin, bovine erythrocyte carbonic anhydrase) did not bind ^{125}I-vinculin.

The nitrocellulose bound α-actinin was initially denatured and its conformation when attached to the nitrocellulose is unclear. Hence, the apparent binding of ^{125}I-vinculin to nitrocellulose bound α-actinin may have been artifactual. Therefore a modification of the overlay assay was also used to demonstrate the specificity of the interaction between α-actinin and vinculin. The nitrocellulose with bound α-actinin was incubated in a ^{125}I-vinculin/α-actinin solution instead of a ^{125}I-vinculin/unlabelled vinculin solution. Since this assay relies on soluble ^{125}I-vinculin binding to soluble α-actinin, both of which are in their native conformation, the results are less open to criticism. The binding of ^{125}I-vinculin ($1.5x10^{-8}$M) to the nitrocellulose bound α-actinin was reduced by 46% by including α-actinin (0.5μM) in the incubation (Table 3.2). Glutatione-S-transferase (GST) (3.7μM) which does not bind to vinculin produced a 14% reduction in the binding of ^{125}I-vinculin. The significant

FIGURE 3.10

^{125}I-VINCULIN OVERLAY OF TALIN AND α-ACTININ.

The figure shows (i) a Coomassie stained SDS-PAGE gel of the samples (ii) the samples electroblotted onto nitrocellulose and overlaid with ^{125}I-vinculin (1.5×10^{-8}M) and (iii) the samples electroblotted onto nitrocellulose and overlaid with I^{125} vinculin plus a 100 fold excess of unlabelled vinculin. As indicated, the lanes contain markers (5μg each of rabbit skeletal muscle myosin, rabbit muscle phosphorylase B, *E. coli* β-galactosidase, BSA, hen egg albumin, and bovine erythrocyte carbonic anhydrase), 2μg talin and proteolytic fragments of talin, and 5μg of α-actinin.

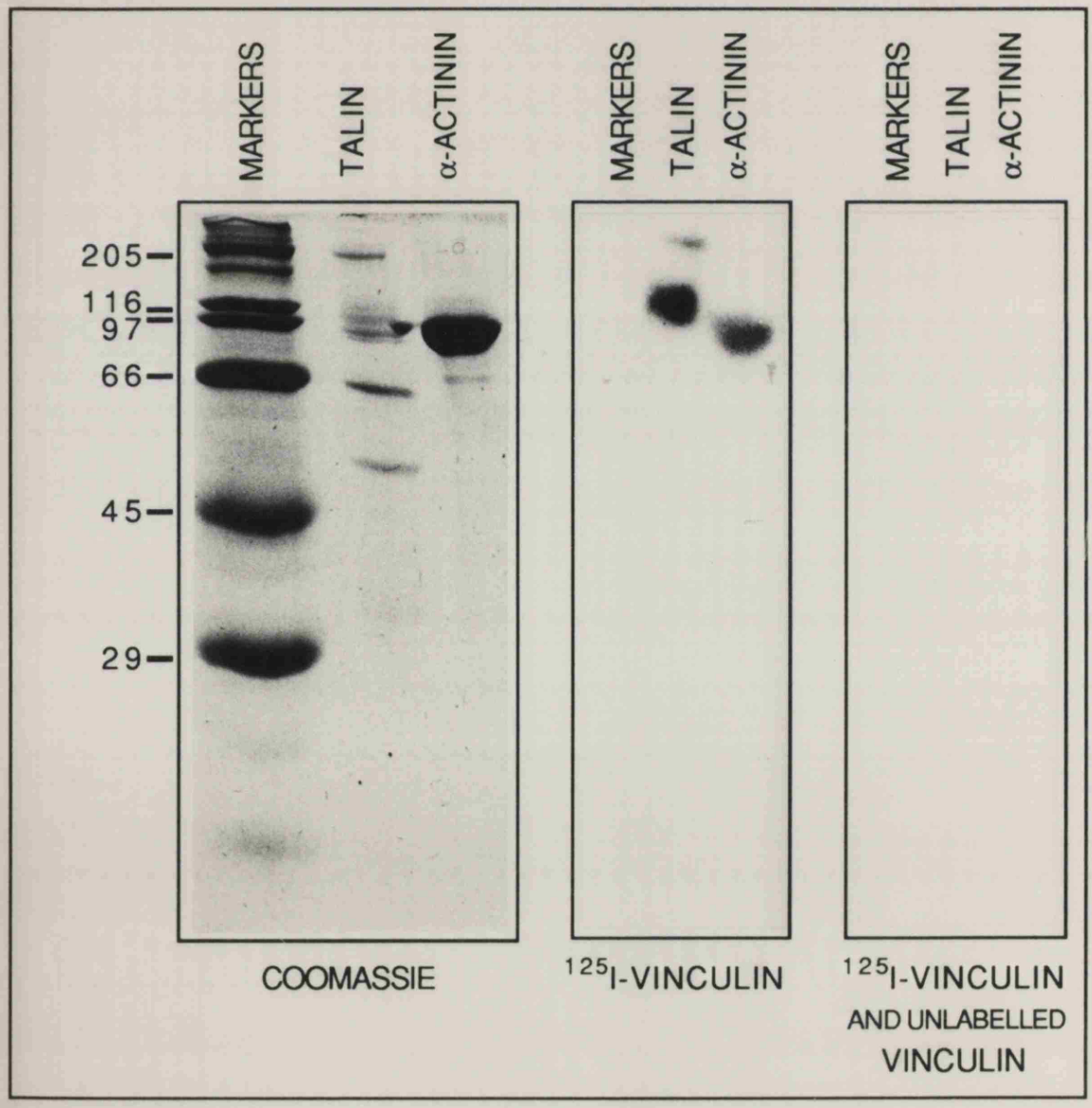

reduction in binding produced by the free α-actinin is because the interaction between the free α-actinin and ^{125}I-vinculin effectively lowered the free concentration of ^{125}I-vinculin. No reduction would have occurred if the concentration of ^{125}I-vinculin had been in large excess of the concentration of free α-actinin as the binding of the ^{125}I-vinculin to the free α-actinin would not have significantly reduced the free ^{125}I-vinculin concentration.

Table 3.2

The inhibition of binding of ^{125}I-vinculin to nitrocellulose bound α-actinin produced by addition of soluble α-actinin.

Added Solute†	Change In Binding (% and standard deviation) Of ^{125}I-Vinculin ($1.5x10^{-8}$M) To Nitrocellulose Bound α-Actinin (5μg)
α-Actinin (0.5μM)	-46 (14)
GST (3.7μM)	-14 (12)

† 500μg of the relevant protein was added to the incubation solution (5ml total) of the overlay assay. The assay was otherwise carried out as previously described. The average of three experiments are shown.

INITIAL LOCALISATION OF THE VINCULIN BINDING SITE IN α-ACTININ.

Initial localisation of the vinculin binding site in α-actinin was carried out using 10μg of a one hour thermolysin digest of α-actinin (as described in section 2.4) and the overlay technique. The main products of thermolysin digestion of α-actinin are fragments of

27kDa and 53kDa (Figure 3.11). The 27kDa fragment contains most of the N-terminal domain (residues 24 to approximately 269) which posseses the actin binding site (Mimura and Asano, 1986). The 53kDa fragment (residues 266 to approximately 750) contains most of the repeats and some sequence C-terminal to repeat 4. Overlays demonstrated that ^{125}I-vinculin binds to the 53kDa fragment but not to the 27kDa fragment. The binding of labelled vinculin to the 53kDa fragment was significantly reduced by the presence of unlabelled vinculin (Figure 3.12).

3.35 ATTEMPTS AT CO-SEDIMENTATION OF VINCULIN WITH α-ACTININ AND F-ACTIN.

One approach to investigate the α-actinin/vinculin interaction would be to examine whether or not vinculin co-sediments with an α-actinin/F-actin complex. It is conceivable that the binding of vinculin, α-actinin, and F-actin were synergistic. The interaction between α-actinin and vinculin, and that between α-actinin and F-actin are of relatively low affinity, but the affinities within a ternary F-actin/α-actinin/vinculin complex might be greater. Examples of such interactions have been reported. The interaction between spectrin tetramers and F-actin is greatly enhanced in the presence of protein 4.1 (Ungewickell et al, 1979; Ohanion et al, 1984).

When F-actin alone was centrifuged as described in Figure 3.13, 30 to 60% of the protein was found in the pellet. Similar values were obtained with F-actin prepared as described in Chapter 2 and with that prepared from G-actin obtained from Sigma. Using F-actin at 4.8, 17.8 and 24μM did not affect the proportion of actin that pelleted.

FIGURE 3.11

FRAGMENTS OF α-ACTININ PRODUCED BY THERMOLYSIN DIGESTION.

Black bars indicate the fragments of α-actinin generated by thermolysin digestion relative to their position in the complete sequence. The N-terminal of each fragment was mapped after N-terminal protein sequencing. The N-terminal sequences (one letter code) were as follows: 92, 81, and 27kDa fragments - LLDPAW; 64 and 53kDa fragments - LAVNQE; 32kDa fragment - DPQQTN; 28kDa fragment - MQPEED; 42.5kDa fragment - FMPSEG; 40.4kDa fragment - LEQAEK; 38.7kDa fragment - IRRLER. The C-terminus of each fragment was estimated from a consideration of its size on SDS-PAGE. The position within the C-terminal domain of the two EF-hand calcium binding motifs is also indicated (residues 750 to 778 and residues 787 to 813).

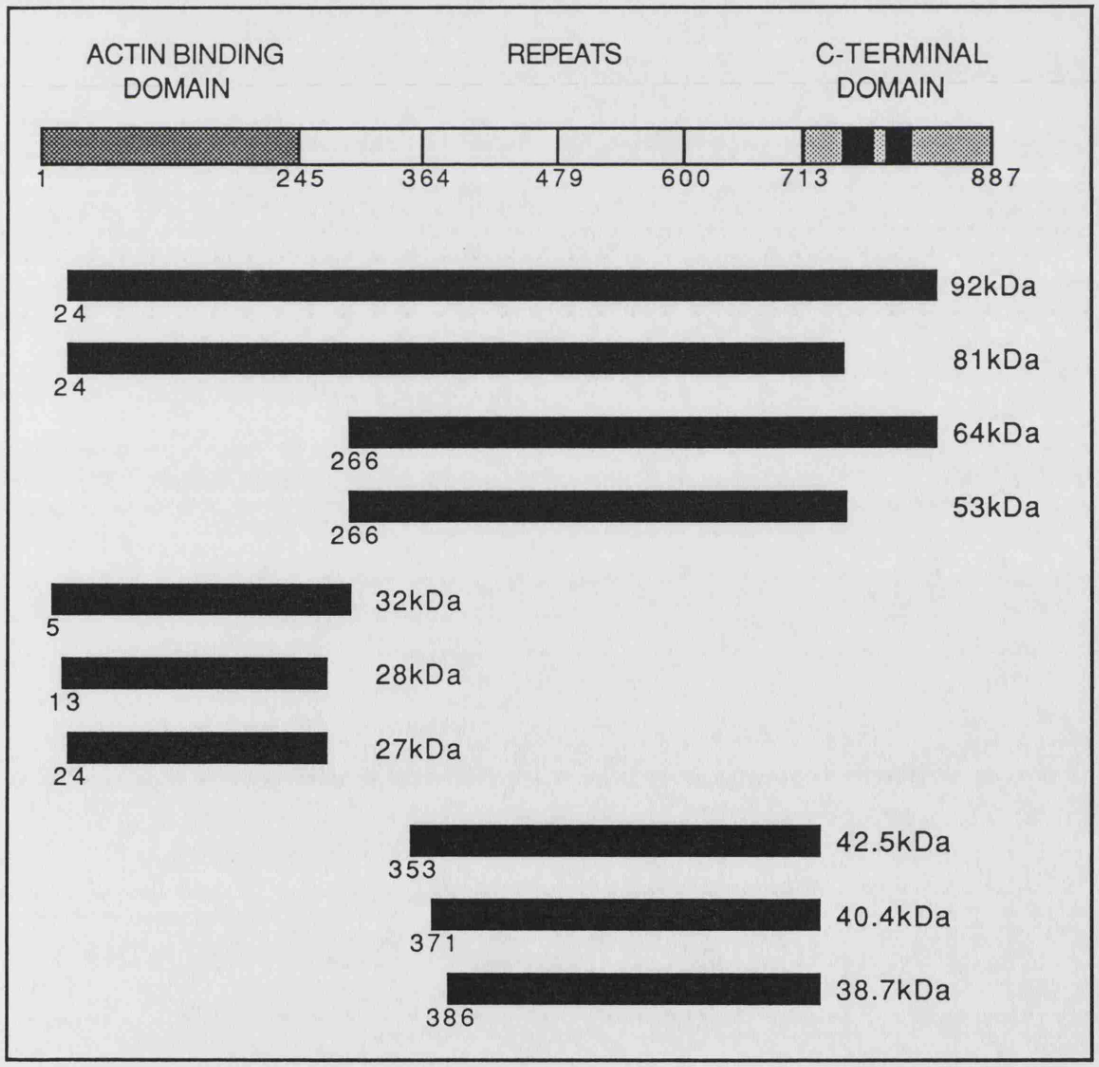

FIGURE 3.12

^{125}I-VINCULIN OVERLAY OF TALIN AND A THERMOLYSIN DIGEST OF α-ACTININ.

The figure shows (i) a Coomassie stained SDS-PAGE gel of the samples (ii) the samples electroblotted onto nitrocellulose and overlaid with ^{125}I-vinculin $(1.5 \times 10^{-8} M)$ and (iii) the samples electroblotted onto nitrocellulose and overlaid with I^{125} vinculin plus a 100 fold excess of unlabelled vinculin. As indicated, the samples were 2μg talin (and proteolytic fragments of talin) and 10μg of a thermolysin digest of α-actinin.

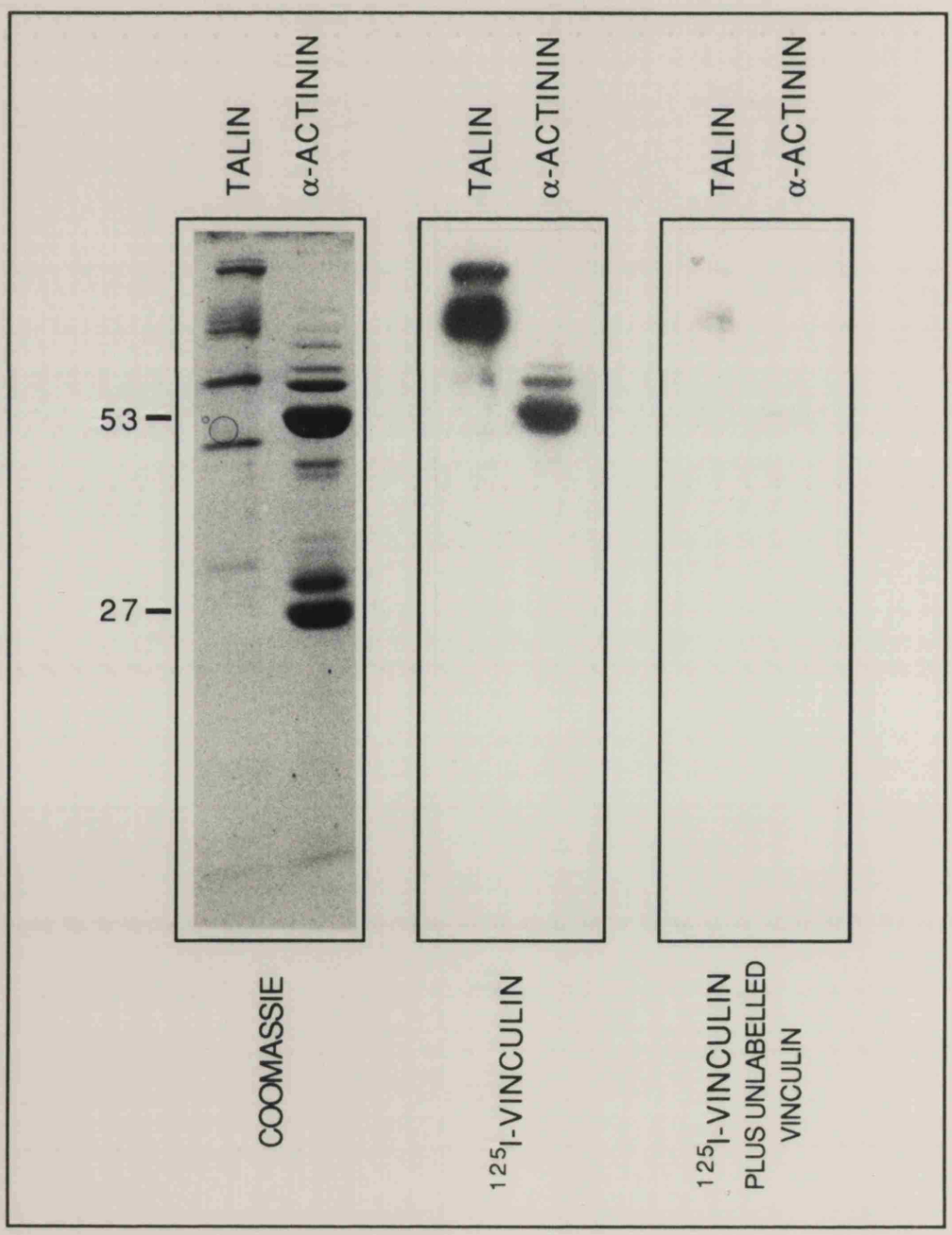

FIGURE 3.13
CO-SEDIMENTATION OF α-ACTININ, VINCULIN, AND α-ACTININ/VINCULIN MIXTURES WITH F-ACTIN.

Samples were centrifuged as described in section 2.48. The buffer used was 10mM Tris/HCL, pH7.5, 100mM KCl, 0.1mM ATP, 4mM $MgCl_2$, 1mM β-mercaptoethanol. S and P indicate the supernatant and pellet after ultracentrifugation of the solutions as follows: actin alone; α-actinin alone; vinculin alone; vinculin and actin; vinculin; α-actinin, and actin; α-actinin and actin. The concentrations of actin, α-actinin, and vinculin were 17.8, 3, and 9μM respectively.

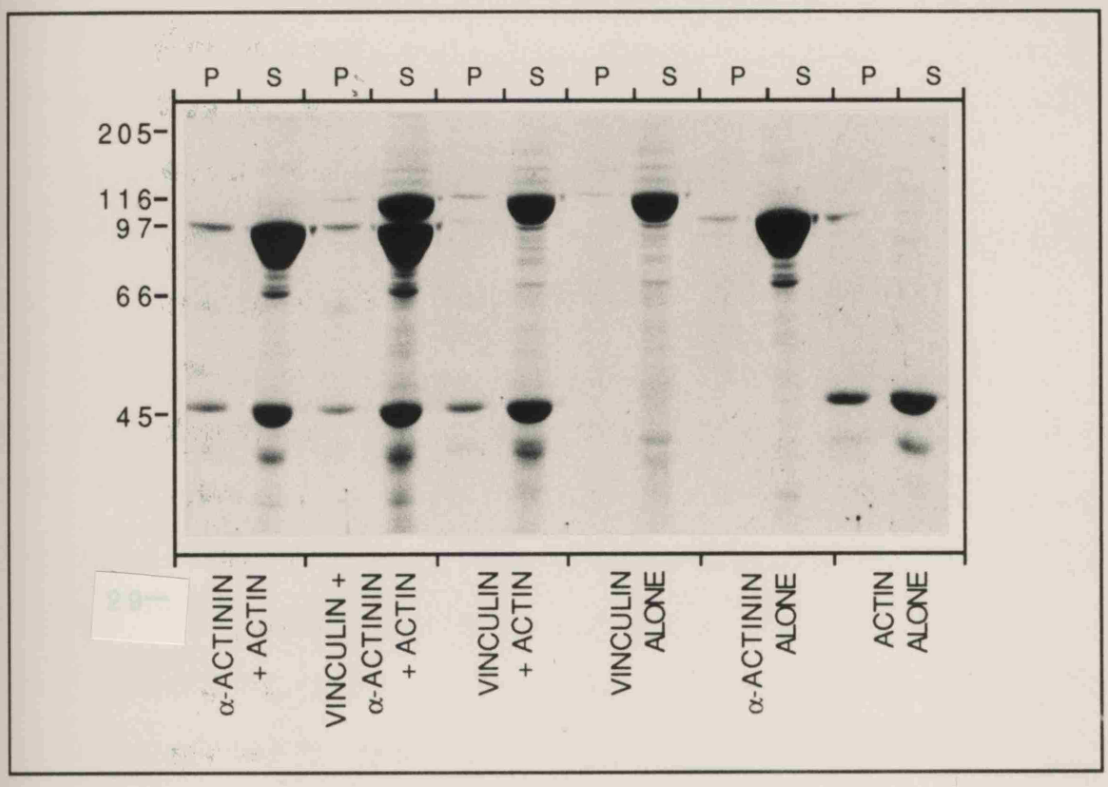

THE FIGURE SHOWS AN EXAMPLE OF ONE OF THE F-ACTIN SEDIMENTATION EXPERIMENTS

THE ACTUAL ACTIN CONCENTRAT" IN THIS FIGURE IS ESTIMATED TO BE 6μM

α-Actinin was shown to co-sediment with F-actin, as previously reported (Mimura and Asano, 1986). As expected, a greater proportion of the α-actinin pelleted when higher concentrations of F-actin were used. When a total concentration of 17.8μM actin was used, between 5 and 26% of the α-actinin was found to co-sediment, depending on the amount of actin in the pellet. If 4.8μM actin was used approximately 9% of the α-actinin co-sedimented. However, using an equation similar to that in section 3.34, the values expected were 46 and 18% respectively. The value for the amount of binding site was taken as the amount of actin that pelleted. The 'ligand' concentration was the concentration of α-actinin dimer. The K_d of the interaction between α-actinin and F-actin was taken as 10^{-5}M (Sato et al, 1987).

Approximately 9% of the vinculin appeared to co-sediment with actin. The presence of α-actinin in a vinculin/F-actin mixture did not affect the amount of vinculin that pelleted. However, the inefficiency of the α-actinin pelleting was such that binding of vinculin to pelleted α-actinin would be negligible. Using the equation from section 3.34 it was estimated that if 26% of the α-actinin co-sedimented with F-actin, then only 4 or 8% of the vinculin would also co-sediment if the K_d between α-actinin and vinculin was 10^{-5}M or 10^{-6}M respectively. Here the value for the amount of binding site was taken as the amount of α-actinin ('monomer') that had pelleted and the 'ligand' concentration was the vinculin concentration.

3.4 DISCUSSION.

Electron microscopy has allowed direct visualisation of α-actinin/vinculin complexes. Negative staining was employed as it is a gentler technique than rotary shadowing. The spraying of the sample required in rotary shadowing produces shear forces which may be detrimental to the stability of any complexes held together by low affinity interactions.

It may be argued that the "dumbell" and "lollipop" images were artifacts and arose by the chance proximity of vinculin and α-actinin molecules. However, there were no examples of structures where a disc lay alongside a rod. Examples of α-actinin molecules adjacent to α-actinin molecules and of vinculin molecules adjacent to vinculin molecules were very infrequent. Trying to demonstrate the presence of complexes in more dilute solutions would not have been helpful. A greater surface area of the sample grid would have to be examined to find α-actinin/vinculin complexes. Hence the argument for the complexes arising due to chance proximity could still be levied. Also, more dilute solutions would have a lower ratio of α-actinin/vinculin complexes to α-actinin dimers and vinculin monomers than the more concentrated samples as the proportion of occupied 'binding sites' is related to the concentration of the 'ligand'.

Two possible methods could be used to generate a greater proportion of complexes: A higher concentration of the α-actinin/vinculin solution could be incubated and diluted immediately prior to preparation for electron microscopy. Alternatively mild fixation of the α-actinin/vinculin mixture with 0.1% glutaraldehyde could be tried.

In the electron micrographs of the α-actinin/vinculin mixture there were very few α-actinin molecules visible despite a mole ratio of α-actinin to vinculin of approximately 1:2. Those that were visible were usually complexed to vinculin. One possible explanation for this observation is that the α-actinin molecules are buried by the stain unless they are elevated by their attachment to vinculin. The micrographs of α-actinin alone showed the presence of a large number of molecules. When α-actinin or vinculin were stained individually the depth of stain only had to accomodate the height of one molecule type.

The number of α-actinin/vinculin complexes visualised was low. However, this is consistent with the low affinity of the interaction between these two proteins. It is known that:-

$$\text{Fraction of binding sites filled} = \frac{[\text{Ligand bound}]}{[\text{Binding sites}]} = \frac{[\text{Free ligand}]}{K_d + [\text{Free ligand}]}$$

The concentrations of α-actinin and vinculin used were 0.25μM and 0.43μM respectively. Considering α-actinin as the binding site, and K_d's of 10^{-5}M and 10^{-6}M, the predicted fractions of occupied binding sites was 0.041 and 0.301 respectively. This considered that the α-actinin dimer has a single binding site for vinculin. Similarly, the predicted fractions of occupied binding sites was 0.024 and 0.200 respectively when considering vinculin as the binding site. Electron micrographs of the α-actinin/vinculin mixture showed an average per field of 660 vinculin molecules and 20 "complexes" with either one or two vinculin molecules attached to one α-actinin molecule. As

discussed above, the uncomplexed α-actinin molecules were largely invisible in the micrographs of the α-actinin/vinculin mixtures. However, the molar ratio of α-actinin to vinculin was known. Since this was 1:1.7, the expected value for the number of α-actinin molecules was 384 per field. This assumes that the amount of α-actinin and vinculin that bound to the grid was representative of the amounts of the two molecules in the solution applied to the grid. The values could only be an approximation as not all of the structures seen in the electron micrographs could be unequivocally assigned. Hence the fraction of binding sites occupied were determined from the electron micrographs. Considering α-actinin as the binding site, the fraction of binding sites occupied was 0.052. Similarly, the value obtained when considering vinculin as the binding site was 0.030. Both of these values were consistent with the interaction between α-actinin and vinculin having a K_d of 10^{-5} to 10^{-6}M.

There appeared to be two distinct vinculin binding sites on the α-actinin dimer. If each site had the same K_d the ratio of α-actinin dimers to the "lollipop" complexes would be the same as the ratio of "lollipop" complexes to "dumbell" complexes. Surprisingly the ratio's of α-actinin dimer to "lollipop" and of "lollipop" to "dumbell" observed were approximately 84:1 and 1:2 respectively. This suggested the possibility that there may be a degree of co-operativity in the binding of vinculin to α-actinin. Such co-operativity is difficult to envisage as the two vinculin binding sites are displaced by about 33nm. However, there are examples of long range intramolecular signalling. Binding of ligand to the large extracellular domain of

receptor tyrosine kinases affects the cytoplasmic kinase activity via a single transmembrane helix (Yarden and Ullrich, 1988).

The binding of vinculin to the ends of the α-actinin dimer gives some indication of the region on α-actinin responsible for binding. The binding site could not be within repeats two or three, as this corresponds to the central region of the α-actinin rod. This suggests that the binding site is contained within the N-terminal or C-terminal domains of α-actinin. However, the binding site could also be within repeat one or four. The location of the vinculin "tail" could not be discerned, though this was probably a reflection of the visualisation technique. Hence no conclusions could be drawn to which region of the vinculin molecule was involved in the interaction.

An interaction between α-actinin and vinculin was also demonstrated by low speed equilibrium centrifugation. This method also enabled the estimation of the dissociation constant, which was shown to be 1.6×10^{-5}M. The affinity of the α-actinin/vinculin interaction, like the α-actinin/F-actin interaction (approximately 1×10^{-6}M), was relatively low (Meyer and Aebi, 1990). Considering the forces that focal contacts are subjected to, it would appear strange that the membrane to microfilament attachment structure should have links with high dissociation constants. With respect to this apparent anomaly a number of points should be considered. (i) The local concentrations of the focal contact proteins is probably quite high. (ii) There are probably linkages other than the integrin-talin-vinculin-α-actinin-F-actin linkage. (iii) Focal contacts are potentially highly dynamic structures and therefore the ability to disassemble is essential. (iv) The mechanisms that control the integrity of the focal contact are

poorly understood. Although unlikely, a proportion of the purified vinculin may have had its binding capacity modified by post translational modification.

The model used for LSE assumed that the α-actinin dimer had two binding sites of equal affinity. It was conceivable that the binding of one vinculin molecule to the α-actinin dimer could have increased the binding affinity of the second binding site. This phenomena would not have been revealed by this approach. Considering the protein concentrations used it was possible to draw a theoretical curve of weight averaged molecular weight against the K_d of the first association given a smaller K_d for the second association (eg 1000 fold). At high K_d's the curve is essentially similar to that shown in Figure 3.8. As the K_d drops the weight averaged molecular weight rises at a larger rate than that shown in Figure 3.8 and reaches a plateau at a higher level. Since the determined weight averaged molecular weights for the mixture are derived from regions of high K_d, no distinction could be made about the second association step. As mentioned above such co-operative binding seems unlikely, though it was tentatively suggested by the electron micrographs.

There were other models that could describe the interaction between α-actinin and vinculin: (i) One model for an interaction would be that an α-actinin dimer and two vinculin monomers were required to bind simultaneously. This binding would be of high affinity, but the low probability of such an interaction occuring *in vitro* would be reflected in the perceived low affinity. The simultaneous binding of two vinculin monomers to an α-actinin dimer may be feasible *in vivo* due to high local concentrations of α-actinin and vinculin at focal

contacts. However, this model seems unlikely due to the significant presence of A2V complexes in the electron micrographs. (ii) α-Actinin could have two vinculin binding sites with distinct K_d's. This model intuitively appeared improbable. Unless the K_d's were markedly different this model would be difficult to distinguish from the model used above. As with the model used above, this model (ii) would favour the formation of A2V rather than A2V2 complexes.

Binding of α-actinin to vinculin was also demonstrated using ^{125}I-vinculin overlays, as performed previously (Otto, 1983; Wilkins et al, 1983; Belkin and Koteliansky, 1987). Nitrocellulose blot overlays have several advantages over the equivalent analysis carried out on the actual gel. Nitrocellulose is easier to handle without damage. Washes and incubations are much quicker as diffusion of solutions through a gel are not involved. Much smaller amounts of reagents are required. However, there are intrinsic problems with this assay. The protein is initially denatured when it is electrophoresed. It is assumed that some reconstitution could occur once the protein was bound to the nitrocellulose and incubated in a suitable buffer. There have been examples of certain epitopes being irreversibly denatured by SDS (Burnette, 1981). A binding site comprised of regions of non-contiguous sequence is less likely to attain its native conformation and thus have a lower or negligible binding affinity. The type of interaction between nitrocellulose and the bound protein, and the constraints that the interaction may impose upon the bound protein are not clearly understood. Another minor drawback to nitrocellulose blot overlays is that although the amount of protein electrophoresed can be determined, the amount

that is transferred to the nitrocellulose and regains 'activity' could not.

^{125}I-Vinculin was shown to interact with α-actinin as demonstrated in previously reported overlays (Otto, 1983; Wilkins et al, 1983; Belkin and Koteliansky, 1987). Furthermore, a reduction in binding of ^{125}I-vinculin to α-actinin was demonstrated when a suitable concentration of unlabelled vinculin was included in the incubation solution. The concentration of unlabelled vinculin required was consistent with a low affinity interaction between α-actinin and vinculin. Interestingly, the concentration of unlabelled ligand required to cause the reduction in binding was greater than the concentration that would have been required if the interaction was of a higher affinity. Otto (1983) failed to demonstrate a reduction in binding of ^{125}I-vinculin to α-actinin despite using an approximately 130 fold excess of unlabelled vinculin. However, two points should be noted that may explain this discrepancy. Increasing the number of binding sites means that a larger excess of unlabelled ligand is required to cause a reduction in the binding of labelled ligand (Figure 3.14). Unfortunately Otto (1983) did not specify the amount of α-actinin that she used. The excess of unlabelled ligand required to reduce the binding of labelled ligand is also affected by the concentration of labelled ligand (Figure 3.15). Lower concentrations of labelled ligand need a greater excess of unlabelled ligand to cause an equivalent reduction in the binding of labelled ligand. Otto (1983) used a lower concentration of ^{125}I-vinculin which would necessitate a larger excess of unlabelled vinculin to reduce the binding of the labelled vinculin.

FIGURE 3.14

GRAPH DEMONSTRATING THE RELATIONSHIP (AT VARIOUS CONCENTRATIONS OF BINDING SITE) BETWEEN THE NUMBER OF BINDING SITES OCCUPIED AND THE EXCESS OF UNLABELLED LIGAND OVER LABELLED LIGAND.

The vertical axis is the amount of occupied binding sites. The horizontal axis is the excess of unlabelled ligand over labelled ligand. The total concentration of labelled ligand was $1x10^{-8}M$. The K_d of the interactions were (i) $10^{-9}M$ and (ii) $10^{-6}M$.

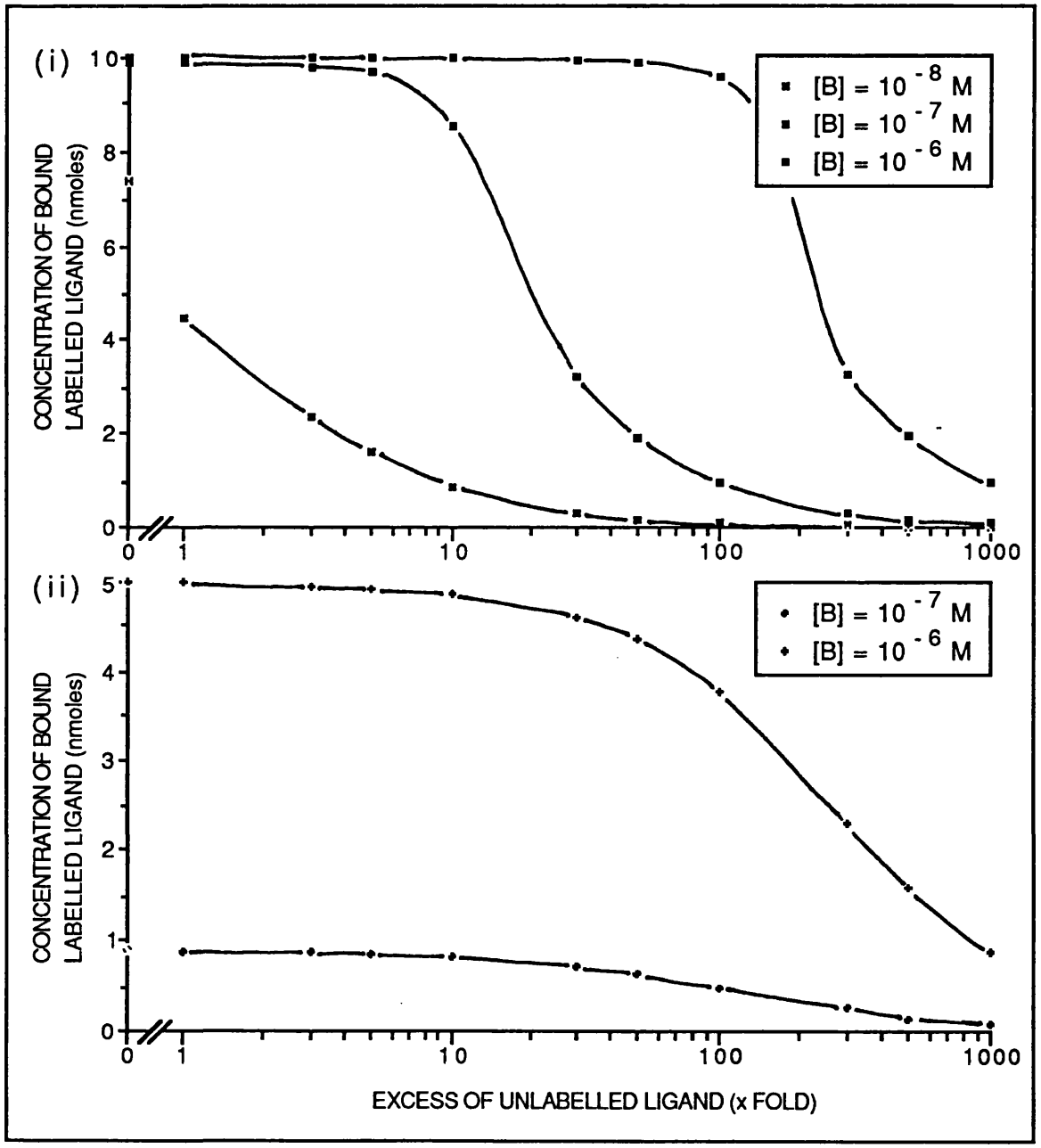

FIGURE 3.15

GRAPH DEMONSTRATING THE RELATIONSHIP (AT VARIOUS TOTAL CONCENTRATIONS OF LABELLED LIGAND) BETWEEN THE NUMBER OF BINDING SITES OCCUPIED AND THE EXCESS OF UNLABELLED LIGAND OVER LABELLED LIGAND.

The vertical axis is the amount of occupied binding sites. The horizontal axis is the excess of unlabelled ligand over labelled ligand. The total concentration of binding sites was $2x10^{-8}M$.

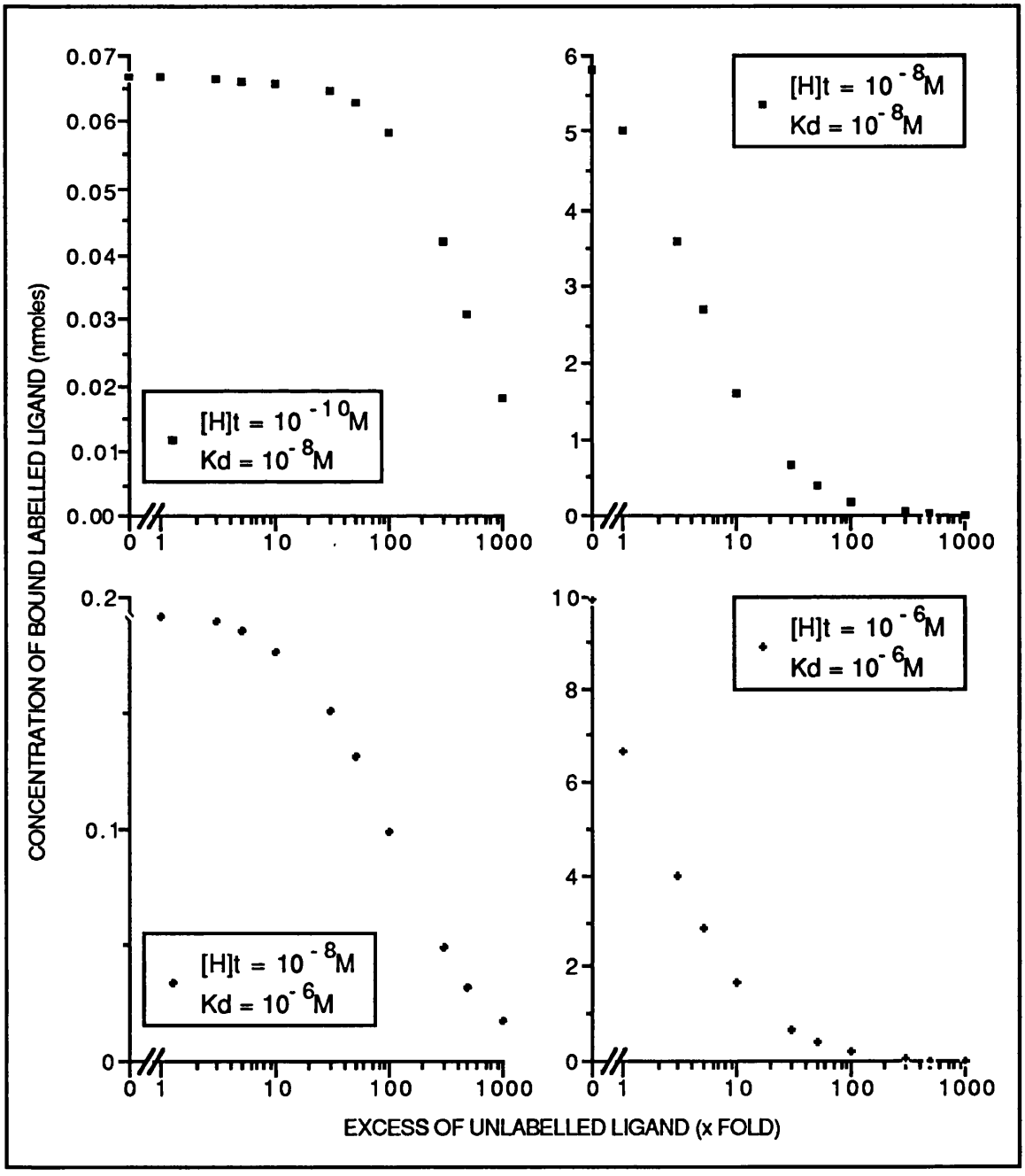

In addition, when nitrocellulose bound α-actinin was incubated in a solution containing ^{125}I-vinculin and native α-actinin, the binding of the ^{125}I-vinculin to the nitrocellulose bound α-actinin was reduced. This assay depended on the free α-actinin binding to the ^{125}I-vinculin, lowering the free concentration of the ^{125}I-vinculin, and hence reducing its interaction with the nitrocellulose bound α-actinin. Therefore this assay was less likely to be affected by artifacts arising due to the binding of α-actinin to nitrocellulose or the membrane bound protein not being native. Hence this modified overlay assay suffers fewer criticisms than the basic overlay assay discussed above.

When considered with the electron microscopy data, the ^{125}I-vinculin overlay data provides a further insight into the region of α-actinin responsible for binding vinculin. The electron micrographs indicated that vinculin bound to the ends of the α-actinin dimer. The ^{125}I-vinculin overlays indicated that the vinculin binding site was within the 53kDa fragment produced by thermolysin digestion of α-actinin. Hence the binding site is likely to be within repeat 1 (from residue 266) or within residues 600 to approximately 750.

In contrast to the data presented here, a recent report (Pavalko and Burridge, 1991) suggested that the 27kDa fragment of α-actinin bound ^{125}I-vinculin in an overlay assay. The 53kDa fragment did not bind ^{125}I-vinculin. However, the ^{125}I-vinculin (labelled with Iodogen) used by Pavalko and Burridge (1991) did not appear to be specific for α-actinin. Pavalko and Burridge (1991) did not demonstrate that the binding of ^{125}I-vinculin could be inhibited with unlabelled

vinculin or free α-actinin. In their assay ^{125}I-vinculin also bound to thermolysin. The ^{125}I-vinculin appeared to bind to thermolysin more strongly than it did to α-actinin or the 27kDa fragment. Pavalko and Burridge (1991) did not use any proteins as negative controls. The results presented in this chapter (see section 3.33) showed that the α-actinin/vinculin interaction was specific. This was demonstrated in three ways: (i) The presence of unlabelled vinculin in the overlays reduced the amount of ^{125}I-vinculin that bound to the α-actinin. (ii) The inclusion of α-actinin but not GST in the overlays also reduced the binding of ^{125}I-vinculin to the nitrocellulose bound α-actinin. (iii) None of the five marker proteins bound ^{125}I-vinculin in overlays. A possible explanation for the discrepancy between the results of Pavalko and Burridge (1991) and those presented here is the method used to label the protein. Although the Bolton and Hunter reagent labelled ^{125}I-vinculin used in this study bound specifically to α-actinin, the ^{125}I-α-actinin that was labelled with Bolton and Hunter reagent bound non-specifically to a number of proteins including GST (data not shown).

The effect of microinjection of the 27 and 53kDa fragments of α-actinin was also investigated by Pavalko and Burridge (1991). The 27kDa fragment was detected along the stress fibres and focal contacts, consistent with its F-actin binding capability. The 53kDa fragment was confined to the transient focal contacts. Pavalko and Burridge (1991) suggested that this was due to an interaction between the α-actinin repeats and the β_1 subunit of integrin, as previously suggested (Otey et al, 1990). However, the localisation of the microinjected 53kDa fragment is also consistent with this fragment possessing a vinculin binding site.

The actin binding domain (residues 1 to 290) and a construct comprising the repeats and C-terminal domain (residues 222 to 887) of smooth muscle α-actinin have seperately been expressed in COS cells (Hemmings et al, 1992). The localisation of the expressed proteins was then examined using an antibody specific for chick α-actinin. The results obtained with expressed protein differed to that obtained with microinjected protein (Pavalko and Burridge, 1991). The actin binding domain strongly labelled focal contacts but was absent from stress fibres. The stress fibres were shorter and stained less than in normal cells, suggesting that they had been disrupted to some extent. The construct encoding residues 222 to 887 did not localise to either focal contacts or stress fibres. The explanation for the different localisation is unclear. It is possible that the expressed construct comprising the repeats and C-terminus was not at a sufficiently high concentration for it to bind to focal contacts. Similarly, the concentration of the actin binding domain may have been such that it was able to bind the F-actin at the focal contact but was unable to bind the F-actin of stress fibres due to competition by other proteins (Nomura et al, 1987). Alternatively, the localisation of the expressed actin binding domain to focal contacts but not to stress fibres raises the possibility that the actin binding domain is binding to focal contacts via another protein. Recently, using the overlay technique, a phosphoprotein termed zyxin has been shown to bind to the actin binding domain of α-actinin (Crawford et al, 1992). In comparison to α-actinin and vinculin, zyxin is quantitatively a minor component of adherens junctions (Beckerle, 1986; Crawford and Beckerle, 1991). The function of zyxin is unclear.

From the co-sedimentation experiments described, no conclusions could be drawn. Had the actin and α-actinin pelleted efficiently then co-sedimentation of vinculin should have been observed if there was an α-actinin/vinculin interaction. The ideal way to improve this method would be to improve the efficiency of actin sedimentation, and hopefully the concomitant co-sedimentation of α-actinin. The experiments described could then be repeated. Alternatively the concentrations of actin and α-actinin could be increased so that the proportion of α-actinin in the pellet was greater. This would probably necesitate the use of another method to monitor any co-sedimentation of vinculin as it would no longer be distinguishable from α-actinin on an SDS-PAGE gel. The use of ^{125}I-vinculin would be one possible method.

Although none of the techniques alone was conclusive, the results taken together provided convincing support for the existence of an α-actinin/vinculin interaction. The interaction was of relatively low affinity, the deduced K_d being 1.6×10^{-5}M. The low number of α-actinin/vinculin complexes that were seen in electron microscopy and the concentration of unlabelled vinculin required to inhibit the binding of ^{125}I-vinculin to α-actinin in overlays were consistent with this interpretation.

CHAPTER FOUR
THE LOCALISATION WITHIN α-ACTININ OF THE VINCULIN BINDING SITE

4.1 INTRODUCTION.

As discussed in the previous chapter, evidence has been provided for the existence of an interaction between α-actinin and vinculin. However, there is no data concerning the region within α-actinin responsible for vinculin binding. The localisation of the vinculin binding site in α-actinin was therefore investigated. To this end, a number of DNA fragments of smooth muscle α-actinin were cloned into the procaryote expression vector pGEX (Smith and Johnson, 1988) and expressed as glutathione-S-transferase (GST) fusion proteins. The GST permitted the single step purification of the fusion protein from the bacterial cell lysate which could then be tested for their ability to bind to ^{125}I-vinculin.

The ^{125}I-vinculin overlay assay was used for initial screening of the α-actinin fusion proteins. This assay was relatively simple to perform. Bacterial cell lysates could be used directly with no special preparation. This assay also permitted the screening of fusion proteins that were largely insoluble in cell lysates. Two further assays were used to substantiate the results of the overlays. A modification of the overlay assay was used (see section 3.34) in which purified GST-α-actinin fusion proteins were tested for their ability to inhibit the interaction between ^{125}I-vinculin and nitrocellulose bound α-actinin (or fragments of α-actinin). A solid phase binding assay was also used. GST-α-actinin fusion proteins were immobilised on glutathione-linked agarose beads. Their ^{125}I-vinculin binding capacity was then assayed.

This chapter describes the various α-actinin constructs and the results of binding studies with these fragments.

4.2 METHODS.

4.21 GENERATION OF α-ACTININ CONSTRUCTS.

Specific regions of α-actinin DNA were generated from the α-actinin smooth muscle cDNA C17 using the polymerase chain reaction (PCR). PCR primers were designed such that BamH1 and EcoR1 restriction enzyme sites were engineered onto the ends of the α-actinin PCR product. The DNA was then ligated into the procaryote expression vector pGEX (Smith and Johnson, 1988). The clones were transformed into *E. coli* strain JM101 for expression. Transformants were then assayed for the presence of the correct fragment by at least two of the following methods: Restriction enzyme mapping: Western Blotting: DNA sequencing.

The PCR reactions were set up as follows:-

5μl 10x Taq polymerase buffer (Cambio)
4μl dNTP (each 0.2mM final concentration)
0.5μl (1ng) C17 in Bluescript
2.5μl each oligonucleotide primer (0.5mM final concentration)
35μl water
0.5μl Taq polymerase (Cambio)

A drop of paraffin was applied to the surface to prevent evaporation. The PCR oligonucleotide primers used to amplify different regions of the α-actinin cDNA are listed in table 4.1.

TABLE 4.1

The PCR primers used to generate the DNA fragments for the α-actinin constructs. See table 4.3 for details of constructs.

CONSTRUCT	PCR PRIMERS	
R1-697	Oligo 5'R1	Oligo 3'697
R1-632	Oligo 5'R1	Oligo 3'632
R1-3	Oligo 5'R1	Oligo 3'R3
Rep 2/3	Oligo 5'R2	Oligo 3'R3
V1-V2	Oligo 5'V1	Oligo 3'V2
V3-V4	Oligo 5'V3	Oligo 3'V4
V1-V5	Oligo 5'V1	Oligo 3'V5

The PCR primers are described in table 4.2. The bases 4 to 9 in the 5' and 3' primers respectively coded for BamH1 and EcoR1 restriction endonuclease sites. This meant that the amplified fragment could be digested with BamH1 and EcoR1 and cloned in the correct orientation into the BamH1/EcoR1 site of the relevant pGEX plasmid. The sequence of bases 1 to 3 of each primer was not important but their presence was required for efficient cutting of the restriction sites engineered onto the ends of the PCR products (New England Biolabs Catalogue, 1990/1991) The remainder of each 5' primer was identical to nucleotides of the sense strand of the α-actinin smooth muscle cDNA C17. Similarly the remainder of each 3' primer was identical to the nucleotides of the antisense strand of C17 denoted in column three of table 4.2. The length of the primers (excluding the restriction site) was designed such that each had a similar melting

TABLE 4.2

PRIMERS USED FOR PCR AMPLIFICATION

Primer	Primer Sequence (5'→3')(1)	Nucleotides In C17 cDNA(2)
Oligo 5'R1	AAA GGA TCC TTC TAC CAC GCC TTC TCA GGA	850-870
Oligo 3'697	AAA GAA TTC CTC CTG GAT CTG TTG GTG GT	2208-2189
Oligo 3'632	AAA GAA TTC ACG AAG TCG CTC ATT TTG TTG C	2013-1992
Oligo 3'R3	AAA GAA TTC CTC CTG TGG GGT GAT TGT AGT	1914-1894
Oligo 5'R2	AAA GGA TCC ATA AAC AAT GCC TGG GGT GGC	1207-1227
Oligo 5'V1	AAA GGA TCC ATT CGT GTG GGC TGG GAG CA	2254-2271
Oligo 3'V2	AAA GAA TTC CCG GGA CAT GAA GTC AAT GAA	2556-2536
Oligo 5'V3	AAA GGA TCC GAA ACA GCA GAT ACA GAT ACT G	2557-2578
Oligo 3'V4	AAA GAA TTC AAG GTC ACT TTC GCC ATA GAG C	2778-2757
Oligo 3'V5	AAA GAA TTC ATT CAT CTG TTC CTG GCT TAT TC	2364-2342

(1) The sequence of bases 1 to 3 was not important, but their incorporation allows efficient cutting of the PCR product by restriction enzymes. Bases 4 to 9 code for BamH1 and EcoR1 restriction endonuclease sites in the 5' and 3' primers respectively. The remaining nucleotides of the 5' and 3' primers were respectively identical to the sense and antisense strands of the α-actinin smooth muscle cDNA C17.

(2) Indicates the position of the PCR primers in the corresponding full length smooth muscle α-actinin clone C17 (Baron et al, 1987).

temperature (based on the rough guide that G+C and A+T contributed 4°C and 2°C respectively to the melting temperature).

A typical PCR cycle used was:-

30 cycles of:-

92°C	1.5 minutes
44°C	1.5 minutes
72°C	2 minutes

then:-

72°C	6 minutes

The reaction mix was then removed, ethanol precipitated, and resuspended in 10µl of water. The PCR product was cut with BamH1 and EcoR1 and purified from agarose gels as described in section 2.6.

The pGEX vector that would allow the incorporation of the PCR product in the correct reading frame was cut with BamH1 and EcoR1 and purified from agarose gels as described in section 2.6. The restriction endonuclease fragment of the α-actinin PCR product was ligated into the cut plasmid and then transformed into *E. coli* strain JM101 cells as described in section 2.6.

The various constructs used in chapter 4 are described in table 4.3.

4.22 SEQUENCING OF DNA CONSTRUCTS.

When necesary the DNA fragments were sequenced to confirm their identity.

TABLE 4.3

Complete list of α-actinin constructs used in chapter 4.

CONSTRUCT	RESIDUES ENCODED	DELETION	FUSION PROTEIN LINKED
ABD[1]	1-268[5]	-	-
E53[1]	240-749	-	-
ΔR1[2]	218-749	238-241[7] 245-363	GST
ΔR2[2]	218-749	238-241[7] 364-478	GST
ΔR3[2]	218-749	238-241[7] 479-599	GST
ΔR4[2]	218-749	238-241[7] 600-712	GST
GST-53[2]	218-749	238-241[7]	GST
CTD[3]	713-887	-	GST
R1-697	290-697[6]	-	GST
R1-632	290-632[6]	-	GST
R1-3	290-599[6]	-	GST
Rep 2/3	364-599	-	GST
V1-V2	713-813	-	GST
V3-V4	814-887	-	GST
V1-V5	713-749	-	GST
GST-ABD[4]	1-268[5]	238-241[7]	GST

[1] The production of these constructs is described in chapter 5. [2] Donated by Dr. A. Blanchard, Department of Biochemistry, Leicester University. [3] Donated by D. Millake, Department of Biochemistry, Leicester University. [4] Obtained from the ABD construct by digestion with BamH1 and EcoR1 followed by ligation into pGEX. [5] Initiating methionine is also encoded [6] Due to a BamH1 site within repeat 1, these constructs start at residue 290. [7] Residues 238 to 241 were deleted as the Met_{239}-Thr_{240} was shown to be susceptible to endogenous *E. coli* proteases.

ISOLATION OF PLASMID DNA FOR SEQUENCING.

DNA was isolated from a 10ml bacterial culture essentially as described in section 2.6. After the potassium acetate step the solution was phenol (1x) and phenol/chloroform (2x) extracted. DNA was then ethanol precipitated and the pellet was resuspended in 10µl of water. 3-5µl of DNA was diluted to 20µl with water and 3µl of freshly prepared 2M NaOH, 2mM EDTA was added and incubated at room temperature for 5 minutes. The DNA was then precipitated by the addition of 4-5µl of 3M sodium acetate and 90µl of ethanol and centrifuged for 15 minutes. The pellet was rinsed with 70% ethanol, air dried, and resuspended in 7µl of water ready for sequencing.

SEQUENCING REACTIONS.

The PCR insert subcloned into pGEX was sequenced using a primer to the reverse strand of pGEX close to the 3' end of the insert. The sequence of the primer was:-

5' ATGTGTCAGAGGTTTTC 3'

This primer was suitable for the 3 pGEX vectors.

Sequencing was carried out using the Sequenase kit obtained from USB (United States Biochemicals). This utilises the dideoxy chain termination method of Sanger et al (1977) with modifications. The enzyme, Sequenase, replaced Klenow fragment. ^{35}S-ATP was used instead of ^{32}P-ATP as it gave better resolution and involved lower levels of radioactivity.

The primer was annealed to the template as follows:-

1ng primer

2µl 5x Sequenase reaction buffer (20mM Tris/HCl, pH7.5, 10mM $MgCl_2$, 25mM NaCl final concentration)

2-4µg template DNA

water to 10µl

The mix was incubated at 37°C for 30 minutes. The reagents specified were those supplied with the USB Sequenase kit, unless otherwise stated.

To extend from the primer the following reagents were added:-

1µl DTT

1µl ^{35}S-ATP (Amersham, Catalogue Number SJ1304)

2µl dNTP mix (67nM final concentration)

2µl Sequenase (1 in 8 dilution with Sequenase dilution buffer)

Incubations were performed at room temperature for 2-3 minutes. The dilutions of dNTP and Sequenase and the time of incubation were such that the sequence could be read close to the primer. 3.5µl aliquots of the mix were then added to tubes containing 2.5µl of ddGTP, ddATP, ddTTP, and ddCTP respectively. These were incubated a for further 4-5 minutes when 4µl of 'stop mix' was added to each. Samples were boiled for 2-4 minutes prior to electrophoresis, as described below.

DENATURING POLYACRYLAMIDE GEL ELECTROPHORESIS.

Samples were electrophoresed on a 6% polyacrylamide gel (40x20x0.04cm) containing 43% urea (w/v). The running buffer was 0.5xTBE (45mM Tris/HCl, pH8.0, 45mM boric acid, 100mM EDTA).

The gel was run at 35W constant power for approximately 1.5 hours. The gel was fixed in 10% acetic acid, 10% methanol for 5 minutes, transferred to Whatman 3MM paper, and dried at 80°C under vacumn. The dried gel was then exposed to Kodak X-OMAT AR film overnight.

4.23 EXPRESSION OF α-ACTININ pGEX CONSTRUCTS.

Liquid cultures were grown in 2xTY with 0.1mg/ml ampicillin. Cultures were grown at 37°C to an optical density at 600nm of approximately 0.5. They were then induced by the addition of IPTG (0.5mM unless otherwise stated) and grown for a further 1-4 hours, depending on the size of the culture. Generally cultures were grown at 37°C post-induction. Some of the constructs were grown at 30°C post-induction as this gave a higher ratio of soluble to insoluble fusion protein. The cells were then harvested by centrifugation.

4.24 PURIFICATION OF GST-LINKED FUSION PROTEINS.

A single step purification was used to obtain soluble GST-linked fusion proteins. Cells were harvested from a bacterial culture that expressed the protein of interest (as described above). The cell pellet was resuspended in 1/50th the culture volume of MT-PBS (150mM NaCl, 12mM sodium phosphate, pH7.3). EDTA was added to 5mM, E64 (trans-Epoxysuccinyl-L-leucylamido-(4-guanidino) butane) (from Sigma) to 5μM, and Leupeptin (from Sigma) to 10μM. PMSF was added to 1mM immediately prior to the addition of Triton X-100 to a final concentration of 1% (v/v). The bacterial suspensions were sonicated on ice (typically 2x45 seconds, amplitude 8 micrometers) and centrifuged (8000g, 5 minutes) to remove insoluble material. 200-500μl of glutathione-agarose beads (50% slurry in MT-PBS;

previously swollen and washed in MT-PBS) were added to the supernatant and gently mixed for 5 minutes. The beads were washed 3 times with MT-PBS to remove unbound material. The fusion protein was then eluted from the beads by 3 successive (5 minute) washes with 0.5ml of 5mM reduced glutathione (in 50mM Tris, pH8.0). The eluates were pooled.

4.25 BINDING OF ^{125}I-VINCULIN TO α-ACTININ FUSION PROTEINS ADSORBED TO GLUTATHIONE-AGAROSE BEADS (SOLID PHASE BINDING ASSAY).

The GST-linked fusion proteins were bound to glutathione beads. The ability of ^{125}I-vinculin to bind to fusion proteins was then assayed by centrifugation.

The soluble fraction from a 50-100ml culture (cells resuspended in 0.5ml of MT-PBS) was obtained as described above. 350µl of glutathione-agarose beads (50% slurry in MT-PBS; previously swollen and washed in MT-PBS) were added to the supernatant and gently mixed for 5 minutes. The beads were washed 3 times with MT-PBS. The volume was made to 500µl and an aliquot was taken for protein estimation. The beads (and the tubes in which the assay was to be performed) were incubated in block buffer (MT-PBS, 0.1% Triton X-100 (v/v), 3% BSA (w/v)), for 2-3 hours with gentle mixing. Incubations were then set up containing immobilised α-actinin fusion protein and ^{125}I-vinculin in block buffer. These were incubated overnight with gentle mixing. The beads were then washed 5 times with MT-PBS. The radioactivity bound was then determined using a Beckman Gamma 5500 counter with a ^{125}I-Iso-window.

4.3 RESULTS.

4.31 CHARACTERISATION OF pGEX-α-ACTININ CONSTRUCTS.

The α-actinin pGEX constructs were characterised to demonstrate that the plasmids contained a DNA insert of the correct size, and that the plasmids expressed a protein of the appropriate size. Restriction enzyme mapping of the constructs using BamH1 and EcoR1 demonstrated that a DNA fragment of the correct size could be liberated from the pGEX plasmid. The V1-V5 plasmid was not tested in this manner as the fragment released by BamH1/EcoR1 digestion would have been difficult to identify on an agarose gel due to its small size. The α-actinin constructs were expressed and the expressed fusion proteins tested for their ability to react with a polyclonal antibody to α-actinin in Western Blotting. Generally the antibody cross reacted with fusion proteins that had a similar molecular weight to that deduced from the sequence (Table 4.4). However, the molecular weight of the R1-3 fusion protein was 49kDa, rather than the expected 63kDa. This suggested that the R1-3 fusion protein may be unstable.

The V1-V5 fragment failed to cross react with the anti-α-actinin antibody. However, this fragment only contained 4.17% of the α-actinin sequence and presumably lacked epitopes recognised by the antibody. Western blotting with a polyclonal anti-GST antibody identified a band at 30kDa, consistent with the expressed protein being a fusion protein rather than GST alone (27kDa). The authenticity of the V1-V5 pGEX construct was confirmed by DNA sequencing.

Table 4.4

Comparison of the expected and observed molecular weights of various α-actinin fusion proteins.

Fragment	Molecular Weight (kDa)†	
	Expected	Observed*
R1-697	75	67
R1-632	67	64
R1-R3	63	49
Rep 2/3	54	49
V1-V2	39	34
V3-V4	35	33
V1-V5	31	30
GST-ABD	58	56

† This value included 27kDa contributed by GST.

* Determined by SDS-PAGE.

4.32 PURIFICATION OF GST-LINKED FUSION PROTEINS.

A number of the GST-linked fusion proteins were purified as described in section 4.2. Purification by this method was dependent on the fusion protein being soluble. The proportion of protein in the soluble and insoluble fractions varied depending on the construct being expressed and the conditions used to induce expression of the fusion protein (see tables 4.5 and 4.6).

The GST-ABD, GST-53, CTD, V1-V2, and V3-V4 constructs were sufficiently soluble for further purification when the induction conditions described above were used. However, the V1-V5 fragment was largely insoluble. A greater proportion of the V1-V5 fusion protein was soluble if cultures were induced at 30°C rather than 37°C (see table 4.6). Varying the IPTG concentration had little effect.

The soluble proteins were purified to about 90% homogeneity, as described in section 4.2 (see figure 4.1). This method gave a good degree of purification. However, the elution of the GST fusion protein from the glutathione agarose beads was inefficient. Approximately 15 to 20% of the fusion protein remained bound to the glutathione beads after two elutions with glutathione. Since large amounts of the fusion protein were produced, the low yield was of little consequence. More fusion protein could be eluted with further washes. Most, if not all, of the endogenous bacterial protein was effectively removed by this purification. Western blotting demonstrated that the bands contaminating the fusion proteins were generally degradation products. Despite the inclusion of inhibitors during cell lysis, the GST-53 construct was especially susceptible to degradation. Prominent bands of 53, 41, and 27kD were produced,

Table 4.5
The solubility of various fusion proteins.

FRAGMENT	PROPORTION SOLUBLE (% and standard deviation)
GST-53	71 (7)
R1-697	12 (12)
R1-632	13 (3)
R1-3	69 (7)
V1-V2	58 (13)
V3-V4	62 (5)
V1-V5	17 (11)
GST-ABD	64 (15)

Cultures were grown and induced at 37°C. They were induced by the addition of IPTG to 0.5mM once the optical density at 600nm of the culture was 0.5. The cultures were grown for a further 80 minutes before harvesting. Following sonication, the soluble and insoluble cell fractions were separated by centrifugation. The cell pellet was resuspended in a volume of TBS equal to that of the supernatant. Equal volumes of supernatant and the resuspended pellet were electrophoresesd on SDS-PAGE. The relevant fragments were quantified using the LKB densitometer. The average of two experiments are shown.

Table 4.6

Affect of various induction conditions on the solubility of the V1-V5 fusion protein.

INDUCTION CONDITIONS		PROPORTION
IPTG	TEMPERATURE	SOLUBLE (%)
0	30	N/A†
0	37	N/A†
0.05mM	30	41
0.05mM	37	28
0.5mM	30	38
0.5mM	37	17

† Not applicable since there was no significant expression of the fusion protein.

Cultures were grown at 37°C until an optical density at 600nm of 0.5 was reached. They were then induced and grown at the stated temperature for a further 80 minutes before harvesting. Following sonication, the soluble and insoluble cell fractions were separated by centrifugation. The cell pellet was resuspended in a volume of TBS equal to that of the supernatant. Equal volumes of supernatant and the resuspended pellet were electrophoresesd on SDS-PAGE. The relevant fragments were quantified using the LKB densitometer. The average of two experiments are shown.

FIGURE 4.1

THE FUSION PROTEINS PURIFIED UTILISING GLUTATHIONE-AGAROSE BEADS.

The figure shows a Coomassie stained SDS-PAGE minigel of the soluble fusion proteins. See table 4.3 for details of the fusion proteins. Molecular weights are indicated at each side.

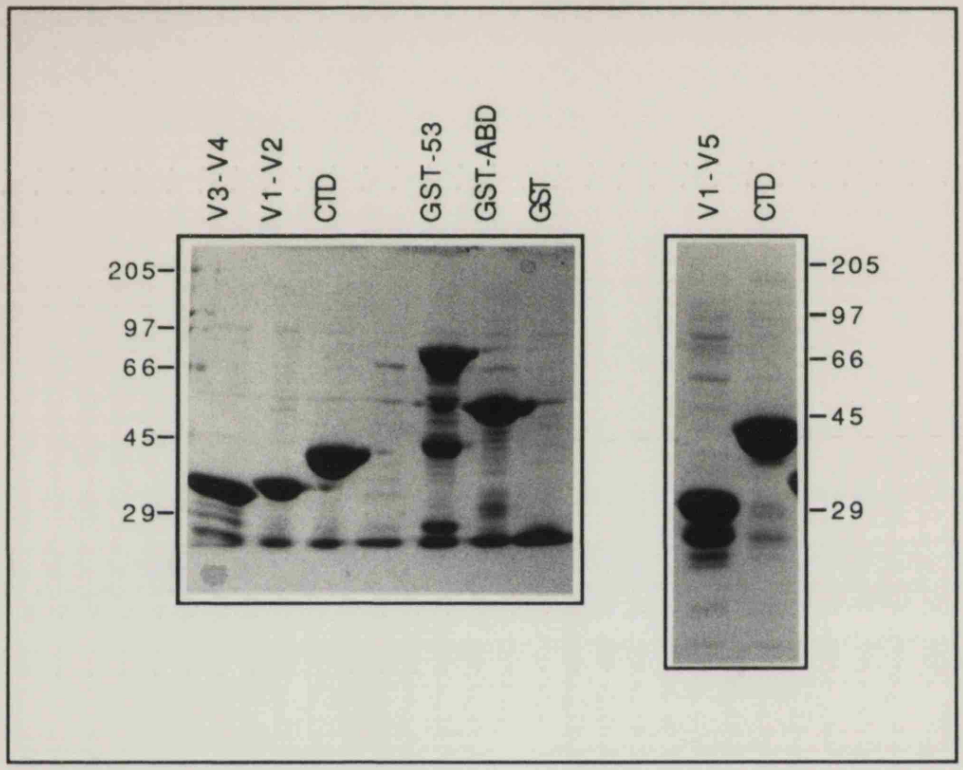

along with various minor bands. Though not purified, the R1-697, R1-632, and R1-3 constructs were also susceptible to degradation by endogenous proteases. The pattern of degradation fragments of the R1-697, R1-632, and R1-3 constructs was similar to that produced by the GST-53 construct.

4.33 ^{125}I-VINCULIN OVERLAYS.

Initial screening of α-actinin fusion proteins was carried out using the ^{125}I-vinculin overlay assay. The assay was performed as described in chapter 3. Each fusion protein was assayed at least three times. The results were reproducible.

The E53 construct bound ^{125}I-vinculin. Binding was markedly reduced by an excess of unlabelled vinculin (see figure 4.2). The ABD construct did not bind even when equivalent amounts (by weight) of the ABD and the E53 construct were used, even though this approximately represented a 2 fold molar excess of the ABD construct.

The region within the E53 construct that was responsible for binding ^{125}I-vinculin was examined. Four constructs that had repeats 1, 2, 3, and 4 deleted were used along with the CTD construct which encodes the C-terminal domain (residues 713 to 887) (Figure 4.6). Surprisingly, the constructs ΔR1, ΔR2, ΔR3, ΔR4, and CTD were all shown to bind ^{125}I-vinculin. Binding of ^{125}I-vinculin was diminished by the presence of unlabelled vinculin in the overlays (see figure 4.3).

FIGURE 4.2

^{125}I-VINCULIN BINDING TO THE EXPRESSED α-ACTININ REPEAT DOMAIN OR ACTIN BINDING DOMAIN ASSAYED USING THE OVERLAY TECHNIQUE.

The figure shows (i) a Coomassie stained SDS-PAGE minigel (12%) of the samples (ii) the samples electroblotted onto nitrocellulose and overlaid with ^{125}I-vinculin (1.5×10^{-8}M) and (iii) the samples electroblotted onto nitrocellulose and overlaid with ^{125}I-vinculin (1.5×10^{-8}M) plus a 100 fold excess of unlabelled vinculin. The samples were the α-actinin actin binding domain (ABD), the repeats from α-actinin (E53), and intact α-actinin. Molecular weights are indicated up the vertical axis of the figure.

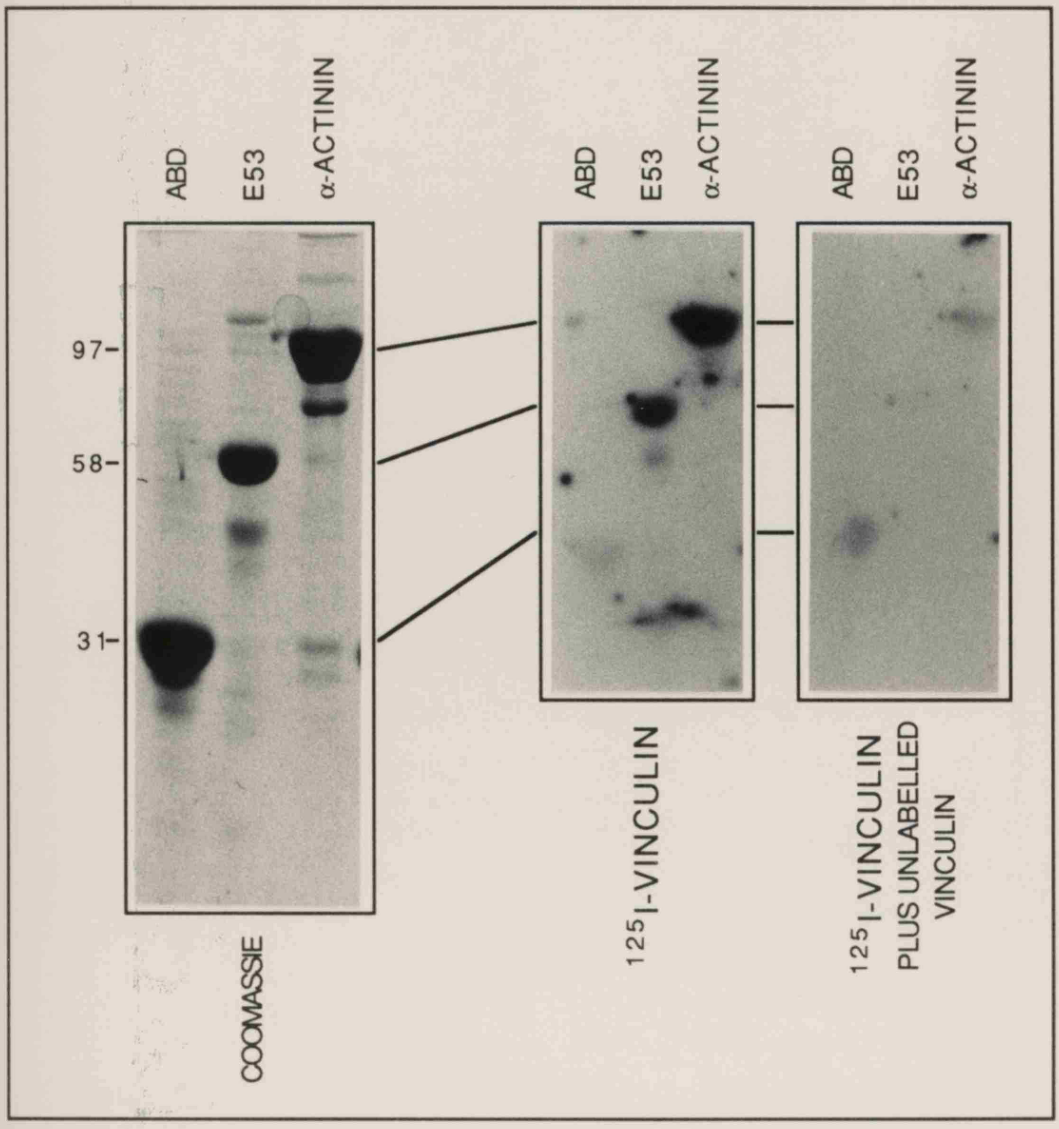

FIGURE 4.3

^{125}I-VINCULIN BINDING TO THE α-ACTININ C-TERMINAL DOMAIN FUSION PROTEIN AND TO FUSION PROTEINS OF THE α-ACTININ REPEATS THAT HAVE INDIVIDUAL REPEATS DELETED, ASSAYED BY THE OVERLAY TECHNIQUE.

The figure shows (i) a Coomassie stained SDS-PAGE minigel of the samples (ii) the samples electroblotted onto nitrocellulose and overlaid with ^{125}I-vinculin (1.5×10^{-8}M) and (iii) the samples electroblotted onto nitrocellulose and overlaid with ^{125}I-vinculin (1.5×10^{-8}M) plus a 100 fold excess of unlabelled vinculin. The samples were cell lysates containing the constructs ΔR1, ΔR2, ΔR3, ΔR4, CTD, GST alone, and molecular weight markers. Refer to table 4.3 for details of fusion proteins.

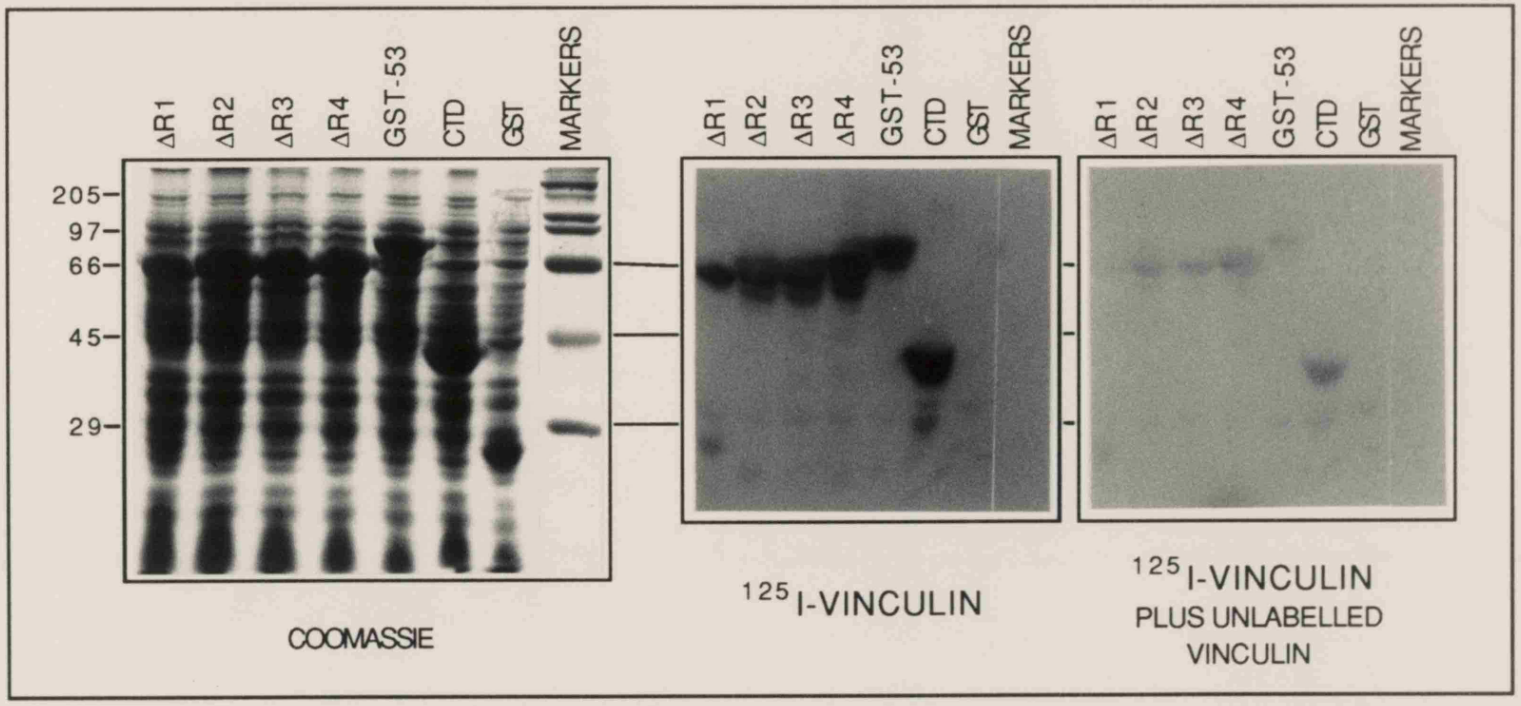

Other constructs were made and assayed for ^{125}I-vinculin binding (Figure 4.6). The reason for making these constructs will be mentioned in the discussion. Of these constructs the Rep 2/3, R1-697, R1-632, R1-3, and V3-V4 fusion proteins did not bind to ^{125}I-vinculin. However, the V1-V2 construct did bind ^{125}I-vinculin (Figure 4.4) and binding was reduced by the presence of unlabelled vinculin (not shown).

The smallest fusion protein tested was the V1-V5 construct (Figure 4.6). This covered α-actinin residues 713 to 749 inclusive. ^{125}I-vinculin bound to V1-V5 fragment in the overlay assay and the binding of the ^{125}I-vinculin was diminished by the presence of unlabelled vinculin (see figure 4.5).

The purified GST-ABD, GST-53, CTD, V1-V5 fragments, and GST alone were then assayed for their ability to inhibit the binding of ^{125}I-vinculin GST-53 and CTD fusion proteins and α-actinin blotted onto nitrocellulose. The GST-53, CTD, and V1-V5 fusion proteins produced a large reduction in the binding of ^{125}I-vinculin to nitrocellulose bound α-actinin, GST-53 fragment, and CTD fragment (Figure 4.7). The GST alone and the GST-ABD caused some inhibition though this was much less than that produced by the GST-53 and CTD fragments.

Hence the fusion protein containing residues 713 to 749 of α-actinin, and larger fusion proteins encompassing that region, were shown to bind ^{125}I-vinculin.

FIGURE 4.4

^{125}I-VINCULIN OVERLAY OF THE FUSION PROTEINS R1-3, R1-632, R1-697, V1-V2, V3-V4, AND GST-ABD.

The figure shows (i) a Coomassie stained SDS-PAGE gel of the samples (ii) and the samples electroblotted onto nitrocellulose and overlaid with ^{125}I-vinculin (1.5×10^{-8}M). The samples were cell lysates containing the constructs R1-3, R1-632, R1-697, V1-V2, V3-V4, GST-ABD, α-actinin, and molecular weight markers.

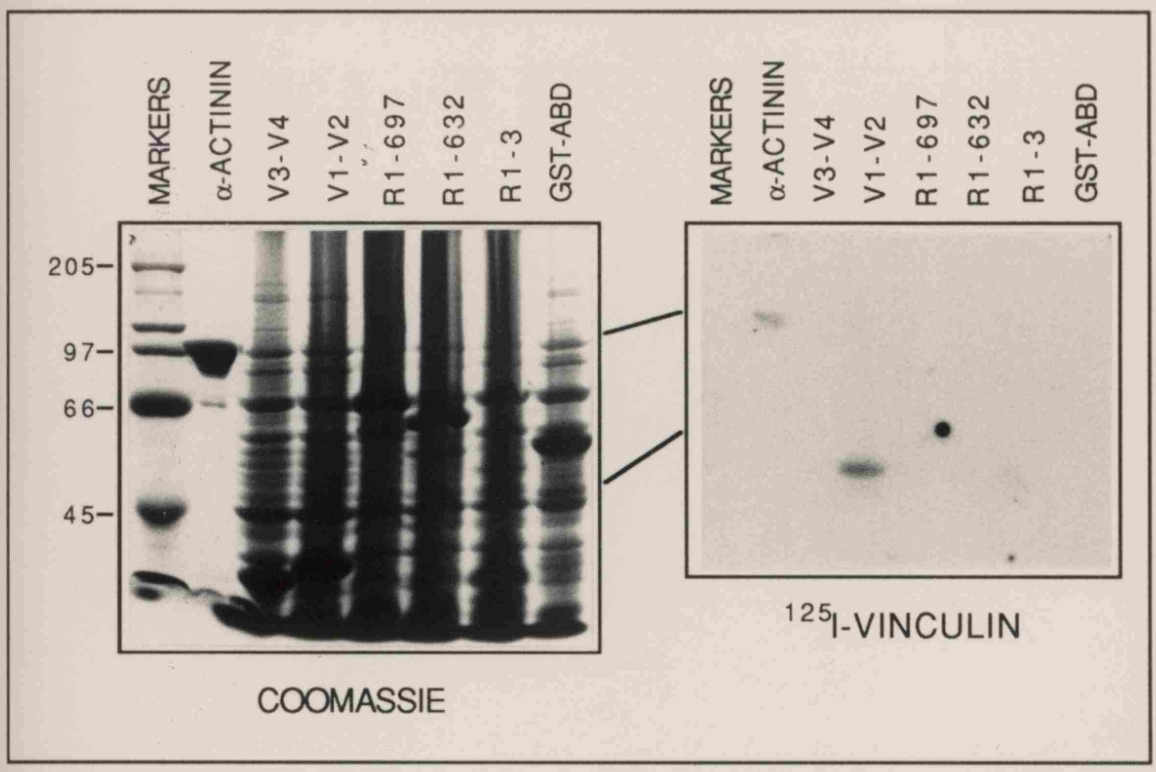

FIGURE 4.5

^{125}I-VINCULIN OVERLAY OF α-ACTININ AND THE V1-V5 FUSION PROTEIN.

The figure shows (i) a Coomassie stained SDS-PAGE gel of the samples (ii) the samples electroblotted onto nitrocellulose and overlaid with ^{125}I-vinculin $(1.5\times10^{-8}M)$ and (iii) the samples electroblotted onto nitrocellulose and overlaid with ^{125}I-vinculin $(1.5\times10^{-8}M)$ plus a 100 fold excess of unlabelled vinculin. As indicated, the samples were α-actinin and a cell lysate containing the V1-V5 fusion protein.

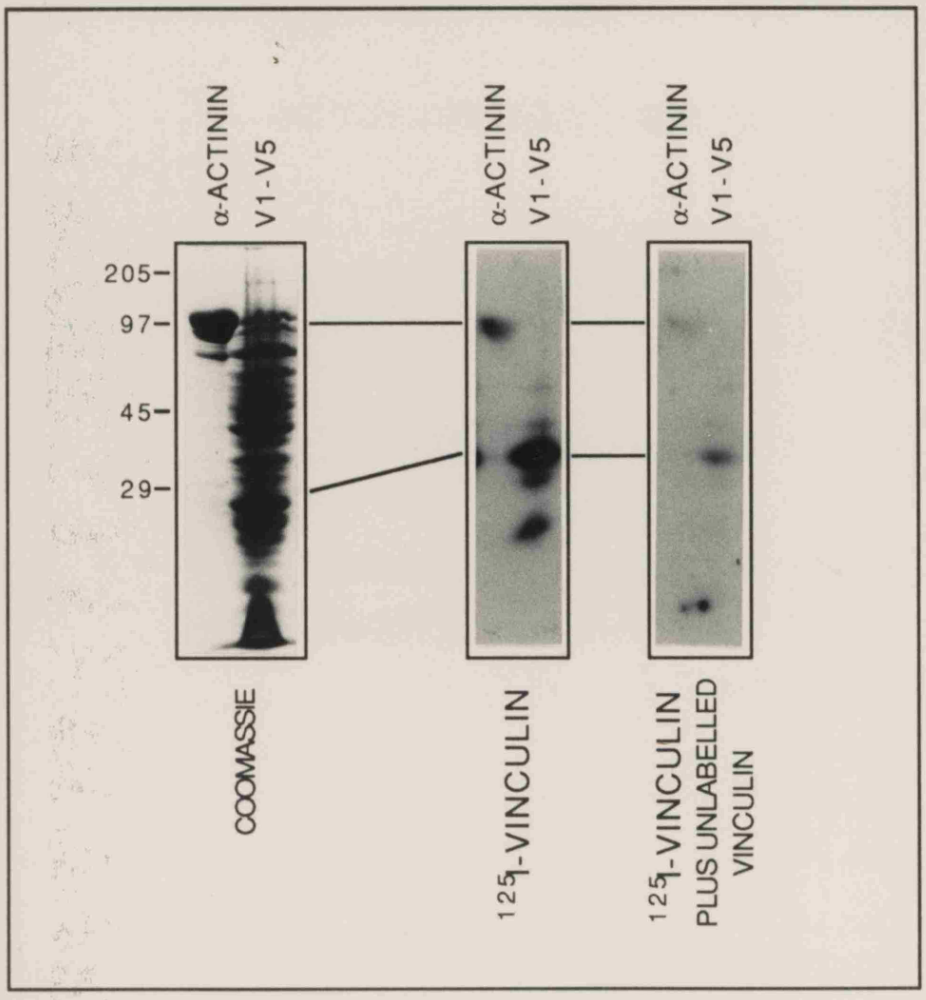

FIGURE 4.6

Diagram showing the various α-actinin fragments tested for their ability to bind ^{125}I-vinculin. Black bars indicate the fragments that bound ^{125}I-vinculin whilst the open bars denote the fragments which did not bind ^{125}I-vinculin. TL53 and TL27 denote the thermolytic fragments of α-actinin described in chapter 3.

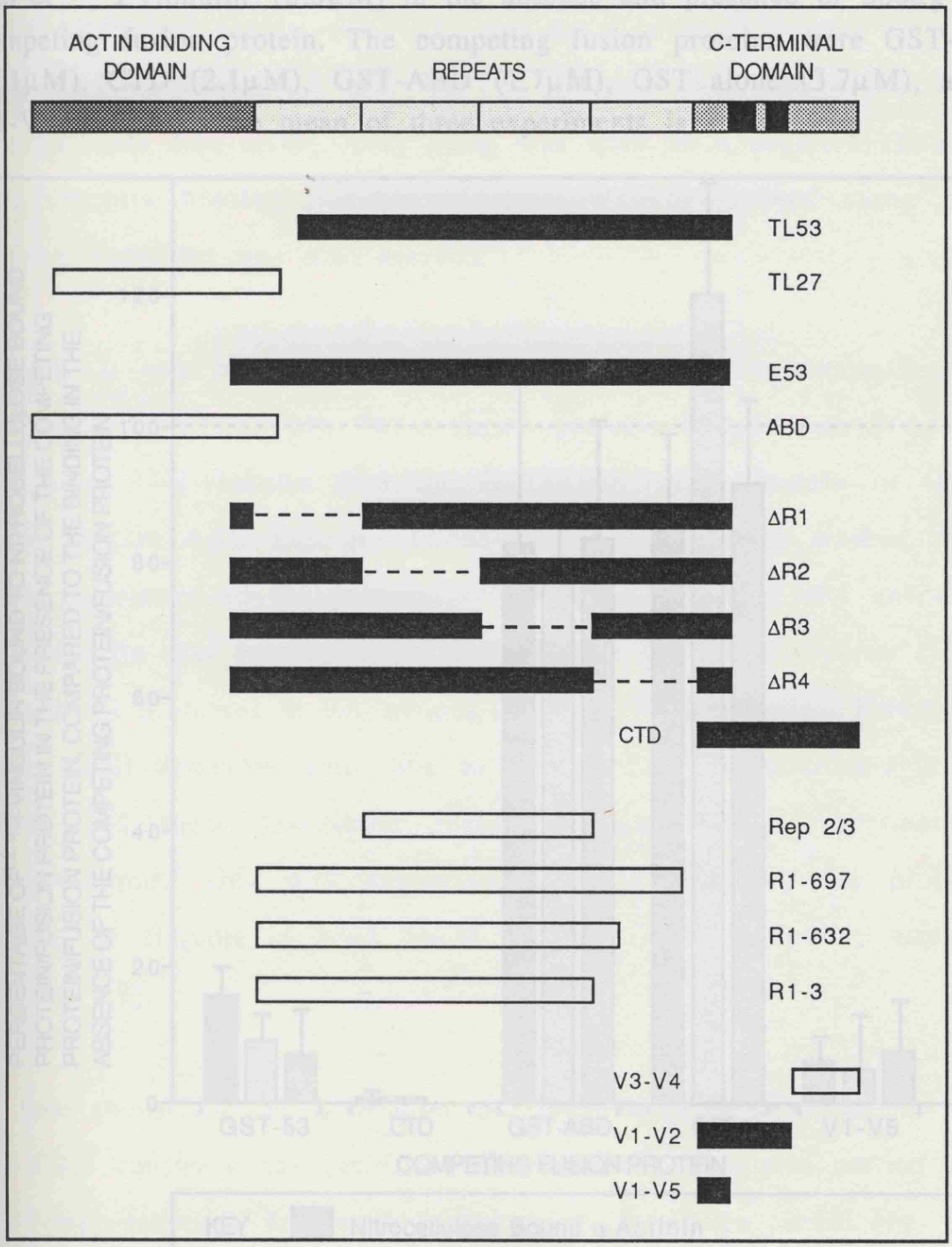

FIGURE 4.7

DEMONSTRATION OF THE EFFECT OF FREE α-ACTININ AND α-ACTININ FUSION PROTEINS ON THE BINDING OF ^{125}I-VINCULIN TO NITROCELLULOSE BOUND α-ACTININ AND α-ACTININ FUSION PROTEINS.

Nitrocellulose bound α-actinin, GST-53, and CTD were incubated in 5ml of ^{125}I-vinculin (8.5μM) in the absence and presence of 500μg of competing fusion protein. The competing fusion proteins were GST-53 (1.1μM), CTD (2.1μM), GST-ABD (1.7μM), GST alone (3.7μM), and V1-V5 (3.2μM). The mean of three experiments is shown.

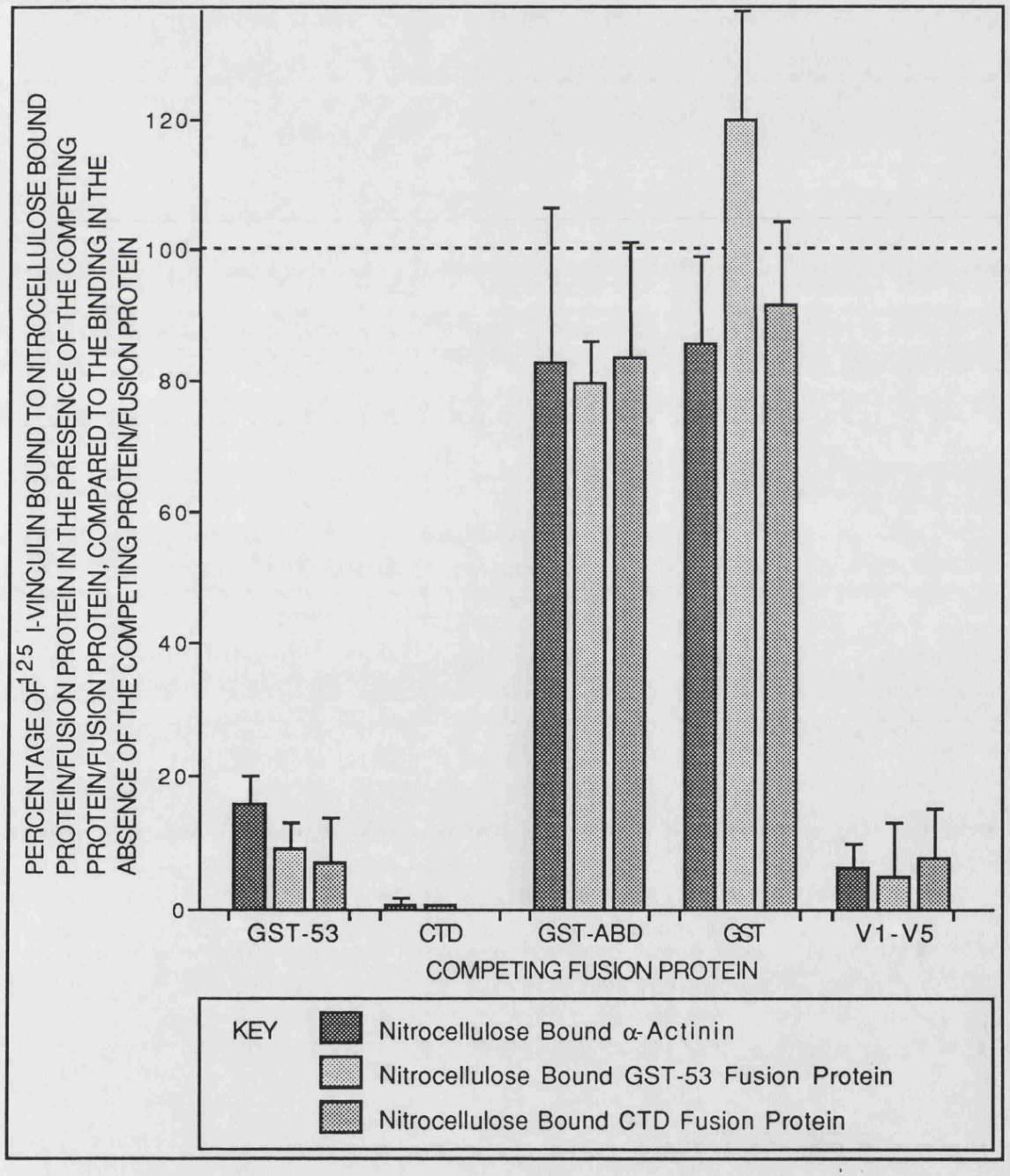

4.34 LOCALISATION OF THE VINCULIN BINDING SITE WITHIN α-ACTININ USING THE SOLID PHASE BINDING ASSAY.

^{125}I-Vinculin was tested for its ability to bind to GST fusion protein/glutathione agarose bead complexes. The three domains of α-actinin were assayed. These were the actin binding domain (GST-ABD), the repeats (GST-53), and the C-terminal domain (CTD). Two fragments (V1-V2 and V3-V4) derived from the C-terminal domain were also tested. GST alone was used as a negative control. The vinculin binding domain (construct V1-V5) defined using the overlay technique was also assayed.

Initially it was shown that the GST-53 and CTD constructs bound ^{125}I-vinculin ($3x10^{-8}$M). These fusion proteins bound some 5 to 10 fold more ^{125}I-vinculin than the GST-ABD fusion protein or GST alone (Figure 4.8). The glutathione-agarose beads were washed five times to remove all the unbound ^{125}I-vinculin. Most of the unbound ^{125}I-vinculin was removed with the first 2-3 washes. Thereafter there were small decreases in the amount of bound ^{125}I-vinculin. However, these small decreases were due to losses of the glutathione-agarose beads and their associated fusion protein during experimental manipulations. This was demonstrated by determining the protein content of aliquots of bead bound construct after successive washes (Figure 4.9).

A time course for the association and dissociation of ^{125}I-vinculin to the CTD construct was performed (Figure 4.10). This was carried out for two reasons. It demonstrated that the time used for the incubation of fusion proteins in ^{125}I-vinculin was sufficient for binding to have occurred. Maximum binding had occurred after

FIGURE 4.8

INVESTIGATION OF THE BINDING OF ^{125}I-VINCULIN TO α-ACTININ USING THE SOLID PHASE BINDING ASSAY.

Approximately 50μg of the fusion proteins indicated (linked to glutathione-agarose beads) was incubated with ^{125}I-vinculin ($3x10^{-8}$M) (specific activity 130,000cpm/μg). The beads were counted following aspiration of the vinculin solution (columns 0). The ^{125}I-vinculin bound to the glutathione-agarose beads was then determined following each of five successive 500μl washes (columns 1 to 5). The protein was then eluted from the beads with 2x1ml washes of 5mM glutathione (columns A and B) and 2 washes of 10mM glutathione (columns C and D). The mean of two experiments is shown.

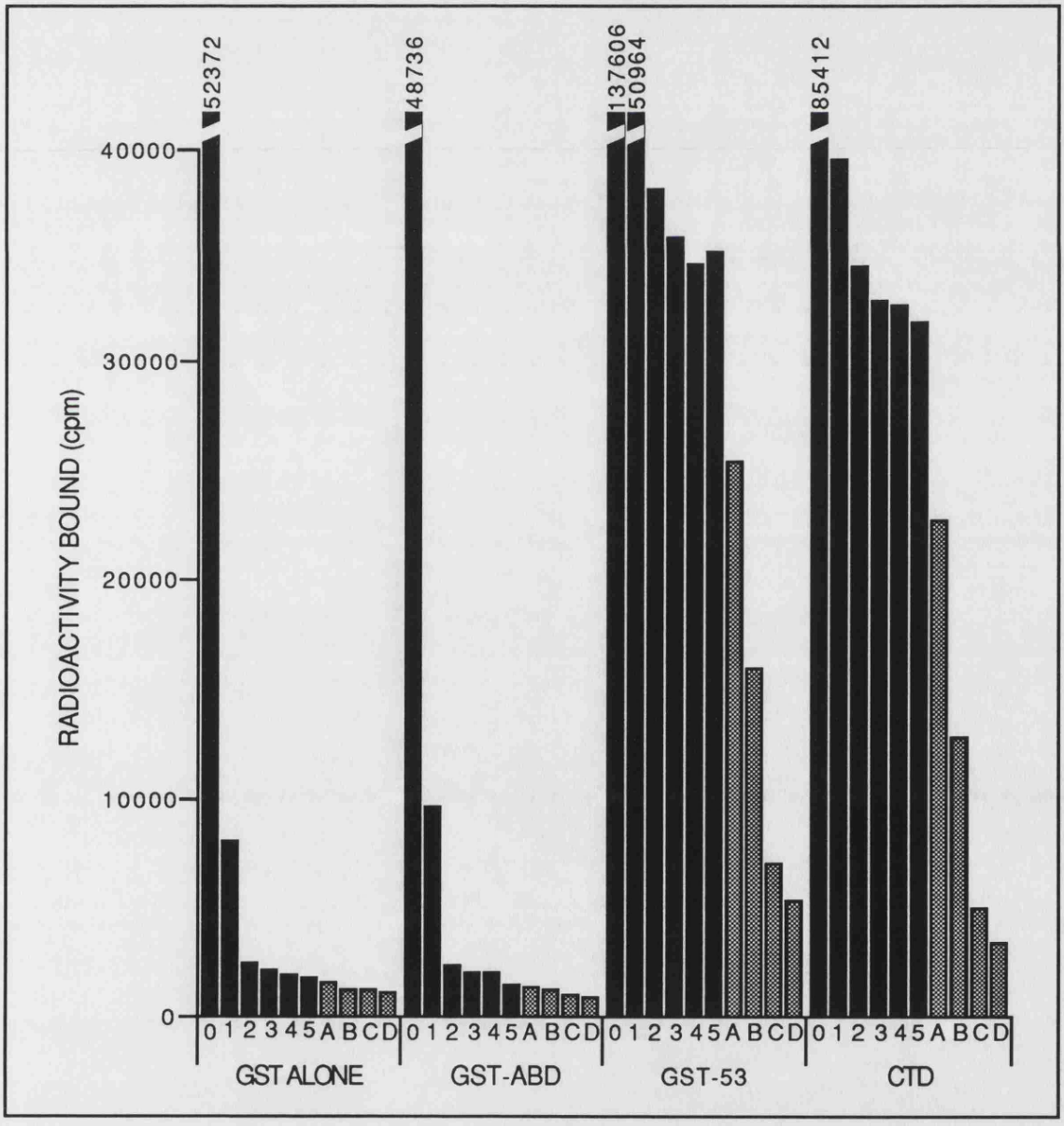

FIGURE 4.9

INVESTIGATION OF THE BINDING OF ^{125}I-VINCULIN TO α-ACTININ USING THE SOLID PHASE BINDING ASSAY: DEMONSTRATION OF BEAD LOSS DURING SUCCESSIVE WASHES.

Approximately 30μg of the CTD fusion protein (bound to 10μl of glutathione-agarose beads) was diluted to 1000μl with MT-PBS. A 100μl aliquot was taken and the protein content assayed (Wash 0). The remaining 900μl was mixed, centrifuged, and the supernatant aspirated. The pellet had MT-PBS added to 900μl. A 100μl aliquot was taken and the protein content assayed (Wash 1). This was repeated several times as shown.

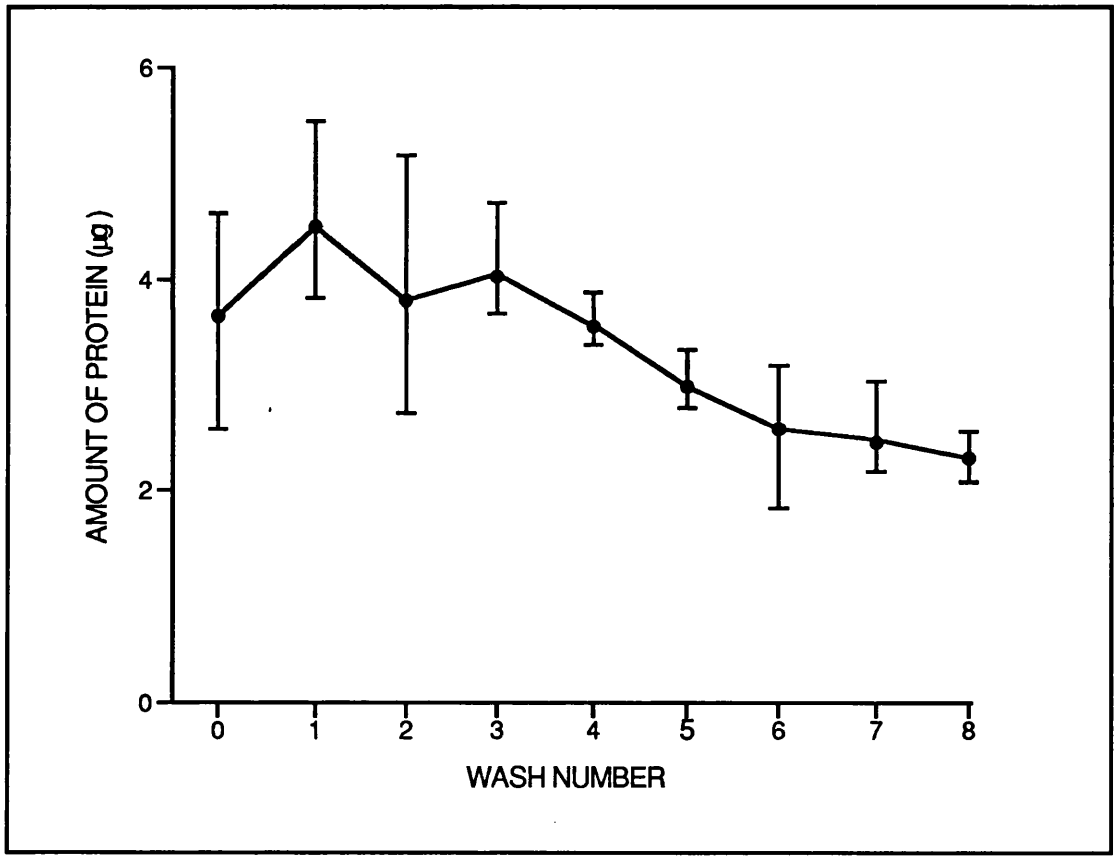

FIGURE 4.10

DEMONSTRATION OF BINDING AND DISSOCIATION OF ^{125}I-VINCULIN TO α-ACTININ FUSION PROTEINS USING THE SOLID PHASE BINDING ASSAY.

The CTD (2.8×10^{-6}M) and V3-V4 (3.6×10^{-6}M) fusion proteins (bound to glutathione-agarose beads) were incubated with ^{125}I-vinculin (8×10^{-8}M)(specific activity 144,000cpm/μg). At the times indicated 200μl (25μg) aliquots were removed. The radioactivity bound was counted following 5 washes of the beads. After 50 hours the ^{125}I-vinculin solution was replaced, after washing, with MT-PBS.

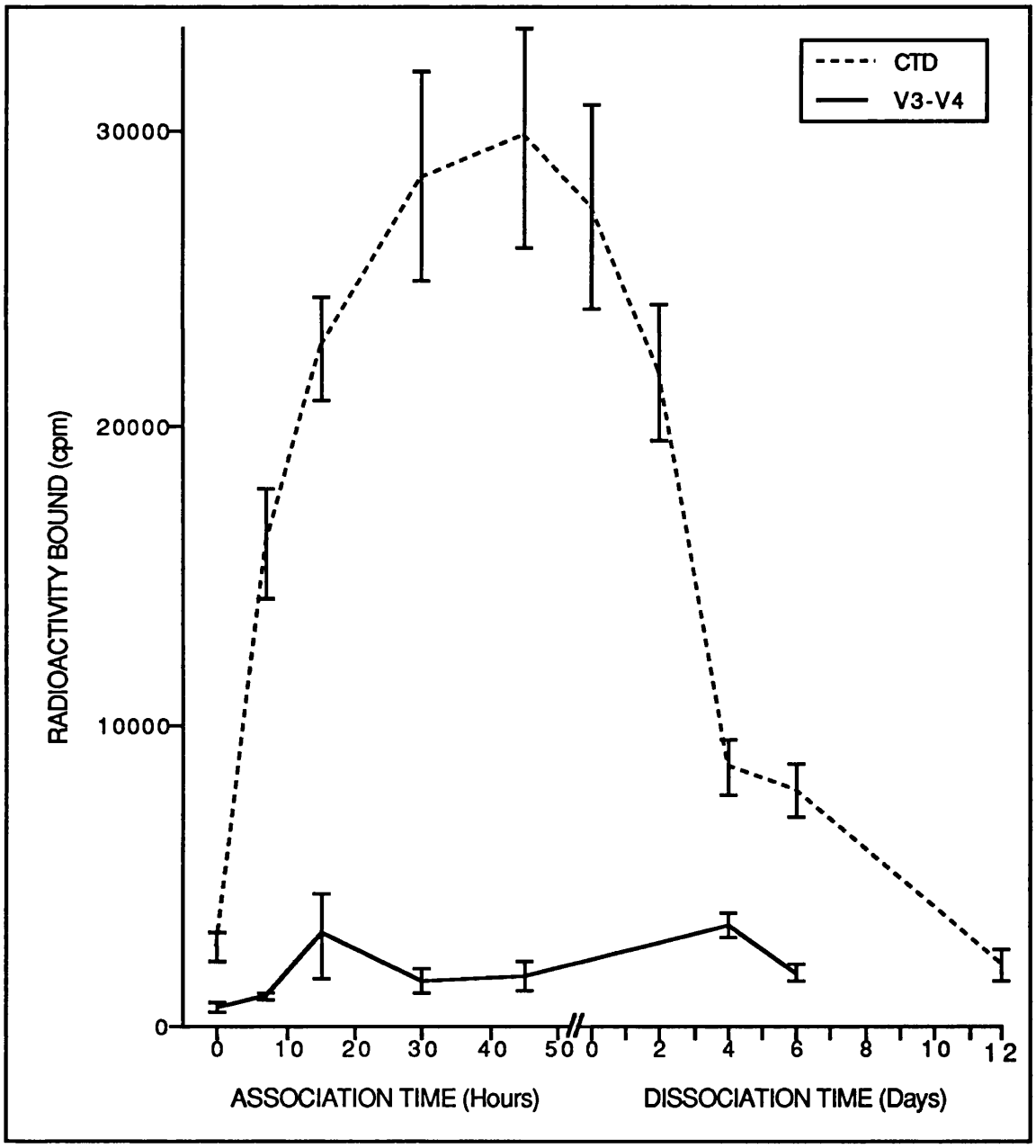

approximately 48 hours. There was appreciable (50%) binding after 8 hours. Dissociation of bound ^{125}I-vinculin following replacement of the ^{125}I-vinculin solution by buffer alone was slow. After 48 hours the CTD fragment retained about 80% of the ^{125}I-vinculin. This showed that any bound ^{125}I-vinculin would not be removed by the washes used in the various assays. The results also demonstrated that binding was reversible. It was assumed that other vinculin binding fusion proteins would exhibit a similar time course.

Binding of ^{125}I-vinculin ($3x10^{-8}$M) to the GST-53 and CTD fusion proteins was diminished by 30-40% when a 50 fold excess of unlabelled vinculin was added to the incubation (Figure 4.11). The reduction of ^{125}I-vinculin binding to the GST-ABD construct and GST alone was approximately +10 to -10%.

Elution of the GST-53 and CTD fusion proteins from the beads with glutathione produced a significant decrease in the amount of radioactivity retained (Figure 4.8). After four elutions the retained activity was some seven fold less. This was not as low as that for the GST-ABD fusion protein or GST alone. However, the retained activity was still falling after the fourth elution. This was consistent with the inefficient elution of fusion proteins from glutathione-agarose beads that was previously noted (see section 4.32). Similar elution of the GST-ABD fusion protein and GST alone with glutathione had little effect on the amount of ^{125}I-vinculin retained by the glutathione-agarose beads. The small decreases in the amount of ^{125}I-vinculin retained by the GST-ABD fusion protein and GST alone following successive elutions were similar to the small decreases due to successive washes.

FIGURE 4.11
INVESTIGATION OF THE BINDING OF ^{125}I-VINCULIN TO α-ACTININ USING THE SOLID PHASE BINDING ASSAY: REDUCTION OF ^{125}I-VINCULIN BINDING PRODUCED BY CO-INCUBATION OF ^{125}I-VINCULIN WITH UNLABELLED VINCULIN.

Approximately 50μg of the fusion proteins indicated (linked to glutathione-agarose beads) was incubated with (i) ^{125}I-vinculin ($3x10^{-8}$M) (specific activity 130,000cpm/μg) and (ii) ^{125}I-vinculin ($3x10^{-8}$M) plus a 50 fold excess of unlabelled vinculin. The ^{125}I-vinculin bound to the glutathione-agarose beads/fusion protein were counted following aspiration of the vinculin solution and five successive washes of 500μl. The protein was then eluted from the beads with 2x1ml washes of 5mM glutathione and two washes of 10mM glutathione and the ^{125}I-vinculin retained by the beads was counted. The mean of duplicate experiments is indicated.

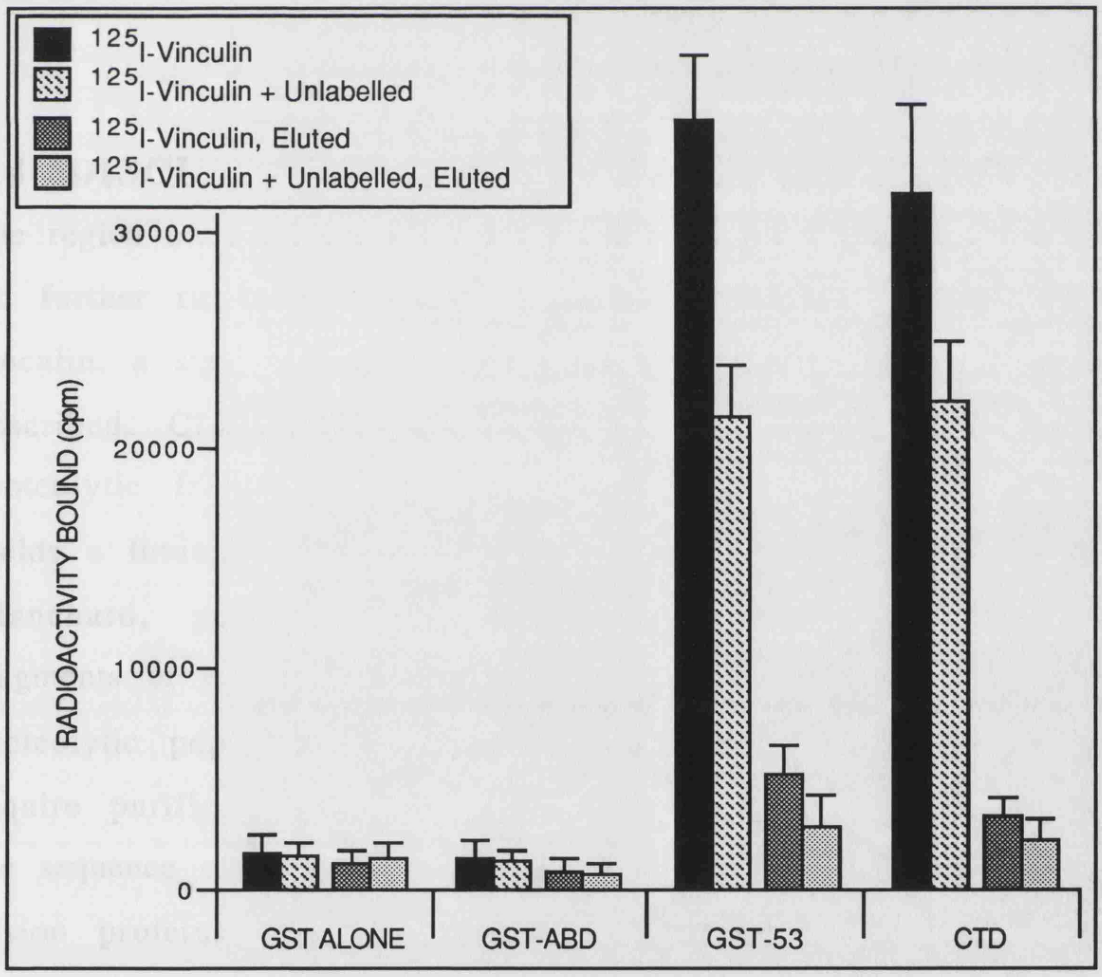

There was a degree of non-specific binding of ^{125}I-vinculin to the glutathione-agarose beads. The non-specific binding to the beads was more marked than any non-specific binding to the GST alone or the GST-ABD fusion protein. This was shown because elution of the fusion protein with glutathione had no apparent effect on the GST and GST-ABD samples.

The V1-V2, V3-V4, and V1-V5 fusion proteins were also assayed (Figure 4.12). The V1-V2 and V1-V5 fragments bound similar amounts of ^{125}I-vinculin to the GST-53 and CTD constructs. The V3-V4 fusion protein bound similar amounts of ^{125}I-vinculin to the GST-ABD construct or GST alone.

4.4 DISCUSSION.

The region of α-actinin that binds to vinculin had not been defined. To further resolve the region of α-actinin involved in binding vinculin, a series of α-actinin fusion proteins were generated as described. Cloned fusion proteins have several advantages over proteolytic fragments of α-actinin. Digestion of native α-actinin yields a limited number of fragments (Imamura et al, 1988; Dr. A. Blanchard, personal communication). Mapping the proteolytic fragments of α-actinin is time consuming and problematical. To use proteolytic peptides in assays other than the overlay assay would require purification protocols tailored to each peptide. In contrast the sequence of the expressed α-actinin fragments is known, and the fusion proteins can be rapidly purified by the same purification protocol in each case. However, the expressed fusion proteins are found to be distributed between both the soluble and insoluble

FIGURE 4.12
INVESTIGATION OF THE BINDING OF ^{125}I-VINCULIN TO α-ACTININ USING THE SOLID PHASE BINDING ASSAY.
Approximately 50μg (in 300μl total) of the fusion proteins indicated (linked to glutathione-agarose beads) was incubated with ^{125}I-vinculin ($3x10^{-8}$M) (specific activity 140,000cpm/μg). The beads were counted following aspiration of the vinculin solution and 5 successive washes of 500μl. The mean of duplicate experiments is indicated.

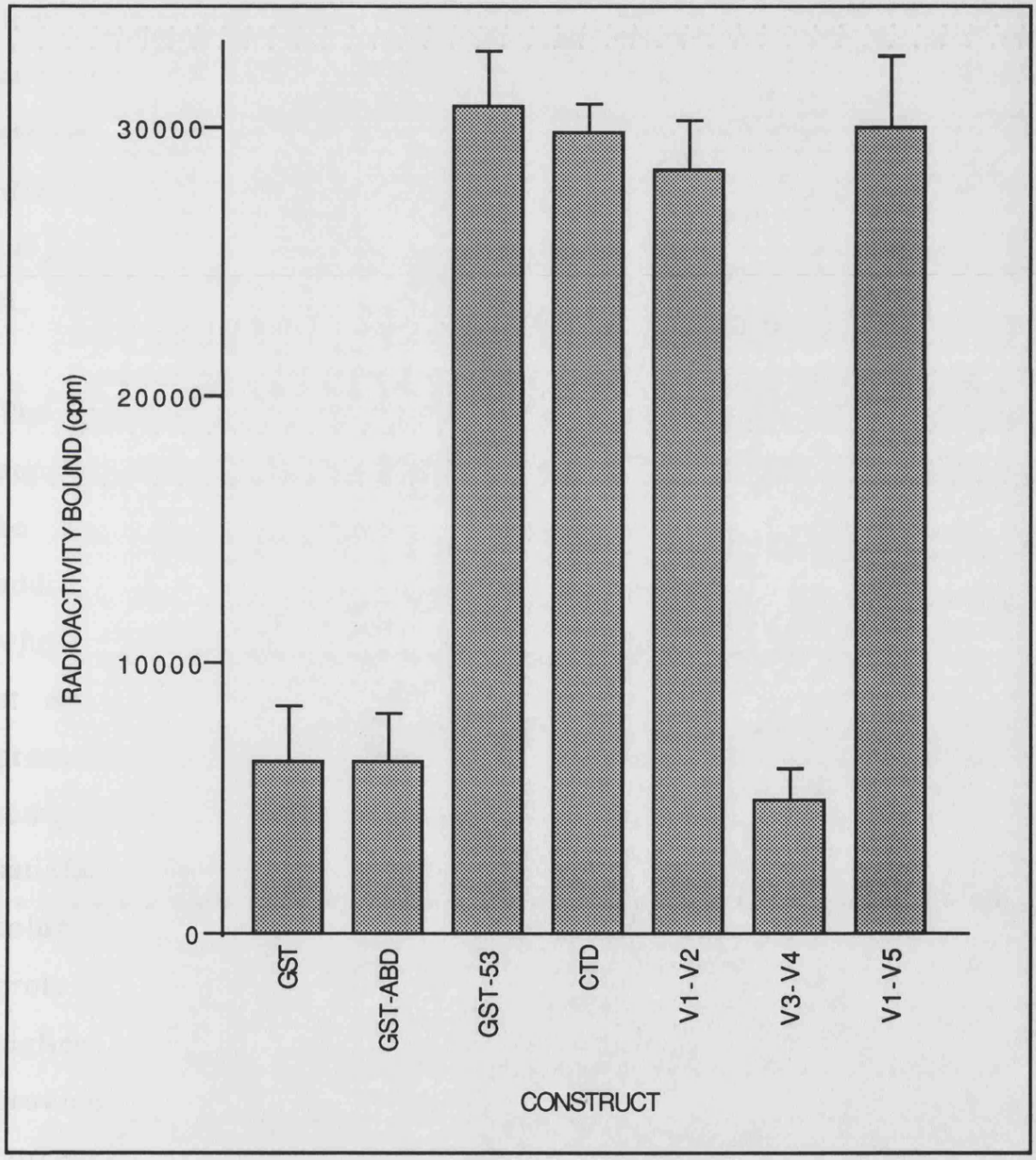

fractions of the cell homogenate. Insoluble protein is probably contained within inclusion bodies. Inclusion bodies are dense amorphous non-membrane bound protein/RNA/DNA aggregates that can be separated easily from bacterial lysates by centrifugation (Mitraki and King, 1989; Schein, 1989). As previously noted, fusion protein solubility is not related to size (Schein, 1989). For example, the GST-53 (88kDa) and R1-3 (63kDa) fusion proteins were largely soluble. However, the R1-697 (75kDa) and R1-632 (67kDa) constructs which contain residues within GST-53 and which both contained R1-3 were largely insoluble. The constructs ΔR1 and ΔR 4 were markedly more soluble than constructs ΔR2 and ΔR3 despite only differing in which of the homologous repeats was removed (Dr. A. Blanchard, personal communication).

The one step purification procedure of the GST fusion proteins was dependent on the protein being soluble. Expressed protein can often be renatured and purified from inclusion bodies, but this entails additional extraction steps. The V1-V5 fragment was largely insoluble when expression was induced at 37°C, but lowering the temperature at which the cells were induced doubled the amount of soluble fusion protein. The increased solubility of proteins expressed at lower temperatures appears to be a general phenomena though no satisfactory explanation has been provided. It has been shown that solubility is not related to the thermal stability of an expressed protein. One suggestion for the formation of inclusion bodies at higher induction temperatures is that high expression rates do not provide sufficient time for the nascent polypeptide chain to fold correctly, though no direct correlation has been demonstrated (Schein, 1989).

A number of the fusion proteins expressed in this study were susceptible to the action of endogenous *E. coli* proteases. Degradation of fusion proteins containing the α-actinin repeats was more marked than that of fusion proteins containing other regions of the α-actinin molecule. Degradation occurred before the protein was extracted, since cell extracts that were immediately boiled in SDS sample buffer also showed evidence of degradation. A possible explanation for the protease sensitivity of the fusion proteins containing α-actinin repeats is that they may be expressed as monomers which may therefore have exposed additional protease sensitive sites hidden in the native dimer. Another possibility is that the fusion proteins are not stable because their termini do not coincide with the functional repeat domain. Recently the start/finish of the spectrin repeat was shown to be residue 23 within the consensus repeat sequence (Winograd et al, 1991). When a single repeat starting and finishing at residue 23 was expressed it formed a stable protease resistant domain. Repeats that were expressed that were a few residues out of phase were sensitive to protease.

The observed molecular weight of some of the fusion proteins differed to the value deduced from the amino acid sequence. However, such differences have previously been observed. The molecular weight of smooth muscle α-actinin was shown to be 96kDa when examined on the same SDS-PAGE gels, whereas the predicted molecular weight was 103kDa (Baron et al, 1987a). It has been demonstrated that a single amino acid substitution can affect the mobility of a protein on SDS-PAGE gels by up to ten percent (De Jong et al, 1978).

Using ^{125}I-vinculin overlays, the localisation of the vinculin binding site to the α-actinin repeats was again tested. However the constructs ABD and E53 were used instead of the fragments produced by thermolysin digestion of α-actinin. The entire sequence of the constructs was known whereas the C-terminus of the proteolytic fragments could only be estimated. The expressed ABD (residues 1 to 268) and E53 (residues 240 to 749) fragments were similar to the 'thermolytic' 27kDa (residues 24 to approximately 269) and 53kDa (residues 266 to approximately 750) fragments respectively.

FIGURE 4.13

Diagram comparing the thermolysin generated 27kDa (TL27) and 53kDa (TL53) proteolytic fragments of α-actinin to the ABD (residues 1 to 268) and E53 (residues 240 to 749) fusion proteins. The C-termini of TL27 and TL53 were estimated from their molecular weights.

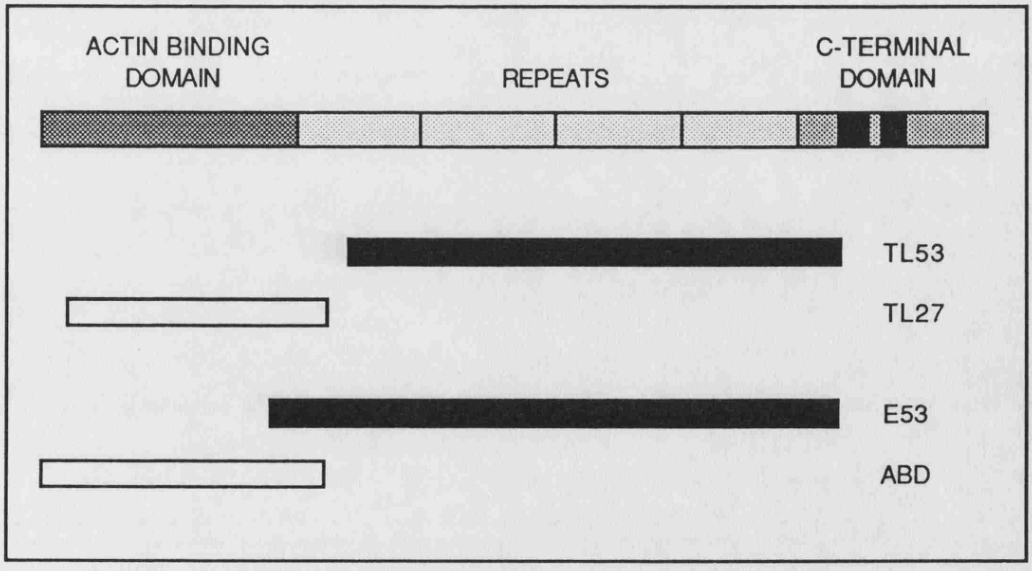

The use of expressed fusion proteins also permitted the assaying of equal amounts (by weight) of both fragments. The results were in agreement with those obtained with the thermolytic α-actinin

fragments, despite the ABD construct being in a two fold excess over the E53 construct. This suggested that the vinculin binding site of α-actinin was contained in one or more of the spectrin-like repeats.

The contribution of each of the four repeats and the C-terminal domain of α-actinin to vinculin binding was examined using the constructs ΔR1, ΔR2, ΔR3, ΔR4, and CTD. ^{125}I-vinculin bound to all of these fusion proteins. There were various possible explanations for this observation. The binding site could have been in the region common to all of the ΔR constructs and the CTD construct, each of which included residues 713-749. Alternatively α-actinin could have more than one binding site for vinculin within residues 218 to 749 in addition to a vinculin binding site within residues 713 to 887. Another disturbing possibility was that the binding of ^{125}I-vinculin was non-specific, and that the vinculin could bind to any fusion protein of a moderate size. However, ^{125}I-vinculin did not bind to GST alone (27kDa) or any of the molecular weight markers which included proteins of 45, 66, 97, 116, and 205kDa. Though *E. coli* lysates containing the fusion protein were used for the overlays, the ^{125}I-vinculin only bound the appropriate fusion protein and not to any of the endogenous *E. coli* proteins. The specificity of binding was confirmed by the fact that binding of ^{125}I-vinculin could be markedly reduced by unlabelled vinculin.

FIGURE 4.14

Diagram comparing the ΔR1, ΔR2, ΔR3, ΔR4, CTD, and Rep 2/3 constructs. The co-ordinates of ΔR1, ΔR2, ΔR3, and ΔR4, are 218 to 749 with the deletions 245 to 363, 364 to 478, 479 to 599, and 600 to 712 respectively. The co-ordinates of CTD and Rep 2/3 are 713 to 887 and 364 to 599 respectively.

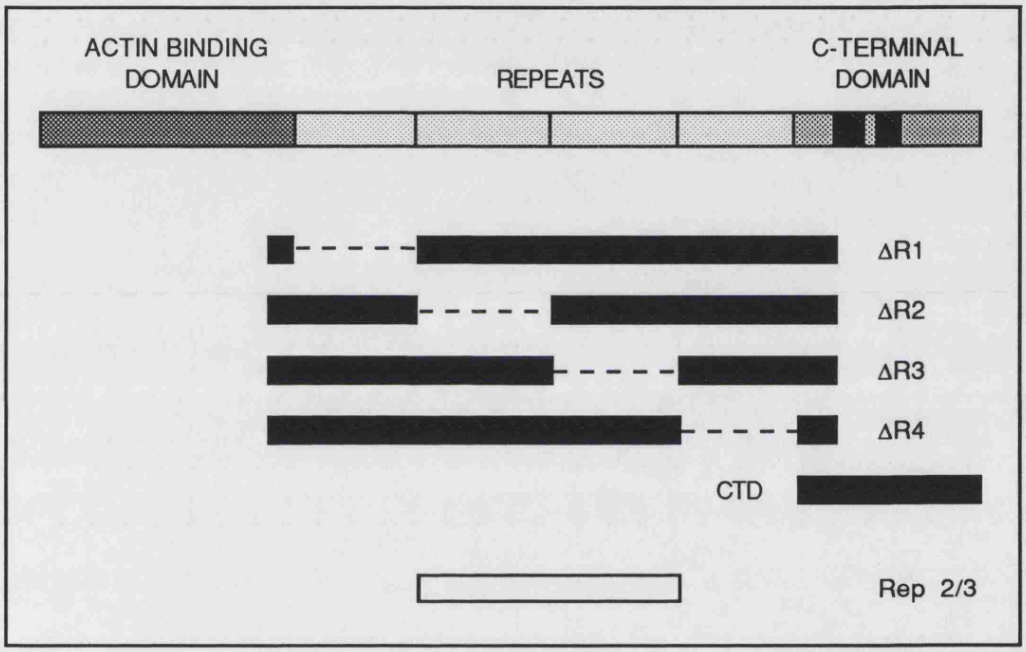

That the Rep 2/3 fusion protein did not bind ^{125}I-vinculin also supported the conjecture that ^{125}I-vinculin was not simply binding non-specifically to larger α-actinin fragments (data not shown). The fact that the Rep 2/3 fusion protein did not bind ^{125}I-vinculin was consistent with the electron micrographs (see section 3.32) which showed that vinculin bound at the ends of the rod shaped molecule.

A fusion protein (RV-H2, donated by B. Patel) that supposedly covered residues 218 to 697 of α-actinin was then examined. The RV-H2 construct expressed a fusion protein of the correct size that

cross reacted with an anti-α-actinin antibody. The binding of the RV-H2 fragment to ^{125}I-vinculin was surprising as it could only be explained by α-actinin having more than one ^{125}I-vinculin binding site. One ^{125}I-vinculin binding site would be within residues 713 to 887. The other one/two ^{125}I-vinculin binding site/s would have been present within repeat 1 (residues 269 to 363) and/or repeat 4 (residues 600 to 697) (Figure 4.15). The constructs R1-697, R1-632, R1-3, V1-V2, and V3-V4 were made to address this question. The R1-697 (residues 290 to 697) construct which was similar to the supposed RV-H2 fragment (except for lacking the N-terminal 72 residues) did not bind ^{125}I-vinculin. This could have been explained by α-actinin having a vinculin binding site within residues 269 to 289 and another within residues 713 to 887. However, this appeared intuitively unlikely. Subsequently DNA sequencing of the 3' region of the RV-H2 construct demonstrated that it coded up to residue 749. Hence only the fusion proteins that contained residues 713 to 749 bound to ^{125}I-vinculin

Residues 713 to 749 of α-actinin were strongly implicated as the ^{125}I-vinculin binding site since only fusion proteins/proteolytic fragments of α-actinin that contained these residues bound to ^{125}I-vinculin. Fusion proteins and proteolytic fragments of α-actinin that did not contain residues 713 to 749 failed to bind ^{125}I-vinculin. The use of the V1-V5 fusion protein which only contains residues 713 to 749 of α-actinin confirmed that the ^{125}I-vinculin binding site is located within this region of the molecule.

As previously explained, other assays were required to substantiate the results obtained from the overlay method described above. The

FIGURE 4.15

DIAGRAM INDICATING THE POSSIBLE VINCULIN BINDING SITES OF α-ACTININ BASED ON THE INCORRECT ASSUMPTION THAT THE RV-H2 FUSION PROTEIN COVERED RESIDUES 218 TO 697.

The fusion proteins that bound ^{125}I-vinculin are indicated as black bars, and those that did not bind ^{125}I-vinculin as open bars. To explain the fusion proteins that bound ^{125}I-vinculin there would need to be two or three ^{125}I-vinculin binding sites; (C) and (A) and/or (B).

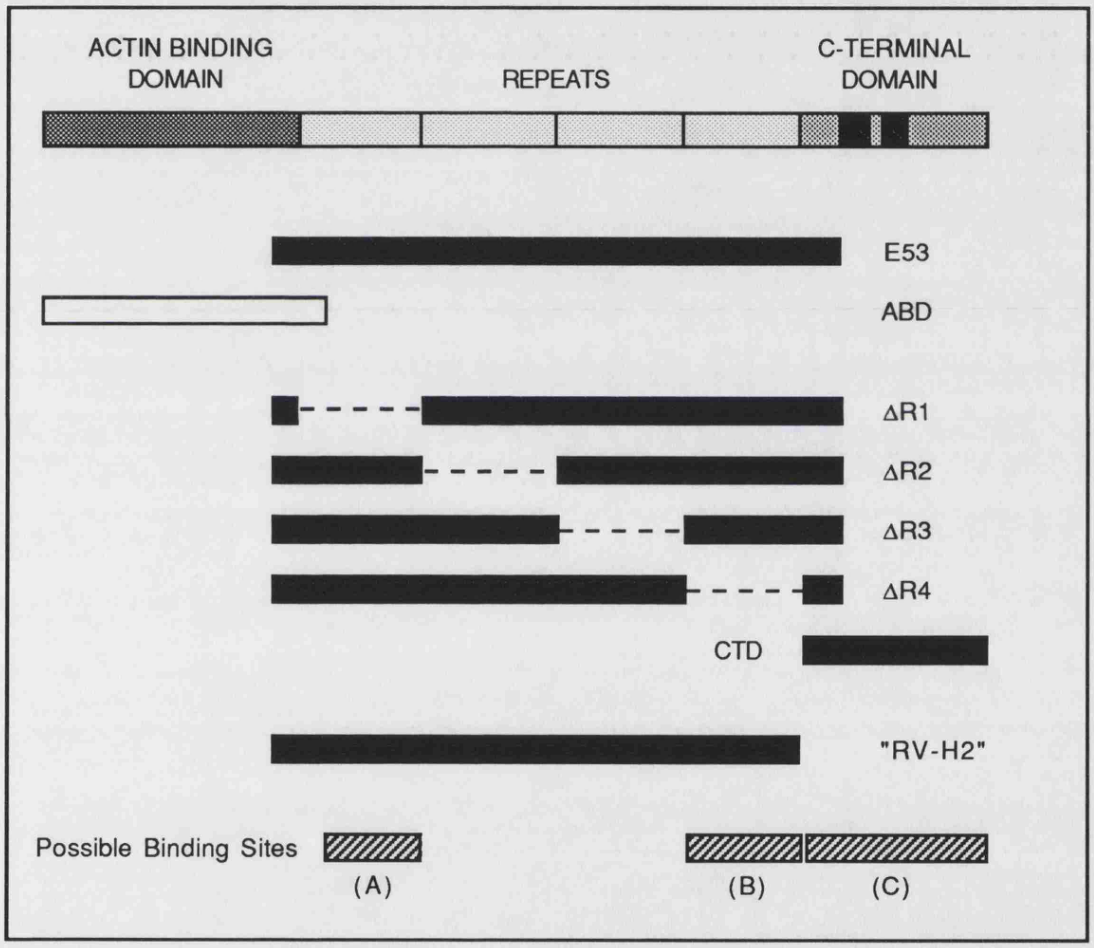

modified overlay assay was used for the reasons discussed in section 3.34. Consistent with the results of the basic overlay, the purified GST-53, CTD, and V1-V5 constructs markedly reduced (84 to 100%) the binding of ^{125}I-vinculin to either nitrocellulose bound whole α-actinin, the GST-53 fusion protein, or the CTD fusion protein. The GST-ABD fusion protein and GST alone generally caused a slight reduction (20%) in the binding of ^{125}I-vinculin to the nitrocellulose bound protein/fusion protein. However, despite equivalent amounts (by weight) of GST and GST-ABD fusion protein to the GST-53, CTD, and V1-V5 fusion proteins being added, the inhibition was considerably less than that produced by the GST-53, CTD, and V1-V5 fusion proteins.

The solid phase binding assay was also used to substantiate the findings of the overlay technique. This assay also demonstrated the specific binding of ^{125}I-vinculin to α-actinin fusion proteins containing residues 713 to 749. A gradual loss of radioactivity was observed during successive washes of the fusion protein bound to glutathione-agarose beads. This downward trend could be attributed to bead losses, which suggests that the assay could have been improved. Rather than removing unbound ^{125}I-vinculin by the repeated addition and aspiration of wash buffer, the glutathione-agarose beads could be filtered and the unbound ^{125}I-vinculin removed by passing wash buffer through the beads/filter. Using the method as described five washes were deemed sufficient to remove unbound vinculin without incurring high bead losses. As demonstrated in figure 4.10, the small losses of glutathione-agarose bead/fusion protein bound ^{125}I-vinculin was not due to dissociation of the protein, but was due to loss of the glutathione-agarose bead

bound fusion protein. The washes used were of very short duration, in contrast to the time required for significant dissociation of the ^{125}I-vinculin. The association between the ^{125}I-vinculin and the CTD fusion protein rose to a peak level over 48 hours. The amount of ^{125}I-vinculin that bound to the glutathione beads/CTD fusion protein complex was close to the expected value given the concentration of the ^{125}I-vinculin and fusion protein and the K_d of the interaction. The GST-53 and CTD fusion proteins bound some 23 to 27% of the total ^{125}I-vinculin. The values that were expected given the concentrations used were 19 to 70% for K_d's of 10^{-5} to 10^{-6}M respectively. Hence the values obtained were consistent with the expected value given a K_d for the α-actinin/vinculin interaction of 1.6×10^{-5}M. The binding of ^{125}I-vinculin to GST-53 and CTD fusion proteins was inhibited by the presence of unlabelled vinculin which was consistent with the binding being specific. However, the amount of inhibition (approximately 30%) was greater than that expected (about 10%).

Three different assays were used to demonstrate an interaction between ^{125}I-vinculin and a 37 residue segment (residues 713 to 749) of α-actinin. The ^{125}I-vinculin overlay assay was used to demonstrate binding. The binding was specific and could be inhibited if unlabelled vinculin was co-incubated with the labelled vinculin. All the proteolytic fragments and fusion proteins of α-actinin that contained residues 713 to 749 bound. The results of the modified overlay assay where soluble α-actinin constructs were tested for their ability to inhibit the binding of ^{125}I-vinculin to nitrocellulose bound α-actinin were also entirely consistent with the overlays. Specific binding was also demonstrated in the solid phase binding assay. The

V1-V5 fusion protein (residues 713 to 749) bound ^{125}I-vinculin, as did the GST-53, CTD, and V1-V2 constructs. The fragments tested that were not expected to bind ^{125}I-vinculin as indicated in the overlay assay did not bind in the solid phase binding assay.

Interestingly, the small V1-V5 fusion protein could bind to ^{125}I-vinculin. This contrasts the 41 amino acid talin binding site of vinculin which is dependent on flanking sequences for its activity (Jones et al, 1989; Gilmore et al, 1992). Though the V1-V5 construct was a GST-linked fusion protein it only had an additional 37 amino acids to GST alone, which did not bind vinculin. This suggested that the 37 amino acids alone could bind vinculin, although this was not tested.

The DNA coding for the vinculin binding site of α-actinin is contained within a single exon, EF1a. The exon covered nucleotides 2251 to 2397 (residues 713 to 760). This exon was common to both the smooth and non-muscle isoforms of α-actinin (Waites et al, 1992). This is consistent with the general observation that functional domains are often located within discrete exons (Gilbert, 1985; Ozawa et al, 1990).

The chick smooth muscle vinculin binding site was homologous to a region of the human non-muscle isoform (100% identity), the skeletal isoform (92% identity), the *Drosophila* skeletal α-actinin (86% identity), and to a lesser extent to *Dictyostelium* α-actinin (24% identity, 78% similarity). The degree of similarity between the 37 amino acid vinculin binding site of chick smooth muscle α-actinin and the equivalent regions of chick skeletal, human non-muscle, and

Drosophila skeletal α-actinin isoforms was generally greater than the degree of similarity exhibited by the other domains of α-actinin (see table 4.7). Such significant conservation is often indicitive of a domain having a functional role. However, since vinculin is absent from the Z-disc, the vinculin binding site of skeletal muscle α-actinin may have lost its vinculin binding capacity. However, this hypothesis has not been examined. Domains within *Dictyostelium* α-actinin exhibited lower levels of similarity with the α-actinins of higher organisms. The 37 residue sequence of *Dictyostelium* α-actinin equivalent to the vinculin binding site of the chick smooth muscle isoform did not have a greater degree of similarity than other domains of *Dictyostelium* α-actinin. The reason for this is as yet unclear. The presence of vinculin has not been demonstrated in *Dictyostelium*, though an equivalent protein might be expected by analogy with other species. If there is a vinculin homologue, sequence divergence of the α-actinin vinculin binding site may reflect the more distant evolution of *Dictyostelium* and chicken α-actinins from a common ancestral α-actinin gene. The sequence divergence between *Dictyostelium* and chicken α-actinins is visible over the entire α-actinin sequence.

The 37 residues immediately prior to the first EF-hand of chicken α-spectrin (Wasenius et al, 1989) are homologous to the vinculin binding site of α-actinin. However, the sequence identity is only 24% whereas that of the EF-hands and remaining C-terminus is 46 and 32% respectively. This is consistent with spectrin not binding vinculin but having the capacity to bind actin in a calcium dependent manner (Fishkind et al, 1987). Both spectrin EF-hands contain the residues required for calcium binding (Da Silva and Reinach, 1991). There was

TABLE 4.7

Examination of the similarity between various α-actinin domains†.

α-Actinin Domain*	Sm vs Sk		Sm vs Hu		Sm vs Dro		Sm vs Dic	
	Id	Sim	Id	Sim	Id	Sim	Id	Sim
Actin Binding(1)	82	95	99	100	79	96	58	84
Repeat 1(2)	90	99	97	100	72	96	38	79
Repeat 2(3)	80	96	96	99	70	91	25	79
Repeat 3(4)	76	97	99	99	60	88	23	70
Repeat 4(5)	76	96	94	98	49	90	27	74
Vinculin Binding(6)	92	97	100	100	84	100	24	78
EF-Hands(7)	78	95	74	87	51	85	33	88
C-terminus(8)	72	94	95	100	77	96	32	71

Sequence comparisons were performed on the multiple alignement package Clustal (Higgins and Sharp, 1988). Id denotes identical residues. Sim denotes identical residues and conservative substutions. Gaps in alignements were counted as mismatches.

† The sequences compared were as follows: Sm - Chicken smooth muscle (Baron et al, 1987); Sk - Chicken skeletal muscle (Arimura et al, 1988); Hu - Human non-muscle (Millake et al, 1989); Dro - *Drosophila* (Fyrberg et al, 1990): Dic - *Dictyostelium* (Noegel et al, 1987).

* The residue numbers of the domains used, as defined in the chick smooth muscle sequence, were: (1) 1 to 245; (2) 245 to 363; (3) 364 to 478; (4) 479 to 599; (5) 600 to 712; (6) 713 to 749; (7) 750 to 813; (8) 814 to 887.

no significant conservation of the vinculin binding site with the analogous region of the dystophin sequence (Koenig et al, 1988).

The α-actinin within cells is found in more than one location. In non-muscle cells α-actinin localises with vinculin at adherens junctions, and in microfilament bundles where vinculin is absent (Lazarides and Burridge, 1975). In skeletal muscle, α-actinin is found in Z-discs and membrane associated plaques. Interestingly, in skeletal muscle the the Z-discs and membrane associated plaques contain different isoforms of α-actinin. The Z-discs contain the skeletal isoform whilst the membrane associated plaques contain either the smooth or non-muscle isoform (Endo and Masaki, 1984). The "anti-smooth muscle" antibody used by Endo and Masaki (1984) would not have distinguished between the α-actinin smooth and non-muscle isoforms due to their sequence similarity. cDNAs encoding both the smooth and non-muscle isoforms of α-actinin have been isolated from a chick skeletal muscle library (Dr. A. Blanchard, unpublished data). There was also evidence for the expression of multiple α-actinin isoforms in non-muscle cells. The smooth muscle cDNA C17 was isolated from a chick fibroblast library (Baron et al, 1987a). This could have arisen due to contaminating tissue, but the identification of other smooth muscle α-actinin clones from the same library suggests that the smooth muscle isoform is present in non-muscle cells (Waites et al, 1992). Using reverse transcription-PCR amplification of mRNA it was recently shown that skeletal, smooth, and non-muscle tissue each contain mRNA for the smooth and non-muscle isoforms of α-actinin (Waites et al, 1992). The percentage of smooth to smooth plus non-muscle mRNA was 53, 94, and 11-29% respectively. The levels were not compared to the amount of skeletal

muscle mRNA. It has been suggested that in non-muscle cells the smooth muscle α-actinin isoform would localise to stress fibres, where it would form structures analagous to the Z-disc of muscle, and that the non-muscle isoform would localise to focal contacts which are subject to disassembly and assembly. However, when chicken smooth muscle α-actinin was expressed in monkey COS cells it localised to both stress fibres and focal contacts (Jackson et al, 1989). Non-muscle α-actinin also localised to stress fibres and focal contacts when expressed in COS cells (D. Millake, personal communication). Conceivably the localisation of the expressed α-actinin is anomalous due to species differences between monkey and chicken α-actinins. The use of monoclonal antibodies to the regions of difference was one possible method of addressing this question.

It is interesting that the smooth and non-muscle α-actinin isoforms only differ in the latter half of the first EF-hand and the linking sequence between the two EF-hands. Presumably, any differential localisation of the two isoforms is due to this divergance. One mechanism that has been suggested is that the calcium sensitivity of the non-muscle isoform is due to steric hindrance of the EF-hands of one α-actinin subunit acting upon the actin binding domain of the adjacent subunit. Although the vinculin binding sites of the smooth and non-muscle α-actinins are identical, it is now conceivable that the EF-hands could also affect the binding of vinculin to α-actinin due to the direct proximity of the vinculin binding site to the first EF-hand, the EF-hand that is predicted to be functional. It is possible that the non-muscle isoform has a higher affinity for vinculin than the smooth muscle isoform due to differences in the EF-hand

adjacent to the vinculin binding site. A more remote possibility is that the vinculin binding capacity of the non-muscle α-actinin isoform could be modulated by calcium. Due to the remarkable similarity between the smooth and non-muscle isoforms it has previously been assumed that the vinculin binding characteristics would be the same. In light of the location of the vinculin binding site it would be worthwhile to compare vinculin binding to the smooth and non-muscle isoforms, and to investigate the possible calcium sensitivity of vinculin binding.

The identification of a discrete vinculin binding site within α-actinin suggests various exciting experiments.

The actual residues responsible for vinculin binding within the 37 amino acids could be defined further. Various approaches could be used to investigate this. The approach used in this chapter was probably close to its limits due to difficulties in manipulating the PCR products. Mutagenesis could be used. However, since the loss of vinculin binding could be due to pertubations of secondary structure, the results of this approach are often difficult to interpret. Another approach would be proton NMR spectroscopy of the 37 amino acids. When vinculin is added to a solution of the peptide the mobility of residues involved in the binding would probably be lowered. This could be observed in the spectral changes of the peptide. Another, and probably simpler approach would be to use synthetic peptides to segments within the 37 residue sequence. These could be assayed for their ability to inhibit the binding of ^{125}I-vinculin to α-actinin. It would be interesting to see whether fluorescently labelled synthetic peptides of sequences within the vinculin binding site or the V1-V5

fusion protein would disrupt focal contacts if micro-injected into adherent fibroblasts.

The V1-V5 construct could be used to identify the α-actinin binding site of vinculin. Proteolytic fragments of vinculin could be assayed for their ability to be co-sedimented by the V1-V5 construct immobilised on glutathione-agarose beads (Prelimary attempts at this suggested that the V8 protease generated 90kDa fragment of vinculin could be co-sedimented in this manner, whereas the 27kDa fragment of vinculin could not). An alternative approach would be to attach the 37 amino acid segment to a column matrix. Affinity chromatography of proteolytic fragments of vinculin could then be used to identify those that bound. Chemical cross-linking of the V1-V5 fragment and protease digestion could also be used to localise the α-actinin binding site in vinculin.

Interestingly vinculin has recently been shown to have extensive regions of similarity to a cadherin associated protein of 102kDa (CAP102) (also termed α-catenin) (Herrenknecht et al, 1991; Nagafuchi et al, 1991). CAP102 localises to cell-cell adherens junctions, and has been shown to bind to the transmembrane cell adhesion molecule cadherin. Residues 22 to 234 of CAP102 share 26% identity with residues 6 to 208 of vinculin, which contain the talin binding site. Whether CAP102 can bind talin has not been demonstrated, but although cell-cell adherens junctions contain both vinculin and CAP102, they do not contain talin. Residues 377 to 585 of CAP102 and 582 to 796 of vinculin show 32% identity. The function of this domain is unclear. Bendori et al (1989) have shown that transfection in COS cells of vinculin residues 380 to

approximately 880 disrupted the actin microfilament system. The expressed vinculin fragment did not localise to focal contacts. They suggest that this region contains a binding site other than those for talin and self association. It is conceivable that this is the α-actinin binding site, though Westermeyer et al (1990) have suggested that it could be an actin binding site. Residues 698 to 848 and 905 to 1053 of CAP102 and vinculin respectively are 34% identical. This C-terminal domain of vinculin has been implicated in self association. It has been suggested that vinculin, which does not appear to bind to cadherin, may bind to CAP102 via their similar C-terminal domains. Alternatively self association of CAP102 may aid in the formation of a cadherin plaque.

SUMMARY.

The vinculin binding site of α-actinin has been localised to a contiguous sequence of 37 residues. This represents 4.17% of the total α-actinin sequence. The vinculin binding site thus far defined (residues 713 to 749) was bounded by the C-terminus of repeat 4 and the N-terminus of the first EF-hand.

CHAPTER FIVE
ATTEMPTS AT CRYSTALLISATION OF α-ACTININ AND OF α-ACTININ DOMAINS

5.1 INTRODUCTION.

It would be immensely useful to know the three dimensional structure of α-actinin. Knowing the structure of the actin binding domain would assist greatly in determining the nature of the interaction between α-actinin and F-actin. At present a biochemical approach is being used to identify α-actinin residues involved in the interaction with F-actin. The three dimensional structure of actin has been determined (Kabsch et al, 1990). Hence, if the three dimensional structure of α-actinin were determined, space filling models of possible actin/α-actinin complexes could be investigated. Similarly, the exact nature of dimerisation between the spectrin like repeats of adjacent α-actinin monomers is not known. Except for the EF-hands, which are assumed to have a helix-turn-helix motif, nothing is known about the structure of the C-terminal domain of α-actinin. Because of the antiparallel orientation of the α-actinin subunits, it is thought that the actin binding domain of one α-actinin subunit is adjacent to the C-terminal domain of the next, though the exact relationship is unclear. It has been suggested that the calcium sensitivity of the non-muscle isoform is due to a conformational change in the EF-hand domain sterically preventing access of actin to the actin binding domain on the adjacent subunit. There is as yet no data in support of this hypothesis.

Various other cytoskeletal proteins have domains homologous to those in α-actinin. Filamin, β-spectrin, dystrophin, ABP-120, and fimbrin, all have a similar actin binding domain (Koenig et al, 1988; Byers et al, 1989; Noegel et al, 1989; De Arruda et al, 1990). The α-actinin repeats are homologous to those found in spectrin and

dystrophin (Baron et al, 1987a; Koenig et al, 1988; Wasenius et al, 1989).

This chapter details the attempts to crystallise intact α-actinin and the actin binding domain of α-actinin. The expression in *E. coli* of the actin binding domain and the purification protocol developed for that domain are also described. A purification protocol for the α-actinin repeats expressed in *E. coli* is described.

5.2 METHODS.

5.21 THE EXPRESSION IN *E. COLI* OF THE ACTIN BINDING DOMAIN OF α-ACTININ AND THE PURIFICATION OF THE EXPRESSED POLYPEPTIDE.

CELL GROWTH AND EXPRESSION.

An Nco1-Hinc2 fragment of the chicken smooth muscle α-actinin cDNA C17 (Baron et al, 1987a), encoding residues 1 to 268, was subcloned into the plasmid pMW172 (Way et al, 1990), which contains the T7 promoter (Figure 5.1) (kindly donated by Mike Way). The plasmid construct was transformed into *E. coli* BL21(DE3) cells using the $CaCl_2$ method (see section 2.6), and the cells grown on agar plates with 0.5mg/ml ampicillin. Liquid cultures were grown in 2x500ml of 2xTY with 0.5mg/ml ampicillin. They were grown from a colony that was no older than seven days, picked from an agar plate. Cultures were grown at 37°C to an optical density at 600nm of 0.5-0.7. They were then induced by the addition of IPTG (0.01mM). The cells were then grown at 30°C for a further 3-5 hours. The cells were

FIGURE 5.1

MAP OF THE PLASMID pMW172 CONTAINING THE INSERT CODING FOR THE ACTIN BINDING DOMAIN OF α-ACTININ.

pMW172 is based on the plasmid pBR322. A segment of pBR322 (indicated by the dashed line) has been replaced by the 'T7' insert. The fragment of the smooth muscle α-actinin cDNA C17 (Baron et al, 1987), that was cloned into pMW172 (Way et al, 1990) is also indicated.

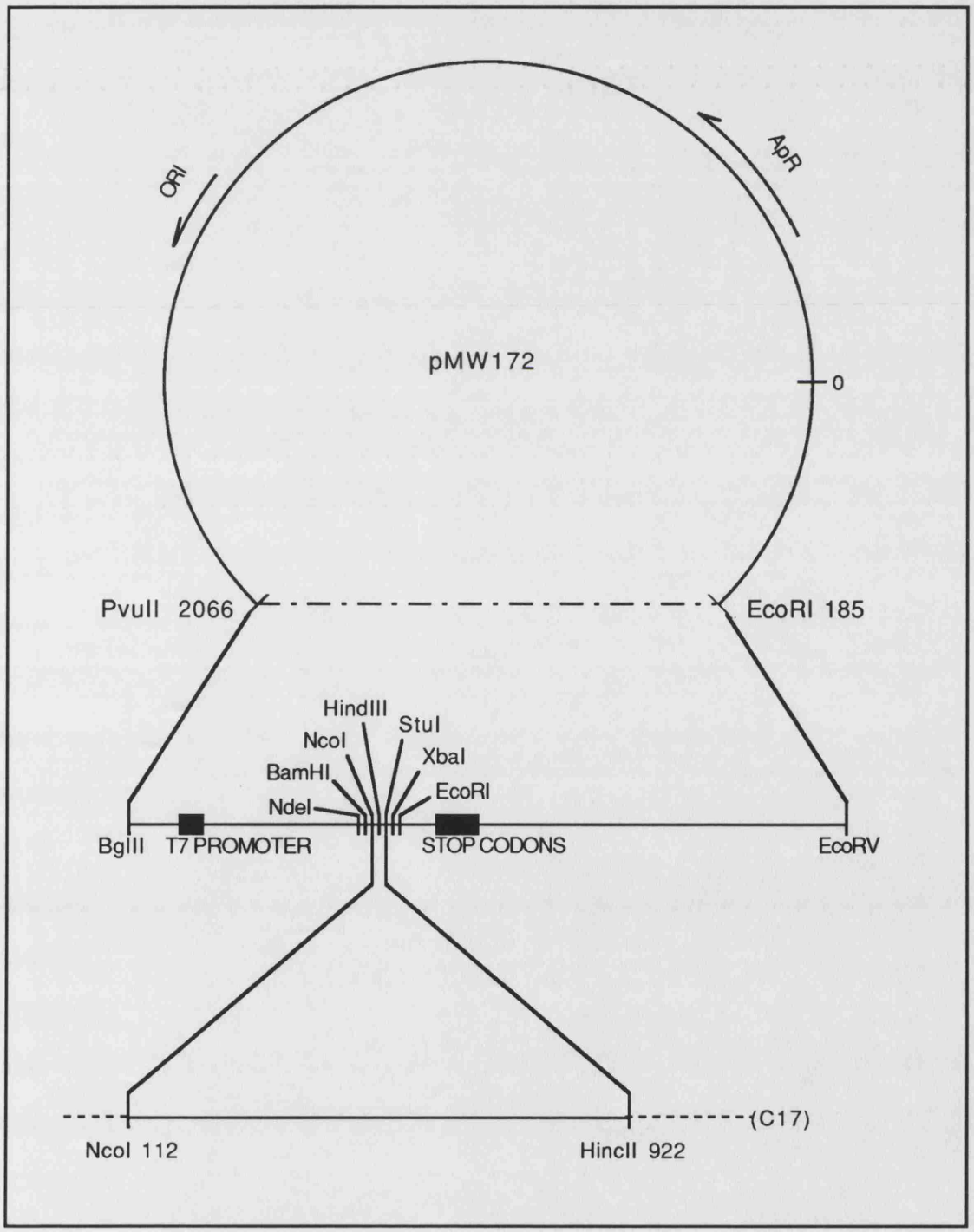

then harvested by centrifugation (10,000g, 15min, 4°C) and frozen until required.

PURIFICATION OF THE EXPRESSED ACTIN BINDING DOMAIN OF α-ACTININ FROM *E. COLI*.

Thawed pellets were resuspended in 16ml of ice cold 150mM NaCl, 12mM sodium phosphate, pH7.3. EDTA was added to 5mM, E64 (trans-Epoxysuccinyl-L-leucylamido-(4-guanidino) butane) to 5μM, and Leupeptin to 10μM (final volume 20ml). PMSF was added to 1mM immediately prior to the addition of Triton X-100 to a final concentration of 1% (v/v). Cells were sonicated on ice for 2x45s. Cell debris was spun down at 4°C (8000g, 15min). The supernatant was then dialysed against 2 litres of buffer T' (10mM Tris/acetate, pH7.6, 10mM NaCl, 2mM EDTA, 0.05% β-mercaptoethanol). The dialysate was applied to a DEAE-Sepharose Fast-Flow column (1x20cm, equilibrated with buffer T') and washed with buffer T'. A 150ml gradient of buffer T' to buffer T' plus 150mM NaCl was applied. A flow rate of 30ml/hr was used and 3ml fractions were collected. Fractions containing the expressed actin binding domain were pooled then concentrated by ammonium sulphate precipitation. Saturated ammonium sulphate solution (pH7.5, 0.1mM EDTA) was added to 60% saturation followed by stirring at 4°C for 1 hour. After centrifugation the pellet was resuspended in 5ml of buffer T' and dialysed against 1 litre of buffer T' before being applied to a Sephadex G75 column (1x70cm, equilibrated in buffer T'). A flow rate of 20ml/hr was used and 2ml fractions were collected. Peak fractions were pooled and loaded onto a hydroxylapatite (BioRad) column (0.5x3cm) previously equilibrated in 10mM potassium phosphate, pH7.0. The column was washed at 10ml/hour with buffer

T'. A 50ml gradient of 10 to 150mM potassium phosphate, pH7.0 was then applied, and 1ml fractions were collected. The major peak was pooled and dialysed against buffer T'. The dialysate was applied to a MonoQ 10/10 column previously equilibrated in buffer T'. After washing, a 100ml gradient of buffer T' to buffer T' plus 200mM NaCl was applied. The flow rate was 3ml/min, and 0.5ml fractions were collected. Peak fractions were pooled and dialysed into buffer B (20mM Tris/acetate, pH7.6, 20mM NaCl, 0.1mM EDTA, 0.1% β-mercaptoethanol).

5.22 THE EXPRESSION IN *E. COLI* OF THE SPECTRIN-LIKE REPEATS OF α-ACTININ AND THE PURIFICATION OF THE EXPRESSED PROTEIN.

CELL GROWTH AND EXPRESSION.

The EcoRV-Xmn1 (nucleotides 474 to 2069) fragment of the chicken non-muscle cDNA C18 (Baron et al, 1987b) had been ligated into the SmaI restriction endonuclease site of pGEX-3X by Dr. A. Blanchard (Department of Biochemistry, Leicester University) (Figure 5.2). The plasmid, termed pAB1, was transformed into *E. coli* strain JM101 and grown on agar plates with 0.1mg/ml ampicillin. 500ml 2xTY liquid cultures were grown from a frozen glycerol stock. Cultures were induced at an optical density at 600 of 0.5-0.7 by the addition of IPTG to 0.5mM. The cells were grown for a further 2.5 hours. Growth was at 37°C before and after induction. The cells were spun down and frozen until required.

FIGURE 5.2

MAP OF THE PLASMID pAB1 WHICH CONTAINS AN INSERT CODING FOR α-ACTININ RESIDUES 218 TO 749.

The plasmid pGEX-3X (Studier and Moffat, 1986) contains the fragment of the smooth muscle clone C18 (Baron et al, 1987), as indicated.

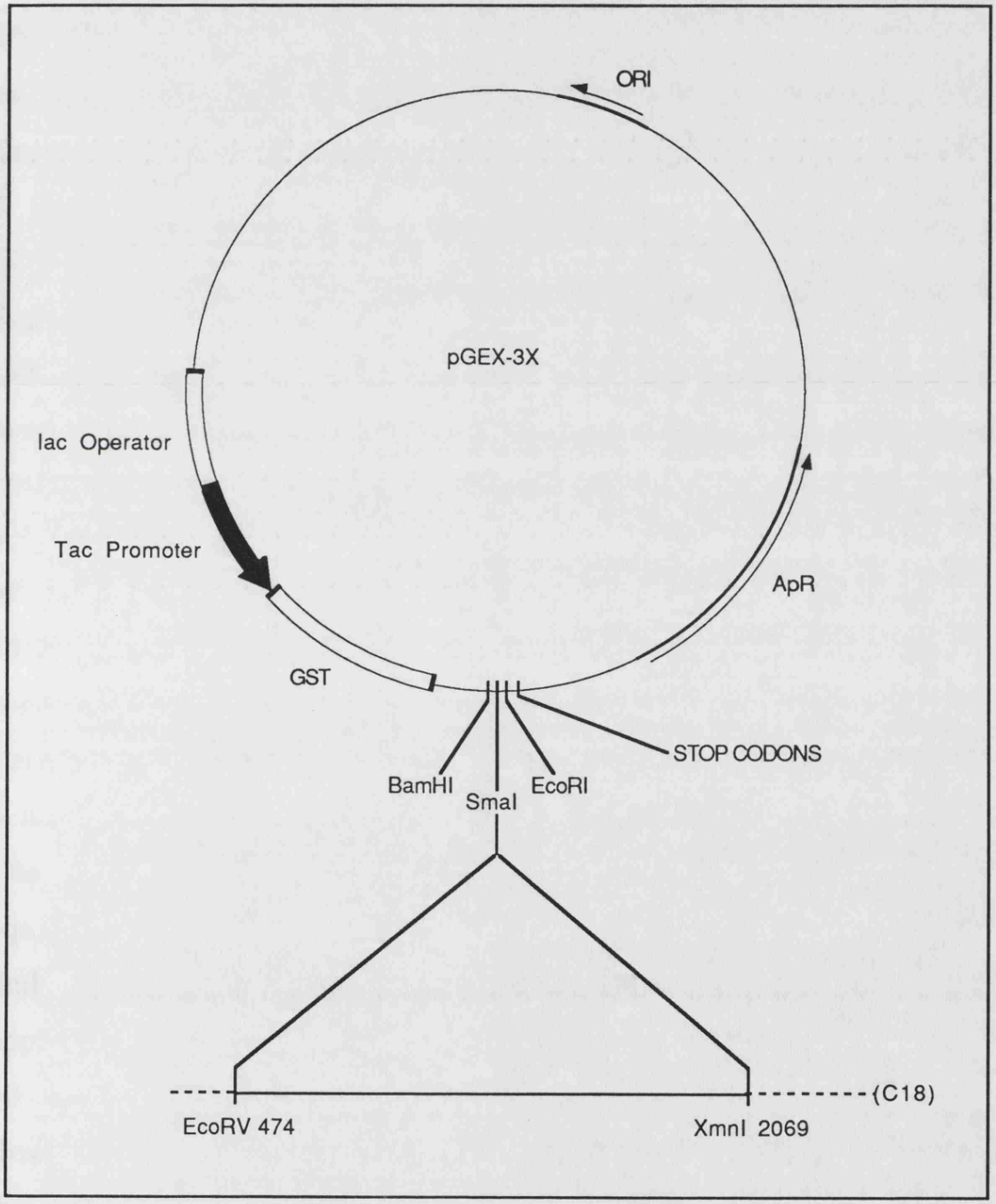

PURIFICATION OF THE EXPRESSED SPECTRIN-LIKE REPEATS OF α-ACTININ FROM *E. COLI*.

The purification of the repeat domain was similar to that of the actin binding domain of α-actinin. The expressed GST fusion protein was cleaved by an endogenous *E. coli* protease between residues 239 and 240 of the α-actinin repeats. Hence the expressed protein could not be purified on glutathione-agarose beads. The soluble fraction of the bacterial cells was extracted as described above and dialysed against 2 litres of buffer T (10mM Tris/acetate, pH7.6, 10mM NaCl, 0.1mM EDTA, 0.1% β-mercaptoethanol). The dialysate was applied to a DEAE-Sepharose Fast-Flow column (1x15cm, equilibrated in buffer T). A salt gradient of buffer T to buffer T plus 300mM NaCl was developed over 300ml. A flow rate of 30ml/hr was used and 3ml fractions were collected. The fractions containing the expressed α-actinin polypeptide were pooled and the protein precipitated by the addition of saturated ammonium sulphate solution (pH7.5, 0.1mM EDTA) to 75% saturation. The solution was stirred at 4°C for 1 hour before centrifugation. The pellet was resuspended in 6ml of buffer B (20mM Tris/acetate, pH7.6, 20mM NaCl, 0.1mM EDTA, 0.1% β-mercaptoethanol) and further dialysed against 2 litres of buffer B. The dialysate was applied to a Sephacryl S200HR column (1.6x83cm, equilibrated in buffer B) and developed at 30ml/hr with buffer B. 2ml fractions were collected. The peak fractions were pooled and applied to a hydroxylapatite column (0.5x3cm). A 100ml gradient of 10 to 150mM potassium phosphate, pH7.0 was then applied. The flow rate was 10ml/hr and 2ml fractions were collected. The peak fractions were pooled and dialysed into buffer B.

5.23 MEANS OF ATTAINING SUPERSATURATION FOR PROTEIN CRYSTALLISATION.

EDTA was removed from the protein solutions by dialysis. Samples were set up for crystallisation using the 'Hanging Drop' method. A small aliquot of the protein sample and of the precipitating solution were mixed on a coverslip until the schlieren lines disappeared. Generally the drop contained 30-45µl of which 30-50% was protein solution. The drop was placed over 2ml of the precipitating solution. An airtight seal between the coverslip and the well was made with silicone grease (Dow Corning). The drops were allowed to stand. Examination was made routinely with a Leitz microscope (16, 25, and 40x magnification).

Diagram Showing The Apparatus Used For Attaining Supersaturation With the 'Hanging Drop' Method.

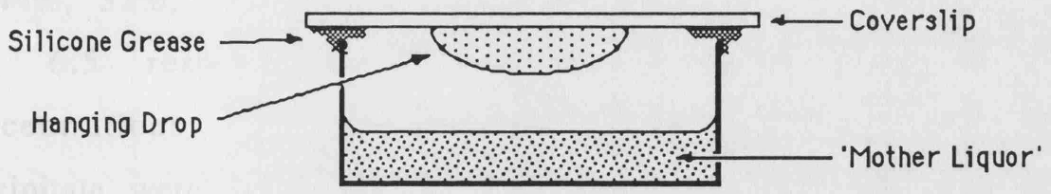

5.24 NATIVE GELS.

Native gels were run on a LKB 'Midget' electrophoresis unit. Gels were made as for SDS-PAGE gels, but omitting the SDS. There was no stacking gel. Gels were pre-run at 100-150V constant voltage for 30 to 60 minutes at 4°C. The samples were not boiled. Samples were run at 80V constant voltage until the bromophenol blue reached the base of the gel. Native gels were stained as for SDS-PAGE gels.

5.3 RESULTS.

5.31 THE PURIFICATION OF α-ACTININ AND ATTEMPTS AT CRYSTALLISATION.

α-Actinin was purified as previously described (see sections 2.5 and 3.31). The sample was shown to be essentially homogenous with light and heavy loadings on SDS-PAGE gels. However, there was a low level of an approximately 70kDa degradation product (Figure 5.3). This was less than 4% of the total protein. Crystallisation was tried with the conditions (all at 4°C) shown in table 5.1.

At the lower ammonium sulphate concentrations some microcrystalline precipitate was seen. A number of angular grains were observed, but these did not grow further. The ammonium sulphate concentrations required for total precipitation were 47%, 41-44%, 32%, and 32% ammonium sulphate for pH's 8.0, 7.5, 7.0, and 6.5 respectively. At pH6.0 and ammonium sulphate concentrations of 24-34%, small amounts of microcrystalline precipitate were observed, but there was no total precipitation.

Nothing significant was observed with the MPD (2-methyl-2,4-pentanediol) concentrations tested. Small grains were sometimes observed but none of these had any distinct shape.

The various PEG (pH7.5) precipitants generally gave a small amount of 'grainy' microcrystalline material up to the precipitating concentration. Occasionally slightly larger and sometimes angular grains were seen, but these did not develop further. The concentration of PEG required for total precipitation was about 10%,

TABLE 5.1

The various conditions tried for the crystallisation of α-actinin. The abbreviations used are MPD, 2-methyl-2,4-pentanediol; PEG, polyethylene glycol; and MES, 2-(N-morpholino) ethane sulphonic acid.

PRECIPITANT		BUFFER	PROTEIN
TYPE	CONC^N		CONC^N
$AmSO_4$	20-50 (3% Steps)	50mM MES, pH6.5	3.8mg/ml
$AmSO_4$	20-50 (3% Steps)	50mM Tris, pH7.0	3.8mg/ml
$AmSO_4$	20-50 (3% Steps)	50mM Tris, pH7.5	3.8mg/ml
$AmSO_4$	20-50 (3% Steps)	50mM Tris, pH8.0	3.8mg/ml
$AmSO_4$	20-50 (3% Steps)	50mM Tris, pH8.5	3.8mg/ml
MPD	5-30 (5% Steps)	10mM Tris, pH7.5	3.8mg/ml
PEG 600	5-30 (5% Steps)	10mM Tris, pH7.5	3.8mg/ml
PEG 1000	5-30 (5% Steps)	10mM Tris, pH7.5	3.8mg/ml
PEG 4000	5-30 (5% Steps)	10mM Tris, pH7.5	3.8mg/ml
PEG 8000	5-30 (5% Steps)	10mM Tris, pH7.5	3.8mg/ml
PEG 20K	5-30 (5% Steps)	10mM Tris, pH7.5	3.8mg/ml
$AmSO_4$	24-34 (1% Steps)	50mM MES, pH6.0	3.8mg/ml
$AmSO_4$	24-34 (1% Steps)	50mM MES, pH6.5	3.8mg/ml
PEG 4000	5-30 (5% Steps)	50mM MES, pH6.5	3.8mg/ml
PEG 4000	5-30 (5% Steps)	10mM MES, pH7.0	3.8mg/ml
PEG 4000	5-30 (5% Steps)	10mM Tris, pH7.5	3.8mg/ml
PEG 4000	5-30 (5% Steps)	10mM Tris, pH8.0	3.8mg/ml
PEG 4000	5-30 (5% Steps)	10mM Tris, pH8.5	3.8mg/ml
PEG 8000	5-30 (5% Steps)	10mM MES, pH6.5	3.8mg/ml
PEG 8000	5-30 (5% Steps)	10mM MES, pH7.0	3.8mg/ml
PEG 8000	5-30 (5% Steps)	10mM Tris, pH7.5	3.8mg/ml
PEG 8000	5-30 (5% Steps)	10mM Tris, pH8.0	3.8mg/ml
PEG 8000	5-30 (5% Steps)	10mM Tris, pH8.5	3.8mg/ml

FIGURE 5.3

PURIFIED α-ACTININ USED IN CRYSTALLISATION STUDIES.

The figure shows a Coomassie stained SDS-PAGE gel (7%) of the α-actinin (25μg) used in crystallisation studies.

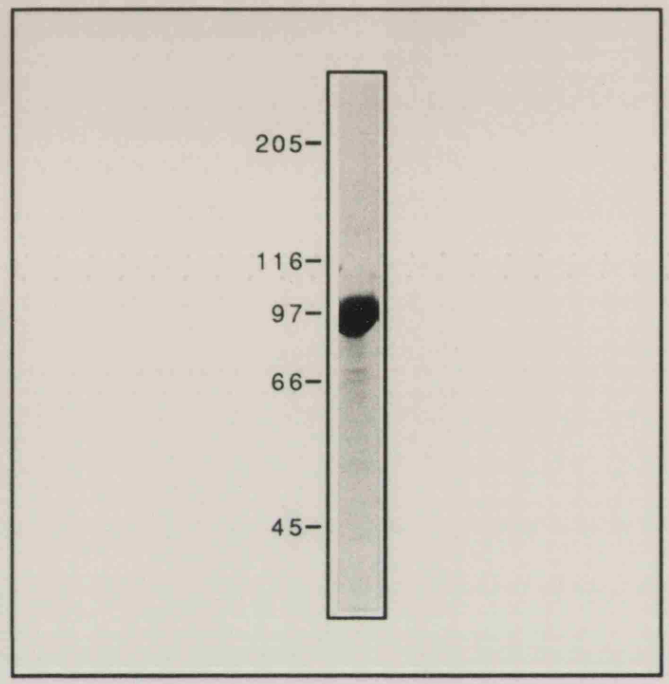

15-20%, 15-20%, 10-15%, and 10% for PEG's 600, 1000, 4000, 8000, and 20k respectively. The pH of the buffer did not markedly affect the concentration of PEG 4000 required for total precipitation. At pH's 6.5, 7.0, 7.5, and 8.0, the concentration needed was 15-20%, while at pH8.5 a concentration of 10-15% was required. The precipitation of α-actinin by PEG 8000 appeared to demonstrate pH dependance. The concentrations of PEG 8000 required 15-20%, 10-15%, 15-20%, 20-25%, and 20-25% at pH6.5, 7.0, 7.5, 8.0, and 8.5 respectively.

5.32 THE EXPRESSION IN *E. COLI* OF THE ACTIN BINDING DOMAIN OF α-ACTININ AND THE PURIFICATION OF THE EXPRESSED POLYPEPTIDE.

CELL GROWTH AND EXPRESSION.

The growth rate of the BL21(DE3) cells containing the plasmid pMW172 was not affected by concentrations of ampicillin added to to the cultures. The maximum concentration of ampicillin examined was 1000μg/ml. The expressed actin binding domain has a molecular weight of 31kDa, as determined by SDS-PAGE. This is in agreement with the molecular weight deduced from the sequence. The proportion of expressed α-actinin actin binding domain that was soluble depended on the conditions used to induce protein expression (Figure 5.4 and table 5.2). Generally the proportion of expressed actin binding domain that was soluble decreased with higher induction temperatures or higher IPTG concentrations. A significant amount of α-actinin actin binding domain was expressed in the absence of IPTG.

FIGURE 5.4

EXAMINATION OF THE EXPRESSION OF THE ACTIN BINDING DOMAIN WITH VARIOUS CONDITIONS OF INDUCTION

Cultures were grown at 37°C until an optical density at 600nm of 0.5 was attained. The cultures were induced by the addition of 0.01, 0.1, and 1.0mM IPTG (final concentration) respectively. Cultures were further grown at 30°C and 37°C. The cultures were sonicated and the soluble (S) and insoluble (P) fractions of the extract were analysed on a 12% minigel.

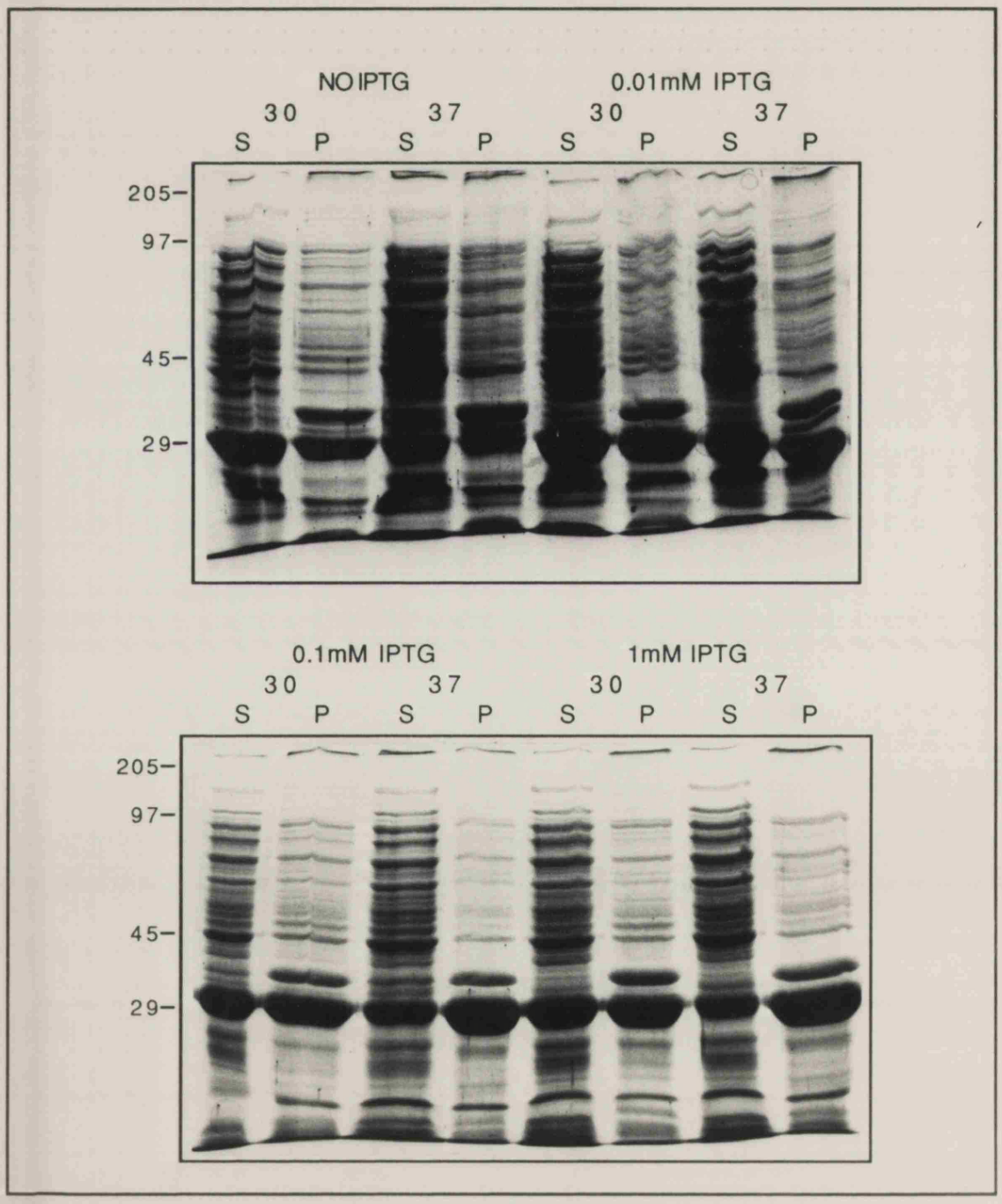

TABLE 5.2

The percentage of soluble expressed α-actinin actin binding domain for various conditions of induction. The soluble and insoluble fractions of a bacterial lysate was electrophoresed on an SDS-PAGE gel. The percentage of the expressed actin binding domain was estimated using laser densitometry.

	INDUCTION TEMPERATURE	
IPTG Conc^{n} (mM)	30°C	37°C
0	68%	72%
0.01	62%	49%
0.10	53%	30%
1.00	49%	27%

PROTEIN PURIFICATION.

The soluble fraction of BL21(DE3) cells expressing the actin binding domain was applied to the DEAE-Sepharose Fast-Flow column after dialysis into Buffer T'. Following extensive dialysis, negligible amounts of the expressed protein eluted with the unbound fraction (Figure 5.5). The expressed actin binding domain eluted at approximately buffer T' plus 20-37mM NaCl. The main contaminants were of approximately 40, 37, 29, 28, and 20kDa.

An ammonium sulphate step was used to concentrate the protein. After precipitation with 50% ammonium sulphate the supernatant and pellet were examined by Bradford protein estimation and SDS-PAGE analysis. This showed that 40-50% of the expressed protein remained in the supernatant. A 60% cut appeared to precipitate all

FIGURE 5.5
PURIFICATION OF THE ACTIN BINDING DOMAIN OF α-ACTININ: ELUTION PROFILE FROM THE DEAE-SEPHAROSE FAST-FLOW COLUMN.

The photographic insert shows a Coomassie stained SDS-PAGE minigel of (A) the unbound protein and the actin binding domain from the peak leading edge (B) and from the peak/trailing edge (C). 25µl aliquots were applied to the minigel. The column bed size was 1x20cm. A flow rate of 30ml/hour was used. Buffer T' with a salt gradient as indicated was used as the eluent. 3ml fractions were collected.

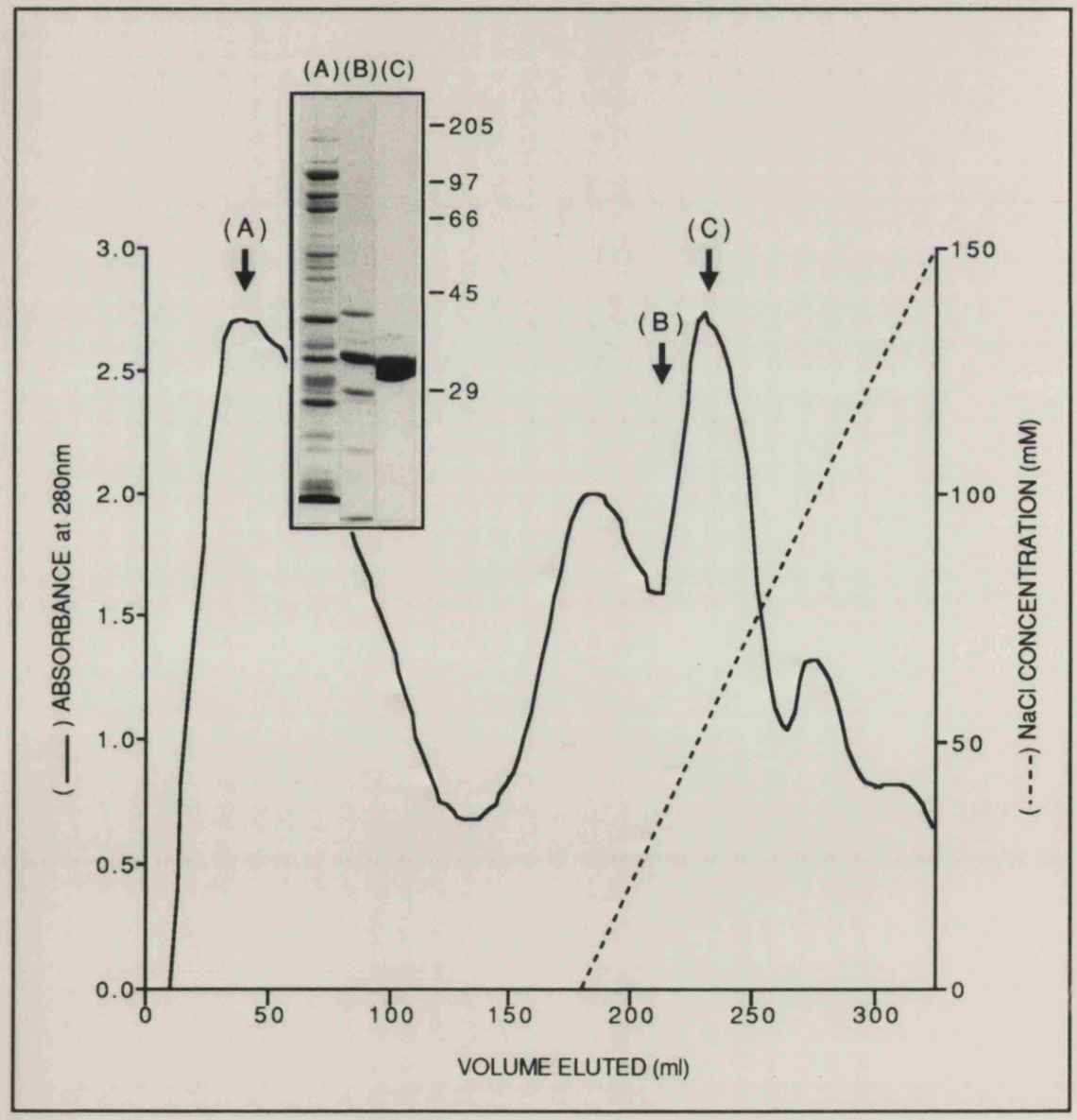

the protein, but to fully redissolve the pellet the sample had to be dialysed against buffer T'.

The expressed protein eluted from the Sephadex G75 column with a K_{av} value of approximately 0.06 (see figure 5.6). This column removed the 40kDa band and various minor high molecular weight contaminants.

The hydroxylapatite column removed the 37 and 20kDa contaminants, as well as concentrating the sample. The only remaining contaminants were bands of 28 and 29kDa (Figure 5.7). These were not removed by the FPLC MonoQ 10/10 or phenyl Superose columns. However, this contamination did not occur when the protease inhibitors were used as described in section 5.21. The expressed protein appeared to elute from the hydroxylapatite column as two adjacent peaks. The first peak was larger than the second and eluted between approximately 26 and 67mM potassium phosphate. The second minor peak eluted between 67 and 118mM potassium phosphate (see figure 5.7). The second peak had the same molecular weight as the major peak as judged by SDS-PAGE. The minor peak eluted from the FPLC Mono-Q 10/10 column at a slightly higher salt concentration. The major and minor peaks eluted from the MonoQ 10/10 column at approximately 44 to 49mM and 49 to 57mM NaCl (in buffer T') respectively (see figure 5.8). The purified actin binding domain appeared to be stable. No degradation was observed in samples kept at 4°C or at room temperature for a month.

Typical yields from a 1 litre culture were 20mg from the major peak of the hydroxylapatite column, plus a further 5mg from the minor

FIGURE 5.6
PURIFICATION OF THE ACTIN BINDING DOMAIN OF α-ACTININ:
ELUTION PROFILE FROM THE SEPHADEX G75 COLUMN.

The photographic insert shows a Coomassie stained SDS-PAGE minigel (12%) of (A) the applied sample (B) the peak fractions containing the actin binding domain, and (C) the proteins in the trailing edge. 10µl aliquots were applied to the minigel. The column bed size was 1x70cm. A flow rate of 20ml/hour was used. The eluent was buffer T'. Fractions of 2ml were collected.

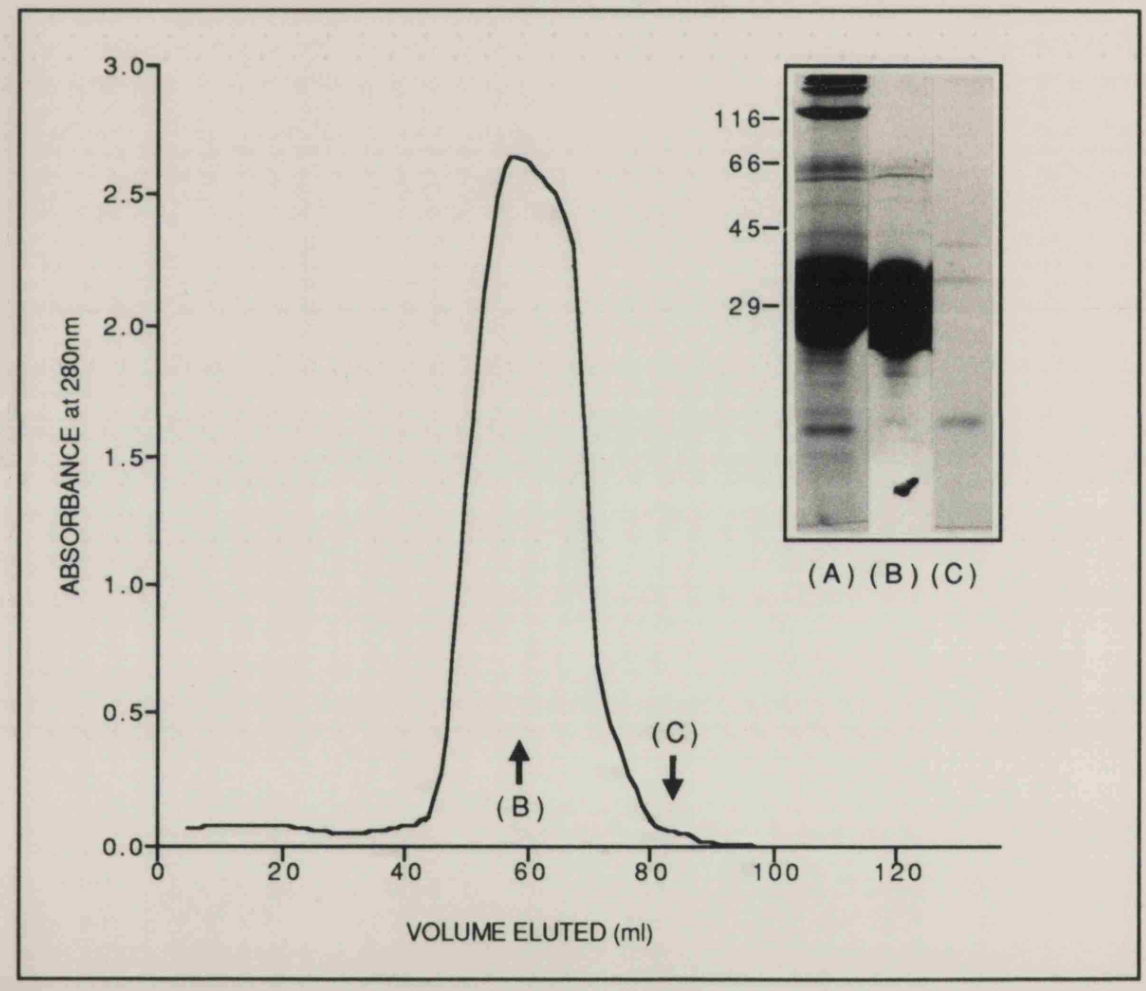

FIGURE 5.7
PURIFICATION OF THE ACTIN BINDING DOMAIN OF α-ACTININ: ELUTION PROFILE FROM THE HYDROXLAPATITE COLUMN.
The photographic insert shows a Coomassie stained SDS-PAGE minigel (12%) of (A) the applied sample, (B) the actin binding domain derived from the major peak, and (C) the actin binding domain derived from the minor peak. Aliquots of 10µl were applied to the minigel. The column bed size was 0.5x3cm. A flow rate of 10ml/hour was used. As indicated, a 50ml gradient of 10mM to 150mM potassium phosphate (pH7.0) was used as the eluent. 1ml fractions were collected.

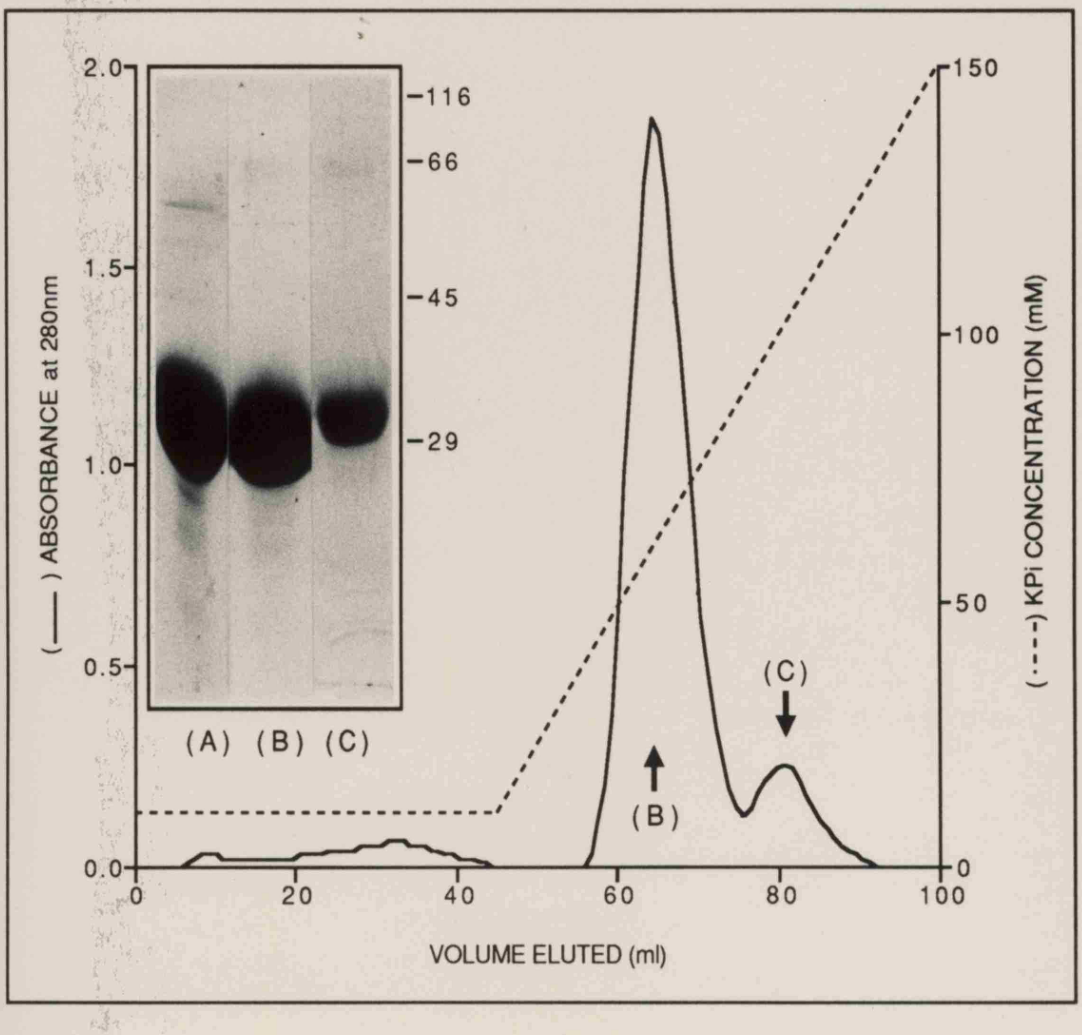

FIGURE 5.8
PURIFICATION OF THE ACTIN BINDING DOMAIN OF α-ACTININ: ELUTION PROFILE FROM THE MONO-Q 10/10 COLUMN.

The photographic insert shows a Coomassie stained SDS-PAGE minigel of the actin binding domain derived from the major (A) and minor (B) peaks. Aliquots of 10µl were applied to the minigel. A flow rate of 3ml/min was used. Buffer T' with a salt gradient as indicated was used as the eluent. 0.5ml fractions were collected.

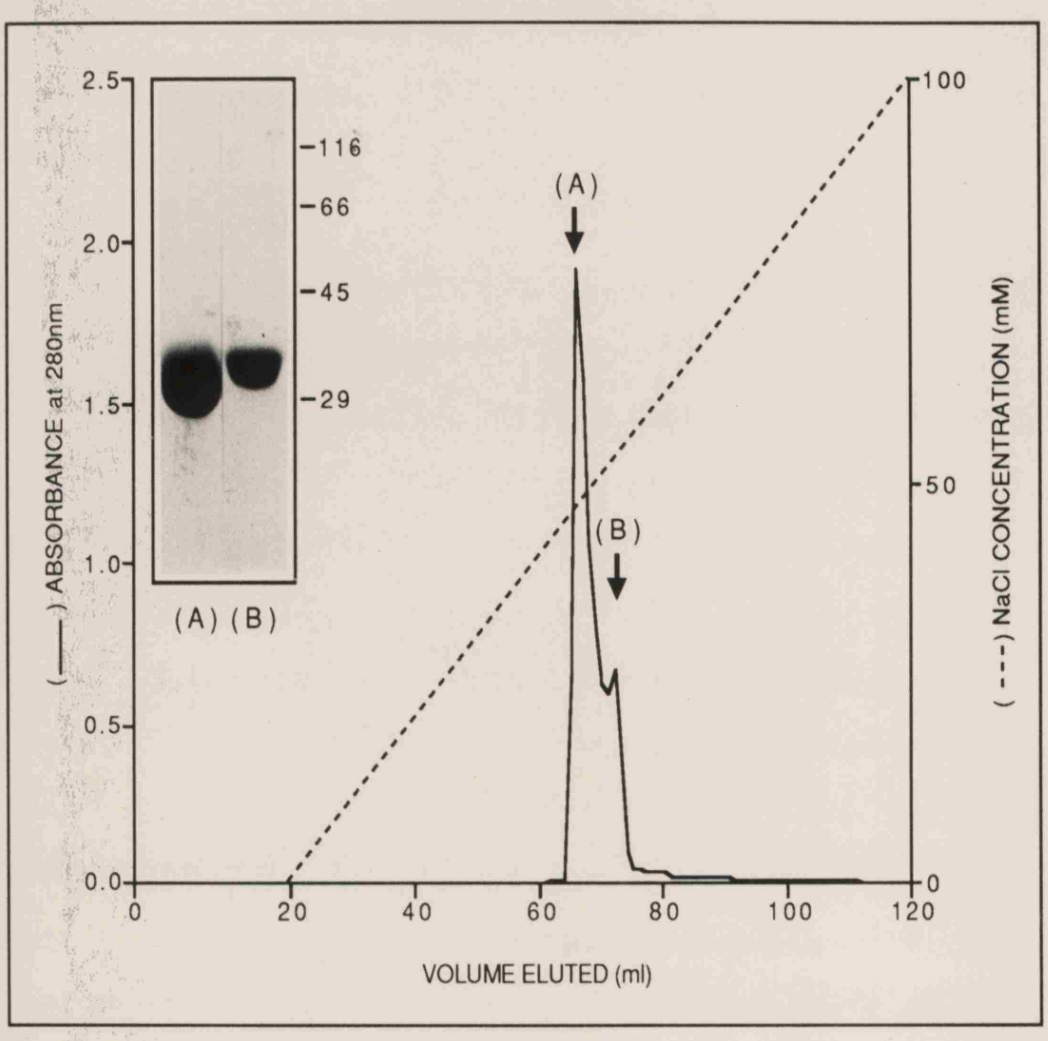

peak. Unless required for crystallisation, the major and minor peaks were be pooled. Following further chromatography of the major peak on a MonoQ 10/10 column, 16mg of crystallisation quality actin binding domain was produced.

5.33 EXAMINATION OF THE INTEGRITY OF THE EXPRESSED ACTIN BINDING DOMAIN OF α-ACTININ.

Three methods were used to investigate the integrity of the expressed actin binding domain.

COMPARISON OF THE THERMOLYSIN GENERATED PEPTIDE MAPS OF α-ACTININ AND THE ACTIN BINDING DOMAIN OF α-ACTININ.

When whole α-actinin was digested by thermolysin, it was rapidly degraded to peptides of 27kDa (via intermediates of 32 and 29kDa) and 53kDa. The thermolysin cleavage sites of α-actinin have previously been mapped (Figure 3.11). The thermolytic 27kDa fragment corresponded to the actin binding domain (residues 24 to approximately 269). The expressed α-actinin actin binding domain contained the whole of the actin binding domain plus part of repeat 1 (residues 1 to 268). The expressed protein was cleaved to a 27kDa fragment which was resistant to further thermolysin digestion, similar to the actin binding domain released from whole α-actinin (Figure 5.9).

CO-SEDIMENTATION OF THE α-ACTININ ACTIN BINDING DOMAIN WITH F-ACTIN.

The ability of the expressed actin binding domain to be co-sedimented with F-actin was examined to show whether it retained an active conformation. 50-60% of the F-actin was present in the pellet

FIGURE 5.9

COMPARISON OF THE PEPTIDE MAPS PRODUCED BY THERMOLYSIN DIGESTION OF α-ACTININ AND THE EXPRESSED ACTIN BINDING DOMAIN OF α-ACTININ.

150μg of α-actinin and 80μg of the expressed α-actinin actin binding domain were digested with 6 and 2μg respectively of thermolysin at 37°C. 30μg aliquots of α-actinin and 20μg aliquots of the actin binding domain were taken at the times indicated (minutes) and the thermolysin inactivated by the addition of EDTA to 10mM. The samples were applied to a 10% SDS-PAGE gel. This was stained with Coomassie. Molecular weights (kDa) are noted down the axis. The two upper bands in the actin binding domain samples are a minor contaminant.

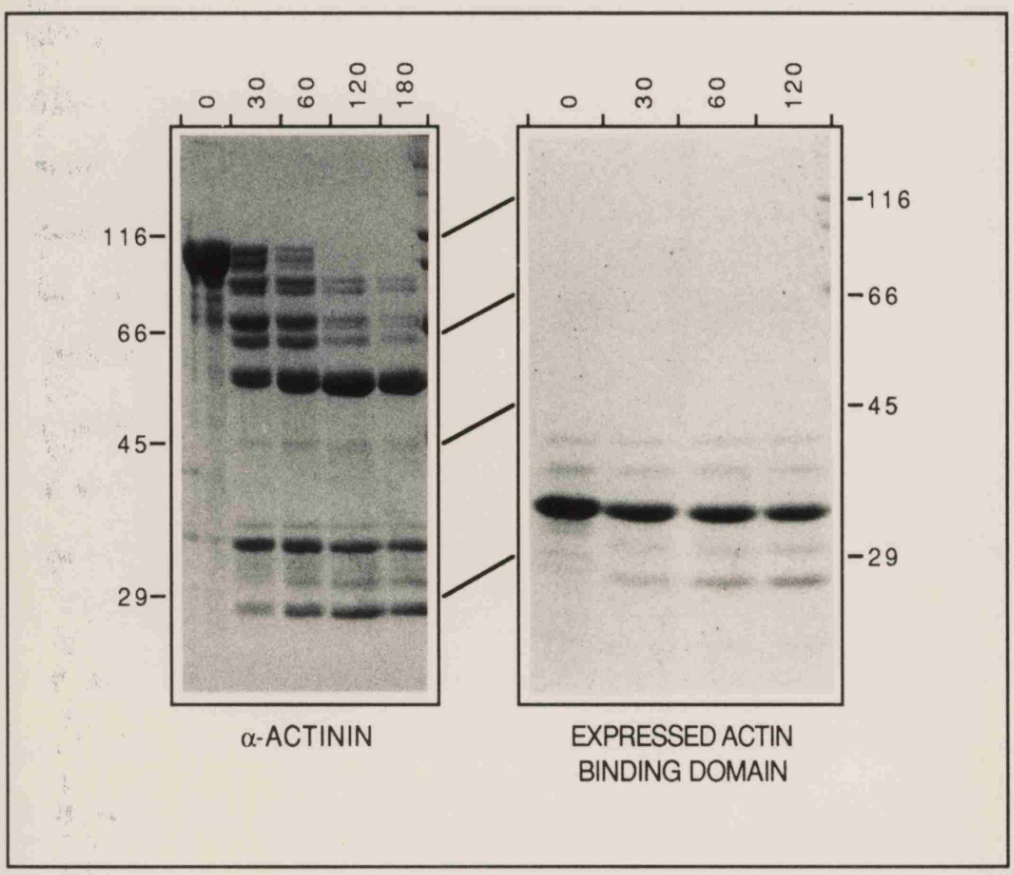

(Figure 5.10). α-Actinin co-sedimented with F-actin. Some α-actinin did sediment in the absence of F-actin. Considering the background sedimentation, approximately 7% of the α-actinin was co-sedimented in the presence of F-actin. There was no noticeable reduction of the amount of α-actinin in the supernatant. Cytochrome c did not co-sediment. About 50% of the expressed actin binding domain co-sedimented in the presence of actin suggesting that it retained an active conformation. No actin binding domain pelleted when F-actin was absent.

EXAMINATION OF THE ACTIN BINDING DOMAIN BY ELECTROPHORESIS ON NATIVE GELS.

The actin binding domain was further examined by electrophoresis on native gels as it failed to crystallise (see below). On native gels, vinculin ran as a single band, and BSA gave two bands. The purified actin binding domain of α-actinin ran as a triplet (Figure 5.11). A similar triplet was obtained for a variety of conditions. The expressed protein was incubated in buffers at pH6, 7, 7.5, and 8. A number of salt concentrations were examined (10, 60, 110, 160, and 210mM NaCl). Various concentrations of actin binding domain were used plus or minus β-mercaptoethanol. An aliquot of the actin binding domain from the major peak of the MonoQ 10/10 column was checked with the MonoQ 5/5 column to show that the major and minor peaks had been separated (see figure 5.12). When re-examined with the MonoQ 5/5 column 10 days later, the peak fractions still produced a single peak. The peak fraction ran as a triplet on native gels.

FIGURE 5.10

CO-SEDIMENTATION OF α-ACTININ AND THE ACTIN BINDING DOMAIN OF α-ACTININ WITH F-ACTIN.

Samples were centrifuged as described in section 2.48. The buffer used was 10mM Tris/HCL, pH7.5, 100mM KCl, 0.1mM ATP, 4mM $MgCl_2$, 1mM β-mercaptoethanol. S and P indicate the supernatant and pellet after ultracentrifugation of the solutions as follows: α-actinin and actin; α-actinin alone; α-actinin actin binding domain alone; α-actinin actin binding domain plus actin; actin alone. The concentrations of actin, α-actinin, and α-actinin actin binding domain were 4.8, 0.5, and 3.2μM respectively.

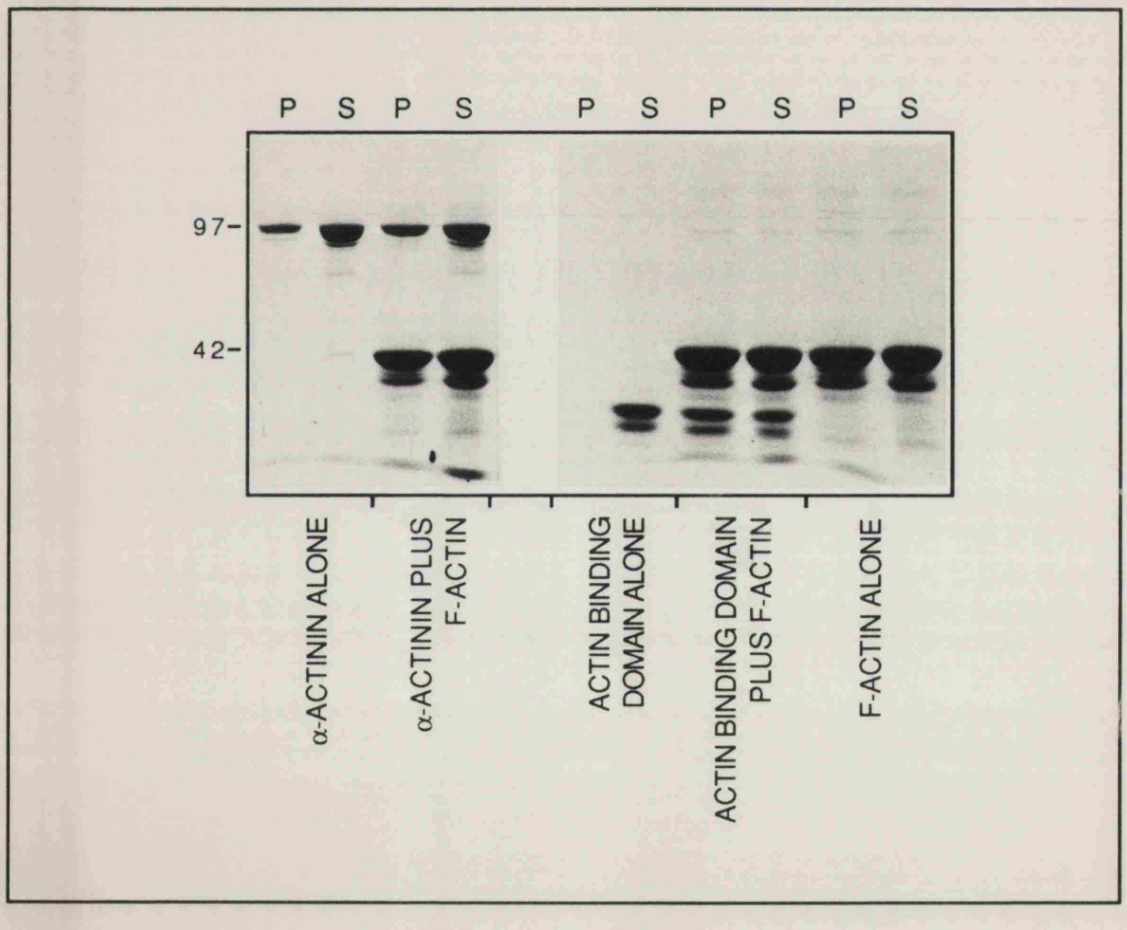

FIGURE 5.11
EXAMINATION OF THE α-ACTININ ACTIN BINDING DOMAIN ON NATIVE GELS.
The α-actinin actin binding domain was dialysed into 50mM MES, pH6.0, 10mM Tris, pH7.0, and 10mM Tris, pH8.0. 11μg aliquots of the actin binding domain and 5μg of vinculin were applied to the native gel.

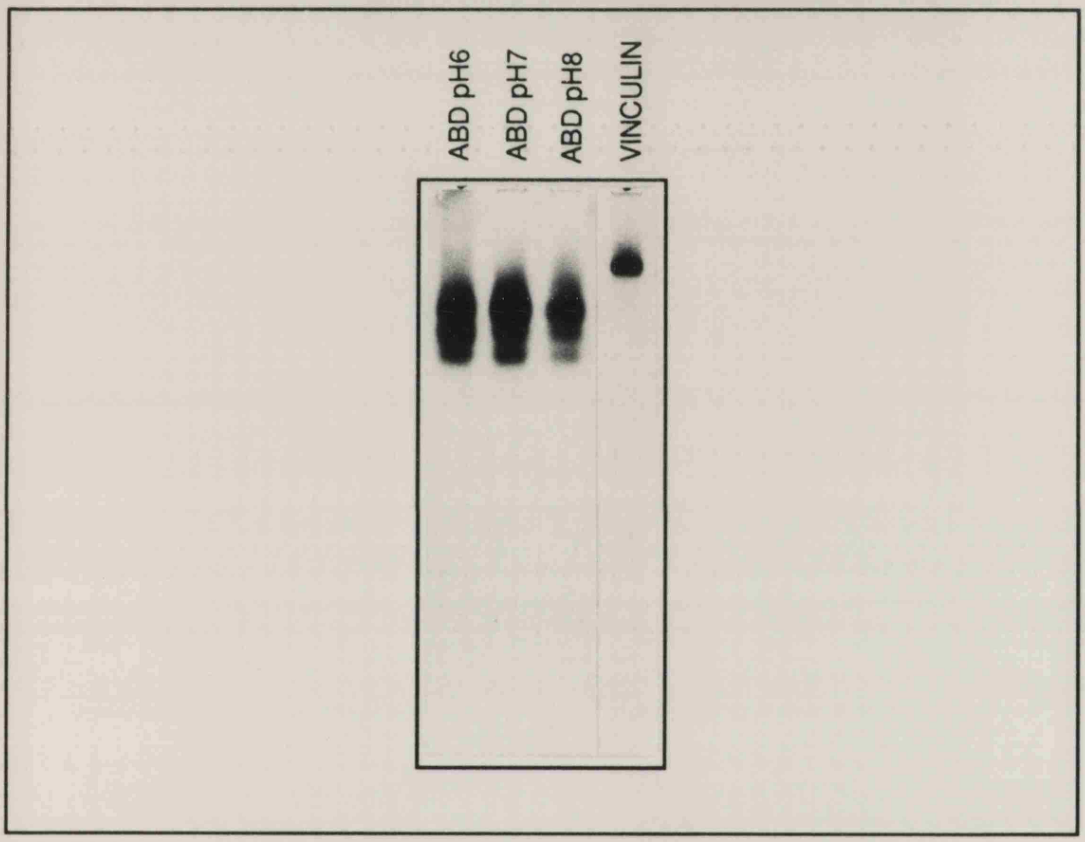

FIGURE 5.12
PURIFICATION OF THE ACTIN BINDING DOMAIN OF α-ACTININ:
ELUTION PROFILE FROM THE MONO-Q 5/5 COLUMN.
Approximately 3.5mg of protein was applied to the column. A flow rate of 1ml/min was used. Buffer T' with a salt gradient as indicated was used as the eluent. 0.5ml fractions were collected.

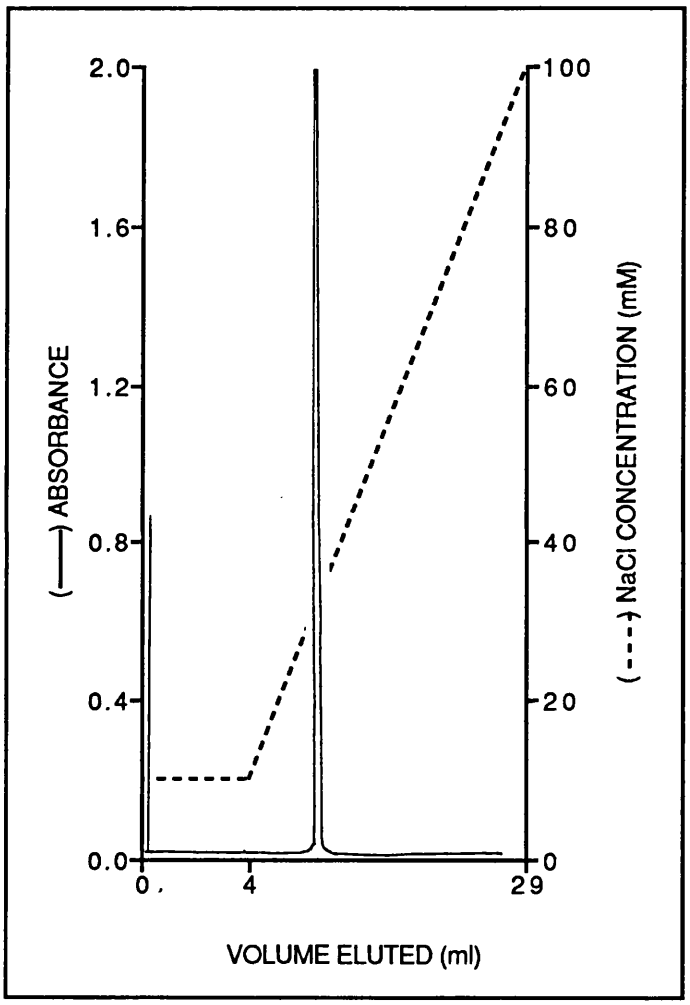

5.34 ATTEMPTS AT THE CRYSTALLISATION OF THE ACTIN BINDING DOMAIN OF α-ACTININ.

Crystallisation was tried with the conditions (all at 4°C) shown in table 5.3

Ammonium sulphate concentrations (7.3mg/ml actin binding domain, pH7.5) to 41% yielded nothing significant. Often small grains would be seen that were sometimes angular, but these did not develop further. From 42% upwards, many grains were observed. These were located towards the centre of the drop, and progressively occupied a larger proportion of the drop as the ammonium sulphate concentration increased. At concentrations of 42-44% there were grains of 25μm, but these did not grow further. The point of total precipitation (where the drop was totally occupied by granular material) was 44-45% when a protein concentration of 3.1mg/ml was used.

Similar results were obtained with ammonium sulphate at pH6, 7, and 8 (3.1mg/ml actin binding domain). The points for total precipitation were approximately 44, 50, and 50% respectively.

The point of total precipitation with MPD (7.3mg/ml actin binding domain, pH7.5) was 23%. The precipitate was fine. A few very small grains were seen.

Below 23% PEG 400 (7.3mg/ml actin binding domain, pH7.5) nothing significant was noted. Occasionally very small (5μm) grains were observed, but these did not have a distinct shape. With 23% PEG the drop was initially opaque (at day 3), but this had disappeared by day

TABLE 5.3

The various conditions tried for the crystallisation of the actin binding domain of α-actinin.

PRECIPITANT		BUFFER	PROTEIN
TYPE	CONC^N		CONC^N
$AmSO_4$	5-60 (5% Steps)	50mM Tris, pH7.5	7.3mg/ml
MPD	5-45 (5% Steps)	10mM Tris, pH7.5	7.3mg/ml
PEG 400	5-45 (5% Steps)	10mM Tris, pH7.5	7.3mg/ml
PEG 4000	5-45 (5% Steps)	10mM Tris, pH7.5	7.3mg/ml
$AmSO_4$	38-49 (1% Steps)	50mM Tris, pH7.5	7.3mg/ml
MPD	20-30 (1% Steps)	10mM Tris, pH7.5	7.3mg/ml
PEG 400	5-29 (2% Steps)	10mM Tris, pH7.5	7.3mg/ml
PEG 4000	7-33 (2% Steps)	10mM Tris, pH7.5	7.3mg/ml
$AmSO_4$	42-53 (1% Steps)	50mM Tris, pH7.5	3.1mg/ml
PEG 400	20-36 (2% Steps)	10mM Tris, pH7.5	3.1mg/ml
PEG 4000	15-30 (3% Steps)	10mM Tris, pH7.5	3.1mg/ml
$AmSO_4$	42-52 (2% Steps)	50mM MES, pH6.0	3.1mg/ml
$AmSO_4$	42-52 (2% Steps)	50mM Tris, pH7.0	3.1mg/ml
$AmSO_4$	42-52 (2% Steps)	50mM Tris, pH8.0	3.1mg/ml

20. The boundary of total precipitation was at 25%. Grains of 25μm were seen that appeared to have some angular sides. However, no advancement from this state was observed. PEG concentrations of 27% upwards contained total precipitates. Similar results were obtained when a protein concentration of 3.1mg/ml was used. The PEG concentration for significant precipitation was 28%.

At low PEG 4000 concentrations (7.3mg/ml actin binding domain, pH7.5) a microcrystalline precipitate was generally seen. The point of total precipitation occurred at about 15% PEG. However, many of the hanging drops at the higher PEG 4000 concentrations developed condensation over their surface making examination difficult. When the final concentration of the actin binding domain was 3.1mg/ml, total precipitation occurred at 24-27% PEG.

In collaboration with David Rice (Sheffield University), the following precipitating concentrations were tried. The buffers used were 0.1M citrate at pH's 4, 5, and 6, 0.1M HEPES at pH's 7 and 8, and 0.05M glycine/NaOH at pH9, each with 1mM EDTA and 10mM β-mercaptoethanol. At pH4 and 5 the protein precipitated. The protein also precipitated at pH6 but not as rapidly as with the lower pH buffers. A range of protein concentrations were examined.

Ammonium sulphate concentrations of 20%, 22.5%, 25%, 30%, 35%, 40%, 45%, 50%, and 55% were used. At the low ammonium sulphate concentrations a low level of microcrystalline precipitate was seen, rising to total precipitation. Total precipitation occurred at approximately 30% at pH7, 45% at pH8, and 40-45% at pH9. No single crystals were detected.

MPD concentrations between 5% and 15% were tested. Low levels of precipitate were seen at low MPD concentrations. High levels of precipitate were seen at 15% MPD at pH's 7 and 8, whilst 10% MPD was sufficient at pH9.

A concentration range of 6% to 30% polyethylene glycol 3000 was examined. These crystallisations initially appeared quite hopeful as the microcrystalline precipitate of the 20% PEG solution at pH8 contained several very small (10μm) crystals. However the number of single crystals was a small fraction of the total and may not represent protein.

5.35 THE EXPRESSION IN *E. COLI* OF THE REPEAT DOMAIN OF α-ACTININ AND THE PURIFICATION OF THE EXPRESSED POLYPEPTIDE.

CELL GROWTH AND EXPRESSION.

Some 60 to 70% of the expressed α-actinin repeats were shown to be soluble when the cells were induced at 37°C with 0.5mM IPTG. However, rather than producing a single glutathione-linked fusion protein of 87kDa, the major products were of 29 and 58kDa. Western Blotting with an anti-α-actinin antibody showed that the 58kDa band was derived from α-actinin. Some intact fusion protein was also observed. The intact fusion protein was less than 5% of the expressed protein (Figure 5.13, track A). Peptide sequencing of the 58kDa fragment showed that the N-terminus was threonine$_{240}$.

FIGURE 5.13
PURIFICATION OF THE REPEAT DOMAIN OF α-ACTININ: ELUTION PROFILE FROM THE DEAE-SEPHAROSE FAST-FLOW COLUMN.
The photographic inserts show Coomassie stained SDS-PAGE minigels (12%) of (A) the applied sample and protein from the leading edge (B), the centre (C), and the trailing edge (D) of the peak. The repeat domain was present in the centre of the peak. 20µl aliquots were applied to the minigel. The column bed size was 1.0x15cm. A flow rate of 30ml/hour was used. Buffer T with a salt gradient as indicated was used as the eluent. 3ml fractions were collected.

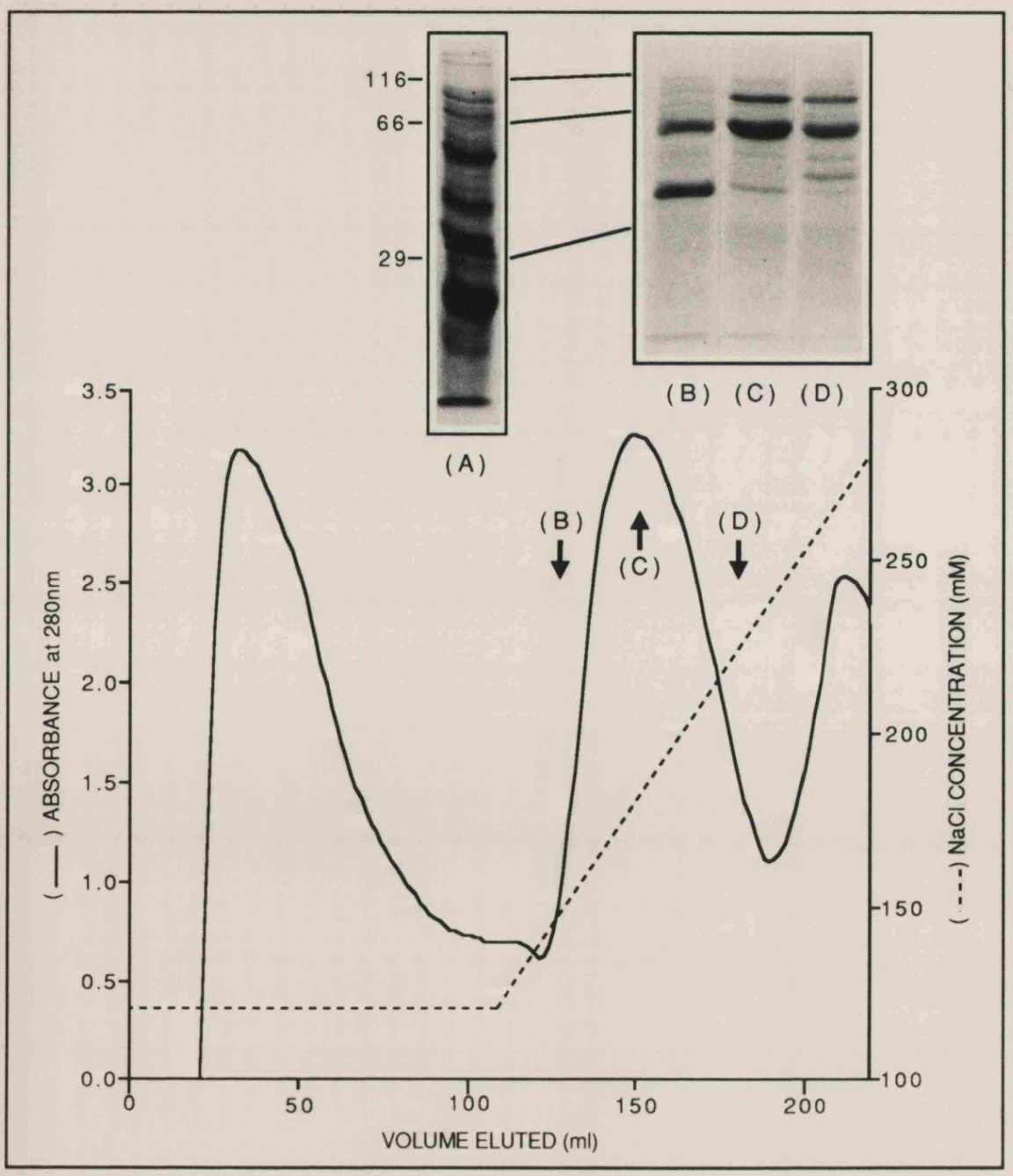

PROTEIN PURIFICATION.

Following dialysis of the soluble fraction of the cell extract against buffer T, the sample was applied to the DEAE-Sepharose Fast-Flow column. The expressed protein eluted at approximately buffer T plus 200-235mM NaCl (Figure 5.13). The main contaminants were proteins of 45 and 87kDa. The 87kDa band was intact fusion protein. In addition there were numerous other bands between 20 and 100kDa. The GST alone eluted at a low salt concentration.

The peak fractions were pooled and concentrated before being applied to a Sephacryl S200HR sizing column. Contaminants below 42kDa were separated from the expressed protein, along with the 45 and 80kDa bands (Figure 5.14).

Minor contaminants of approximately 45, 50, 52, 97 and 120kDa remained after hydroxylapatite chromatography (see figure 5.15). At this stage, degradation of the expressed protein to a closely spaced doublet was apparent. The two proteins were present in similar amounts. They could not be resolved by FPLC monoQ chromatography.

5.4 DISCUSSION.

5.41 ATTEMPTS AT CRYSTALLISATION OF α-ACTININ.

Crystals of α-actinin did not grow using the conditions examined. The precipitates observed suggested that crystallisation was possible, but that crystal growth was being inhibited. There are many reasons why α-actinin may not be forming crystals. The precipitant may not have

FIGURE 5.14
PURIFICATION OF THE REPEAT DOMAIN OF α-ACTININ: ELUTION PROFILE FROM THE SEPHACRYL S200 HR COLUMN.
The photographic insert shows a Coomassie stained SDS-PAGE minigel (12%) of (A) the applied sample (B) the peak repeat domain containing fraction, and (C) protein from the peaks trailing edge. Aliquots of 20μl were applied to the minigel. The column bed size was 1x75cm. A flow rate of 30ml/hour was used. The eluent was buffer B. Fractions of 2ml were collected.

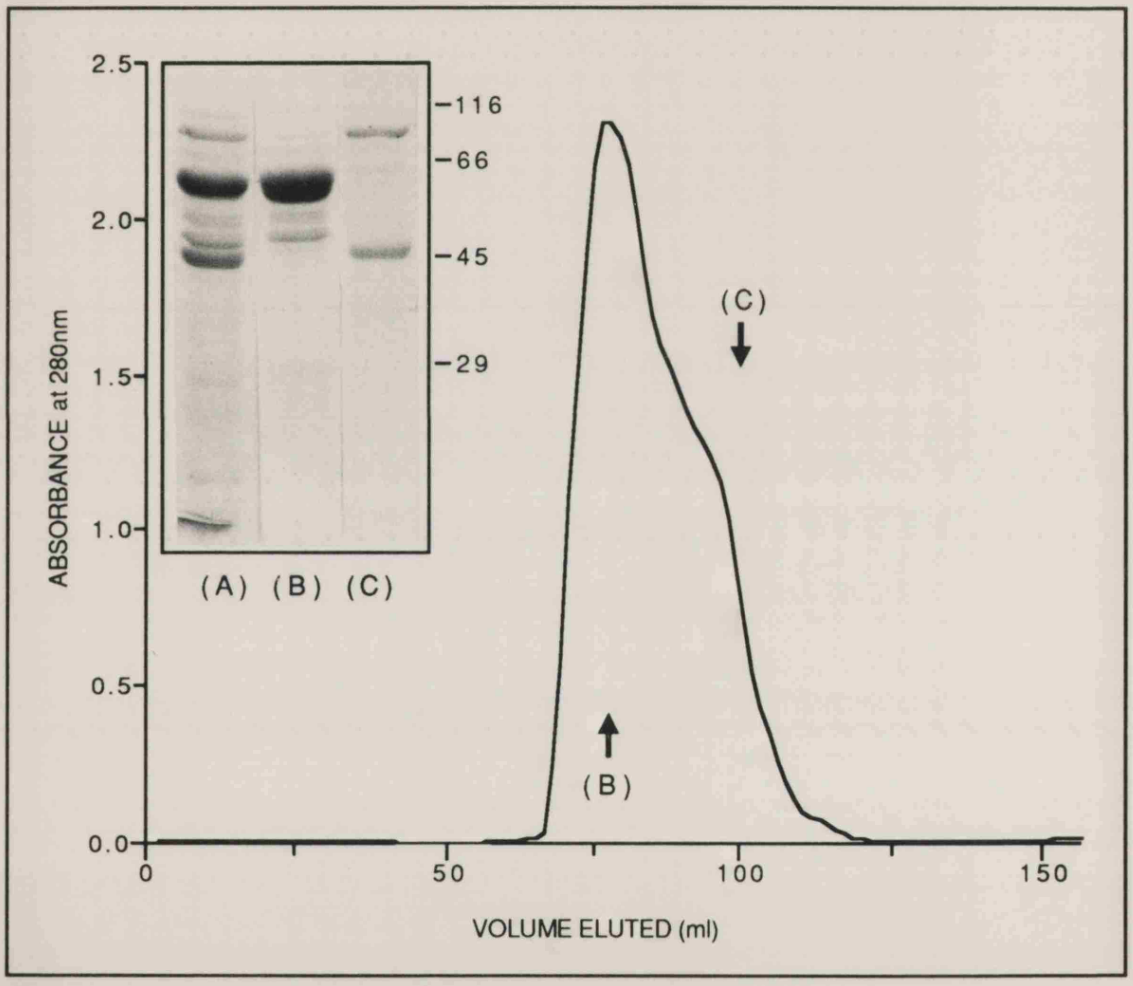

FIGURE 5.15
PURIFICATION OF THE REPEAT DOMAIN OF α-ACTININ: ELUTION PROFILE FROM THE HYDROXYLAPATITE COLUMN.

The photographic insert shows a Coomassie stained SDS-PAGE minigel (12%) of (A) the unbound protein and (B) the peak repeat domain containing fraction. 20µl aliquots were applied to the minigel. The column bed size was 0.5x3cm. A flow rate of 10ml/hour was used. Potassium phosphate, pH7.0, with a salt gradient as indicated was used as the eluent. 2ml fractions were collected.

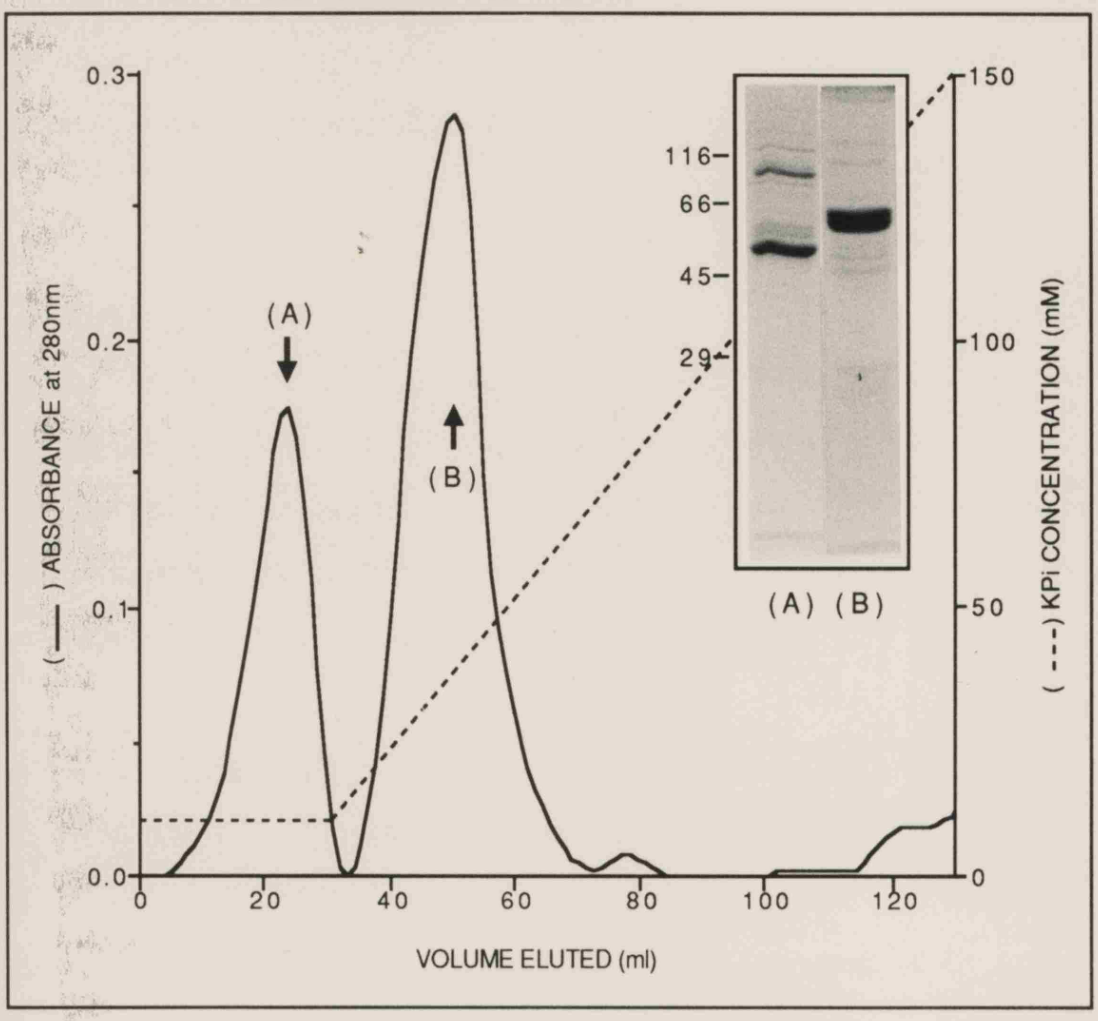

been suitable. The difference between a protein crystallising or not crystallising can be as little as a 0.5% difference in the ammonium sulphate concentration (McPherson, 1982). A more likely explanation was that the sample was slightly contaminated by a 70kDa degradation product. Degradation products pose a greater problem to crystallisation than contaminating proteins (McPherson, 1982). This is because a degraded fragment would be able to incorporate into the growing regular crystal lattice, but would not permit the incorporation of further protein.

Further attempts could be made at improving the purification of α-actinin, such that the trace amounts of the 70kDa degradation product were removed. However, if α-actinin were ultimately crystallised the amount of data to be processed would be vast. Because of this attempts were also made to purify and crystallise distinct domains of α-actinin. Smaller domains would provide more manageable data sets if crystals were obtained.

5.42 THE EXPRESSION IN *E. COLI* OF THE ACTIN BINDING DOMAIN OF α-ACTININ AND THE PURIFICATION OF THE EXPRESSED POLYPEPTIDE.

The actin binding domain was purified after expression in *E. coli* for two reasons. The alternative source for the actin binding domain was from a thermolysin digest of whole α-actinin. This would have required the purification of α-actinin, digestion of that α-actinin, and purification of the 27kDa actin binding domain from the remaining thermolytic fragments. The 27kDa fragment could easily be separated from the fragments containing the repeats (those above 53kDa) by FPLC MonoQ chromatography. However, the 27kDa

fragment was not separated from its slightly larger precursor (29kDa). The 32kDa fragment, a precursor of the 27 and 29kDa fragments, could be separated (data not shown). A purification protocol for the separation of the 27kDa fragment from the repeat containing fragments has been reported (Mimura and Asano, 1986). Whether this column separated the 27, 29, and 32kDa fragments could not be discerned. The expression of the actin binding domain in *E. coli* permitted the purification of high yields of the expressed actin binding domain.

CELL GROWTH AND EXPRESSION.

The NcoI-HincII fragment of the chicken smooth muscle α-actinin cDNA C17 was cloned into the T7 plasmid pMW172. The expressed protein coded for the entire actin binding domain plus 23 residues from repeat 1. The C-terminus had three additional residues derived from the multiple cloning site, whilst the N-terminus had four additional amino acids (including the initiating methionine of the multiple cloning site and the initiating methionine for α-actinin). The pMW172 vector, derived from pBR322, contained a T7 promoter and multiple cloning site (Figure 5.1) (Way et al, 1990). The T7 promoter is specifically recognised by the T7 RNA polymerase but is not recognised by the endogenous *E. coli* RNA polymerase. The plasmid was transformed into the *E. coli* strain BL21(DE3). This cell line had the gene for T7 RNA polymerase integrated into the host chromosome. The T7 RNA polymerase gene was under the control of lacUV5 regulatory elements.

60-80% of the expressed protein was found to be in the soluble fraction if the cultures were grown at 30°C. The proportion of

expressed protein in the soluble fraction was lower if the cultures were grown with higher levels of IPTG or at 37°C after induction. There were significant levels of expression in the absence of IPTG. In complex media the lacUV5 regulatory elements are sometimes "leaky" and allow low levels of transcription of the T7 RNA polymerase. Since the T7 RNA polymerase only affects the T7 promoter and elongates RNA some five times quicker than the *E. coli* RNA polymerase, significant levels of expression of the actin binding domain were observed due to the "leaky" expression of the T7 RNA polymerase (Studier and Moffat, 1986). This could possibly be reduced by growing the cells in minimal media with glucose as the sole carbon source. This was deemed unnecesary as expression was good.

Once the purification protocol was developed, problems were encountered with the expression of soluble α-actinin actin binding domain. Despite following the same procedures each time, cultures often expressed low levels of the actin binding domain, or the expressed protein was insoluble. I have found no explanation for this, although this problem has been observed elsewhere (Dr. A. Weeds, personal communication). One possible explanation is that this cell line/plasmid combination produce large amounts of β-lactamase (Studier and Moffat, 1986). β-lactamase degrades ampicillin, which may have permittted cells lacking plasmid to predominate. An ampicillin concentration of 0.5mg/ml was therefore used. Cell growth was unaffected by the ampicillin concentrations examined (tested up to 1mg/ml). However, although this may have explained the low levels of expression of the actin binding domain, it did not explain the shift of protein expression from the soluble to the

insoluble fraction of the cells. The efficiency of expression declined with the age of the plate used to innoculate cultures. Though plates could be kept for two months, the number of colonies that would give reasonable expression appeared to decline. Cultures innoculated from older plates tended to grow slower than those derived from fresh transformants. Cultures innoculated from a glycerol stock generally, but not always, gave reasonable expression. Re-transforming from plasmid DNA stocks produced cells that expressed soluble protein.

PROTEIN PURIFICATION.

The DEAE-Sepharose Fast-Flow column proved to be a very effective purification step. The actin binding domain eluted at a low NaCl concentration, whilst most of the endogenous *E. coli* proteins required a NaCl concentration of over 150mM to be eluted. Following DEAE-Sepharose Fast-Flow chromatography the expressed protein was approximately 75% pure. The main contaminants were of approximately 40, 37, 29, 28, and 20kDa. If the later fractions were taken, the only contaminant would have been the 37kDa protein. However, although this would have removed the need to use the hydroxylapatite column, the yield would have been reduced by approximately one third.

Hydroxylapatite and molecular sieving chromatography were both examined as the next purification step. As detailed below, both were useful, but the sizing column was chosen as the next step as it was initially thought that this would remove the need to dialyse the sample into buffer T'.

The elution position of the expressed actin binding domain from the DEAE-Sepharose Fast-Flow column suggested that a cation exchanger could be used as the second purification column. Unfortunately this was not viable as the low pH buffer required precipitated the protein.

An ammonium sulphate step was used to concentrate the protein. Addition of ammonium sulphate to 50% saturation only precipitated some 50-60% of the expressed protein. A 60% cut appeared to precipitate all the protein, but to fully redisolve the pellet, the sample had to be dialysed against buffer T'.

The expressed protein eluted from the Sephadex G75 column with a K_{av} value of approximately 0.06. This column removed the 40kDa contaminant. The resolution could possibly be improved if the sample was split and run as two aliquots.

The hydroxylapatite column was an effective concentration step. It also removed the 37 and 20kDa contaminants. The peak fractions were pooled and shown to be at least 98% pure on SDS-polyacrylamide gels. When the inhibitors E64 and leupeptin were omitted, there were contaminants of 28 and 29kDa, which were not removed by the FPLC MonoQ 10/10 or phenyl Superose columns. Western Blotting with anti-α-actinin antibody demonstrated that the 28 and 29kDa bands were degradation products of the expressed actin binding domain. One point of concern was the way that the expressed protein appeared to elute from the hydroxylapatite column as two peaks (Figure 5.7). The second smaller peak apparently had the same molecular weight as the major peak. The two peaks also eluted from the FPLC monoQ 10/10 column at different salt

concentrations. One possible explanation for the two bands was that these were two entirely different proteins that initially co-purified. However, this was shown not to be the case as protein in the minor peak fractions also cross-reacted with the anti-α-actinin antibody. The most likely explanation is that the expressed protein had been very slightly nicked so that its ionic character differed, though its mobility on SDS-polyacrylamide gels was apparently unaffected. Considering the N- and C-termini of the expressed protein, whose sequences were:-

```
          1       *
M G S M D H H Y   D P Q Q T - - -

                        *    268
- - - - R I C K V   L A V P L V
```

Two thermolysin cleavage sites are shown (*) as these indicate regions of native α-actinin that are accessible to protease. Assuming that the secondary peak is the nicked protein, it should have had a greater net negative charge than the major peak as it eluted at a higher salt concentration from the MonoQ column. The number of residues removed should also have been small to account for the apparent lack in change of molecular weight. Both these criteria are fulfilled by trimming of the C-termini to residue 263, which removes one basic residue and approximately 0.8kDa, or trimming to residue 260, which removes two basic residues and about 1.2kDa. Furthermore, the 28 and 29kDa contaminants can also be explained by trimming of approximately 18 residues from the N- and C-termini.

Although the protein obtained from the hydroxylapatite column (both major and minor peaks) was adequate for most purposes, the charge heterogeneity was such that it could not have been used for crystallisation studies. For this, the major peak from the hydroxylapatite column was further purified on the MonoQ 10/10 column. Pure protein was produced by this method, as judged by SDS-PAGE (Coomassie stained and Western Blotted) and analytical FPLC using the MonoQ 5/5 column.

5.43 EXAMINATION OF THE INTEGRITY OF THE EXPRESSED ACTIN BINDING DOMAIN OF α-ACTININ.

For the expressed protein to be useful, it had to be in the correct conformation. Both α-actinin and the actin binding domain of α-actinin could be digested with thermolysin yielding a thermolysin resistant fragment of 27kDa. This suggested that the expressed actin binding domain had a similar core to that within intact α-actinin. As previously shown (see section 3.35), α-actinin co-sediments with F-actin. However, the amount of α-actinin that pelleted was some 5 to 10 times less that expected, considering an α-actinin/F-actin interaction having a K_d of 10^{-6}M (Meyer and Aebi, 1990). The expressed actin binding domain was also shown to bind F-actin. A greater proportion of the expressed actin binding domain was co-sedimented than intact α-actinin. This suggested that the actin binding domain alone had a higher affinity for F-actin than did intact α-actinin. However, it has previously been suggested that the thermolysin derived 27kDa fragment of α-actinin had a lower affinity for F-actin than did whole α-actinin (Mimura and Asano, 1986). More recently Way et al (in press) have shown that the expressed actin binding domain (residues 1 to 268) has a ten fold lower affinity for

F-actin than whole α-actinin. The reason for this discrepancy is unclear. Taken together these results strongly suggested that the expressed actin binding domain had the conformation of the native actin binding domain.

The expressed actin binding domain was thought to be homogenous. Three methods were used to demonstrate homogeneity. The expressed protein yielded a single band on SDS-PAGE gels at low and high protein loadings. Western Blotting showed no evidence for the presence of minor degradation products. The purified actin binding domain produced a very sharp and symmetrical peak when examined on the MonoQ 5/5 column. However, since the actin binding domain failed to crystallise (see below), the sample was examined by electrophoresis on native gels. Native gels revealed a degree of microheterogeneity.

Microheterogeneity can arise in a number of ways. These include binding of a prosthetic group, modification with carbohydrate or lipid, proteolytic degradation, side chain oxidation, amino acid modification, genetic variation, aggregation, and partial denaturation. Binding of prosthetic groups and genetic variation would not have been responsible for the microheterogeneity observed with the actin binding domain. The only post-translational modification of α-actinin is acetylation of the N-terminus (Singh et al, 1977). However, differences due to acetylation would not have been detected on native gels. Whether expression in *E. coli* would affect acetylation is unclear. β-mercaptoethanol was included throughout the purification, so that cysteines should have remained in their reduced form. Proteolytic degradation could have been responsible

for the microheterogeneity, though this seemed unlikely. No charge heterogeneity was noted on the MonoQ column. Removal of a few residues from the actin binding domain with no alteration in charge would probably not have been discerned on the native gel. The cleavage of larger fragments would have been revealed on SDS-PAGE gels. Partial denaturation would probably not be revealed by native gels. Aggregation is a likely possibility to explain the presence of the three bands on native gels. Indeed, the K_{av} with which the actin binding domain eluted from the Sephadex G75 column (0.06) suggested that the protein had a molecular weight of 70kDa. A 35kDa protein would be expected to have a K_{av} of approximately 0.2. Since aggregation may be via charge to charge interactions, the association could be affected by pH, ionic strength, and ionic species. However, the ratio of the three bands in native gels was not markedly affected by the pH's and ionic strengths (NaCl) examined. Even if the actin binding domain could be stabilised in a specific oligomeric form (assuming aggregation is the problem) by defined pH/ionic conditions, this would restrict the range of conditions that could be used in crystallisation studies. Aggregation of the actin binding domain may be due to the hydrophobic nature of this domain, therefore the addition of low levels of mild detergents to the buffers may prevent aggregation.

5.44 ATTEMPTS AT THE CRYSTALLISATION OF THE ACTIN BINDING DOMAIN OF α-ACTININ.

Unfortunately the α-actinin actin binding domain did not crystallise under the conditions examined. Larger grains were often observed, but these never exceeded 25μm. Although they were sometimes slightly angular, the grains did not have the regular sides expected of

a crystal and did not grow further. A crystal of some 100μm would be required for X-ray diffraction using a good X-ray source, whilst a crystal of 2-300μm would be required using a lesser X-ray sources. There were many possible reasons for crystallisation being difficult. It could have simply been that the parameters for crystallisation examined were not quite correct. Many aspects could be changed, such as the protein concentration, temperature, precipitant concentration, and the type of precipitating agent. A more likely explanation for the lack of crystallisation was the microheterogeneity revealed on native gels. It would be worthwhile seeing if the microheterogeneity could be eliminated, as mentioned above. The expressed protein contains the whole actin binding domain plus part of repeat 1. It is conceivable that the residues that constitute the actin binding domain formed a stable structure whilst the remaining sequence derived from the interdomain linker and repeat 1 could not form its proper conformation and was fairly flexible. Such dynamic microheterogeneity would prevent crystallisation but would be difficult to diagnose. One possible approach to solving such dynamic microheterogeneity would be to use a shorter fragment of the actin binding domain.

Various other things could be tried. These include trying to co-crystallise the actin binding domain with actin, as has been successful with the actin/DNAse I (Kabsch et al, 1990) and actin/gesolin complexes, or trying to co-crystallise with actin peptides.

5.45 THE EXPRESSION IN *E. COLI* OF THE SPECTRIN-LIKE REPEATS OF α-ACTININ AND THE PURIFICATION OF THE EXPRESSED POLYPEPTIDE.

CELL GROWTH AND EXPRESSION.

An EcoRV-Xmn1 fragment of the chick non-muscle α-actinin cDNA C18 was cloned into the plasmid pGEX-3X. This fragment coded for residues 218-749 (ie, 27 residues of the actin binding domain, the repeats, and 37 residues of the C-terminal domain). This plasmid produced a GST-linked fusion protein which would normally allow the single step purification of the target protein. The target protein could then have been cleaved from the GST using thrombin. However, during expression, this fusion protein was cleaved between residues 239-240 of the target protein (cleavage site demonstrated by amino terminus peptide sequencing). Therefore the GST could not be utilised for purification.

Generally the expressed protein was difficult to discern on SDS-PAGE gels of the cell extract. The pGEX plasmids are not high level expression vectors like that used in the expression of the α-actinin actin binding domain (see above). They will produce up to 15μg protein/ml of culture (Smith and Johnson, 1988) which, providing the GST fusion protein remained intact would be relatively easy to purify. Western Blotting with anti-α-actinin antibody showed that 60-70% of the expressed protein was found to be in the soluble fraction if the cultures were grown as described. The majority of the fusion protein was cleaved after residue 239. Less than 5% of the expressed protein was in the intact form. The proportion of the intact expressed protein in the soluble fraction was the same as that for the cleaved expressed protein.

PROTEIN PURIFICATION.

The cleaved expressed protein formed a distinct band on SDS-PAGE gels once it had eluted from the DEAE-Sepharose Fast-Flow column. It eluted at salt concentrations similar to those required to displace whole α-actinin.

The peak fractions from the DEAE-Sepharose Fast-Flow column were pooled, concentrated, and dialysed into buffer T. The sample was applied to a Sephacryl S200HR sizing column. Using gel filtration chromatography, the 53kDa thermolysin fragment of α-actinin has been demonstrated to be a dimer (Mimura and Asano, 1987). The expressed protein eluted with a K_{av} of 0.07. This was consistent with the expressed protein being a dimer.

The hydroxylapatite column produced some purification. However it was observed that the expressed protein ran as a doublet on SDS-PAGE gels following this step. This doublet was observed whether or not protease inhibitors were included in the purification. These bands could not be resolved on a MonoQ column.

Unfortunately the purified α-actinin repeats were unsuitable for crystalisation studies due to the partial degradation. As noted previously (see chapter 4), the α-actinin repeats appeared especially susceptible to the action of endogenous *E. coli* proteases. The GST fusion protein GST-53 also coded for residues 218 to 749 of α-actinin. However residues 238 to 241 had been deleted as this was a major protease sensitive site. Although the GST-53 fusion protein was rapidly purified with glutathione beads in the presence of protease inhibitors, there was still marked degradation. Three

predominant degradation products were generated of approximately 55, 42, and 29kDa. The 55kDa degradation product was not separated from the intact fusion protein by chromatography on DEAE-Sepharose Fast-Flow or Sephacryl S200HR columns. An alternative approach would be to express a single repeat. One possible region would be Leu_{266} to Ala_{352}. The Val_{265}-Leu_{266} and Ala_{352}-Phe_{353} peptide bonds have previously been shown to be thermolysin cleavage sites (Dr. A. Blanchard, unpublished results) whereas no proteolysis within the intervening sequence has been reported.

CHAPTER SIX
INVESTIGATION OF POSSIBLE STRUCTURAL HOMOLOGIES BETWEEN THE ACTIN BINDING DOMAIN OF α-ACTININ AND FILAMIN

6.1 INTRODUCTION.

Although over sixty different actin binding proteins have been identified (Pollard and Cooper, 1986), it has become apparent that certain domains are shared by various actin binding proteins. Thus, the rod like domains of α-actinin, spectrin, and dystrophin, are each composed of a series of homologous repeats (Baron et al, 1987a; Koenig et al, 1988; Davison et al, 1989; Wasenius et al, 1989), the number of repeats determining the length of the molecule (Figure 6.1). An actin binding domain homologous to that of α-actinin has been demonstrated in β-spectrin (Byers et al, 1989), dystrophin (Koenig et al, 1988), and the *Dictyostelium* 120kDa Gelation Factor (also termed ABP-120) (Noegel et al, 1989). Fimbrin contains two domains that each show weak homology to the actin binding domain of α-actinin (De Arruda et al, 1990).

Data presented by Mimura and Asano (1986) suggest that filamin may also have an actin binding domain homologous to that of α-actinin. They demonstrated that a monoclonal antibody which recognised an epitope in the actin binding domain of α-actinin cross reacted with intact filamin in a 'dot blot' assay. However, this assay does not rule out the possibility that the filamin used was contaminated as the filamin sample was simply spotted onto nitrocellulose, rather than being resolved by electrophoresis on SDS-PAGE and subsequently electroblotted onto nitrocellulose.

Filamin is a high molecular weight (2x250 kDa) actin binding and cross linking protein (Wang et al, 1975). Initially identified in avian smooth muscle, filamin is also present in skeletal and cardiac muscle and several non-muscle sources (Wang et al, 1975; Wallach et al,

FIGURE 6.1

FIGURE DEMONSTRATING THE MODULAR ORGANISATION OF VARIOUS ACTIN CROSSLINKING PROTEINS

The various modules are depicted as follows: The actin binding domain is an open oval; The spectrin-like repeats are shaded rectangles; The EF-hand motifs are shaded circles; The β-sheet repeats of ABP-120 are shown as striped ovals. Dystrophin is shown as an anti-parallel homodimer. This is suggested by analogy with α-actinin and spectrin.

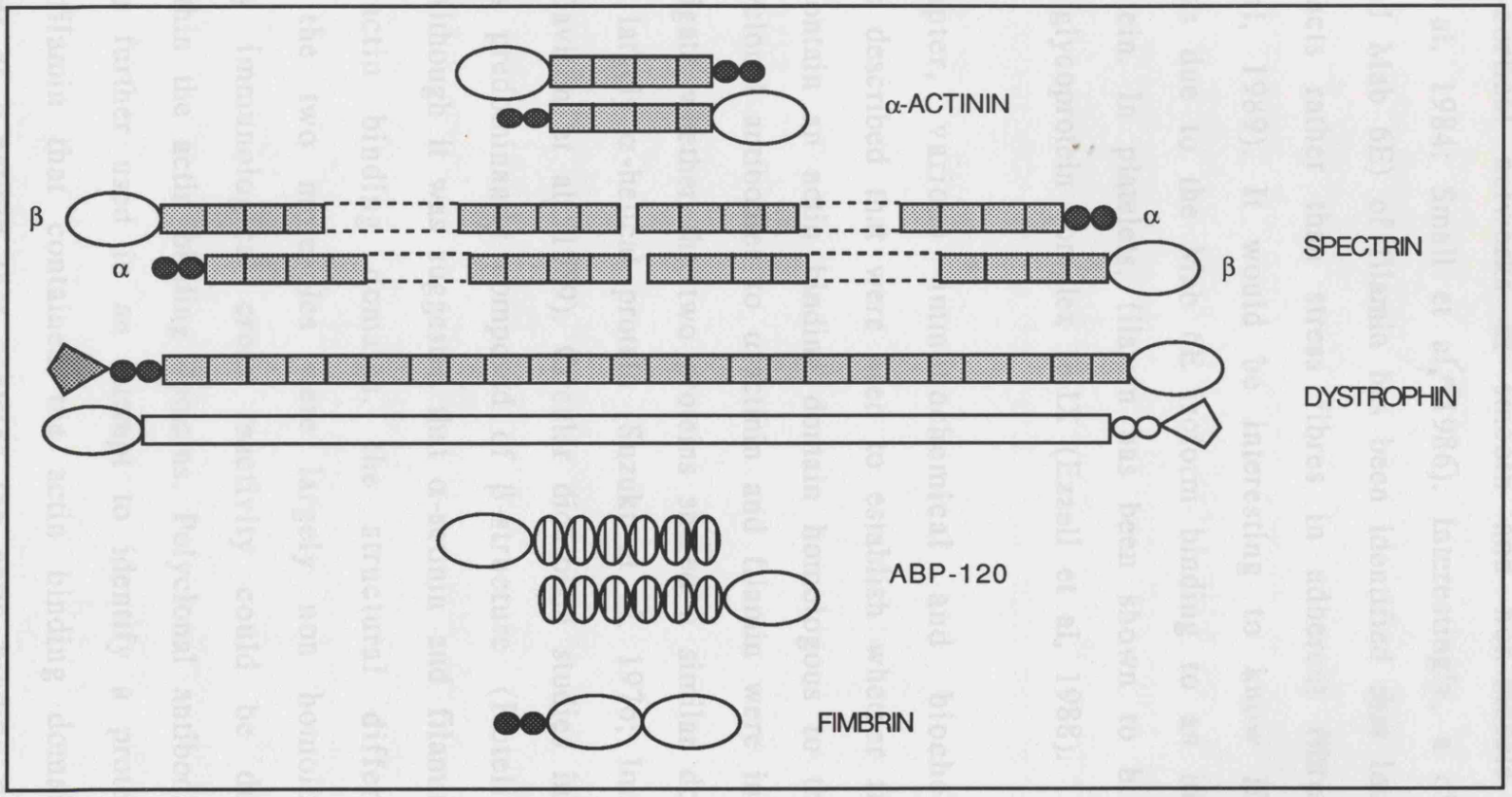

1978; Bechtel, 1979). Filamin is localised in the microfilament bundles and cortical networks of smooth and non-muscle cells (Langanger et al, 1984; Small et al, 1986). Interestingly, a distinct isoform (termed Mab 6E) of filamin has been identified that localises to focal contacts rather than stress fibres in adherent fibroblasts (Pavalko et al, 1989). It would be interesting to know if this localisation was due to the Mab 6E isoform binding to an integral membrane protein. In platelets, filamin has been shown to bind to the membrane glycoprotein complex Ib-IX (Ezzell et al, 1988).

In this chapter, various immunochemical and biochemical approaches are described that were used to establish whether filamin does indeed contain an actin binding domain homologous to that of α-actinin. Polyclonal antibodies to α-actinin and filamin were initially used to investigate whether the two proteins shared a similar domain. α-Actinin is a largely α-helical protein (Suzuki et al, 1976; Imamura et al, 1988; Davison et al, 1989). Circular dichroism studies indicate that filamin is predominantly composed of β-structure (Koteliansky et al, 1982). Although it was suggested that α-actinin and filamin had homologous actin binding domains, the structural differences implied that the two molecules were largely non homologous. Therefore any immunological cross reactivity could be due to similarities within the actin binding domains. Polyclonal antibodies to α-actinin were further used in an attempt to identify a proteolytic fragment of filamin that contained the actin binding domain. A 27kDa fragment of α-actinin that contains the actin binding domain can be generated by thermolysin digestion of α-actinin. The 27kDa fragment is resistant to further proteolysis by thermolysin and retains its ability to bind to F-actin (Mimura and Asano, 1986). If

filamin does contain a homologous actin binding domain to that of α-actinin, it would be predicted that thermolysin treatment of filamin would also liberate a fragment of approximately 27kDa. Antibodies specifically to the actin binding domain of α-actinin were also used to examine thermolysin digests of filamin. In addition, attempts were made at co-sedimenting the actin binding domain of filamin with F-actin. An overlay technique using ^{125}I-labelled F-actin was also used to identify any proteolytic fragments of filamin that could bind to F-actin. Providing the actin binding domain of filamin could be identified, the polypeptide might be purified in sufficient quantities for its sequence to be determined.

6.2 METHODS.

6.21 FILAMIN PURIFICATION.

Filamin was purified according to the method of Davies et al (1982). All steps were carried out at 4°C. Approximately 25g of chicken gizzard were homogenised in a low salt buffer (5mM EDTA, pH7.0, 5mM DTT). The homogenate was centrifuged, and the resulting pellet was homogenised in a high salt buffer (50mM potassium phosphate, pH7.5, 600mM KCl, 1mM EDTA, 1mM DTT). After centrifugation, the supernatant was filtered through glass wool. The supernatant was then dialysed overnight against 10 litres of 50mM potassium phosphate, pH7.5, 100mM KCl, 1mM EDTA, 0.033% β-mercaptoethanol. The dialysate was centrifuged. Solid ammonium sulphate was added slowly to the supernatant to 35% saturation whilst stirring. The pH was maintained at 7.2-7.5 with ammonium hydroxide. The resulting precipitate was removed by centrifugation

and resuspended in 50mM potassium phosphate, pH7.2-7.5, 100mM KCl, 1mM EDTA, 1mM DTT. Following two hours stirring, the solution was centrifuged and the pellet discarded. An ammonium sulphate precipitation was carried out as previously on the supernatant. After centrifugation the pellet was resuspended in 20mM potassium phosphate, pH7.5, 100mM KCl, 1mM EDTA, 1mM DTT and then dialysed into the buffer (20mM potassium phosphate, pH7.5, 50mM KCl, 1mM EDTA, 0.1% β-mercaptoethanol) for the first column chromatographic step. Both this buffer and the elution buffer for the first column had a relatively high salt concentration (equivalent to 120mM NaCl). The sample was run (25ml/hr) through the first DE52 column (1.6x20cm). 5ml fractions were collected. The filamin fractions were pooled and the salt concentration lowered (to 40mM NaCl equivalent) by the addition of distilled water. This solution was applied to a second DE52 column (1.6x20cm) that had previously been equilibrated with 10mM potassium phosphate, pH7.5, 25mM KCl, 1mM EDTA, 0.1% β-mercaptoethanol. Protein was eluted using a 200ml gradient of 50 to 500mM KCl in 20mM potassium phosphate, pH7.5, 1mM EDTA, 0.1% β-mercaptoethanol. A flow rate of 25ml/hr was used and 5ml fractions were collected. The filamin fractions were pooled and dialysed into 50mM potassium phosphate, pH7.5, 100mM KCl, 1mM EDTA, 0.1% β-mercaptoethanol. The sample was then applied to a Sepharose CL-6B sizing column (0.8x70cm). The column was developed at 10ml/hr with 50mM potassium phosphate, pH7.5, 100mM KCl, 1mM EDTA, 0.1% β-mercaptoethanol. Fractions of 2ml were collected. The peak fractions were pooled and stored at -20°C in 50% glycerol.

6.22 SOURCE OF ANTIBODIES.

The rabbit anti-α-actinin antiserum was raised by Kellie et al (1983). The α-actinin used to raise the antiserum was purified as previously described (Feramisco and Burridge, 1980). It was electrophoresed on SDS-PAGE and electroblotted onto nitrocellulose. The α-actinin was excised from the nitrocellulose and dissolved in dimethyl sulphoxide before injection with Freunds adjuvant. Two anti-filamin antibodies were used. An anti-filamin (chicken gizzard) IgG raised in rabbits was kindly supplied by Dr. Wilkinson (London University). A goat anti-filamin (chicken gizzard) IgG was supplied by ICN ImmunoBiologicals (Catalogue number 65-780).

6.23 AFFINITY PURIFICATION OF POLYCLONAL ANTIBODIES TO THE ACTIN BINDING DOMAIN AND SPECTRIN-LIKE REPEATS OF α-ACTININ USING PROTEINS IMMOBILISED ON NITROCELLULOSE.

A SDS-polyacrylamide gel with a single well that covered the entire length of the stacking gel was prepared. The sample applied contained at least 1mg of the protein of interest or a protein digest including the fragment of interest. The proteins were then electroblotted onto nitrocellulose as previously described. Following staining and destaining of the nitrocellulose with Ponceau S, the band of interest was excised and the remaining dye was washed off with TBS. The nitrocellulose strip was then incubated for at least 30 minutes in a 3% BSA/TBS solution to block unoccupied sites on the nitrocellulose. The strip was then incubated overnight at 4°C in a solution containing the required antibody (100μl of neat anti-serum diluted into 5ml of BSA/TBS). Loosely bound material was removed by washing the strip 5 times (5 minutes each) in 10mM sodium

phosphate, pH7.4, 500mM NaCl, 0.2% Triton X-100, 1mM EDTA, 1mM sodium azide; 5 times in 2M urea, 100mM glycine, 1% Triton X-100; and 3 times in 50mM sodium acetate, pH5.0. The antibody was then eluted by repeatedly rinsing the strip with 250µl of 200mM glycine/HCl, pH2.3. The eluted antibody was neutralised by the addition of 1M Tris. It was then dialysed overnight against 100mM sodium phosphate, pH7.2. The nitrocellulose strip was washed in TBS-T (TBS with 0.1% Tween 20). The incubation of the nitrocellulose strip in the initial antibody solution and the elution of specific antibody from the strip was repeated four times. The eluted antibody was pooled and then stored at 4°C with sodium azide (0.02%).

6.24 CLEVELAND PEPTIDE MAPPING.

Peptide mapping of proteolytic fragments excised from SDS-PAGE gels was carried out according to Cleveland et al (1977). A primary digestion of the protein was carried out. The fragments were separated on a SDS-polyacrylamide gel, then stained and destained as normal. The required band was excised and equilibrated into 125mM Tris/HCl, pH6.8, 15% glycerol, 0.1% SDS, 1mM EDTA. (1 hour, with 3 changes of buffer). The gel slices were then inserted into the wells of a 7 to 20% SDS-polyacrylamide gel or a Tris-Tricine gel. The secondary protease, in the above buffer, was applied to the wells and incubated for 10 minutes. Following electrophoresis, the gel was stained and destained as previously described.

6.25 TRICINE-SDS-POLYACRLAMIDE GEL ELECTROPHORESIS (TRIS-TRICINE GELS).

Tris-Tricine gels were run according to the method of Schagger and Von Jagow (1987) on a BioRad 'Protean' vertical electrophoresis

system (16cm by 18cm). This gel system, which gave excellent resolution of low molecular weight peptides/proteins had a 'spacer' gel between the stacking gel and the separating gel. Samples were prepared as those for SDS-polyacrylamide gels. Gels (16.5%) were run at 30V constant voltage for one hour, then 45mA constant current until the bromophenol blue reached the base of the gel (approximately 10 hours). Gels were initially fixed in 50% methanol, 10% glacial acetic acid for one hour. They were then stained in 0.025% Coomasie blue (R250), 10% glacial acetic acid for 1-2 hours. Background staining was removed by washing the gel in 10% methanol.

6.26 SAMPLE PREPARATION FOR PROTEIN SEQUENCING.

Protein samples (or proteolytic fragments of) were electrophoresed on SDS-polyacrylamide gels and electroblotted onto Polyvinylidene Difluoride membrane (PVDF) as described by Matsudaira (1987). After staining and destaining, the required band was excised and loaded onto an Applied Biosystems 470A Protein Sequencer. This was run using standard programs.

6.3 RESULTS.

6.31 THE PURIFICATION OF FILAMIN.

The purification developed by Davies et al (1982) was used to purify filamin. The first homogenisation, after centrifugation, yielded a pellet enriched in cytoskeletal proteins. The supernatant contained actin, myosin, and various soluble proteins. The second homogenisation released cytoskeletal proteins into the supernatant.

Fat was removed by filtering the supernatant through glass wool. Dialysis overnight produced a gelatinous precipitate which was removed by centrifugation. This precipitate was composed of actin and myosin, though some filamin was lost at this stage. After centrifugation of the first ammonium sulphate cut, the pellet was enriched in filamin. Re-precipitation of the resuspended pellet with ammonium sulphate had no apparent effect on the purification, but was required to concentrate the sample. The major remaining contaminant was actin, although there were still significant amounts of a 97kDa and a 116kDa protein, along with various other minor proteins. The pellet was resuspended and applied to a DE52 column. Because of the high salt content of the buffer used, filamin did not bind to the DE52 column. However actin did bind (Figure 6.2). The pooled filamin fractions still contained many contaminants, but negligible amounts of actin. After lowering the ionic strength of the buffers the filamin bound to a second DE52 column. A number of low molecular weight contaminants did not bind and hence were resolved from filamin. A salt gradient was used to elute bound protein. Filamin eluted between 70 and 240mM NaCl equivalents (Figure 6.3). The remaining contaminants were removed by the Sepharose CL-6B sizing column. Filamin eluted shortly after the void volume (Figure 6.4). This resulted in filamin of greater than 95% purity, as judged by SDS-PAGE. An equal volume of glycerol was added to the purified filamin and it was stored at -20°C. It was stable for many weeks. It could not be frozen as this resulted in irreversible aggregation and precipitation. Storage at 4°C could only be limited due to aggregation and breakdown of the protein.

FIGURE 6.2
PURIFICATION OF FILAMIN: ELUTION PROFILE FROM THE FIRST DE52 COLUMN.

Filamin did not bind to the column and was present in the first peak. The second peak contains the protein that initially bound to the column. The column bed size was 1.6x20cm. A flow rate of 25ml/hr was used. 20mM Potassium phosphate, pH7.5, 50mM KCl, 1mM EDTA, 0.1% β-mercaptoethanol was used as the eluent. At the point indicated the KCl concentration of the buffer was raised to 1M. 5ml fractions were collected. The inserts show Coomassie stained SDS-PAGE gels (7%) of (A) unbound protein and (B) protein that initially bound and was then eluted by 1M KCl. 50µl aliquots of each was applied to the gel.

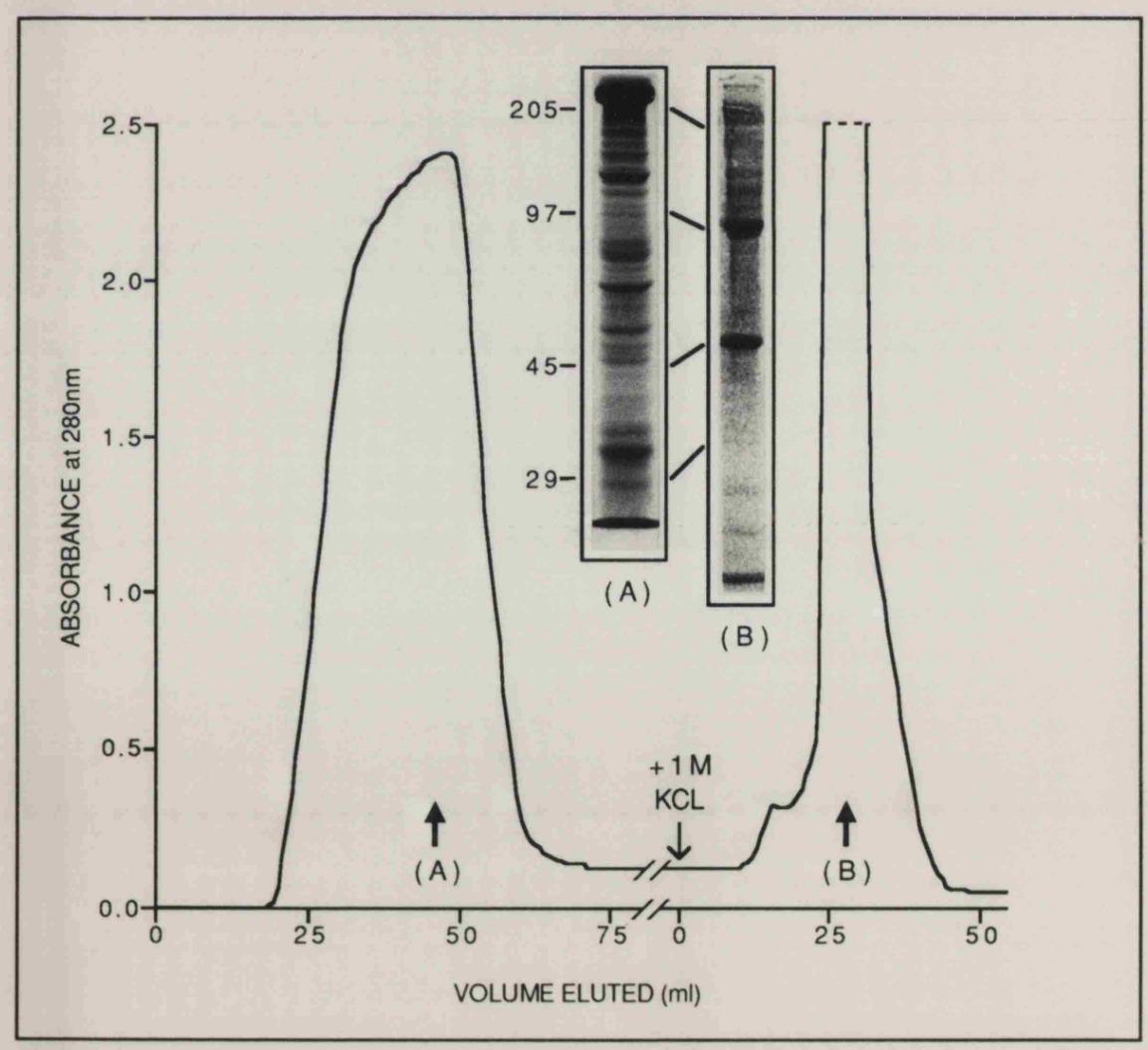

FIGURE 6.3

PURIFICATION OF FILAMIN: ELUTION PROFILE FROM THE SECOND DE52 COLUMN.

The column bed size was 1.6x20cm. A flow rate of 25ml/hr was used. 20mM Potassium phosphate, pH7.5, 1mM EDTA, 0.1% β-mercaptoethanol with a salt gradient of 50 to 500mM KCl over 200ml was used as the eluent. 5ml fractions were collected. The insert shows a Coomassie stained SDS-PAGE gel (7%) of fractions from the positions indicated. 50µl aliquots of each was applied to the gel.

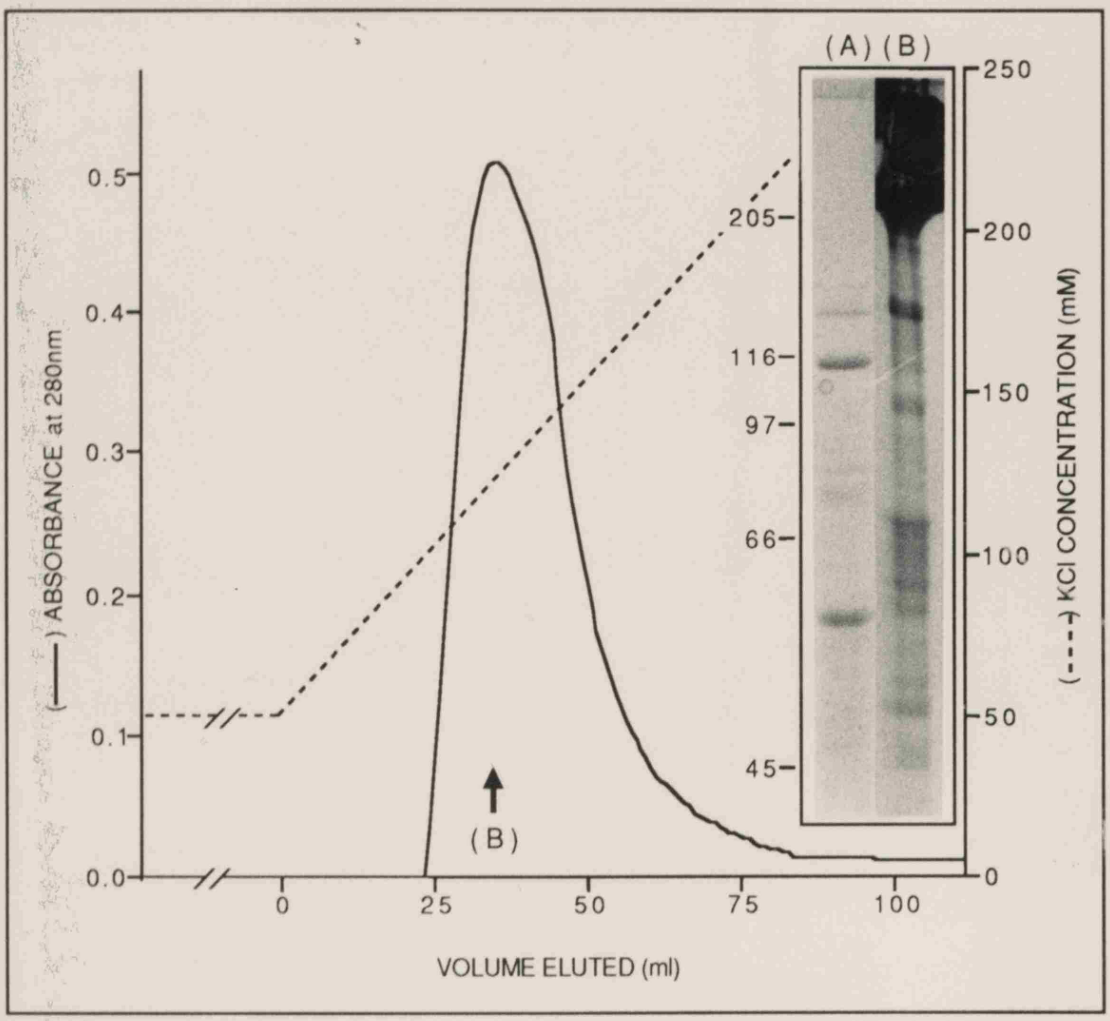

(A) – PROTEIN IN FLOW THROUGH

FIGURE 6.4

PURIFICATION OF FILAMIN: ELUTION PROFILE FROM THE SEPHAROSE CL-6B COLUMN.

The column bed size was 0.8x70cm. A flow rate of 10ml/hr was used. 50mM Potassium phosphate, pH7.5, 100mM KCl, 1mM EDTA, 0.1% β-mercaptoethanol was used as the eluent. 2ml fractions were collected. The inserts shows a Coomassie stained SDS-PAGE gel (7%) of the peak filamin fraction from the major peak. 50µl aliquots was applied to the gel.

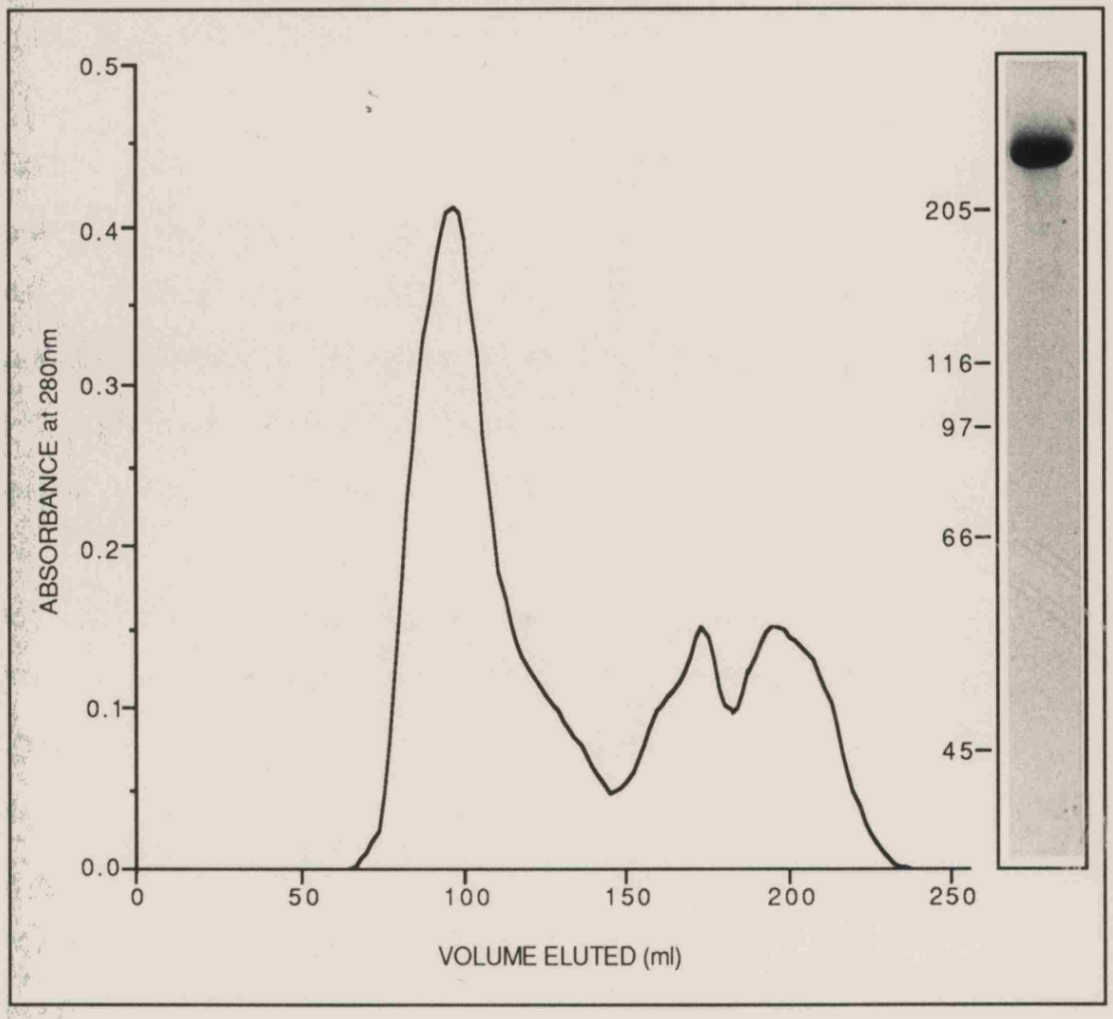

6.32 THE USE OF POLYCLONAL ANTIBODIES TO INVESTIGATE A POSSIBLE HOMOLOGY BETWEEN α-ACTININ AND FILAMIN.

The actin binding domain of α-actinin is highly conserved and may have a low immunogenicity. This possibility had to be excluded. A thermolysin digest of α-actinin was electroblotted onto nitrocellulose and probed with the polyclonal anti-α-actinin antibody. The antibody picked out all the α-actinin fragments, including the 27kDa fragment which contained the actin binding domain (not shown).

Western Blots of intact α-actinin and filamin were performed with the antibodies to each of the other two proteins. (Figure 6.5). Filamin cross reacted significantly with the polyclonal anti-α-actinin antibody. Similarly α-actinin showed a marked cross reactivity with the anti-filamin antibody. There was no cross reactivity of either protein with the pre-immune sera.

To test whether the antibody to filamin was cross reacting with epitopes in the actin binding domain of α-actinin or the spectrin-like repeats, α-actinin that had been digested with thermolysin was Western Blotted with the anti-filamin antibody (Figure 6.6). The 27kDa fragment of α-actinin cross reacted with the anti-filamin antibody. The 53kDa fragment of α-actinin, which comprised most of the remainder of the molecule, did not cross react, despite a good transfer of this polypeptide onto nitrocellulose. There was no cross reactivity when the pre-immune serum was used.

These immunological experiments strongly suggested that α-actinin and filamin do have a homologous actin binding domain. To isolate the putative actin binding domain from filamin, it was digested with

FIGURE 6.5
DEMONSTRATION OF THE CROSS REACTIVITY OF INTACT α-ACTININ AND FILAMIN WITH POLYCLONAL ANTIBODIES AGAINST FILAMIN AND α-ACTININ.

10μg of α-actinin (with some slight filamin contamination) and 5μg of filamin were electroblotted onto nitrocellulose. As indicated, the samples were probed with a rabbit polyclonal anti-α-actinin antibody (6μg/ml) and a goat polyclonal anti-filamin antibody (1:5000 dilution). The appropriate pre-immune seras were used at the same concentrations.

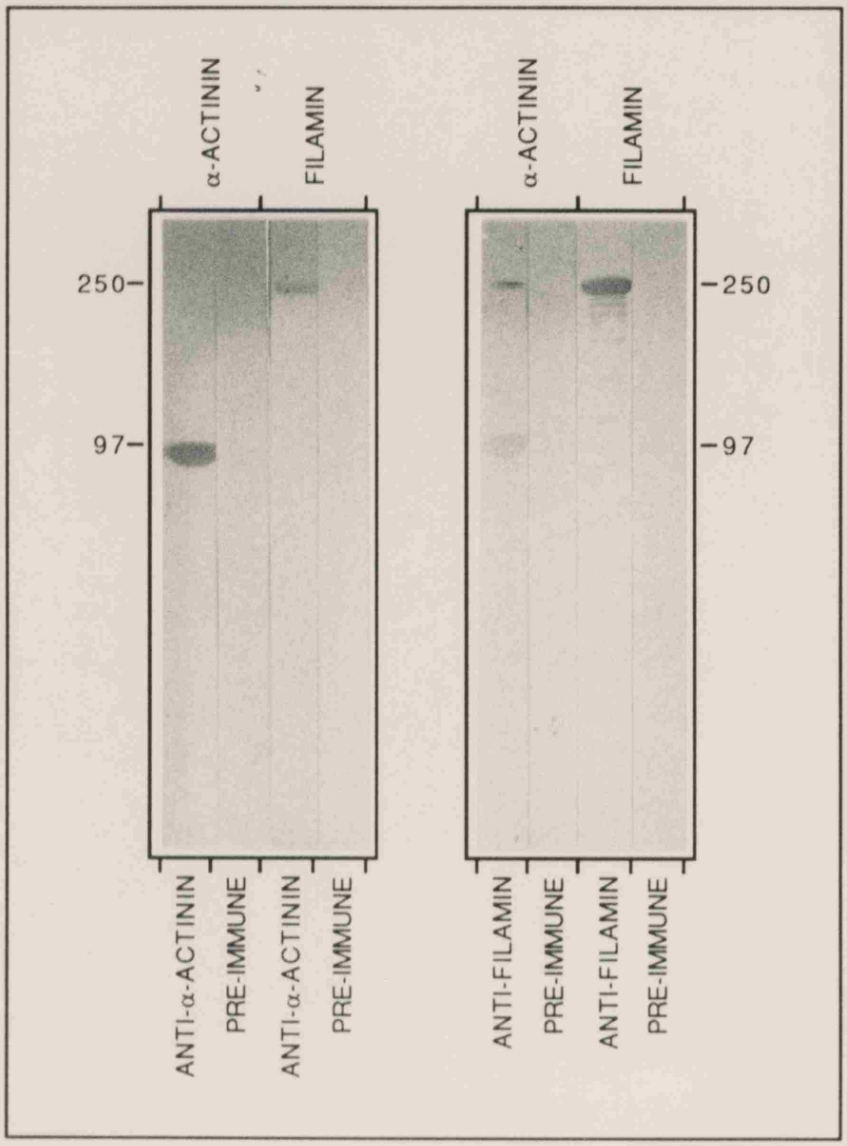

FIGURE 6.6

DEMONSTRATION OF THE CROSS REACTIVITY OF THERMOLYSIN DIGESTS OF α-ACTININ AND FILAMIN WITH POLYCLONAL ANTIBODIES AGAINST FILAMIN AND α-ACTININ.

60μg of thermolysin digested α-actinin and 120μg of thermolysin digested filamin were electroblotted onto nitrocellulose. As indicated, the samples were probed with a goat polyclonal anti-filamin antibody (1:5000 dilution) and a rabbit polyclonal anti-α-actinin antibody (6μg/ml). The appropriate pre-immune seras were used at the same concentrations.

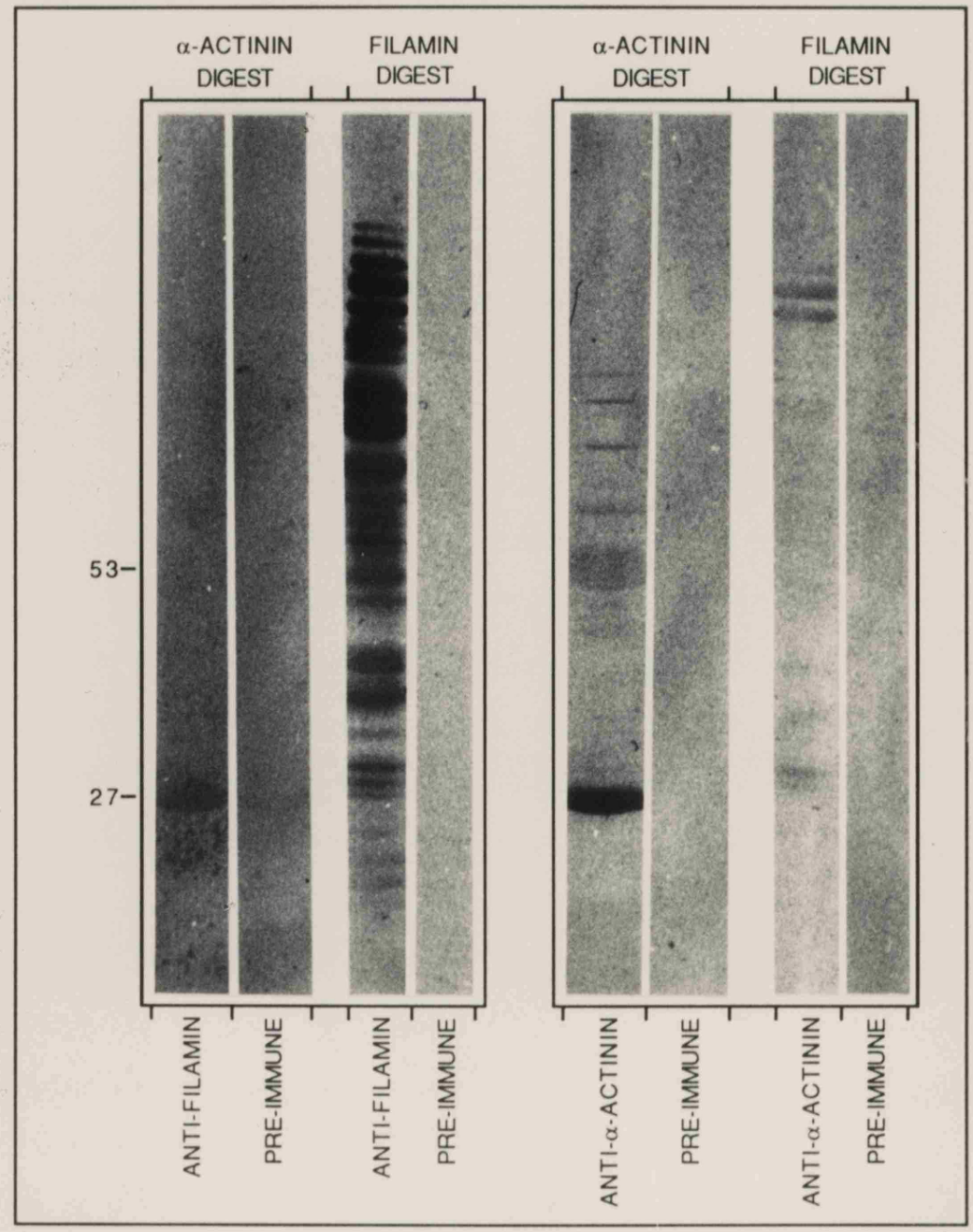

thermolysin and Western Blotted with anti-α-actinin antibody. Filamin that had been subjected to limited thermolysin digestion was used as this contained a wide range of fragment sizes (Figure 6.7). A doublet of 29/29.5kDa (designated Bands E and E-1) was shown to be cross reactive with the anti-α-actinin antibody (Figure 6.6). A number of larger bands of around 110kDa were also cross reactive. These may have been precursor fragments of Bands E and E-1. There was also a slight suggestion that a 14kDa band was also cross reactive (designated Band G) (not visible in figure 6.6). This was interesting as the 27kDa actin binding fragment of α-actinin could be digested further by thermolysin to yield a 14kDa fragment. Whether or not the anti-α-actinin antibody recognises epitopes within the 14kDa fragment of α-actinin has not been shown. Controls with pre-immune serum were not cross reactive.

Antibodies to the 27kDa and 53kDa fragments of α-actinin were affinity purified from the anti-α-actinin serum to more specifically investigate the immunological relatedness between α-actinin and filamin. The purified antibodies were designated EL27 and EL53 respectively. The antibodies were shown to be specific for the appropriate regions of the α-actinin molecule (Figure 6.8). A very slight degree of cross reactivity of the EL27 antibody with α-actinin fragments not containing the actin binding domain was revealed when an ^{125}I-conjugated goat anti-rabbit secondary antibody (obtained from ICN, Catalogue number 68-086) followed by prolonged autoradiography was used as the detection system. Similarly slight cross reactivity of the EL53 antibody with the α-actinin actin binding domain was observed when the more sensitive detection system was used. Western Blotting of a thermolysin digest

FIGURE 6.7

TIME COURSE OF THERMOLYSIN DIGEST OF FILAMIN.

180µg of filamin was digested with 9µg of thermolysin in 100mM ammonium bicarbonate, pH7.6, 5mM $CaCl_2$, at 37°C. 30µg filamin aliquots were taken at the times indicated (minutes) and inactivated by the addition of EDTA to 10mM. The samples were applied to a 7 to 15% SDS-PAGE gradient gel. This was stained with Coomassie. Molecular weights (kDa) are noted down the left axis. The designations given to the filamin fragments are noted down the right axis.

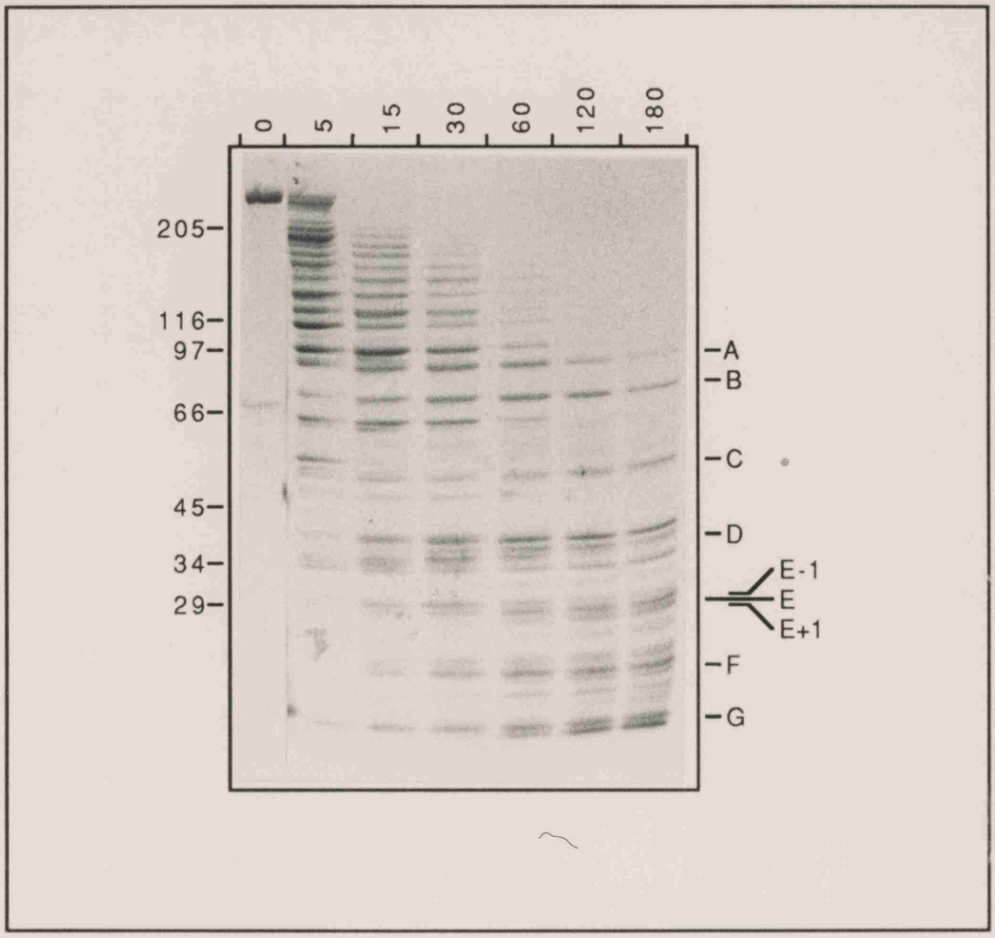

FIGURE 6.8
CHARACTERISATION OF THE α-ACTININ ANTIBODIES EL27 AND EL53 AND THERE USE IN INVESTIGATING A POSSIBLE HOMOLOGY BETWEEN THE ACTIN BINDING DOMAINS OF α-ACTININ AND FILAMIN.

50μg and 120μg samples (intact protein) of thermolysin digested α-actinin and filamin were electroblotted onto nitrocellulose after electrophoresis on a 7 to 15% SDS-PAGE gradient gel. The primary antibodies used were EL27, EL53, and polyclonal anti-α-actinin (pAB) (6μg/ml). An ^{125}I-linked secondary antibody (1:500 dilution) and autoradiography were used to reveal cross reactivity. The length of exposure is indicated.

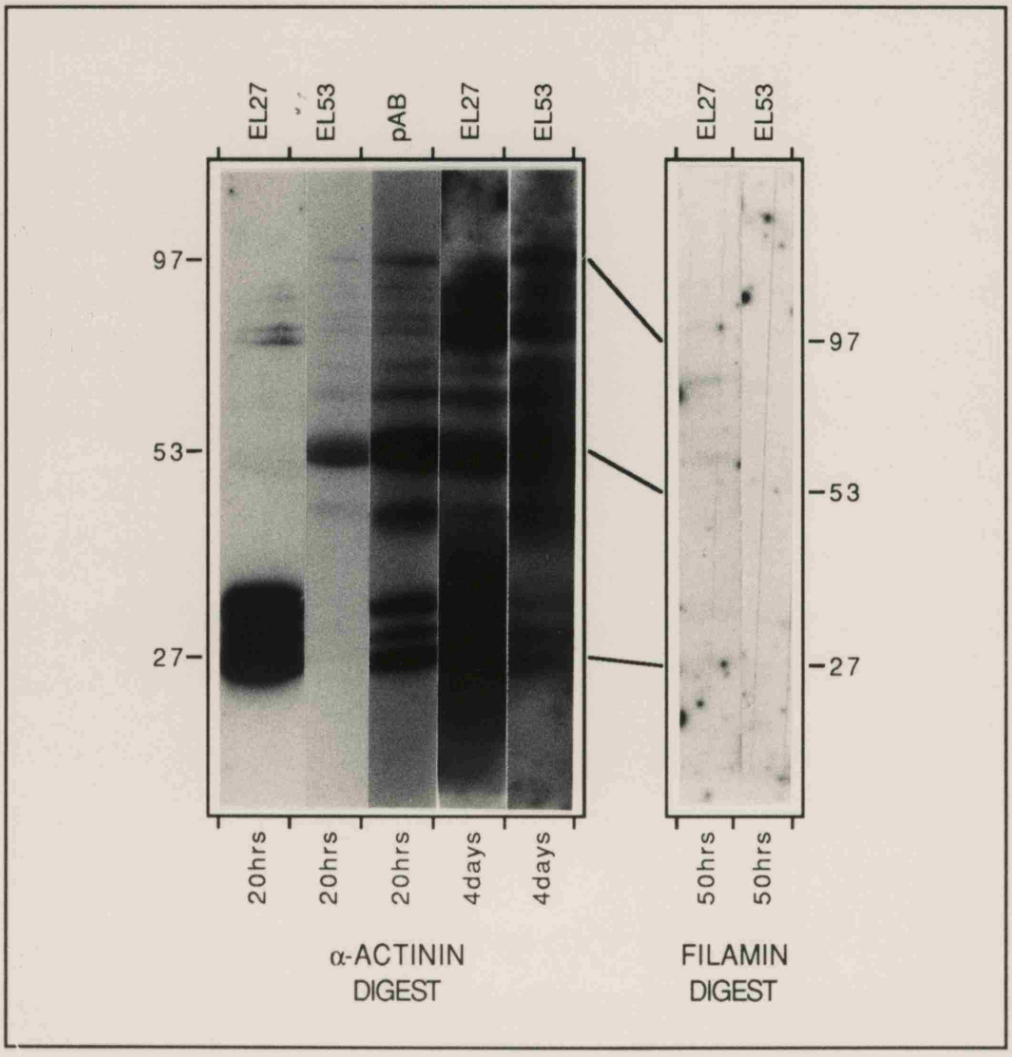

of filamin suggested very weak cross reactivity of Band E to the EL27 antibody when the alkaline phosphatase detection system was used (not shown). However, no cross reactivity of Band E to the EL27 antibody could be demonstrated when an ^{125}I-labelled secondary antibody was used (Figure 6.8), unless autoradiography was prolonged. None of the filamin fragments cross reacted with the EL53 antibody.

Because filamin cross reacted with the anti-α-actinin antibody but not with EL27 or EL53, the antibodies were examined further. Chick embryo fibroblast and chick skeletal muscle extracts were Western Blotted with EL27, EL53, and the anti-α-actinin antibody. The only significant cross reaction of antibodies EL27 and EL53 was with a 97kDa protein (Figure 6.9). The anti-α-actinin antibody cross reacted with the 97kDa protein. Surprisingly, the anti-α-actinin also cross reacted with proteins of approximately 115, 130, 200, and 250kDa (figure 6.9). However, when the anti-α-actinin antibody was purified from nitrocellulose (designated ELαA) (as the EL27 and EL53 antibodies) its cross reactivity to the 115, 130, 200, and 250kDa bands was greatly reduced (Figure 6.10). In comparison, the serum from which ELαA was derived (termed ELαR) contained significant cross reactivity with the 200kDa protein.

6.33 PEPTIDE MAPPING COMPARISON OF THE ACTIN BINDING DOMAIN OF α-ACTININ AND BANDS E AND E-1 OF FILAMIN.

The V8 protease peptide maps of Bands E and E-1 were compared to that of the α-actinin 27kDa fragment (Figure 6.11). Bands E and E-1 yielded similar peptide maps. The larger fragment, Band E-1, produced two extra bands to Band E. There appeared to be one V8

FIGURE 6.9

INVESTIGATION OF CHICK EMBRYO FIBROBLAST AND CHICKEN SKELETAL MUSCLE EXTRACTS USING THE ANTIBODIES EL27, EL53, AND POLYCLONAL ANTI-α-ACTININ.

Extracts of chick embryo fibroblasts and chicken skeletal muscle were electroblotted onto nitrocellulose following electrophoresis on a 7% SDS-PAGE gel. The primary antibodies used were EL27, EL53, polyclonal anti-α-actinin (pAB) (6μg/ml), and a pre-immune sera (6μg/ml). An ^{125}I-linked secondary antibody (1:500 dilution) and autoradiography were used to reveal cross reactivity. The autoradiograph was exposed for 12 hours.

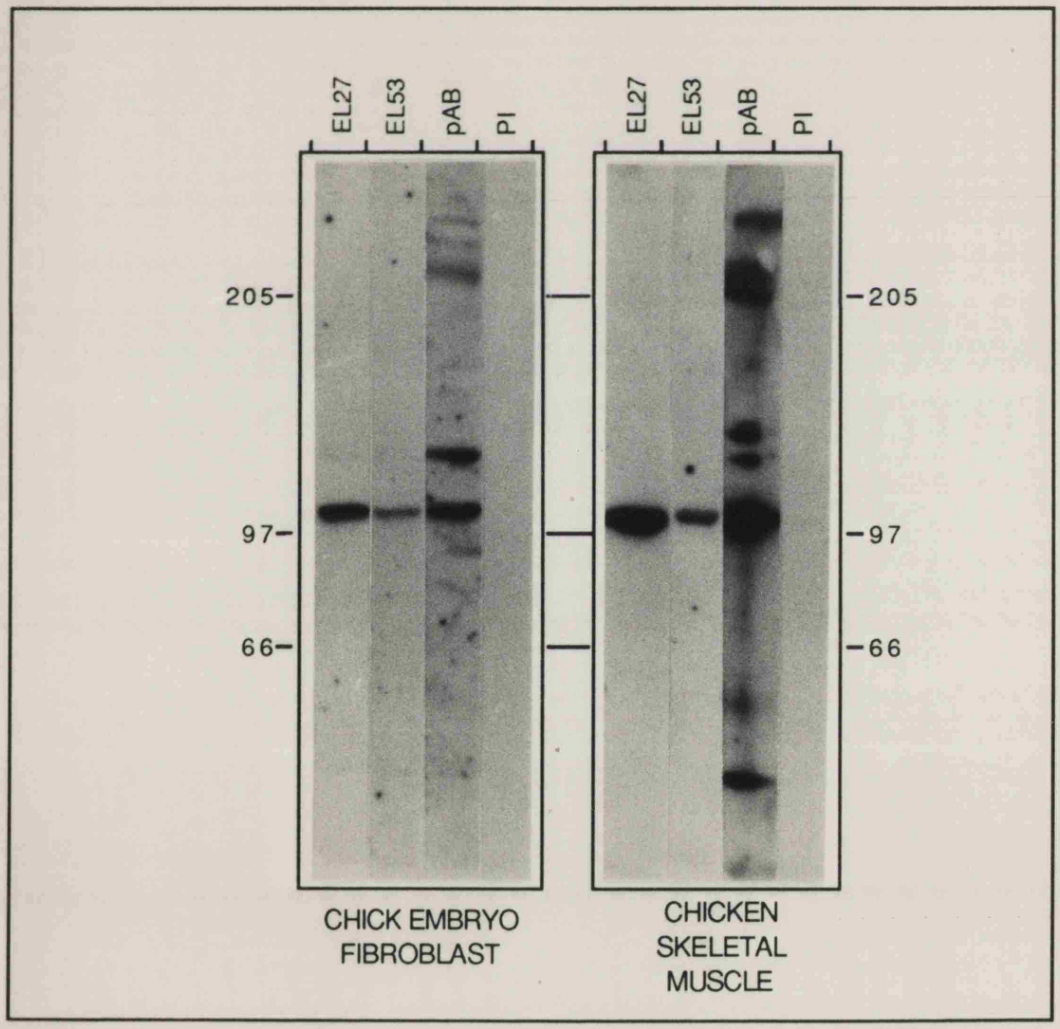

FIGURE 6.10

EXAMINATION OF THE POLYCLONAL ANTI-α-ACTININ ANTIBODY.

Extracts of chick embryo fibroblasts (CEF) and chicken skeletal muscle (CSM) were electroblotted onto nitrocellulose following electrophoresis on a 7% SDS-PAGE gel. The primary antibodies used were the polyclonal antiserum to α-actinin following affinity purification on nitrocellulose (ELαA), and the residual antiserum from which ELαA was derived, termed ELαR. The alkaline phosphatase detection method was used to reveal cross reactivity.

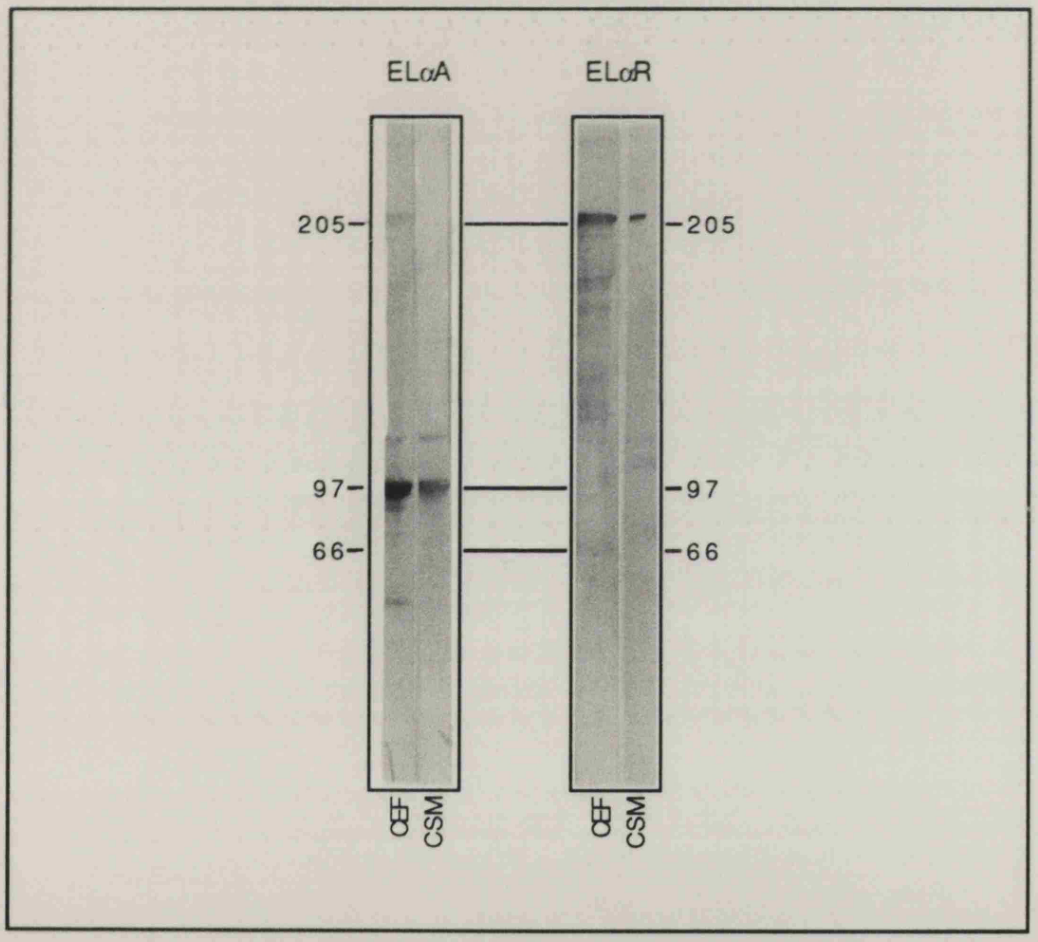

FIGURE 6.11

COMPARISON OF THE PEPTIDE MAPS GENERATED FROM THE 27kDa FRAGMENT OF α-ACTININ AND FROM BANDS E AND E-1 OF FILAMIN USING V8 PROTEASE

60μg samples of α-actinin digested with thermolysin and 80μg samples of filamin digested with thermolysin were electrophoresed on an SDS-PAGE gel. The appropriate bands were excised and equilibrated into 125mM Tris/HCl, pH6.8, 15% glycerol, 0.1% SDS, 1mM EDTA (1 hour, with 3 changes of buffer). The gel slices were then inserted into the wells of a 7 to 20% gradient SDS-PAGE gel. Samples were digested by 0.01, 0.1, and 1.0μg of papain and V8 protease. The gel was silver stained.

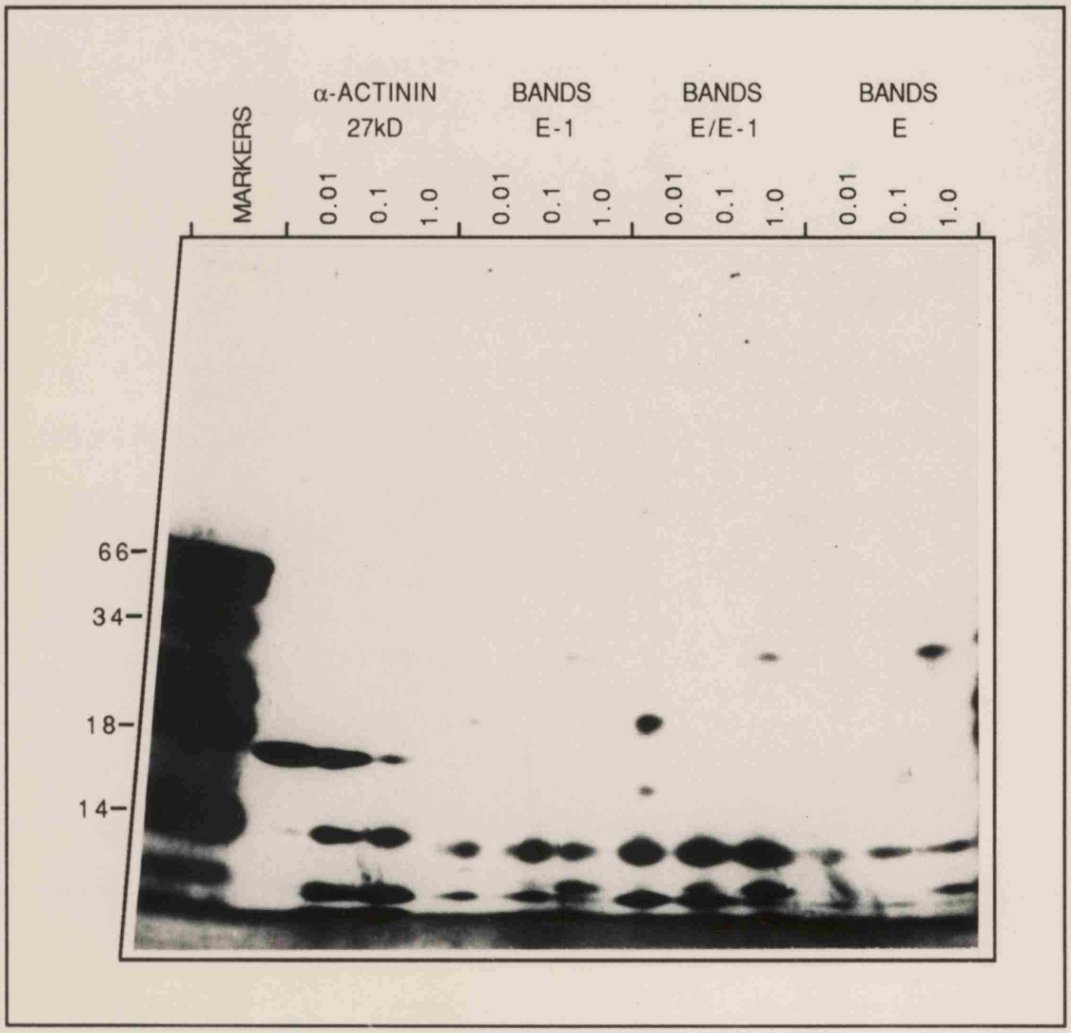

generated fragment common to the α-actinin actin binding domain and filamin Band E/E-1 digests. However, the resolution of the gel at these molecular weights was limited. Some fragments were not resolved from the dye front. The determined molecular weights of small fragments were anomolous in this gel system. The intact α-actinin actin binding domain appeared to have a molecular weight of approximately 16kDa. Such discrepancies have previously been reported (Schagger and Von Jagow, 1987).

16.5% Tris-Tricine gels (high cross-linker) provided excellent resolution of fragments between 30kDa to below 2.5kDa. V8 protease digestion of the α-actinin actin binding domain yielded four distinct fragments of about 22, 14, 11, and 4kDa (Figure 6.12). Similar digestion of Bands E/E-1 from filamin generated a larger number of fragments. More prominent fragments of approximately 18, 14, and 6kDa (doublet) were observed. 10 other fragments were also generated. The only fragment common to both digests was a 14kDa polypeptide. Peptide maps of the α-actinin actin binding domain and Bands E/E-1 of filamin were also generated using papain. The actin binding domain of α-actinin yielded about nineteen proteolytic fragments. Bands E/E-1 yielded at least sixteen fragments. Both digests had a fragment of approximately 10kDa, but otherwise the peptide maps were different.

6.34 ATTEMPTS AT CO-SEDIMENTATION OF THE ACTIN BINDING DOMAIN OF FILAMIN WITH F-ACTIN.

Attempts were made at co-sedimenting any F-actin binding polypeptides from a thermolysin digest of filamin. Initially it was demonstrated that intact filamin did co-sediment with F-actin.

FIGURE 6.12

COMPARISON OF THE PEPTIDE MAPS GENERATED FROM THE 27kDa FRAGMENT OF α-ACTININ AND FROM BANDS E/E-1 OF FILAMIN USING PAPAIN AND V8 PROTEASE

60μg samples of α-actinin digested with thermolysin and 80μg samples of filamin digested with thermolysin were electrophoresed on an SDS-PAGE gel. The appropriate bands were excised and equilibrated into 125mM Tris/HCl, pH6.8, 15% glycerol, 0.1% SDS, 1mM EDTA (1 hour, with 3 changes of buffer). The gel slices were then inserted into the wells of a 16.5% Tris-Tricine gel (high cross linker). Samples were digested by 0.01, 0.1, and 1.0μg of papain and V8 protease. Papain was activated by the addition of 50% β-mercaptoethanol (in glycerol). The gel was electrophoresed and silver stained as described in sections 6.25 and 2.43 repectively.

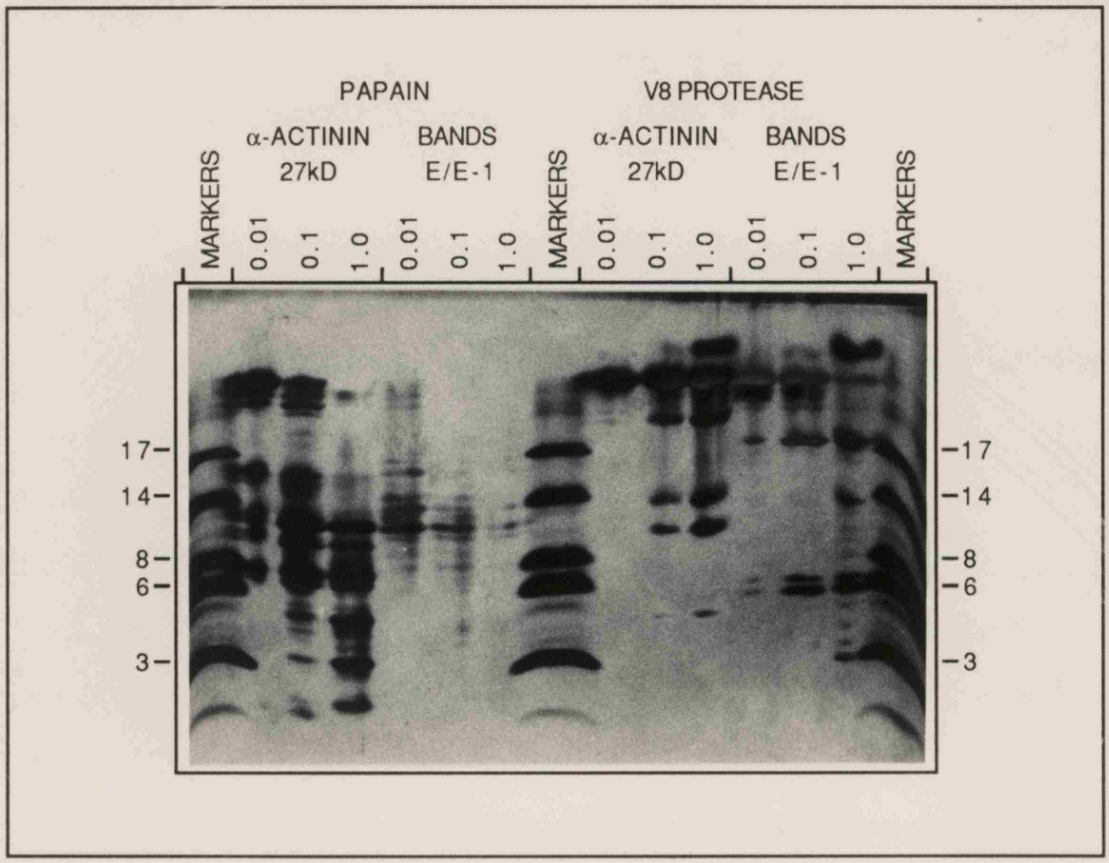

Filamin did pellet in the absence of F-actin, but to a lesser degree than in its presence. Pre-spinning the filamin sample in the airfuge prior to use in the experiment did not alleviate the non-specific pelleting of filamin. It was also shown that actin was not degraded by thermolysin in the sedimentation buffer. Thermolysin-generated proteolytic fragments of filamin and α-actinin were assayed for their ability to bind F-actin. No co-sedimenting fragments could be observed when the gels were stained with Coomassie staining or Western Blotted. Silver staining of the gels suggested that a filamin fragment of 37kDa pelleted in the presence of F-actin (Figure 6.13). Some of the 37kDa fragment pelleted in the absence of F-actin but to a lesser degree. None of the other filamin fragments sedimented in the presence or absence of F-actin.

6.35 PROTEIN SEQUENCE DATA DERIVED FROM FILAMIN BANDS E AND E-1.

The cross reactivity of the filamin Bands E and E-1 with the anti-α-actinin antibody initially suggested that they may have been homologous to the actin binding domain of α-actinin. Therefore Bands E and E-1 were both partially sequenced. Thermolysin digests of filamin were run on 7 to 15% SDS-PAGE gels and electroblotted onto PVDF as previously described. The required bands were then excised for sequencing. The results obtained were:-

Band E: L R P E/K A/L N(?) L D/R Y(?) A R V(?)

Band E-1: L K P G A P L R P/K K L N Y G

FIGURE 6.13

INVESTIGATION OF THE ACTIN BINDING DOMAINS OF FILAMIN AND α-ACTININ BY CO-SEDIMENTATION WITH F-ACTIN.

Samples were centrifuged as described in section 2.48. The buffer used was 10mM Tris/HCL, pH7.5, 100mM KCl, 0.1mM ATP, 4mM $MgCl_2$, 10mM EGTA, 1mM β-mercaptoethanol. S and P indicate the supernatant and pellet after ultracentrifugation of the solutions as follows: actin alone; thermolysin digested filamin and actin; thermolysin digested filamin alone. The concentrations of actin and digested filamin were 3.7 and 1.3μM (intact filamin concentration) respectively. Protein was detected by silver staining.

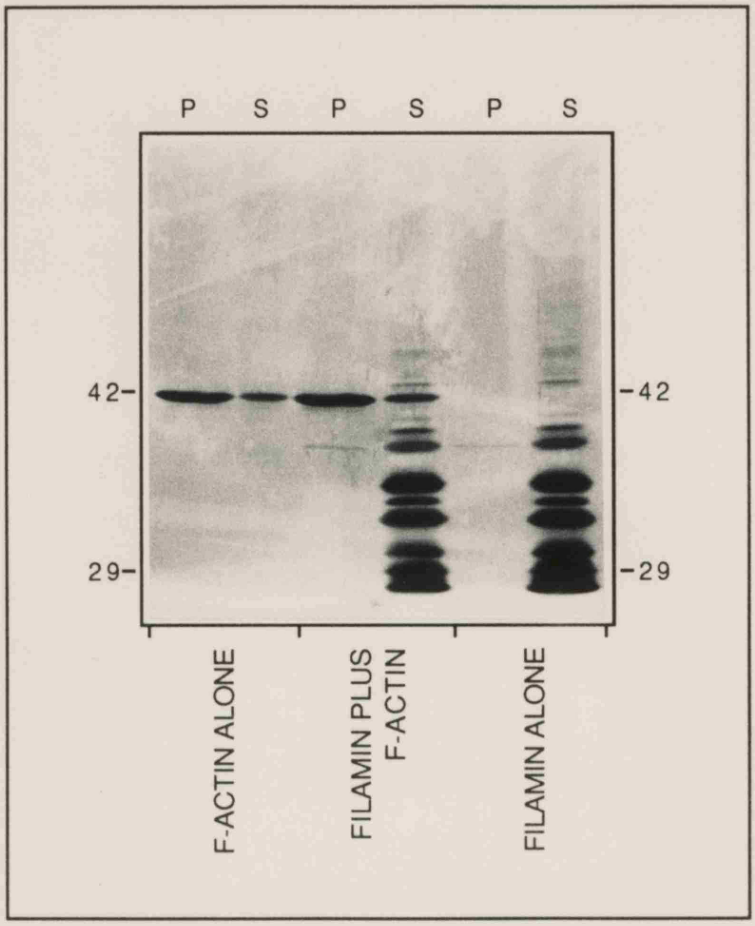

6.4 DISCUSSION.

An immunological approach was used to investigate the possible homology between the actin binding domains of α-actinin and filamin. Similarities between proteins have previously been demonstrated this approach. Thus, an α-actinin isoform specific to fast twitch glycolytic muscle was identified using antibodies raised against a region of 207 amino acids from the repeats of dystrophin (Hoffman et al, 1989). Narvanen et al (1987) generated a monoclonal antibody to a synthetic eight residue peptide identical to residues within the brain α-spectrin repeats. The monoclonal antibody cross reacted with α-actinin. Sequence analysis of α-actinin suggested two putative epitopes, one within the actin binding domain and one within the first repeat. The proposed epitope in α-actinin was similar but not identical to the spectrin sequence suggesting that the antibody recognised a specific peptide conformation rather than a defined sequence. It was hoped that some of the antigenic determinants within the actin binding domain would be to regions conserved between α-actinin, dystrophin, β-spectrin, and the ABP-120. Hence filamin may have had similar epitopes providing it shared a homologous actin binding domain. However, there are examples of low or zero immunological cross reactivity between tissue and species specific isoforms of a protein eg (Weihing, 1983). This could arise if the antigenic determinants were to regions of sequence divergence. This would mean that an immunological approach would not detect a homologous actin binding domain.

The cross reactivity of the anti-α-actinin antibody to intact filamin and of the anti-filamin antibodies to intact α-actinin suggested that the two proteins had common epitopes. Circular dichroism of

α-actinin indicates that it is largely α-helical and that this helix is contained within the repeats (Suzuki et al, 1976; Imamura et al, 1988). Secondary structure predictions for the α-actinin repeats also suggested that they are predominantly composed of α-helix (Davison et al, 1989). In contrast, spectroscopic studies indicate that the secondary structure of filamin is mainly β-form (Koteliansky et al, 1982). No significant α-helix is detected. The marked difference in secondary structure suggests that the immunological cross reactivity of α-actinin and filamin was not due to similarities within the bulk of the α-actinin and filamin molecules. However, the cross reactivity could have been due to both proteins having similar actin binding domains. Furthermore, the anti-filamin antibody cross reacted with the thermolysin generated 27kDa fragment of α-actinin which contains the actin binding domain, but did not cross react with the 53kDa spectrin-like repeat containing fragment of α-actinin. These results suggested that α-actinin and filamin posses a number of common epitopes within the actin binding domain. A thermolysin digest of filamin was then examined with the anti-α-actinin antibody to identify the actin binding domain. The anti-α-actinin antibody cross reacted with five/six filamin polypeptides. Two fragments, designated Bands E and E-1, had molecular weights of approximately 29kDa. This was consistent with the actin binding domain of filamin being released as a protease resistant domain of about 27kDa. The larger cross reactive bands may have been precusor fragments of Bands E and E-1.

Bands E and E-1 were sequenced. The polypeptides had different N-termini. There were two possible explanations for this. Bands E and E-1 could have been non-overlapping fragments that contained the C

and N-terminal regions of the actin binding domain. Alternatively, the two bands could be identical except for N-terminal trimming of Band E-1. It was possible that the two pieces of protein sequence determined overlapped, although alignment of the two sequences would have involved mismatches. The mismatched residues were at the end of the determined amino acid sequence where assignment of amino acid identity is more difficult. During thermolysin digestion of filamin the quantity of Band E-1 diminished whilst the amount of Band E increased, although such changes could have been linked to intensity changes of other bands within the filamin digest. Peptide mapping of Bands E and E-1 strongly suggested that the two bands were closely related. Analysis on SDS-PAGE of V8 protease generated peptide maps of Bands E and E-1 revealed three common fragments. Band E-1 had two additional fragments.

No homology was observed between the determined filamin sequence and that of α-actinin. This was not entirely surprising as the determined sequence was limited (12 and 14 residues). The N-terminal 10 to 30 residues of the actin binding domain from the α-actinin family of F-actin cross linking proteins show no homology (Arimura et al, 1988; Blanchard et al, 1989; Noegel et al, 1989). Therefore it was possible that the regions of homology between α-actinin and filamin within Bands E and E-1 had not been reached. The amount of digested filamin used was limited because of the proximity of Bands E and E-1 after being resolved by gel electrophoresis. The yield of the initial residue was approximately 10pmole. To sequence significantly further would have required an initial yield of about 100pmoles. Two approaches to obtaining further sequence could have been attempted. Purification of Band E

from E-1 would have permitted a greater loading of Band E. Alternatively one of the V8 protease generated fragments from Bands E/E-1 could have been sequenced. This may have provided sequence information within Band E which would have been closer to regions of homology.

However, further investigation suggested that the 27kDa fragment of α-actinin and Band E of filamin were not similar. The V8 protease and papain generated peptide maps of the 27kDa fragment of α-actinin and Band E of filamin differed markedly when analysed by Tris-Tricine gel electrophoresis. However, the generation of different peptide maps by protease digestion of the 27kDa fragment of α-actinin and Band E of filamin did not rule out a possible homology. Despite being homologous, the peptide maps of chicken smooth and skeletal α-actinins differed notably (Bretscher et al, 1979). The antibody cross reactivity described above was re-evaluated using more specific polyclonal antisera. A polyclonal antibody (EL27) specific to the actin binding domain of α-actinin was generated to re-evaluate the cross reaction of filamin with anti-α-actinin antiserum. This was specific to α-actinin fragments containing the actin binding domain when alkaline phosphatase or ^{125}I-conjugated secondary antibody were used as the detection method. A polyclonal antibody (EL53) to the α-actinin repeats was also generated for use as a control. Slight cross reactivity of EL27 with α-actinin fragments not containing the actin binding domain was observed when the ^{125}I-labelled secondary antibody and prolonged autoradiography were used for detection. Bands E and E-1 did not cross react with either the EL27 or EL53 antisera. These results were unexpected as EL27 and EL53 were purified from the polyclonal anti-α-actinin serum

that did cross react with Bands E and E-1 of filamin. Another anomaly was revealed when chicken tissue extracts were examined with EL27, EL53, and the anti-α-actinin antibodies. As expected the EL27 and EL53 antibodies cross reacted with a single protein of approximately 97kDa. However, the anti-α-actinin antiserum cross reacted with four proteins in addition to the 97kDa protein. The cross reactivity could have been due to homology of α-actinin with these proteins but this was unlikely as neither EL27 or EL53 cross reacted with the additional proteins. The anti-α-actinin serum was further affinity purified on nitrocellulose (ELαA) to address the discrepancy. ELαA and the serum (ELαR) from which ELαA had been extracted were then compared using chicken tissue extracts. The cross reactivity of ELαA to the 97kDa protein was enhanced in comparison to its cross reactivity with the 200kDa protein. The converse was true when ELαR was tested. This strongly suggested that the anti-α-actinin serum had antibodies to a high molecular weight protein other than α-actinin. This was surprising as the antiserum was raised against α-actinin that had been purified as described (see section 2.5) and then resolved further by SDS-PAGE. It was possible that the contaminating antibody was raised to a degradation product of the high molecular weight protein which comigrated with α-actinin on SDS-PAGE. It was not shown whether the contaminating antibody was responsible for the cross reactivity exhibited by Bands E and E-1. The cross reactivity of the anti-filamin antibody with the 27kDa fragment of α-actinin could still have been due to conserved epitopes.

α-Actinin and filamin could be co-sedimented by F-actin. A proportion of the α-actinin and filamin sedimented in the absence of F-actin, but this was markedly less than the amount that sedimented

in the presence of F-actin. Interestingly a fragment from the thermolysin digest of filamin appeared to co-sediment in the presence of F-actin. The amount of the fragment to sediment was small, but was markedly greater than the amount of fragment to sediment in the absence of F-actin. The fragment had a molecular weight of approximately 37kDa. Whether the co-sedimentation of the 37kDa fragment represented specific or non-specific binding was unclear.

Unfortunately investigation of the actin binding domain of filamin using an ^{125}I-labelled F-actin overlay approach could not be carried out due to technical difficulties. Background labelling was always excessive. A number of proteins examined that should not bind actin appeared to bind. Similar difficulties with F-actin overlays have been observed previously (Dr. V. Ohanion, Manchester University).

Whilst work was in progress the complete sequence of human endothelial filamin was published (Gorlin et al, 1990). The sequence showed that filamin was composed of two types of domain. There was a single N-terminal domain that was homologous to the actin binding domain of α-actinin. The rest of the molecule comprised twenty four repeats of approximately 96 amino acids that were predicted to form β-sheet.

The N-terminal residue of Band E-1 and of Band E corresponded to residue 269 and 275 respectively of the human filamin sequence Figures 6.14 and 6.15). This confirmed that the sequence derived for Band E of filamin overlapped with that of Band E-1 (Figure 6.15). Fifteen of the eighteen residues sequenced from Bands E/E-1 were

FIGURE 6.14

COMPARISON OF THE N-TERMINAL DOMAINS OF FILAMIN AND α-ACTININ

The sequence of the actin binding domain and the first repeat of filamin (Fil) and α-actinin (αA) are shown (Baron et al, 1987; Gorlin et al, 1990). The β-sheet repeat of filamin and the spectrin-like repeat of α-actinin are shown in italics. Identical residues in the two sequences are indicated *; conservative substitutions are denoted |. The sequence derived for the N-terminus of Bands E/E-1 is underlined.

```
                    .         .         .         .         .         .         .         .
Fil      (1) MSSSHSRAGQSAAGAAPGGGVDTRDAEMPATEKDLAEDAPWKKIQQNTFTRWCNEHLKCVSKRIANLQTDLSDGLVLIAL (80)
αA       (1)             DHHYDPQQTNDYMQPEEDWDRDLLLDPAWEKQQRKTFTAWCNSHLRKAGTQIENIEEDFRDGLKLMLL (68)
                        |       |||  |   | ||**  *||*|* *||*** ***|**| ||||*|*|||*||*** *| *
                    .         .         .         .         .         .         .         .
Fil     (81) LEVLSQKKMHRKHNQRPTFRQMQLENVSVALEFLDRES-IKLVSIDSKAIVDGNLKLILGLIWTLILHYSISMPMWDEEE (159)
αA      (69) LEVISGERLA-KPERGKMRVHKISNVNKALDFIASKGV--KLVSIGAEEIVDGNVKMTLGMIWTIILRFAIQDISVEE-- (143)
             ***|* |||  * ||     ||  |  || |   |||   *****||||*****|*||**|***|**|||*     |*
                    .         .         .         .         .         .         .         .
Fil     (160) DEEAKKQTPKQRLLGWIQNKLPQLPITNFSRDWQS---GRALGALVDSCAPGLCPDWDSWDASKPVTNAREAMQQADDWL (236)
αA      (144) ------TSAKEGLLLWYQRKTAPYKNVNIQNFHISWKDGLGFCALIHRHRPELIDYGKLRKDDPLTNLNTAF-DVAEKYL (216)
                  | *| ** * *|*      |*| | | *   * || **||   *|*    |  |||  ||   |  | *|||*
                    .         .         .         .         .         .         .         .
Fil     (237) GIPQVITPEEIVDPNV-DEHSVMTYLSQFPKAKLKPGAPLRPKLNPKKARAYGPGIEPTGNMVKKRAEFTVETRSAGQGE (315)
αA      (217) DIPKMLDAEDIVGTARPDEKAIMTYVSSFYHAFSGAQKAETAANRICKVLAVNQENEQLMEDYEKLASDLLEWIRRTIPW (296)
             |**|||||*|**||   **|||***|* * |*              *| *   | *   |  |* *|  |*    |
                    .         .         .         .         .         .         .         .
Fil     (316) VLVYVEDPPAGHQEEAKVTANNDKNRTFSVWYVPEVTGTHKVTVLFAGQHLAKSPFEVYV (375)
αA      (297) -LENRAPENTMQAMQQKLEDFRDYRRLHKPPVQEKCQLEINFNTLQTKLRLSNRPAFMPSEGKMVSD (363)
              *   |   | || ||*||| |* |*  |     |   | | ||* |  |*|| *
                    .         .         .         .         .         .
```

FIGURE 6.15
DIAGRAM ALIGNING THE SEQUENCES OF BANDS E AND E-1 OF FILAMIN WITH THAT OF HUMAN FILAMIN.
(a) and (b) indicated uncertain residues of the sequences determined for Band E and Band E-1 respectively. (c) denoted the identical residues between chicken gizzard filamin and human endothelial filamin.

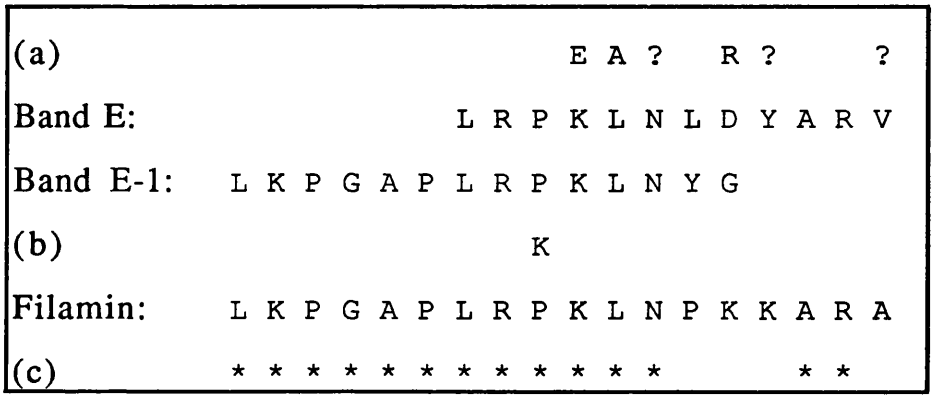

identical to those in the corresponding region of human filamin. The residues that do not match may reflect species differences between chicken and human filamins. Alternatively the differences may be due to incorrect assignment of the sequenced amino acids from Bands E/E-1. Band E-1 corresponds to residues 269 to approximately 538 of human filamin. This region was directly adjacent to the actin binding domain of filamin (residues 33 to 265). Although the actin binding domains of α-actinin and filamin are 32% identical, there is no significant homology C-terminal of the actin binding domain.

REFERENCES

Abercrombie, M., Heaysman, J.E.M., and Pegrum, S.M. (1971) Experimental Cell Research 67: 359-367.

Aitken, A., Cohen, P., Sartikern, S., Williams, B.H., Calder, H.G., Smith, A., and Klee, C.B. (1982) FEBS Lett 150: 314-318.

Akiyama, S.K., Hasegawa, E., Hasegawa, T., and Yamada, K.M. (1985) Journal of Biological Chemistry 260: 13256-13260.

Altruda, F., Cervella, P., Tarone, G., Botta, C., Balzac, F., Stefanuto, G., and Silengo, L. (1990) Gene 95: 261-266.

Andre, E., Brink, M., Gerisch, G., Isenberg, G., Noegel, A., Schleicher, M., Segall, J.E., and Wallraff, E. (1989) Journal of Cell Biology 108: 985-995.

Argraves, W.S., Dickerson, K., Burgess, W.H., and Ruoslahti, E. (1989) Cell 58: 623-629.

Argraves, W.S., Tran, H., Burgess, W.H., and Dickerson, K. (1990) Journal of Cell Biology 111: 3155-3164.

Arimura, C., Suzuki, T., Yanagisawa, M., Imamura, M., Hamada, Y., and Masaki, T. (1988) European Journal Of Biochemistry 177: 649-655.

Armstrong, L. and Molony, L. (1991) Journal of Cell Biology 129a.

Barnes, D.W. and Silnutzer, J. (1983) Journal of Biological Chemistry 258: 12548-12552.

Baron, M.D., Davison, M.D., Jones, P., and Critchley, D.R. (1987a) Journal of Biological Chemistry 262: 17623-17629.

Baron, M.D., Davison, M.D., Jones, P., Patel, B., and Critchley, D.R. (1987b) Journal of Biological Chemistry 262: 2558-2561.

Barstead, R.J. and Waterston, R.H. (1989) Journal of Biological Chemistry 264: 10177-10185.

Barstead, R.J. and Waterston, R.H. (1991) Journal of Cell Biology 114: 715-724.

Bechtel, P.J. (1979) Journal of Biological Chemistry 254: 1755-1758.

Beck, K. (1989) FEBS Lett 249: 1-4.

Beckerle, M.C. (1986) Journal of Cell Biology 103: 1679-87.

Beckerle, M.C., Burridge, K., DeMartino, G.N., and Croall, D.E. (1987) Cell 51: 569-577.

Belkin, A.M. and Koteliansky, V.E. (1987) FEBS Lett 220: 291-294.

Belkin, A.M., Ornatsky, O.I., Glukhova, M.A., and Koteliansky, V.E. (1988) Journal of Cell Biology 107: 545-553.

Bendori, R., Salomon, D., and Geiger, G. (1989) Journal of Cell Biology 108: 2383-2393.

Bennett, J.P., Zaner, K.S., and Stossel, T.P. (1984) Biochemistry 23: 5081-5086.

Birnboim, H.C. and Dolby, J. (1979) Nucleic Acids Research 7:1513

Blanchard, A., Ohanion, V., and Critchley, D.R. (1989) Journal of Muscle Research and Cell Motility 10: 280-289.

Bradford, M.M. (1976) Analytical Biochemistry 72: 248-254.

Brands, R., De Boer, A., Feltkamp, C.A., and Roos, E. (1990) Experimental Cell Research 186: 138-148.

Bresnick, A.R., Warren, V., and Condeelis, J. (1990) Journal of Biological Chemistry 265: 9236-9240.

Bresnick, A.R., Janmey, P.A., and Condeelis, J. (1991) Journal of Biological Chemistry 266: 12989-12993.

Bretscher, A. (1981) Proc. Natl. Acad. Sci. USA 78: 6849-6853.

Bretscher, A., Vandekerckhove, J., and Weber, K. (1979) European Journal Of Biochemistry 100: 237-243.

Bretscher, A. and Weber, K. (1980) Journal of Cell Biology 86: 335-340.

Buck, C.A., Shea, E., Duggan, K., and Horwitz, A.F. (1986) Journal of Cell Biology 103: 2421-2428.

Burn, P., Rotman, A., Meyer, R.K., and Burger, M.M. (1985) Nature 314: 469-72.

Burn, P. and Burger, M.M. (1987) Science 235: 476-9.

Burn, P., Kupfer, A., and Singer, S.J. (1988) Proc. Natl. Acad. Sci. USA 85: 497-501.

Burnette, W.N. (1981) Analytical Biochemistry 112: 195-203.

Burridge, K. and Feramisco, J.R. (1980) Cell 19: 587-95.

Burridge, K. and Feramisco, J.R. (1981) Nature 294: 565-567.

Burridge, K. and Connell, L. (1983) Journal of Cell Biology 97: 359-367.

Burridge, K. and Mangeat, P. (1984) Nature 308: 744-746.

Burridge, K., Fath, K., Kelly, T., Nuckolls, G., and Turner, C. (1988) Annual Reviews of Cell Biology 4: 487-525.

Byers, T.J., Husain-Chishti, A., Dubreuil, R., Branton, D., and Goldstein, L.S.B. (1989) Journal of Cell Biology 109: 1160-1166.

Chelly, J., Gilgenkrantz, H., Lambert, M., Hamard, G., Chafey, P., Recan, D., Katz, P., De la Chapelle, A., Koenig, M., Ginjaar, L.B., Fardeau, M., Tome, F., Kahn, A., and Kaplan, J.-C. (1990) Cell 63: 1239-1248.

Chen, M. and Stracher, A. (1989) Journal of Biological Chemistry 264: 14282-14289.

Chen, W.-T. and Singer, S.J. (1982) Journal of Cell Biology 95: 205-222.

Cheresh, D.A. (1987) Proc. Natl. Acad. Sci. USA 84: 6471-6475.

Clark, R.A.F. (1989) Current Opinion in Cell Biology 1: 1000-1008.

Cleveland, D.W., Fischer, S.G., Kirschner, M.W. and Laemmli, U.K. (1977) Journal of Biological Chemistry 252: 1102-1106.

Conboy, J., Kan, Y.W., Shohet, S.B., and Mohandas, N. (1986) Proc. Natl. Acad. Sci. USA 83: 9512-9516.

Correas, I., Speicher, D.W., and Marchesi, V.T. (1986) Journal of Biological Chemistry 13362-13366.

Coutu, M.D. and Craig, S. (1988) Proc. Natl.Acad. Sci. USA 85: 8535-9.

Crawford, A.W. and Beckerle, M.C. (1991) Journal of Biological Chemistry 266: 5847-5853.

Crawford, A.W., Michelsen, J.W., and Beckerle, M.C. (1992) Journal of Cell Biology 116: 1381-1393.

Da Silva, A.C.R. and Reinach, F.C. (1991) TIBS 16: 53-57.

Dana, N., Fathallah, D.M., and Arnaout, M.A. (1991) Proc. Natl. Acad. Sci. USA 88: 3106-3110.

David-Pfeuty, T. and Singer, S.J. (1980) Proc. Natl. Acad. Sci. USA 77: 6687-6691.

Davies, P.J.A., Shizuta, Y. and Pastan, I. (1982) Methods In Enzymology 85: 322-328.

Davison, M.D., Baron, M.D., Wootton, J.C., and Critchley, D.R. (1989) Int. J. Biol. Macromol. 11: 81-90.

De Arruda, M.V., Watson, S., Lin, C.-S., Leavitt, J., and Matsudaira, P. (1990) Journal of Cell Biology 111: 1069-1079.

De Jong, W.W., Zweers, A., and Cohen, L.H. (1978) Biochemical and Biophysical Research Communications 82: 532.

DeLozanne and Spudich. (1987) Science 236: 1086.

DePasquale, J.A. and Izzard, C.S. (1987) Journal of Cell Biology 105: 2803-2809.

DePasquale, J.A. and Izzard, C.S. (1991) Journal of Cell Biology 113: 1351-1359.

Detwiler, T.C., Charo, I.F., and Feinman, R.D. (1978) Thromb. Haem. 110: 207-211.

Dower, W.J., Miller, J.F., and Ragsdale, C.W. (1988) Nucleic Acids Reaearch 16: 6127-6145

Duhaiman, A.S. and Bamburg, J.R. (1984) Biochemistry 23: 1600-1608.

Edelman, G.M. (1986) Annual Reviews of Cell Biology 2: 81-116.

Elmore, M.A., Anand, R., Horvath, A.R., and Kellie, S. (1990) FEBS Lett 269: 283-287.

Endo, T. and Masaki, T. (1984) Journal of Cell Biology 99: 2322-2332.

Engel, J. (1991) Current Opinion in Cell Biology 3: 779-785.

Evans, R.R., Robson, R.M., and Stromer, M.H. (1984) Journal of Biological Chemistry 259: 3916-3924.

Ezzell, R.M., Kenney, D.M., Egan, S., Stossel, T.P., and Hartwig, J.H. (1988) Journal of Biological Chemistry 263: 13303-13309.

Feltkamp, C.A., Pijnenburg, M.A.P., and Roos, E. (1991) Journal of Cell Science 100: 579-587.

Feramisco, J.R. and Burridge, K. (1980) Journal of Biological Chemistry 255: 1194-1199.

Fishkind, D.J., Bonder, E.M., and Begg, D.A. (1987) Cell Motility and the Cytoskeleton 7: 304-314.

Folkman, J.A. and Moscona, A. (1978) Nature 273: 345-349.

Fox, J.E.B., Goll, D.E., Reynolds, C.C., and Phillips, D.R. (1985) Journal of Biological Chemistry 260: 1060-1066.

Freifelder, D. Physical Biochemistry: Applications to Biochemistry and Molecular Biology. Second ed., Freeman, 1976.

Funayama, N., Nagafuchi, A., Sato, N., Tsukita, S., and Tsukita, S. (1991) Journal of Cell Biology 115: 1039-1048.

Gache, Y., Landon, F., Touitou, H., and Olomucki, A. (1984) Biochemical and Biophysical Research Communications 124: 877-881.

Geiger, B. (1979) Cell 18: 193-205.

Geiger, B. (1981) In *International Cell Biology* Springer Verlag: pp761-773.

Geiger, B., Tokuyasu, K.T., Dutton, A.H., and Singer, S.J. (1980) Proc. Natl. Acad. Sci. USA 77: 4127-4133.

Geiger, B., Volk, T., and Volberg, T. (1985) Journal of Cell Biology 101: 1523-1531.

Gilbert, W. (1985) Science 228: 823-824.

Gilmore, A.P., Jackson, P., Waites, G.T., and Critchley, D.R. (1992) (in press)

Gimona, M., Furst, D.O., and Small, J.V. (1987) Journal of Muscle Research and Cell Motility 8: 329-341.

Gimona, M., Small, J.V., Moeremans, M., Van Damme, J., Puype, M., and Vandekerckhove, J. (1988) European Molecular Biology Organisation Journal 7: 2329-2334.

Glenney Jr, J.R. and Zokas, L. (1989) Journal of Cell Biology 108: 2401-2408.

Goll, D.E., Dayton, W.R., Singh, I., and Robson, R.M. (1991) Journal of Biological Chemistry 266: 8501-8510.

Gorlin, J.B., Yamin, R., Egan, S., Stewart, M., Stossel, T.P., Kwiatkowski, D.J., and Hartwig, J.H. (1990) Journal of Cell Biology 111: 1089-1105.

Grinnell, F. (1986) Journal of Cell Biology 103: 2697-2706.

Grinnell, F., Toda, K.-I., and Takashima, A. (1987) Journal of Cell Science 8: 199-209.

Hamaguchi, M. and Hanafusa, H. (1987) Proc. Natl. Acad. Sci. USA 84: 2312-2316.

Hartwig, J.H. and Stossel, T.P. (1981) Journal of Molecular Biology 145: 563-581.

Hartwig, J.H., Thelen, M., Rosen, A., Janmey, P.A., Nairn, A.C., and Aderem, A. (1992) Nature 356: 618-622.

Hayashi, Y., Haimovich, B., Rezka, A., Boettiger, D., and Horwitz, A. (1990) Journal of Cell Biology 110: 175-184.

Heise, H., Bayerl, T., Isenberg, G., and Sackmann, E. (1991) Biochim. Biophys. Acta. 1061: 121-131.

Hemler, M.E. (1990) Ann. Rev. Immunol. 8: 365-400.

Hemmings, L., Kuhlman, P., and Critchley, D.R. (1992) Journal of Cell Biology 116: 1369-1380.

Herman, B. and Pledger, W.J. (1985) Journal of Cell Biology 100: 1031-1040.

Herman, B., Harrington, B.A., Olashaw, N.E., and Pledger, W.J. (1986) Journal of Cellular Physiology 126: 115-125.

Herrenknecht, K., Ozawa, M., Eckerskorn, C., Lottspeich, F., Lenter, M., and Kemler, R. (1991) Proc. Natl. Acad. Sci. USA 88: 9156-9160.

Hirst, R., Horwitz, A., Buck, C., and Rohrschneider, L. (1986) Proc. Natl. Acad. Sci. USA 83: 6470-6474.

Hoffman, E.P., Watkins, S.C., Slayter, H.S., and Kunkel, L.M. (1989) Journal of Cell Biology 108: 503-510.

Horwitz, A., Duggan, K., Greggs, R., Decker, C., and Buck, C. (1985) Journal of Cell Biology 101: 2134-2144.

Horwitz, A., Duggan, K., Buck, C., Beckerle, M.C., and Burridge, K. (1986) Nature 320: 531-533.

Humphries, M.J., Akiyama, S.K., Komoriya, A., Olden, K., and Yamada, K.M. (1986) Journal of Cell Biology 103: 2637-2647.

Hynes, R.O. (1992) Cell 69: 11-25.

Igarashi, M., Saito, S., and Komiya, Y. (1990) European Journal Of Biochemistry 193: 551-558.

Imamura, M., Endo, T., Kuroda, M., Tanaka, T., and Masaki, T. (1988) Journal of Biological Chemistry 263: 7800-7805.

Isenberg, G., Leonard, K., and Jockusch, B.M. (1982) Journal of Molecular Biology 158: 231-249.

Ito, S., Werth, D.K., Richert, N.D., and Pastan, I. (1983) Journal of Biological Chemistry 258: 14626-31.

Izzard, C.S. (1988) Cell Motility and the Cytoskeleton 10: 137-42.

Izzard, C.S. and Lochner, L.R. (1976) Journal of Cell Science 21: 129-159.

Jackson, P., Smith, G., and Critchley, D.R. (1989) European Journal Of Biochemistry 50: 162-169.

Jaken, S., Leach, K., and Klauck, T. (1989) Journal of Cell Biology 109: 697-704.

Jenne, D. and Stanley, K. (1987) Biochemistry 26: 6735-6742.

Jones, P., Jackson, P., Price, G.J., Patel, B., Ohanion, V., Lear, A.L., and Critchley, D.R. (1989) Journal of Cell Biology 109: 2917-2927.

Kabsch, W., Mannherz, H.G., Suck, D., Pai, E.F., and Holmes, K.C. (1990) Nature 347: 37-44.

Kamps, M.P., Buss, J.E., and Sefton, B.M. (1986) Cell 45: 105-112.

Kaufmann, S., Piekenbrock, T., Goldmann, W.H., Barmann, M., and Isenberg, G. (1991) FEBS Lett 284: 187-191.

Kellie, S., Patel, B., Pierce, E.J. and Critchley, D.R. (1983) Journal of Cell Biology 97: 447-454.

Kellie, S., Patel, B., Wigglesworth, N.M., Critchley, D.R., and Wyke, J.A. (1986) Experimental Cell Research 165: 216-218.

Kellie, S. and Wigglesworth, N.M. (1987) FEBS Lett 213: 428-432.

Kimizuka, F., Ohdate, Y., Kawase, Y., Shimojo, T., Taguchi, Y., Hashino, K., Goto, S., Hashi, H., Kato, I., Sekiguchi, K., and Titani, K. (1991) Journal of Biological Chemistry 266: 3045-3051.

Knecht and Loomis. (1987) Science 236: 1081-1085.

Koenig, M., Monaco, A.P., and Kunkel, L.M. (1988) Cell 53: 219-228.

Kornblihtt, A.R., Vibe-Pederson, K., and Baralle, F.E. (1984) European Molecular Biology Organisation Journal 3: 221-226.

Koteliansky, V.E., Glukhova, M.A., Shirinsky, V.P., Smirnov, V.N., Bushueva, T.L., Filimonov, V.V., and Venyaminov, S.Y. (1982) European Journal Of Biochemistry 121: 553-559.

Koteliansky, V.E., Ogryzko, E.P., Zhidkova, N.I., Weller, P.A., Critchley, D.R., Vancompernolle, K., Vandekerckhove, J., Strasser, P., Way, M., Gimona, M., and Small, J.V. (1992) European Journal Of Biochemistry 204: 767-772.

Kulesza-Lipka, D. and Jakubiec-Puka, A. (1985) FEBS Lett 187: 354-358.

Kupfer, A., Singer, S.J., and Dennert, G. (1986) J. Exp. Med. 163: 489-498.

Laemmli, U.K. (1970) Nature 227: 680-685.

Lamb, N.J.C., Fernandez, A., Conti, M., Adelstein, R., and Glass, D.B. (1988) Journal of Cell Biology 106: 1955-1971.

Landon, F., Gache, Y., Touitou, H., and Olomucki, A. (1985) European Journal Of Biochemistry 153: 231-237.

Langanger, G., De Mey, J., Moeremans, M., Daneels, G., De Brabander, M., and Small, J.V. (1984) Journal of Cell Biology 99: 1324-1334.

Langer, B.G. and Pepe, F.A. (1980) Journal of Biological Chemistry 255: 5429-5434.

Lankes, W.T. and Furthmayr, H. (1991) Proc. Natl. Acad. Sci. USA 88: 8297-8301.

Laterra, J., Norton, E.K., Izzard, C.S., and Culp, L.A. (1983) Experimental Cell Research 146: 15-27.

Lazarides, E. and Burridge, K. (1975) Cell 6: 289-298.

Leader, W.M., Stopak, D., and Harris, A.K. (1983) Journal of Cell Science 64: 1-11.

Lehtonen, E., Lehto, V.-P., Badley, R.A., and Virtanen, I. (1983) Experimental Cell Research 144: 191-197.

Leto, T.L., Correas, I., Tobe, T., Anderson, R.A., and Horne, W.C. In Membrane skeleton and cytoskeletal membrane associations., ed. V. Bennet, C.M. Cohen, S.E. Lux, and J. Palek. 201-209. New York: Alan R. Liss Inc., 1986.

Litchfield, D.W. and Ball, E.H. (1986) Biochemical and Biophysical Research Communications 134: 1276-1283.

Maher, P. and Singer, S.J. (1983) Cell Motil. 3: 419-29.

Maher, P.A. and Pasquale, E.B. (1988) Journal of Cell Biology 106: 1747-1755.

Maniatis, T., Fritsch, E.F., and Sambrook, J. Molecular cloning: A laboratory manual. 2nd ed., Cold Spring Harbour Laboratory press, 1982.

Marcantonio, E.E. and Hynes, R.O. (1988) Journal of Cell Biology 106: 1765-1772.

Marchesi, V.T. (1985) Annual Reviews of Cell Biology 1: 531-61.

Matsudaira, P.T., Mandelkow, E., Renner, W., Hesterberg, L.K., and Weber, K. (1983) Nature 301: 209-214.

Matsudaira, P.T. (1987) Journal of Biological Chemistry 262: 10035-10038.

McClay, D.R. and Ettensohn, C.A. (1987) Annual Reviews of Cell Biology 3: 319-345.

McPherson, A. Preparation and analysis of protein crystals. Wiley Interscience, 1982.

Meigs, J.B. and Wang, Y.-L. (1986) Journal of Cell Biology 102: 1430-1438.

Menke, A. and Jockusch, H. (1991) Nature 349: 69-71.

Merisko, E.M., Welch, J.K., Chen, T.-Y., and Chen, M. (1988) Journal of Biological Chemistry 263: 15705-15712.

Meyer, R.K. (1989) European Journal of Cell Biology 50: 491-9.

Meyer, R.K., Schindler, H., and Burger, M.M. (1982) Proc. Natl.Acad. Sci. USA 79: 4280-4.

Meyer, R.K. and Aebi, U. (1990) Journal of Cell Biology 110: 2013.

Milam, L.M. (1985) Journal of Molecular Biology 184: 543-545.

Mimura, N. and Asano, A. (1986) Journal of Biological Chemistry 261: 10680-10687.

Mimura, N. and Asano, A. (1987) Journal of Biological Chemistry 262: 4717-23.

Miron, T., Vancompernolle, K., Vandekerckhove, J., Wilchek, M., and Geiger, B. (1991) Journal of Cell Biology 114: 255-261.

Mitraki, A. and King, J. (1989) Bio/Technology 7: 690-697.

Molony, L., McCaslin, D., Abernethy, J., Paschal, B., and Burridge, K. (1987) Journal of Biological Chemistry 262: 7790-7795.

Monaco, A.P. (1989) TIBS 14: 412-415.

Mould, A.P., Wheldon, L.A., Komoriya, A., Wayner, E.A., Yamada, K.M., and Humphries, M.J. (1990) Journal of Biological Chemistry 265: 4020-4024.

Mould, A.P., Komoriya, A., Yamada, K.M., and Humphries, M.J. (1991) Journal of Biological Chemistry 266: 3579-3585.

Mueller, S.C., Kelly, T., Dai, M., Dai, H., and Chen, W.-T. (1989) Journal of Cell Biology 109: 3455-3464.

Muguruma, M., Matsumura, S., and Fukasawa, T. (1990) Biochemical and Biophysical Research Communications 171: 1217-1223.

Nagafuchi, A., Takeichi, M., and Tsukita, S. (1991) Cell 65: 849-857.

Narvanen, O., Narvanen, A., Wasenius, V-M., Partanen, P. and Virtanen, I. (1987) FEBS Lett 224: 156-160.

Nave, R., Furst, D., and Weber, K. (1990) FEBS Lett 269: 163-166.

Niggli, V., Dimitrov, D.P., Brunner, J., and Burger, M.M. (1986) Journal of Biological Chemistry 261: 6912-18.

Nishizuka, Y. (1984) Science 308: 693-698.

Noegel, A., Witke, W., and Schleicher, M. (1987) FEBS Lett 221: 391-396.

Noegel, A.A., Rapp, S., Lottspeich, F., Schleicher, M., and Stewart, M. (1989) Journal of Cell Biology 109: 607-618.

Nomura, M., Yoshikawa, K., Tanaka, T., Sobue, K., and Maruyama, K. (1987) European Journal Of Biochemistry 163: 467-471.

Nuckolls, G. and Burridge, K. (1990) Journal of Cell Biology 111: 299a.

Nuckolls, G.H., Turner, C.E., and Burridge, K. (1990) European Journal of Cell Biology 110: 1635-1644.

O'Halloran, T., Beckerle, M.C., and Burridge, K. (1985) Nature 317: 449-451.

O'Halloran, T. and Burridge, K. (1986) Biochim. Biophys. Acta. 869: 337-349.

O'Halloran, T., Molony, M., and Burridge, K. (1986) Methods In Enzymology 69-77.

Obara, M., Kang, M.S., Rocher-Dufour, S., Kornblihtt, A., Thiery, J.-P., and Yamada, K.M. (1987) FEBS Lett 213: 261-264.

Oesch, B. and Birchmeier, W. (1982) Cell 31: 671-679.

Ohanion, V., Wolfe, L.C., John, K.M., Pinder, J.C., Lux, S.E., and Gratzer, W.B. (1984) Biochemistry 23: 4416-4420.

Onji, T., Takagi, M., and Shibata, N. (1987) Biochimica et Biophysica Acta 912: 283-286.

Otey, C.A., Pavalko, F.M., and Burridge, K. (1990) Journal of Cell Biology 111: 721-729.

Otto, J.J. (1983) Journal of Cell Biology 97: 1283-1287.

Ozawa, M., Ringwald, M., and Kemler, R. (1990) Proc. Natl. Acad. Sci. USA 87: 4246-4250.

Pakkanen, R., Hedman, K., Turunen, O., Wahlstrom, T., and Vaheri, A. (1987) Journal of Histochemistry and Cytochemistry 135: 809-816.

Pasquale, E.B., Maher, P.A., and Singer, S.J. (1986) Proc. Natl. Acad. Sci. USA 83: 5507-5511.

Pastan, I. and Willingham, M. (1978) Nature 274: 645-650.

Paul, J.I., Schwarzbauer, J.E., Tamkun, J.W., and Hynes, R.O. (1986) Journal of Biological Chemistry 261: 12258-12265.

Pavalko, F.M., Otey, C., and Burridge, K. (1989) Journal of Cell Science 94: 109-118.

Pavalko, M.K. and Burridge, K. (1991) Journal of Cell Biology 114: 481-491.

Pellman, D., Garber, E., Cross, F.R., and Hanafusa, H. (1985) Proc. Natl. Acad. Sci. USA 82: 1623-1627.

Pierschbacher, M.D. and Ruoslahti, E. (1984a) Nature 309: 30-33.

Pierschbacher, M.D. and Ruoslahti, E. (1984b) Proc. Natl. Acad. Sci. USA 81: 5985-5988.

Plantefaber, L.C. and Hynes, R.O. (1989) Cell 56: 281-290.

Podlbnaya, Z.A., Tskhovrebova, L.A., Zaalishvili, M.M., and Stefanenko, G.A. (1975) Journal of Molecular Biology 92: 357-359.

Pollard, T.D. and Cooper, J.A. (1986) Annual Review of Biochemistry 55: 987-1035.

Price, G.J., Jones, P., Davison, M.D., Patel, B., Bendori, R., Geiger, B., and Critchley, D.R. (1989) Biochem. J. 259: 453-461.

Pytela, R., Pierschbacher, M.D., and Ruoslahti, E. (1985) Cell 40: 191-198.

Rees, D., J,G., Ades, S.E., Singer, S.J., and Hynes, R.O. (1990) Nature 347: 685-689.

Risinger, M.A., Wilkins, J.A., and Lin, S. (1987) Journal of Cell Biology 105: 130a (abstr).

Rohrschneider, L.R. (1980) Proc. Natl. Acad. Sci. USA 77: 3514-3518.

Rosen, A., Keenan, A.F., Thelen, M., Nairn, A.C., and Aderem, A.A. (1990) J. Exp. Med. 172: 1211-1215.

Rowe, A.J. (1988) Nature 333: 16th June.

Ruhnau, K. and Wegner, A. (1988) FEBS Lett 228: 105-8.

Ruhnau, K., Gaertner, A., and Wegner, A. (1989) Journal of Molecular Biology 210: 141-148.

Ruoslahti, E. (1988) Annual Review of Biochemistry 57: 375-413.

Sato, M., Schwarz, W.H., and Pollard, T.D. (1987) Nature 325: 828-830.

Sato, R., Komira, J., Imanaka, T., and Takano, T. (1990) Journal of Biological Chemistry 265: 21232-21236.

Schagger, H. and Von Jagow, G. (1987) Analytical Biochemistry 166: 368-379.

Schein, C.H. (1989) Bio/Technology 7: 1141-1149.

Schleicher, M., Noegel, A., Schwarz, T., Walraff, E., Brink, M., Faix, J., Gerisch, G., and Isenberg, G. (1988) Journal of Cell Science 90: 59-71.

Schroer, E. and Wegner, A. (1985) European Journal Of Biochemistry 153: 515-20.

Sefton, B.M., Hunter, T., Beeman, K., and Eckhart, W. (1980) Cell 20: 807.

Sefton, B.M., Hunter, T., Ball, E.H., and Singer, S.J. (1981) Cell 24: 165-174.

Sefton, B.M. and Buss, J.E. (1987) Journal of Cell Biology 104: 1449-1453.

Senecal, J.L., Fortin, S., Roussin, S., and Joyal, F. (1987) J. Clin. Invest. 80: 778-85.

Seykora, J.T., Ravetch, J.V., and Aderem, A. (1991) Proc. Natl. Acad. Sci. USA 88: 2505-2509.

Shaw, L.M., Messier, J.M., and Mercurio, A.M. (1990) Journal of Cell Biology 110: 2167-2174.

Shimizu, Y., Van Seventer, G.A., Horgan, K.J., and Shaw, S. (1990) Nature 345: 250-253.

Shizuta, Y., Shizuta, H., Gallo, M., Davies, P., Pastan, I., and Lewis, M. (1976) Journal of Biological Chemistry 251: 6562-6567.

Shoeman, R.L. and Traub, P. In Intracellular calcium dependent proteolysis., ed. R.L. and Murachi Mellgren T. 191-209. CRC Press, 1990.

Singer, I.I., Kawka, D.W., Scott, S., Mumford, R.A., and Lark, M.W. (1987) Journal of Cell Biology 104: 573-584.

Singh, I., Goll, E.D., Robson, R.M., and Stromer, M.H. (1977) Biochimica et Biophysica Acta 491: 29-45.

Skorstengaard, K., Jensen, M.S., Sahl, P., Petersen, T.E., and Magnusson, S. (1986) European Journal Of Biochemistry 161: 441-453.

Small, J.V., Furst, D.O., and De Mey, J. (1986) Journal of Cell Biology 102: 210-220.

Smith, D.B. and Johnson, K.S. (1988) Gene 67: 31-40.

Solowska, J., Guan, J.-L., Marcantonio, E.E., Trevithick, J.E., Buck, C.A., and Hynes, R.O. (1989) Journal of Cell Biology 109: 853-861.

Speicher, D.W. and Marchesi, V.T. (1984) Nature 311: 177-180.

Stickel, S.K. and Wang, Y.-L. (1988) Journal of Cell Biology 107: 1231-1239.

Studier, F.W. and Moffat, B.A. (1986) Journal of Molecular Biology 189: 113-130.

Stumpo, D.J., Graff, J.M., Albert, K.A., Greengard, P., and Blackshear, P.J. (1989) Proc. Natl. Acad. Sci. USA 86: 4012-4016.

Suzuki, A., Goll, D.E., Singh, I., Allen, R.E., Robson, R.M., and Stromer, M.H. (1976) Journal of Biological Chemistry 251: 6860-6870.

Suzuki, S., Pierschbacher, M.D., Hayman, E.G., Nguyen, K., Ohgren, Y., and Ruoslahti, E. (1984) Journal of Biological Chemistry 259: 15307-15314.

Takada, Y., Elices, M.J., Crouse, C., and Hemler, M.E. (1989) European Molecular Biology Organisation Journal 8: 1361-1368.

Tamkun, J.W., Schwarzbauer, J.e., and Hynes, R.O. (1984) Proc. Natl. Acad. Sci. USA 81: 5140-5144.

Tapley, P., Horwitz, A., Buck, C., Duggan, K., and Rohrschneider, L. (1989) Oncogene 4: 325-333.

Tsukita, S., Hieda, Y., and Tsukita, S. (1989) Journal of Cell Biology 108: 2369-2382.

Turner, C.E. (1991) Journal of Cell Biology 115: 201-207.

Turner, E.T., Pavalko, F.M., and Burridge, K. (1989) Journal of Biological Chemistry 264: 11938-11944.

Turner, C.E., Glenney Jr, J.R., and Burridge, K. (1990) Journal of Cell Biology 111: 1059-1068.

Turunen, O., Winqvist, R., Pakkanen, R., Grzeschik, K.-H., Wahlstrom, T., and Vaheri, A. (1989) Journal of Biological Chemistry 264: 16727-16732.

Ungewickell, E., Bennett, P.M., R., C., Ohanion, V., and Gratzer, W.B. (1979) Nature 280: 811-814.

Volberg, T., Sabanay, H., and Geiger, G. (1986) Differentiation 32: 34-43.

Wachsstock, D.H., Wilkins, J.A., and Lin, S. (1987) Biochem. Biophys. Res. Comm. 146: 554-560.

Waites, G.T., Graham, I.R., Jackson, P., Millake, D.B., Patel, B., Blanchard, A.D., Weller, P.A., Eperon, I.C., and Critchley, D.R. (1992) Journal of Biological Chemistry

Wallach, D., Davies, P.J.A., and Pastan, I. (1978) Journal of Biological Chemistry 253: 4739-4745.

Walraff, E., Schleicher, M., Modersitski, M., Rieger, D., Isenberg, G., and Gerisch, G. (1986) European Molecular Biology Organisation Journal 5: 61-67.

Wang, K. (1977) Biochemistry 16: 1857-1865.

Wang, K., Ash, J.F., and Singer, S.J. (1975) Proc. Natl. Acad. Sci. USA 72: 4483-4486.

Wasenius, V.-M., Saraste, M., Salven, P., Eramaa, M., Holm, L., and Lehto, V.-P. (1989) Journal of Cell Biology 108: 79-93.

Way, M., Pope, B., Gooch, J., Hawkins, M., and Weeds, A.G. (1990) European Molecular Biology Organisation Journal 9: 4103-4109.

Weihing, R.R. (1983) Biochemistry 22: 1839-1847.

Weller, P.E., Ogryzko, E.P., Corben, E.B., Zhidova, N.I., Patel, B., Price, G.J., Spurr, N.K., Koteliansky, V.E., and Critchley, D.R. (1990) Proc. Natl.Acad. Sci. USA 87: 5667-5671.

Werth, D.K., Niedel, J.E., and Pastan, I. (1983) Journal of Biological Chemistry 258: 11423-11426.

Werth, D.K. and Pastan, I. (1984) Journal of Biological Chemistry 259: 5264-5270.

Westmeyer, A., Ruhnau, K., Wegner, A., and Jockusch, B.M. (1990) Molecular Biology Organisation Journal 9: 2071-8.

Wilkins, J.A. and Lin, S. (1982) Cell 86: 83-90.

Wilkins, J.A., Chen, K.Y., and Lin, S. (1983) Biochem. Biophys. Res. Comm. 116: 1026-1032.

Wilkins, J.A. and Lin, S. (1986) Journal of Cell Biology 102: 1085-1092.

Wilkins, J.A., Risinger, M.A., and Lin, S. (1986) Journal of Cell Biology 103: 1483-1494.

Wilkins, J.A., Risinger, M.A., Coffey, E., and Lin, S. (1987) Journal of Cell Biology 105: 130a (abstr).

Winograd, E., Hume, D., and Branton, D. (1991) Proc. Natl. Acad. Sci. USA 88: 10788-10791.

Woods, A., Couchman, J.R., Johansson, S., and Hook, M. (1986) European Molecular Biology Organisation Journal 5: 665-670.

Woods, A. and Couchman, J.R. (1992) Journal of Cell Science 101: 277-290.

Yang, Q. and Tonks, N.K. (1991) Proc. Natl. Acad. Sci. USA 88: 5949-5953.

Yarden, Y. and Ullrich, A. (1988) Annual Review of Biochemistry 57: 443-474.

Zhang, Z., Lawrence, J., and Stracher, A. (1988) Biochemical and Biophysical Research Communications 151: 355-360.

Zhuang, Q.Q., Rosenberg, S., Lawrence, J., and Stracher, A. (1984) Biochemical and Biophysical Research Communications 118: 508-513.